

INVESTIGATION INTO THE FUNCTIONAL ROLES OF TAU AND
ALPHA-SYNUCLEIN IN NEURODEGENERATIVE DISEASE

by

Meaghan Morris

A dissertation submitted to Johns Hopkins University in conformity with the requirements for the degree of
Doctor of Philosophy

Baltimore, Maryland

June, 2014

Abstract

Tau and α -synuclein (SYN) are two intrinsically disordered proteins that aggregate in several common neurodegenerative diseases, including Alzheimer's disease (AD) and Parkinson's disease (PD). We investigated the functional roles and interactions of tau and SYN in mouse models of neurodegenerative disease. We first determined that reduction and ablation of tau in aging mice is benign, validating tau reduction as a safe potential therapeutic target. Tau ablation prevents many AD-like behavioral and biochemical alterations in the human amyloid precursor protein mouse model (hAPP-J20) of AD, but how tau mediates these phenotypes is unknown. Using mass spectrometry to identify and quantify endogenous post-translational modifications of tau, we found similar levels of tau modifications in hAPP-J20 and wildtype mice suggesting that abnormal tau modification may not mediate AD-like phenotypes in hAPP-J20 mice. Because hyperphosphorylated and aggregated tau can also be found in PD, we explored whether tau mediated PD-like phenotypes in a mouse model of toxic dopaminergic cell death and a wildtype SYN transgenic mouse model. Tau knockout tended to worsen toxicity in the dopaminergic cell death model and did not affect motor impairments in SYN transgenic mice, implying that tau does not mediate PD-like deficits in these models. We went on to describe SYN-induced cortical network dysfunction by electroencephalography and compared it to network dysfunction in patients with dementia with Lewy bodies (DLB), a disease closely related to PD. We identified two types of neural network dysfunction in SYN transgenic mice: a shift in power from higher to lower frequency brain oscillations and seizures. Human DLB patients show a similar shift in oscillatory power and signs of aberrant network excitability, implying that SYN accumulation may contribute to neural network dysfunction in DLB. Tau ablation and acute anti-epileptic treatment reduced epileptiform activity in SYN mice, but did not affect the oscillatory shift. We propose that tau mediates aberrant network excitability induced by $A\beta$ in hAPP-J20 mice, however, SYN can induce oscillatory and motor network dysfunction independently of tau function. In human dementia patients, tau lowering therapies may benefit patients with $A\beta$ pathology but additional SYN-targeted therapies would be required for patients with SYN pathology.

Advisors: Dr. Gerald Hart and Dr. Lennart Mucke

Preface

I would like to begin by saying thank you to my mentors, Jerry Hart and Lennart Mucke, who worked together to support my work in highly unusual circumstances. Without the unwavering support of both my mentors, this work would have been impossible. I am deeply indebted to Jerry's flexibility and generosity in taking on a graduate student as a long-distance, collaborative effort and Lennart has been a role model and wonderful mentor in writing, experimental design, lab management and professional conduct. I'd also like to thank Robert Silicano and Carolyn Machamer for facilitating the unusual arrangements of my thesis work and my thesis committee, Michela Gallagher and Paul Worley, for their helpful critiques and advice.

Many people have contributed to this work, only some of whom contributed as authors. Many thanks to Win Cheung, who got me started in the Hart lab; Sumihiro Maeda, who did the same in the Mucke lab; Laure Verret, my EEG instructor; Keith Vossel, my labmate and collaborator on human studies; and the many friends and colleagues I've had the pleasure of working with in the Mucke and Hart labs. My special thanks go to Gui-Qiu Yu, Daniel Kim, Xin Wang, Weikun Guo, Kaitlyn Ho, and Jing Kang for technical contributions, but also for teaching me a great deal of experimental technique and patiently answering all of my questions. The smooth functioning of the Mucke lab is entirely due to this group of very talented people. I'd like to thank Nino Devidze, Iris Lo, and the past and present staff of the Gladstone behavioral core, who have been a pleasure to work through some difficult experiments over the past several years, and Monica dela Cruz, Amy Cheung and Emily Loeschinger for extremely capable administrative support.

My thesis work has allowed me to learn a great variety of biological techniques in collaboration with groups within Johns Hopkins and the Gladstone Institutes, and at other institutions. I would like to thank everyone I've had the pleasure of collaborating with over the past several years, especially Gigi Knudsen, Al Burlingame, Namrata Udeshi, Donald Hunt, and Eliezer Masliah. A special thank you goes to Mariel Finucane, who has a talent for clearly explaining statistical analysis to biologists. For their contributions to this work, I'd like to thank Marie-Francoise Chesselet for Thy1-SYN (line 61) transgenic mice on a pure C57Bl/6J background; Raymond Johnson at the Vanderbilt Neurochemistry Core for measuring dopamine levels; Kirsten Eilertson from the Gladstone Bioinformatics core for additional advice on statistical analysis; Alexxai Kravitz for advice on gait analysis; the Gladstone Genomics Core for RNA integrity

measurements; the Gladstone Electron Microscopy Core for spinal electron microscopy; and Giovanni Maki and John Carroll for figure preparation and advice. Additional thanks go to the large number of people contributing to the human studies in chapter 5, including Bruce Miller, Alexandra Nelson and Kate Possin for helpful discussions; Heidi E. Kirsch for EEG interpretation; Srikantan Nagarajan for EEG oversight; and Danielle Mizuiri and Susanne M. Honma for technical support.

Financial support for this work includes NIH grants AG022074, AG039259, NS041787 and NS065780 to Lennart Mucke, AG5131 and AG022074 to Eliezer Masliah, GM103481 to Al Burlingame, K23 AG038357 to Keith Vossel, a MetLife Foundation Award to Lennart Mucke, a grant from the John Douglas French Alzheimer's Foundation to Keith Vossel, and a University of California, San Francisco Alzheimer's Disease Research Center pilot project grant to Keith Vossel, and by a gift from the S.D. Bechtel, Jr. Foundation to the Gladstone institutes.

Last, but certainly not least, thank you to my amazing family. Our daughter, Michaela, has been a near constant source of amusement and joy for the past year and none of this would have been possible without the support of my husband, Pat. I love you both very much!

Table of Contents

Abstract	ii
Preface	iii
List of Tables	vi
List of Figures	vii
Chapter 1: Tau and α -Synuclein, Two Intrinsically Disordered Proteins That Cause Neurodegeneration in Humans	1
Part I: Tau, a microtubule-associated protein involved in disease	2
Part II: α -Synuclein, a pre-synaptic protein involved in disease	31
Part III: Pathologic interactions between SYN, tau and A β	44
Chapter 2: Age-Appropriate Cognition and Subtle Dopamine-Independent Motor Deficits in Aged Tau Knockout Mice	47
Chapter 3: How Tau Mediates A β -induced Dysfunction: Gain-of-Function versus Physiological Mediator	58
Chapter 4: Tau Reduction Does Not Prevent Motor Deficits in Two Mouse Models of Parkinson's Disease	77
Chapter 5: Network Dysfunction in α -Synuclein Transgenic Mice and Human Lewy Body Dementia	87
Chapter 6: Insights into the Functional Roles of Tau and α -Synuclein in Neurodegenerative Disease	102
Appendix A: Methods	110
Appendix B: Mouse Cohorts Studied	132
Bibliography	140
Curriculum Vitae	161

List of Tables

Table 1.1: Partial list of tau binding partners.....	6
Table 1.2: Behavioral tests in tau knockout mice.....	13
Table 1.3: Electrophysiological abnormalities of hAPP-J20 mice prevented by tau knockout.....	17
Table 3.1: Summary of unambiguously assigned tau modifications in wildtype mice.....	64
Table 3.2: Endogenous tau modifications in wildtype and hAPP mice.....	65
Table 3.3: Tau modifications quantified in hAPP and wildtype mice.....	71
Table 5.1: Human EEG cohort.....	89
Table 5.2: Human <i>postmortem</i> tissues.....	96
Table 5.3: Humans with DLB analyzed.....	96
Table 5.4: Incidence of seizures and myoclonus in humans with DLB by age.....	98
Table B.1: Mouse cohorts used in aged tau knockout studies.....	132
Table B.2: Summary of mice and experiments used to identify post-translational modifications of tau.....	133
Table B.3: Mouse cohorts used for quantitative mass spectrometry experiments.....	137
Table B.4: Mouse cohorts used in PD model studies.....	138
Table B.5: Mouse cohorts used in SYN transgenic studies of neural network dysfunction.....	139

List of Figures

Figure 1.1: Tau structure and function.....	3
Figure 1.2: Endogenous tau exists in dendrites.....	8
Figure 1.3: Tau reduction suppresses drug-induced seizures in mice and neuronal bursting activity in acute hippocampal slices.....	15
Figure 1.4: Tau reduction does not change amyloid pathology but prevents A β -dependent cognitive and functional neuronal deficits.....	15
Figure 1.5: Potential mechanisms of tau-dependent A β toxicity.....	19
Figure 1.6: Determining the pathologic interactions between A β , SYN and tau.....	46
Figure 2.1: Lack of tau since early development does not impair learning and memory in middle-aged and old mice.....	50
Figure 2.2: Complete, but not partial, tau reduction and aging are associated with weight gain and subtle motor deficits.....	51
Figure 2.3: Correlation between weight and motor performance in 12–15-month-old <i>Tau</i> ^{-/-} mice.....	53
Figure 2.4: Mild dopaminergic deficits do not contribute to motor deficits in <i>Tau</i> ^{-/-} mice.....	54
Figure 2.5: Lack of iron staining in the brains of 14-month-old <i>Tau</i> ^{-/-} mice.....	56
Figure 3.1: Identification of O-GlcNAc modification of S400 on tau by chemical/enzymatic enrichment.....	62
Figure 3.2: Post-translational modifications identified in endogenous mouse tau.....	63
Figure 3.3: Comparison of post-translational modifications in hAPP and wildtype mice.....	68
Figure 3.4: Differential modification of tau in the post-synaptic density.....	69
Figure 4.1: Tau reduction does not prevent motor deficits induced by acute striatal 6-OHDA injection.....	80
Figure 4.2: Tau reduction does not alter recovery of motor function after 6-OHDA injection.....	81
Figure 4.3: Tau reduction does not prevent loss of tyrosine hydroxylase after striatal injection of 6-OHDA.....	83
Figure 4.4: Tau reduction does not prevent motor deficits in SYN transgenic mice.....	84
Figure 5.1: Dementia with Lewy bodies (DLB) in humans and neuronal expression of wildtype human α -synuclein (SYN) in transgenic mice cause a similar left shift in EEG spectral power.....	90
Figure 5.2: Epilepsy and related immunohistochemical alterations in SYN mice.....	92

Figure 5.3: Neuronal expression of SYN directed by the PDGF promoter also causes hippocampal changes in activity-dependent proteins in an independent line of transgenic mice.....	93
Figure 5.4: Modulation of epileptic activity does not shift spectral power.....	95
Figure 5.5: Reduction of calbindin mRNA levels in the dentate gyrus of humans with DLB and/or AD pathology.....	97
Figure 6.1: Model of pathologic interactions between A β , SYN and tau in neurodegenerative disease.....	109
Figure A.1: Workflow of the chart review analysis.....	110

Chapter 1

Tau and α -Synuclein, Two Intrinsically Disordered Proteins That Cause Neurodegeneration in Humans

By

Meaghan Morris, Sumihiro Maeda, Keith Vossel and Lennart Mucke

Tau review modified from *Neuron* 2011; 70: 410-426

Used with permission

Part I: Tau, a microtubule-associated protein involved in disease

The microtubule-associated protein tau was identified as a microtubule-assembly factor in the mid-1970s^{1,2}. Subsequently, hyperphosphorylated, insoluble, filamentous tau was shown to be the main component of neurofibrillary tangles (NFTs), a pathological hallmark of Alzheimer's disease (AD)³⁻⁷. Neurodegenerative disorders with tau inclusions are referred to as tauopathies⁸. These include AD; frontotemporal lobar degeneration with tau inclusions (FTLD-tau) such as Pick's disease, progressive supranuclear palsy and corticobasal degeneration; agyrophillic grain disease; some prion diseases; amyotrophic lateral sclerosis/parkinsonism–dementia complex, chronic traumatic encephalopathy; and some genetic forms of Parkinson's disease⁸⁻¹¹. Although associations *per se* cannot prove cause-effect relationships, tau inclusions are widely thought to contribute to the pathogenesis of these disorders because they occur in specific brain regions whose functions are altered by these conditions, and NFT formation correlates with the duration and progression of AD^{12,13}. Tau inclusions also appear to modulate the clinical features of other neurodegenerative diseases. In dementia with Lewy bodies, an α -synuclein disorder, accumulation of insoluble tau inclusions is associated with a more AD-like phenotype¹⁴.

Tau is expressed in the central and peripheral nervous system and, to a lesser extent, in kidney, lung and testis¹⁵. It is most abundant in neuronal axons^{8,16}, but can also be found in neuronal somatodendritic compartments¹⁷ and in oligodendrocytes¹⁸. Tau can be subdivided into four regions: an N-terminal projection region, a proline-rich domain, a microtubule-binding repeat domain (MBRD), and a C-terminal region¹⁹. Alternative splicing around the N-terminal region and MBRD generates six main isoforms in adult human brain²⁰. Tau isoforms are named by how many microtubule binding repeat sequences are expressed (termed R) and by which N-terminal exons are included (termed N) (Figure 1.1). For example, 3R tau has three microtubule binding repeat sequences, while 4R tau has four due to inclusion of exon 10. 0N tau includes no N-terminal exons, 1N tau exon 2, and 2N tau exons 2 and 3⁸. Tau mutations and post-translational modification sites are numbered by their location in 4R2N human tau⁸. Six additional isoforms are formed by alternative splicing around exon 6, resulting in a total of 12 tau isoforms expressed in brain²¹, although these additional splice variants have not yet been widely studied.

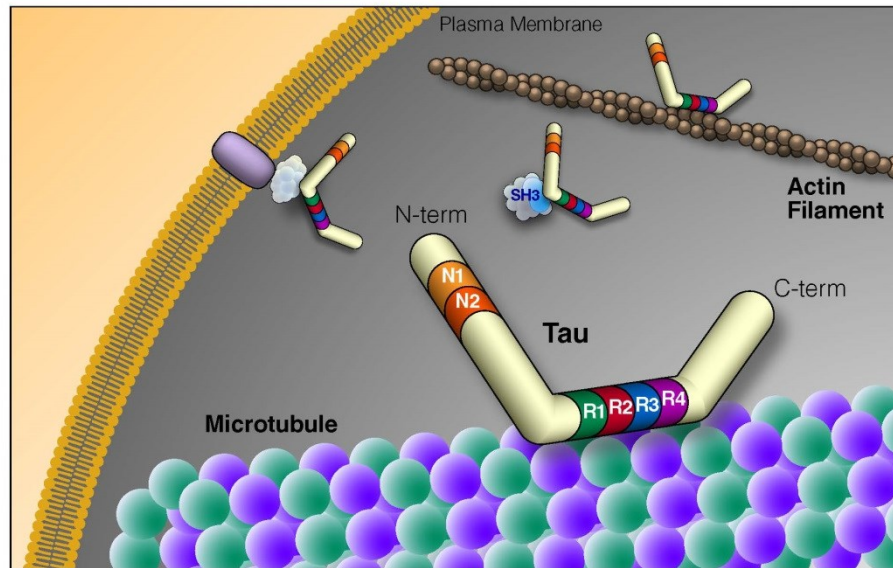


Figure 1.1. Tau structure and function. Tau is an intrinsically disordered protein that can be alternatively spliced at N terminal exons (N1, 2) and the microtubule repeat domains (R). The domains of tau bind many different types of molecules, suggesting a central role in signaling pathways and cytoskeletal organization. The diversity of tau binding partners is highlighted in Table 1.1. N-term, N-terminus; C-term, C-terminus; SH3, protein SH3 domain.

Physiological tau has an intrinsically disordered structure and is subject to a complex array of post-translational modifications. Many serine and threonine residues on tau are phosphorylated by a variety of kinases in both physiological and pathological conditions (for a comprehensive table of tau phosphorylation and corresponding kinases, see <http://cnr.iop.kcl.ac.uk/hangerlab/tautable>). Tau is also post-translationally modified by tyrosine phosphorylation²², acetylation^{23,24}, cross-linking by transglutaminase²⁵, glycation²⁶, isomerization²⁷, nitration²⁸, sumoylation²⁹, O-GlcNAcylation³⁰, and ubiquitination³¹. The diversity of these modifications suggests that tau is highly regulated.

Tau can bind to the outside and, possibly, also the inside of microtubules, with its N- and C-terminal regions projecting outward^{32,33}. Its N-terminal region can associate with the cell membrane, likely as part of a membrane-associated complex (Figure 1.1), and regulate the spacing between microtubules³⁴⁻³⁶. Its proline-rich domain includes many phosphorylation sites^{37,38} and can bind to SH3 domains of other proteins³⁹, including the tyrosine kinase Fyn⁴⁰. Tau's ability to bind microtubules depends on the MBRD and on adjacent regions⁴¹. The tandem repeat sequences within the MBRD are thought to directly bind microtubules through their positive net charge, which interacts with negatively charged residues in tubulin^{32,42}. Phosphorylation of tau can decrease its binding to microtubules, allowing tau to diffuse out of the axon⁴³, and is associated with tau aggregation in disease. Phosphorylation of tau in and around the MBRD may neutralize the positive charge⁴² and alter the conformation of the MBRD of tau⁴⁴, detaching tau from microtubules. The detached tau mislocalizes, diffusing out of the axon⁴³ and accumulating in neuronal cell bodies and neurites, and forms insoluble filaments and, ultimately, NFTs^{8,45}. The MBRD also contains PHF6 (VQIVYK) and PHF6* (VQIINK), critical sequences that can assume the beta-sheet structures necessary for tau aggregation and formation of pathological inclusions^{45,46}

Evidence for multiple functions of tau

Although tau has been studied ever more intensely in recent years, its precise functions and roles have, if anything, become more mysterious. Some of its activities are known in great molecular detail, but were

established in rather reductionist paradigms, and their *in vivo* significance remains uncertain. Other functions were revealed by analysis of tau knockout mice, but the precise mechanisms are poorly understood. A major advantage of tau knockout models is that they can reveal unique functions of tau that are not redundant with the functions of other proteins. For example, tau reduction prevents behavioral deficits in several models of AD (see below), suggesting that unique functions of tau are important in the pathogenesis of this condition. It remains controversial whether animal models with high levels of tau overexpression can provide relevant insights into human conditions in which such overexpression does not occur. However, the accumulation and abnormal distribution of hyperphosphorylated and aggregated tau in these models does simulate key aspects of human tauopathies. Concerns may also be raised about the relevance of studies investigating tau in non-neuronal cells. Although neurons are probably the most relevant cell type to study in relation to tauopathies, some tauopathies are associated with tau pathology in glial cells⁴⁷ and the proteins that interact with tau in different cell types likely overlap.

Tau has numerous binding partners (Table 1.1), including signaling molecules, cytoskeletal elements and lipids, suggesting that it is a multifunctional protein. Indeed, tau can bind to and affect cytoskeletal components and regulate signaling pathways by acting as a protein scaffold for signaling complexes; tau binding also activates or inhibits several enzymes.

Cytoskeletal binding functions

The most extensively described activity of tau—binding to microtubules—occurs *in vitro* and *in vivo*. In fact, the majority of tau in the cell is bound to microtubules. In cell-free conditions, this microtubule binding activity promotes microtubule assembly and stability¹. However, in cell culture, tau co-localizes with those microtubules that are most dynamic and most susceptible to drug-induced depolymerization⁴⁸. Moreover, the population of tau-bound microtubules has the highest basal turnover rate of any microtubule population, both in rat primary neuronal culture and in mouse hippocampus *in vivo*⁴⁹, raising doubts about the essential role of tau in microtubule stabilization postulated on the basis of *in vitro* findings. In addition,

Table 1.1. Partial list of tau binding partners

Tau Binding Partners	Function of Binding Partner
ApoE3	Lipid carrier ^{50,51}
Beta tubulin	Cytoskeleton ³²
cSrc	Src-family kinase ^{39,40}
F-actin	Cytoskeleton ⁵²
Fgr	Src-family kinase ³⁹
Fyn	Src-family kinase ^{39,40}
Growth factor receptor-bound protein 2 (Grb2)	Adaptor protein for growth factor signaling ³⁹
Lck	Src-family kinase ⁴⁰
p85 α	Regulatory subunit of PI3K ³⁹
Phosphatidylinositol	Signaling lipid ⁵³
Phosphatidylinositol bisphosphate	Signaling lipid ⁵⁴
PLC γ	Cleaves phospholipids into signaling molecules ^{39,55,56}

knockdown of tau by siRNA is not lethal to primary neurons in culture and does not decrease the number of microtubules or their polymerization state^{57,58}. Thus, microtubule stabilization may not be a unique or critical function of tau *in vivo*.

The *in vitro* and *in vivo* functions of tau appear to overlap with those of MAP1B, another microtubule-associated protein found in axons^{59,60}. In mice, complete ablation of tau by homologous recombination does not significantly impair longevity or most critical brain functions, but clearly worsens the MAP1B knockout phenotype of premature mortality and

brain dysgenesis⁶⁰. Knockout of both tau and MAP1B results in severe brain dysgenesis and is lethal within the first month of life. Assuming that this phenotype relates to the microtubule-binding activities of tau and MAP1B, which is uncertain, it is reasonable to speculate that MAP1B is more important for microtubule stabilization than tau and that their overlapping functions are critical for postnatal brain maturation. However, because of the early lethality, it is impossible to draw firm conclusions from the double-knockout phenotype on the functions of tau and MAP1B in the adult or aging brain.

In principle, tau's binding to microtubules could regulate axonal transport. Tau can interfere with the binding of motor proteins to microtubules^{61,62}, and there is a gradient of tau along the axon; the highest

levels are closest to the synapse⁶³. This distribution might facilitate the detachment of motor proteins from their cargo near the presynaptic terminal, increasing axonal transport efficiency⁶¹. Independent of the microtubule binding ability of tau, the N-terminus of tau impairs fast-axonal transport through activation of protein phosphatase 1 and glycogen-synthase kinase 3 β (GSK3 β), a mechanism which may be relevant in overexpression or disease conditions⁶⁴. However, ablation of tau does not alter axonal transport in primary neuronal culture⁶⁵ or *in vivo*⁶⁶, making an essential role of tau in this physiological function less likely.

Tau can also bind to and bundle actin filaments^{52,67,68}, activities mediated primarily by its MBRD^{69,70} and assisted by the adjacent proline-rich domain⁶⁷ (Figure 1.1). It is possible that tau connects microtubule and actin filament networks⁶⁹.

Modulation of signaling pathways through scaffolding

Tau could also act as a protein scaffold, and regulation of its binding partners may alter signaling pathways. For example, tau modulates the activity of Src family kinases. In mouse brain tissues, tau co-immunoprecipitates with both the tyrosine kinase Fyn and the scaffolding protein PSD95, and in the absence of tau, Fyn can no longer traffic into postsynaptic sites in dendrites (Figure 1.2)⁷¹. The authors speculated that tau normally tethers Fyn to PSD-95/NMDA receptor signaling complexes. Although very little tau is normally present in dendrites, it may be enough to ensure proper localization of postsynaptic components⁷¹. Similarly, tau acts as a protein scaffold in oligodendrocytes, connecting Fyn and microtubules to enable process extension¹⁸. In cell culture, tau binds to and activates both cSrc and Fyn and facilitates cSrc-mediated actin rearrangements following platelet-derived growth factor stimulation⁷².

Tau may also regulate signaling cascades that control neurite extension, although this is a somewhat controversial area. Some investigators have reported a defect in neurite extension in tau knockout neurons *in vitro*⁷³, whereas others found no such defect despite observing decreased numbers of microtubules⁷⁴.

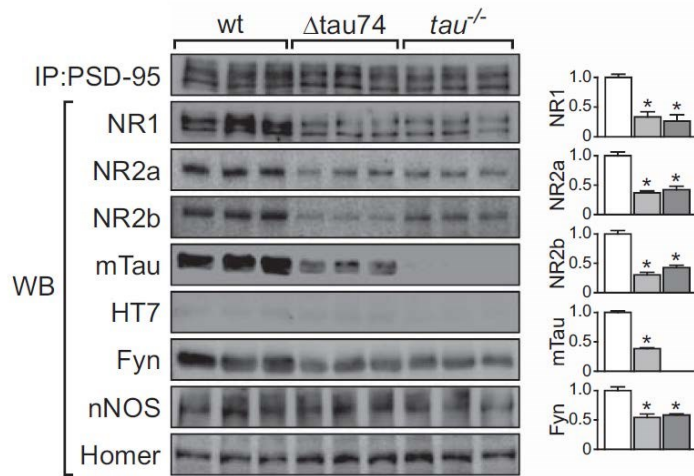


Figure 1.2. Endogenous tau exists in dendrites. Tau immunoprecipitates with PSD95, a postsynaptic protein, and regulates the association of PSD95 with NMDAR subunits and the tyrosine kinase Fyn. Overexpression of a human N-terminal truncation of tau (Δtau74 , light grey) or knocking out tau ($\text{Tau}^{-/-}$, dark grey) reduced the amount of NR1, NR2a, NR2b, and Fyn within PSD95 complexes. From Ittner, *et.al.* 2010⁷¹ with permission from Elsevier.

Knockdown of tau by siRNA decreased the length of neurites^{57,75} but not the number of microtubules^{57,58}, and overexpression of tau promoted neurite extension in cell culture⁷⁶. These effects may relate to tau's ability to thwart microtubule-severing proteins⁵⁷, but could also involve facilitation of nerve growth factor (NGF) signaling.

In PC12 cells, overexpression of full-length tau was associated with normal neurite extension and an increased number of neurites per cell, whereas overexpression of the N-terminus of tau suppressed NGF-induced neurite extension⁷⁶. Thus, increased levels of tau may enhance NGF function, whereas the N-terminus of tau may impair NGF signaling, possibly by a dominant-negative mechanism. Enhancement of NGF signaling by tau may involve increased association of tau with actin filaments, which occurs after stimulation with NGF and is mainly mediated by the MBRD⁷⁰ rather than the N-terminus. In PC12 cells, tau facilitates signaling through receptors for NGF and epidermal growth factor (EGF), thereby increasing activity in the mitogen-activated protein kinase (MAPK) pathway⁷⁷. Stimulation of PC12 cells with NGF or EGF causes tau phosphorylation at T231, a modification necessary for the growth factor-induced activation of the Ras-MAPK pathway⁷⁷, nicely illustrating the functional significance of a single tau phosphorylation site. As tau is not known to directly interact with growth factor receptors, it may facilitate signaling by binding to adapter proteins such as Grb2³⁹. The enhancement of growth factor signaling by increased tau expression may explain why several forms of chemotherapy-naive cancer cells overexpress tau^{78,79}.

Tau may contribute to neuronal migration during a critical period in embryogenesis. While mice with genetic tau ablation show normal brain anatomy, tau reduction at embryonic day 14 by shRNA electroporation impaired the migration of cortical neurons by embryonic day 18⁸⁰. The neurons lacking tau had shorter neurites, and abnormal mitochondrial and cellular morphology⁸⁰. It is unclear whether these neurons would have recovered over a longer time period, however, tau appears to play a specific, unknown role in the health and normal migration of cortical neurons during embryogenesis which may be compensated for in genetic tau knockouts.

Other roles of tau in signaling pathways

Recent evidence suggests that tau plays a role in synaptic plasticity. Long-term potentiation (LTP) of synapses in the hippocampal CA1 region of acute slices caused translocation of tau into the post-synaptic density (PSD), possibly driven by post-synaptic actin polymerization⁸¹. In primary neuronal cultures, treatment with brain-derived neurotrophic factor (BDNF), a neurotrophin associated with LTP, increases tau protein levels and increases neuronal spine density in a tau-dependent manner⁸². However, the physiologic significance of the function is unclear; generally there is no effect of tau ablation on LTP in acute slices^{83,84} or *in vivo*⁸⁵. Only one study has found tau ablation with enhanced green fluorescent protein (EGFP) knock-in to be associated with impaired LTP⁵¹. Endogenous tau may be required for long-term depression (LTD) of synaptic activity *in vitro* and in 7-11 month old mice *in vivo*⁸⁵, though this finding has not been confirmed by studies of LTD in slices from older mice⁵¹.

Tau binds phospholipase C (PLC) γ in human neuroblastoma (SH-SY5Y) cells⁵⁶. Under cell-free conditions and in the presence of unsaturated fatty acids, tau activates PLC γ independently of the tyrosine phosphorylation usually required to activate this enzyme⁵⁵. At high tau concentrations, this activation does not require fatty acids⁵⁵ and may involve binding of tau to both the enzyme and the substrates phosphatidylinositol⁵³ or phosphatidylinositol 4,5-bisphosphate⁵⁴, which could facilitate the cleavage reaction. Activation of PLC γ by tau was particularly facilitated by arachidonic acid⁵⁵. Arachidonic acid is released from phospholipids by cytosolic phospholipase A2, whose activity in the brain is increased in AD patients and related mouse models⁸⁶. Thus, increased levels of tau and arachidonic acid may jointly increase signaling through the PLC γ pathway in AD.

Tau can also act as a direct enzyme inhibitor. For example, it can bind to and inhibit histone deacetylase-6⁸⁷, which deacetylates tubulin and may regulate microtubule stability⁸⁷. Thus, tau may affect microtubule stability by a mechanism independent of tubulin binding, although reports regarding the levels of acetylated tubulin in tau knockout mice vary^{87,88}.

Tau also appears to participate in the cellular response to heat shock. During heat shock of neurons, tau bound DNA and facilitated DNA repair, and tau knockout neurons showed increased DNA damage⁸⁹. However, when cultured neurons were allowed to recover from heat shock, tau knockout actually protected against heat shock-induced cell damage, as determined by measurements of neurite length and lactate dehydrogenase release⁹⁰. Compared with wildtype neurons, tau knockout neurons showed a delayed and prolonged activation of Akt and less GSK3 β activity during recovery from heat shock⁹⁰, suggesting that the protective effect of tau knockout may be upstream of Akt/GSK3 β phosphorylation. In sensory neurons of *C. elegans*, overexpression of 4R0N tau decreased the response to touch, and this phenotype was exacerbated by heat shock when tested after a recovery period of 24 hours⁹¹. These results suggest that tau has a role in the cellular response to heat shock, both during the insult and in the subsequent recovery phase.

The association of tau with DNA during cellular challenge may alter chromatin structure, possibly accounting for the effects of tau on DNA damage and heat shock recovery⁸⁹. Tau can translocate into the nucleus in cellular stress conditions⁸⁹. In transgenic *Drosophila*, mutant and wildtype tau overexpression was associated with loss of histone H3 dimethylation of lysine 9, which implies heterochromatin relaxation, and increased transcription of silenced genes⁹². The effect of tau on DNA structure under challenge conditions may partly account for the prevention of DNA damage in the J20 human amyloid precursor protein (J20-hAPP) mouse model of AD on a tau knockout background⁹³.

Adult Neurogenesis

Tau affects adult neurogenesis. Three-repeat tau is expressed and highly phosphorylated in adult-born granule cells in the dentate gyrus^{94,95}. In one strain of tau knockout mice, adult neurogenesis was found to be severely reduced⁹⁵. However, tau does not appear to be needed for embryonic neurogenesis, as tau knockout mice have grossly normal brain anatomy. The functional significance of adult neurogenesis is a

topic of intense study and debate⁹⁶. Notably, adult tau knockout mice showed no deficits in a variety of learning and memory paradigms^{71,83,97,98}.

Mechanisms by which tau contributes to disease

As mentioned above, tau probably fulfills multiple functions and may contribute to neuropathogenesis in multiple ways. In principle, this might include both gain- and loss-of-function effects, although the latter mechanism has recently been called into question by several lines of experimental evidence. Furthermore, tau does not act alone. For example, in AD it appears to enable the pathogenic effects of both A β and apolipoprotein E4 (apoE4)^{71,83,98,99}.

Loss of function

A prominent theory about tau pathology was that disease phenotypes were caused by loss of tau function due to hyperphosphorylation and sequestration of soluble tau¹⁰⁰. In many tauopathies, tau is hyperphosphorylated, which releases tau from microtubules, apoE¹⁰¹, Src¹⁰², and possibly other binding partners. Although it is conceivable that this process results in loss of specific tau functions, increased phosphorylation of tau *per se* is probably not detrimental, as it occurs naturally during hibernation¹⁰³ and fetal development¹⁰⁴. Although phosphorylated tau from AD brains may seed the aggregation of control human tau¹⁰⁵, we are unaware of any evidence that tau aggregation actually lowers levels of soluble tau *in vivo*.

Recent experimental studies have shown more directly that loss of tau function is an unlikely cause of neurodegeneration and neuronal dysfunction. In our opinion, longevity and behavioral functions are among the most compelling outcome measures for the evaluation of biologically meaningful functions affecting the central nervous system. Complete ablation of tau in knockout mice does not cause premature mortality or major neurological deficits^{66,73,74,83,98,106}. Four independent tau knockout lines have been established and most of them have normal behavior throughout most of their lives (Table 1.2). Only one of these lines was

reported to have motor deficits, hyperactivity in the open field test, and learning impairments in contextual fear conditioning at 10–11 weeks of age¹⁰⁶. Using fear conditioning to assess learning and memory in hyperactive mice is problematic because the hyperactivity confounds the interpretation of diminished freezing¹¹⁰. Because tau ablation has so little impact on neural functions, two of the tau knockout lines were actually generated as indicator tools for neuron-specific expression of EGFP¹⁰⁸ or Cre¹⁰⁹. Contextual fear

Table 1.2. Behavioral tests in Tau knockout mice

Behavioral Test	Knockout Line ¹	Age (months)	Result
Anxiety			
Elevated Plus Maze	2	4–7 and 12–16	Normal anxiety and exploration ⁹⁸
	3	4.5–7.5	Normal anxiety and exploration ⁸³
Motor and Coordination			
Balance Beam	1	10–11 weeks	Impaired motor function ¹⁰⁶
Open Field	1	10–11 weeks	Hyperactive ¹⁰⁶
	2	6, 12 and 24	Decreased movement velocity at 12+ months ¹⁰⁷
	3	6	Normal activity ⁵¹
Pole Test	2	6, 12 and 24	Impaired motor function at 12+ months ¹⁰⁷
Rotor Rod	2	10–12	Normal motor function ⁹⁷
	2	6, 12 and 24	Impaired motor function at 12+ months ¹⁰⁷
Wire Hang	3	6	Normal motor function ⁵¹
	1	10–11 weeks	Impaired motor function ¹⁰⁶
Y-maze	2	4–7	Normal activity ⁹⁸
Learning and Memory			
Contextual Fear Conditioning	1	10–11 weeks	Impaired learning/memory ¹⁰⁶
	3	6	Impaired memory ⁵¹
Morris Water Maze	2	4-7	Normal learning/memory ⁹⁸
	2	10–12	Normal learning/memory ⁹⁷
	3	6	Enhanced learning in acquisition week 2 ⁵¹
Novel Arm Y-maze	2	6 and 12	Impaired memory at 12 months ¹⁰⁷
Novel Object Recognition	3	4.5–7.5	Normal learning/memory ⁸³
Radial Arm Water Maze	2	10–12	Normal learning/memory ⁹⁷
T Maze	3	8	Normal learning/memory ⁷¹
None	4	–	–

¹Tau knockout line numbering based on order of publication: line 1⁷⁴, line 2⁷³, line 3 EGFP-knock-in¹⁰⁸, line 4 Cre knock-in¹⁰⁹

conditioning deficits have been reported in the EGFP-tau knockout line at 6 months of age, however the same cohort showed improvement in the Morris water maze⁵¹, another test of hippocampal-dependent memory. Although axonal abnormalities have been reported in the cingulate cortex and genu of the corpus callosum of 10- and 12-month-old tau knockout mice from line 2, these mice showed no behavioral deficits in the Rota rod test, Morris water maze, or radial arm water maze⁹⁷. By contrast, a second study of 12 month-old tau knockout mice from the same line showed extensive motor and memory impairments related to iron accumulation and loss of dopaminergic neurons in the substantia nigra¹⁰⁷. To our knowledge, no deficits of any kind have been identified in hemizygous knockout mice, which have roughly half normal tau levels^{98,106}.

Based on electrophysiological recordings in acute hippocampal slices, tau knockout mice and wildtype controls have similar NMDA/AMPA receptor currents, synaptic transmission strength, and short-term as well as long-term synaptic plasticity^{83,84}.

Surprisingly, tau knockout mice are more resistant to seizures elicited by disinhibition, excitotoxins, or amyloid- β ($A\beta$) peptides than wildtype mice (Figure 1.3A)^{71,83,98}. Compared with wildtype controls, neurons in hippocampal slices from tau knockout mice are more resistant to disinhibition-induced bursting activity (Figure 1.3B), which may be due, at least in part, to an increased frequency of spontaneous inhibitory postsynaptic currents in tau knockout mice⁸³. Mimicking the effects of genetic tau reduction, reducing tau in adult mice with anti-sense oligonucleotides (ASO) also reduced susceptibility to PTZ-induced seizures¹¹¹. These findings suggest that tau has a complex role in regulating neural network activity and that tau reduction could prevent aberrant neuronal excitability, synchrony, or both.

The resistance of tau knockout mice to seizures may also relate to alterations in brain oscillatory patterns. Tau knockout mice have decreased peak frequency of theta waves in the hippocampus and decreased coherence of gamma waves in the frontal cortex¹¹². The potential effects of these alterations on $A\beta$ -induced dysrhythmias and cognitive abnormalities remain to be determined.

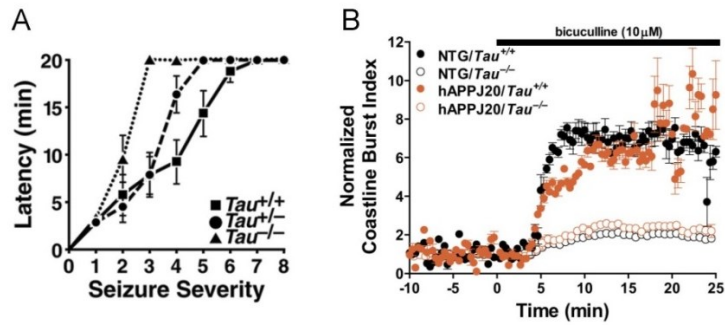


Figure 1.3. Tau reduction suppresses drug-induced seizures in mice and neuronal bursting activity in acute hippocampal slices. A) Partial or complete reduction of tau in mice without hAPP expression delayed the onset and reduced the severity of seizures induced by pentylenetetrazole, a GABA_A receptor antagonist⁹⁸. Reprinted from Roberson, *et.al.* 2007⁹⁸ with permission from AAAS. B) Tau knockout reduced aberrant neuronal discharges in acute hippocampal slices after disinhibition with the GABA_A receptor antagonist bicuculline, as illustrated by measurements of the coastline burst index⁸³. Reprinted from Roberson, *et.al.* 2011⁸³ with permission from the Society for Neuroscience. NTG, no hAPP expression; hAPPJ20, hAPP mice from line J20.

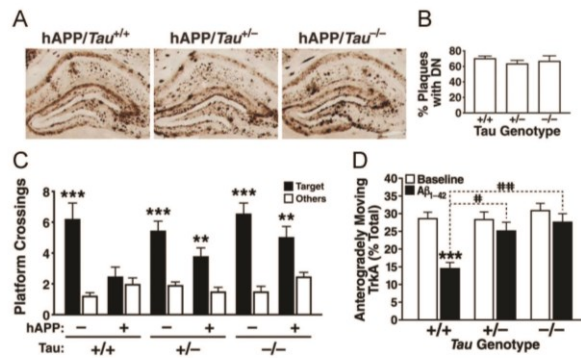


Figure 1.4. Tau reduction does not change amyloid pathology but prevents A β -dependent and functional neuronal deficits. Tau reduction did not affect (A) A β deposition or (B) the number of plaques with dystrophic neurites (DN) in hAPP-J20 mice. However, even partial tau reduction prevented (C) memory deficits in the Morris water maze (72 hour probe trial) in hAPP-J20 mice⁹⁸ and (D) A β oligomer-induced axonal transport deficits in primary hippocampal neurons, although it had no effect on axonal transport at baseline⁶⁵. Reprinted A-C from Roberson, *et.al.* 2007⁹⁸ and D from Vossel, *et.al.* 2010⁶⁵ with permission from AAAS.

In conventional tau knockout mice, other microtubule associated proteins might compensate for tau loss, particularly MAP1A and MAP1B. However, no changes in MAP1A, MAP1B or MAP2 protein levels were detected in 12-month-old adult tau knockout mice⁷³. Acute tau reduction by intraventricular ASO infusion in adult mice was effective and well tolerated¹¹¹. Notably, tau ASO treated mice performed at normal levels in a battery of sensory and motor tasks, had normal anxiety behaviors in the elevated plus maze and normal learning and memory in the Morris water maze¹¹¹. The findings summarized above suggest that partial reduction of tau may be well tolerated and could effectively protect the brain against A β , epileptogenesis and excitotoxicity.

Tau functions enabling pathogenesis

In transgenic mice, wildtype levels of tau are required for A β and apoE4 to cause neuronal, synaptic and behavioral deficits^{58,65,71,83,88,93,98,99}. However, whether A β and apoE4 contribute to AD-related cognitive decline through the same or distinct tau-dependent mechanism(s) remains to be determined. Acute exposure of neuronal cultures to A β led to hyperphosphorylation¹¹³ and mislocalization of tau into dendritic spines¹¹⁴, which, at least in some dendrites, was associated with spine collapse and dendritic degeneration. Tau knockout neurons are resistant to spine loss and cytoskeletal alterations following A β treatment¹¹⁵. As tau phosphorylation releases tau from many of its binding partners, it is tempting to speculate that tau is initially hyperphosphorylated in AD to reduce its function, in an effort to counteract A β -induced neuronal dysfunction. With time, though, this compensatory mechanism fails because hyperphosphorylated tau becomes detrimental at concentrations sufficient to form toxic tau aggregates^{58,65,71,83,88,98,99}.

In some mouse models of AD, tau reduction may also reduce APP cleavage. In mice expressing hAPP and presenilin 1 (PS1), tau ablation improved motor and working memory impairments, prevented spine loss and reduced neurodegeneration¹¹⁶. In addition to the inhibitory effects of tau ablation on A β -induced impairments, tau ablation also reduced the production and deposition of A β in this model, presumably by

preventing the induction of beta-secretase 1 (BACE1) in hAPP/PS1 mice¹¹⁶. The mechanism by which tau ablation prevents BACE1 induction is unknown and is likely related to the mutant PS1 transgene as A β production and deposition are unaffected by tau ablation in transgenic models expressing hAPP alone⁹⁸.

While tau is abnormally phosphorylated in apoE4 transgenic mice¹¹⁷, we have so far found no evidence of abnormal phosphorylation or aggregation of tau in hAPP-J20 mice, whose robust A β -dependent neuronal and behavioral deficits were prevented by reduction of wildtype murine tau (Table 1.3 and Figure 1.4)^{83,98}. While we continue to search for a direct pathogenic tau mediator and a pathogenic mislocalization of tau in hAPP-J20 mice, the above findings raise the possibility that physiological functions of tau, rather

Table 1.3. Electrophysiological abnormalities of hAPP-J20 mice prevented by tau knockout⁸³. Similar results were observed after exposure of hippocampal slices to recombinant A β aggregates^{84,101}.

Electrophysiological Measure ¹	Tau ^{-/-} Mice ²	hAPP/Tau ^{+/+} Mice ²	hAPP/Tau ^{-/-} Mice ²
Action Potential-driven IPSC Frequency	Normal	↓	Normal
Coastline Burst Index	↓	↑	↓
EEG epileptiform activity (cortex)	Normal	↑	Normal
eEPSC Amplitude	Normal	↑	Normal
eIPSC Amplitude	Normal	↓	Normal
Long-term Potentiation	Normal	↓	Normal
mEPSC Frequency	Normal	↓	Normal
mIPSC Frequency	Normal	↑	Normal
NMDAR/AMPA Ratio	Normal	↓	Normal
Paired Pulse Ratio	Normal	↓	Normal
sIPSC Frequency	↑	↓	↑
Synaptic Strength (CA1)	Normal	↓	Normal

EPSC, excitatory post-synaptic current; IPSC, inhibitory post-synaptic current; e, evoked; m, miniature; s, spontaneous

¹Recorded at perforant path to granule cell synapse in dentate gyrus unless indicated otherwise. All recordings were obtained in acute hippocampal slices.

²Relative to Tau^{+/+} mice

than an abnormal tau gain of function, permit A β and other AD-related factors to elicit aberrant neuronal excitation^{71,83,98}, abnormalities in axonal transport⁶⁵, and impairment of inhibitory interneurons⁹⁹ (Figure 1.5). Phosphorylation of tau at S262, in the MBRD, mediates at least part of A β -induced spine loss in primary culture and in hAPP-J20 mice¹¹⁸, possibly by recruiting microtubule severing proteins into dendritic spines¹¹⁵, however, this phosphorylation was not altered in the hippocampus of hAPP-J20 mice⁹⁸. Notably, even partial tau reduction improved longevity and cognitive functions in hAPP-J20 mice (Figure 1.4)⁹⁸. Tau knockout also improved longevity and cognitive functions in APP23 mice and in both lines markedly increased resistance to seizures in mice with or without hAPP^{71,83,98}. For unclear reasons, tau reduction was not beneficial in the Tg2576 hAPP mouse model⁹⁷.

The tyrosine kinase Fyn appears to be important in the development of A β - and tau-dependent neuronal deficits. A β oligomer treatment of primary neurons increases bromodeoxyuridine (BrdU) incorporation into DNA¹¹⁹, which could represent either DNA synthesis or repair. This DNA alteration depends on the activation of Fyn, PKA and CaMKII and their convergent phosphorylation of tau¹¹⁹. Neuronal overexpression of Fyn sensitizes hAPP mice to A β -induced neuronal, synaptic, and cognitive deficits^{120,121} which are prevented by knocking out tau in hAPP-J9/FYN doubly transgenic lines⁸³. Tau knockout prevented behavioral deficits in the Morris water maze and elevated plus maze of hAPP/FYN mice and premature mortality in two separate lines of hAPP/FYN mice⁸³. In addition, tau knockout prevented spontaneous epileptic activity in hAPP/FYN mice and hAPP-J20 mice (Table 1.3)⁸³. This striking antiepileptic effect could result from the reduction of tau in axons, dendrites, or both. Although tau knockout did not affect axonal transport at baseline^{65,66}, it precluded A β -induced deficits in the axonal transport of cargoes that could affect neuronal excitability (Figure 1.4D)⁶⁵. Tau is also required for Fyn to gain access to and phosphorylate the NR2B subunit of dendritic NMDA receptors⁷¹. Consistent with our hypothesis that tau reduction protects against A β by preventing neuronal overexcitation⁹⁸, targeted perturbation of the NR/PSD-95 interaction, which prevents excitotoxicity, also prevented premature mortality and memory deficits in APP23 mice⁷¹. These findings suggest that modulating tau, its interaction with Fyn, or key proteins involved in or affected by this interaction may be of therapeutic benefit in AD.

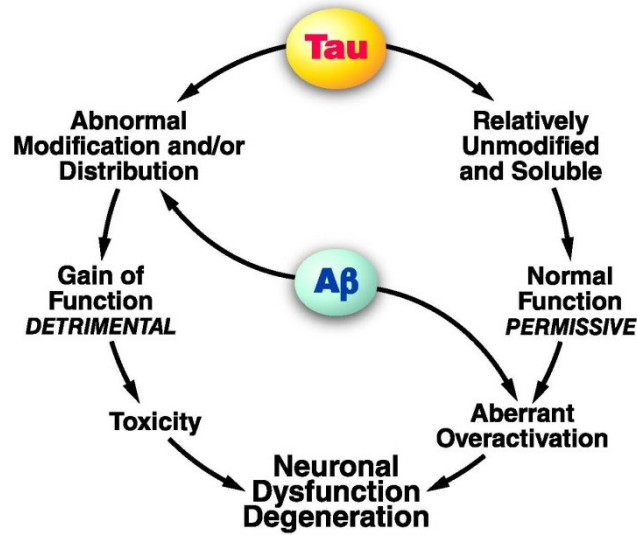


Figure 1.5. Potential mechanisms of tau-dependent A β toxicity. Experiments in which neurons were acutely exposed to A β suggest that A β can trigger tau-mediated neurotoxicity by enhancing tau phosphorylation, which in turn directs pathogenic tau species into dendritic spines where they exert adverse effects (left). In hAPP mice, though, in which neurons are chronically exposed to elevated A β levels, it has so far been impossible to find clear evidence for a similar process. Nonetheless, A β -induced neuronal dysfunction in these models strictly depends on the presence of tau, raising the possibility that physiological functions of tau permit A β to cause neuronal dysfunction (right). Such functions may involve the intraneuronal trafficking of factors that regulate synaptic activity at the pre- or postsynaptic level.

The interaction between Fyn and tau may also contribute to FTLD. Several forms of FTLD-mutant tau and pseudohyperphosphorylated tau bind Fyn more tightly than wildtype tau¹⁰², which may increase neuronal Fyn activity. Furthermore, Fyn binds more tightly to 3R0N tau than 4R0N tau¹⁰², implying that FTLD mutations that alter tau splicing could also alter the activity or localization of Fyn. In mice overexpressing P301L 4R0N tau under the mouse prion promoter (JNPL3 model), phosphorylation of tau at Y18 by Fyn increases simultaneously with tau hyperphosphorylation on serine/threonine sites before the onset of behavioral deficits¹²².

The physiological actin-bundling function of tau may also contribute to pathology. Filamentous actin inclusions, closely resembling Hirano bodies in AD, were found in *Drosophila* models overexpressing wildtype or R406W 4R0N tau and in mice overexpressing P301L 4R0N tau under the TRE promoter with the Tet-off element under the CaMKII promoter (rTg4510 model)⁵². Knocking out or destabilizing actin filaments in the *Drosophila* models prevented tau-induced degeneration⁵², implicating alterations in actin dynamics as a mediator of tau toxicity.

Abnormal gain of function

The largest amount of work in this field has focused on tau phosphorylation and aggregation. Tau is highly phosphorylated in fetal brain without eliciting toxicity and is also phosphorylated on many sites in adult brain, albeit with lower frequency^{104,123}. Tau is transiently hyperphosphorylated during hibernation without long-term harm to neural networks¹⁰³. Tau phosphorylation is also markedly increased in response to various stressors. In humans, tau becomes hyperphosphorylated and aggregated after head trauma, following earlier increases in APP expression, axonal swelling and microtubule disruption^{9,124}. Tau also becomes hyperphosphorylated in mouse brain in response to hypothermia and experimental insulin-dependent diabetes¹²⁵. In cell culture and brain slice models of neuronal injury, tau is hyperphosphorylated during recovery from heat shock⁹⁰, in response to A β oligomer treatment^{113, 114}, hypoxia, and glucose deprivation¹²⁶. In cell culture, ATP, glutamate, hydrogen peroxide, serum deprivation and A β oligomer

treatment all cause tau mislocalization into dendrites¹¹⁴, a process that is likely triggered by hyperphosphorylation-induced dissociation of tau from microtubules and cell membranes. Thus, increased phosphorylation and redistribution of tau may be common responses to neuronal stress.

Findings in *Drosophila* models suggest that tau phosphorylation may cause neurotoxicity in a combinatorial fashion rather than through the modification of individual phosphorylation sites and involves the folding of tau into an abnormal conformation resembling tau conformations found in AD¹²⁷. Hyperphosphorylated tau has a tighter, more folded conformation and an increased propensity to aggregate¹²⁸, as does tau with mutations found in FTL⁸. In *C. elegans*, overexpression of wildtype or mutant 4R1N tau causes axonal degeneration and an uncoordinated phenotype indicative of neuronal dysfunction¹²⁹. The extent of phosphorylation was similar across mutant and wildtype tau lines, but more insoluble tau was found in the former¹²⁹. Worms overexpressing mutant tau that formed aggregates had a more severe phenotype¹²⁹.

Although filamentous tau inclusions are a pathologic hallmark of tauopathies, experimental evidence suggests that filamentous tau may not be responsible for neuronal dysfunction. In a regulatable P301L 4R0N tau transgenic mouse (rTg4510 model), inhibiting tau production after filamentous tau inclusions had formed reversed behavioral deficits in the Morris water maze, even though inclusion formation progressed¹³⁰. Acute tau reduction by methylene blue treatment in this model improved memory scores in correlation with the reduction of soluble tau in the brain but did not alter the number or length of tau fibrils or the amount of Sarkosyl-insoluble tau compared to untreated transgenic mice¹³¹. In other mouse lines, Tet-off transgenes were regulated by the CaMKII promoter to express either the 4R microtubule repeat domain of human tau with a deletion of lysine 280 (termed TauRD), which is highly prone to aggregation, or the TauRD construct with an additional two mutations (I277P/I308P) that prevent TauRD aggregation¹³². The pro-aggregation transgenic mouse, which formed hyperphosphorylated tau inclusions containing TauRD and endogenous mouse tau, developed synaptic loss¹³², memory deficits and electrophysiological deficits¹³³. In contrast, the anti-aggregation transgenic mouse showed none of these abnormalities. Turning

off the transgene in the pro-aggregation mouse reversed behavioral and electrophysiological deficits without eliminating insoluble tau aggregates, which were composed entirely of endogenous mouse tau after the transgene had been turned off for 4 months¹³³. These data highlight that tau aggregation causes toxicity, possibly through the formation of tau oligomers.

This conclusion is also supported by studies using *in vivo* two-photon microscopy demonstrating that very few neurons containing tau inclusions in regulatable rTg4510 transgenic mice have caspase activation or membrane disruption^{134,135}. Decreasing the levels of soluble tau reduced caspase activation in inclusion-positive neurons without affecting the number or size of tau inclusions¹³⁵, implicating soluble tau, not tau inclusions, in the activation of pro-apoptotic pathways. Neurons with or without tau inclusions in this regulatable P301L tau model showed similar electrophysiological deficits, relative to wildtype neurons¹³⁶. Studies in young transgenic flies overexpressing wildtype or mutant 4R0N tau constructs also indicated that toxicity was conferred by soluble tau species, possibly dimers¹³⁷.

Collectively, these studies suggest that tau inclusions are not very toxic and that neuronal toxicity is caused by a smaller, soluble aggregate of a specific conformation of tau. Tau oligomers have been identified in *in vitro* and *in vivo* models as well as in AD brains¹³⁸⁻¹⁴⁰. In regulatable P301L 4R0N transgenic mice (rTg4510 model), the extent of memory deficits correlated with the level of putative tau oligomers¹³⁸.

Tau can also be cleaved in various places by caspase-3, calpain, and cathepsin L, and several of the resulting fragments are thought to increase tau aggregation. In primary neurons exposed to A β , calpain generates a 17-kDa tau fragment. However, the toxicity and *in vivo* relevance of this fragment are debated; its presence is variable in both control and AD brains^{141,142} and it appears to be absent from brains of hAPP-J20 mice⁹⁸. A β treatment of cortical neurons causes caspase cleavage of tau at N421, and cleavage at this site facilitates the formation of tau aggregates in cell-free conditions¹⁴³. Caspase activation precedes formation of filamentous tau inclusions in P301L 4R0N tau transgenic mice (rTg4510 model), raising the

possibility that caspase cleavage is important for aggregation of FTLD-mutant tau *in vivo*¹³⁵. In an inducible cell culture model overexpressing the microtubule repeat domain of tau missing K280, cytosolic cleavage by unknown proteases generated putative tau oligomers associated with lysosomal membranes and inhibited chaperone-mediated autophagy; smaller fragments produced by cathepsin L seeded tau aggregation¹⁴⁴.

Tau may also exert toxic effects from the extracellular milieu¹⁴⁵. The death of degenerating neurons or extrusion of tau from living cells containing tau aggregates¹⁴⁶ may result in the release of pathogenic tau species into the extracellular space, where they may adversely affect neighboring cells. For example, a peptide in the C-terminus of tau (amino acids 391–407) increased intracellular calcium concentrations by activating the muscarinic receptors M1 and M3¹⁴⁷. Tau aggregates released from cells were taken up by and triggered tau aggregation within co-cultured cells that had no pre-existing tau aggregates¹⁴⁶.

Injection of insoluble P301S human 4R0N tau from transgenic mouse brainstem extracts into the hippocampus of transgenic mice expressing wildtype 4R2N human tau under the mouse Thy1.2 promoter caused intraneuronal formation of wildtype 4R2N human tau inclusions in the hippocampus that spread along synaptic connections to distant brain regions¹⁴⁸. However, we are unaware of any evidence that this transfer of tau aggregation causes neuronal dysfunction or neurodegeneration. Injecting soluble P301S tau into the transgenic mice or insoluble P301S tau into nontransgenic mice failed to cause extensive pathology.

Thus, artificial introduction of insoluble tau into the brain parenchyma triggers propagation of tau pathology along neuronal pathways, but only in the presence of the correct tau template. It is unknown whether the potential progression of AD from one brain region to another¹⁴⁹ depends on similar processes, the presynaptic release of A β ¹⁵⁰, or other mechanisms. Tau is physiologically released from neurons in response to neuronal activity in cultured neuron and *in vivo*^{151,152}, so it is possible that the aberrant network excitability induced by A β increases the release of tau and spread of tau pathology.

Do FTLT mutations simulate tau pathology in AD?

Interestingly, mutations in the tau gene cause FTLT disorders such as progressive supranuclear palsy, corticobasal degeneration, and frontotemporal dementia, but never AD. A rare tau variant, with a single base pair mutation in the tau coding sequence converting A152 to T, confers an increased risk for both FTD and AD but does not appear to be a causal mutation^{153,154}. While the clinical spectrum associated with the many rare tau mutations varies, most FTLT disorders differ from AD both in the types of tau inclusions and in the brain regions affected¹⁵⁵, indicating a possible divergence in the roles of tau in these conditions. The trigger for increased phosphorylation and aggregation of tau is also likely different in AD and FTLT.

Two recent studies set out to compare the consequences of overexpressing wildtype human 4R2N tau versus P301L-mutant human 4R2N tau in transgenic mice. Each group generated two mouse lines with approximately matched tau expression levels and patterns directed by the Thy1 promoter¹⁵⁶ or the CaMKII promoter¹⁵⁷. In both studies, P301L tau mice differed from wildtype tau mice in tau phosphorylation patterns and in that P301L tau aggregated more readily than wildtype tau, consistent with previous findings⁴⁶. Remarkably, in both studies, behavior was impaired earlier in wildtype tau transgenic mice than in P301L tau transgenic mice, even though tau was similarly expressed under the same promoter and only P301L mutant tau transgenic mice had tau aggregates. Thy1-wildtype-tau mice had early motor impairments and axonopathy, whereas Thy1-P301L-tau mice had late motor impairments, insoluble tau inclusions and no axonopathy¹⁵⁶. CaMKII-wildtype-tau mice had earlier memory deficits in the Morris water maze and synaptic loss than CaMKII-P301L tau mice, but tau inclusions and neuronal loss were observed only in CaMKII-P301L tau mice¹⁵⁷. These findings suggest that P301L tau causes neuronal loss through its propensity to aggregate and, possibly, to form toxic oligomeric tau species, whereas wildtype human tau may cause early neuronal and cognitive dysfunction without neuronal cell death, possibly by enhancing normal functions of tau or altering the regulation of endogenous tau.

Another recent study compared transgenic mice expressing P301L human 4R0N tau (rTg4510 model) or wildtype human 4R0N tau directed by the TRE promoter and tTA (Tet-off) directed by the CaMKII promoter. Both lines showed deficits in the Morris water maze; however, the deficits worsened with aging in the P301L tau line but not in the wildtype tau line¹⁵⁸. As in the lines described above, neurodegeneration was identified only in the P301L tau line but not in the wildtype tau line. In primary cultures, neurons expressing P301L tau showed tau in dendritic spines more frequently and had greater reductions of miniature excitatory postsynaptic potentials (mEPSCs) and dendritic GluR1, GluR2/3 and NR1 levels than neurons expressing wildtype tau¹⁵⁸. Tau phosphorylation was required for tau to enter into dendritic spines and to impair mEPSCs in transfected primary rat neurons¹⁵⁸. Consistent with these synaptic alterations, a line of mice expressing tau with G272V and P301L mutations had impaired NMDA receptor function and phosphorylation, and NR2B mislocalized into Sarkosyl-insoluble tau aggregates¹⁵⁹.

In slice cultures, wildtype human 3R0N tau and R406W human 4R2N tau each enhanced A β -induced neuronal cell death in the hippocampal CA3 region, whereas P301L human 4R2N tau did not¹⁶⁰. A 3R0N tau mutant that prevents phosphorylation and a 3R0N tau mutant that mimics hyperphosphorylation showed no synergistic neurotoxic effect with A β , implying that dynamic tau phosphorylation may be required for the enhancement of A β toxicity by tau¹⁶⁰. These results are consistent with findings indicating that tau requires phosphorylation to enter the dendritic spine in order to affect synaptic function¹⁵⁸ and that A β oligomers acutely increase phosphorylation and mislocalization of wildtype tau into dendritic spines¹¹⁴.

It may be that P301L tau is already phosphorylated and present in dendritic spines, and therefore no further toxicity is seen in the presence of A β oligomers. Interestingly, the adverse effects of wildtype tau were dependent on the activity of both NMDAR and GSK3 β , whereas the effects of R406W tau were dependent only on NMDAR activity, suggesting partly distinct mechanisms of toxicity¹⁶⁰. These results imply that AD-relevant pathogenic mechanisms and therapeutic interventions might be missed in FTLN mutant transgenic mice due to the overriding effect of the FTLN mutations.

Treatments targeting tau

Treatments targeting various aspects of tau biology are under intense investigation. Inhibitors of tau phosphorylation and aggregation and microtubule stabilizers are already in clinical trials for people with MCI, AD, or FTLD (for more information see <http://www.alzforum.org/therapeutics>), while tau reduction strategies are still in preclinical stages of development. Tau imaging compounds are currently undergoing testing in tau transgenic mice and in humans¹⁶¹, which should greatly facilitate the assessment of target engagement by tau therapies in clinical trials. As we learn more about how tau expression is regulated and about tau's involvement in cell signaling and cytoskeletal organization, additional approaches are likely to emerge.

Tau phosphorylation inhibitors

The function and aggregation of tau appear to be regulated by phosphorylation, as reviewed above. Of the numerous tau kinases implicated in AD pathogenesis, the most widely studied are GSK-3 β , CDK5, MARK, and MAPK^{38,162}. Lithium, which inhibits GSK-3 β and is used to treat bipolar disorder, improved behavior and reduced tau pathology in transgenic mice overexpressing P301L human 4R0N tau (JNPL3 model)¹⁶³. However, because lithium has multiple targets, the rescue observed may not have been solely due to a reduction in GSK3 β activity. Lithium also has a narrow safety margin¹⁶⁴, and reduction of GSK-3 β impairs NMDAR-mediated long-term depression¹⁶⁵ and memory consolidation¹⁶⁶, raising concerns about potential side effects of GSK-3 β inhibitors. In a similar vein, CDK5 inhibitors prevent A β -induced hyperphosphorylation of tau and cell death in culture^{167,168}, but CDK5 is essential for multiple cell signaling pathways and adult neurogenesis, limiting its appeal as a tau-targeting therapy for AD. However, CDK5 and p25, a truncated form of the CDK5 subunit p35, can promote neurodegeneration through mechanisms that are independent of tau phosphorylation, involving inhibition of histone deacetylase 1 (HDAC1) and aberrant expression cell cycle genes¹⁶⁹, raising possibilities for additional therapeutic intervention.

Tau aggregation inhibitors

In vitro, tau aggregation is induced by polyanionic compounds such as RNA¹⁷⁰, heparin¹⁷¹⁻¹⁷³ and lipid micelles¹⁷⁴. Many of the drugs that block the aggregation of tau also block the pathological aggregation of other proteins under cell-free conditions, including A β and α -synuclein¹⁷⁵, suggesting that they might be of benefit in diverse proteinopathies. Some tau aggregation inhibitors are effective in Neuro2A cell lines overexpressing a 4R tau microtubule repeat domain fragment with a K280 deletion, which promotes its aggregation¹⁷⁶. In human AD patients, the phenothiazine methylene blue showed some promise for slowing disease progression in a phase II clinical trial conducted for 1 year¹⁷⁷. Methylene blue was originally thought to inhibit tau–tau interactions¹⁷⁸, but it may also reduce soluble tau through other mechanisms¹³¹ as it is known to have many targets¹⁷⁹. Phase III trials with a newer formulation of methylene blue (LMTX) are planned¹⁸⁰.

The immunosuppressant FK506 reduces microgliosis and tau aggregation in transgenic mice overexpressing P301S human 4R1N tau under the mouse prion promoter (PS19 model)¹⁸¹. Since FK506 affects diverse signaling pathways in many cell types, it may act directly on neurons or influence the neuronal environment by modulating microglial activation. Inhibition of tau aggregation may also be mediated by direct binding of tau to the FK506 binding protein 52¹⁸² or by inhibiting FK506 binding protein 51 (FKBP51), which promotes the formation of tau oligomers in conjunction with heat-shock protein 90¹⁸³. Notably, tau levels are reduced in FKBP51 knockout mice¹⁸³, so targeting FKBP51 may also contribute to the reduction of total tau.

As discussed above, it is far from certain that filamentous tau is actually toxic. Indeed, it is not known which tau assembly or conformation is responsible for tau-dependent neuronal dysfunction and degeneration. Not surprisingly, it is equally uncertain whether the abundance of this entity is lowered by any of the available tau aggregation blockers. In fact, some tau aggregation inhibitors enhance the formation of potentially toxic tau oligomers¹⁸⁴. This scenario is reminiscent of the current state of anti-A β treatment, where it is also unclear whether any of the anti-A β strategies that have undergone or are

currently in clinical trials significantly reduce the abundance of A β oligomers in human brain tissues, which are suspected to be the main mediators of A β -induced neuronal dysfunction¹⁸⁵⁻¹⁸⁸.

Reduction of overall tau levels

In mice, genetic reduction of tau is well tolerated, increases resistance to chemically induced seizures, and markedly diminishes A β - and ApoE-induced neuronal and cognitive impairments *in vivo*^{71,83,98}. Similar tau reduction was achieved through intraventricular infusion of ASOs in adult mice, which provided resistance against PTZ-induced seizures without impairing memory in the Morris water maze¹¹¹. Alternatively, tau levels could be reduced indirectly by targeting molecules that regulate the expression or clearance of tau.

Tau is thought to be degraded *via* the ubiquitin-proteasome and lysosomal pathways. The ubiquitin ligase for tau was identified as the C-terminus of HSP70-interacting protein (CHIP)¹⁸⁹⁻¹⁹¹. Reduction of CHIP levels increased the accumulation of tau aggregates in P301L human 4R0N tau mice (JNPL3 model), and CHIP levels are reduced in AD brains¹⁹². Furthermore, as its name suggests, CHIP works in combination with heat shock proteins to regulate tau degradation¹⁹³; levels of heat shock protein 90 (Hsp90) correlate inversely with the levels of soluble tau and tau oligomers¹⁹⁴.

In AD brains, tau is hyperacetylated, which should increase its half-life²³ and decrease its microtubule binding²⁴. Because both acetylation and ubiquitination target lysine residues, acetylation of tau by the acetyltransferase p300 inhibits ubiquitination and stabilizes tau²³, but can inhibit the aggregation of tau into filaments¹⁹⁵. Acetylation by Creb binding protein (CBP) inhibits the binding of tau to microtubules and enhances tau aggregation, possibly due to acetylation of the 6 amino acid motif VQIINK (PHF6*)²⁴. This motif is critical for the formation of tau oligomers and filaments^{46,196}. While the effects of tau acetylation on aggregation may be site-specific, the combination of a tau acetylation inhibitor and a ubiquitination-proteasome enhancer might synergize to lower the level of pathogenic tau species.

Larger aggregates of tau are not likely to be accessible to the proteasome but can be degraded by the lysosomal pathway, in which autophagosomes engulf the aggregates and fuse with lysosomes. In cells overexpressing the microtubule repeat domain of tau with a deletion of K280, aggregated tau is removed by the lysosomal pathway¹⁴⁴. In slice culture, inhibition of the lysosomal pathway produces NFT-like tau deposition¹⁹⁷. The lysosomal pathway of tau degradation is also involved in Niemann-Pick type C (NPC) disease, an autosomal recessive disorder associated with neurological symptoms and NFT formation in the brain¹⁹⁸. NPC disease is caused by a loss of function of NPC1, a lysosomal trafficking protein¹⁹⁹, suggesting that tau is degraded in lysosomes and that lysosomal dysfunction leads to tau accumulation. Consistent with this notion, phosphorylated tau is increased in the brains of NPC1-deficient mice and of NPC patients²⁰⁰. However, crossbreeding of NPC1-deficient mice with tau knockout mice worsened the phenotype²⁰¹, suggesting that the role of tau in this disease is complex. The autophagic-lysosomal pathway has also been interrogated in a mouse model of tauopathy with parkinsonism overexpressing human 4R2N tau under the mouse Thy1 promoter with deletion of Parkin (PK^{-/-}/TauVLW)²⁰². Treatment of 3-month-old PK^{-/-}/TauVLW mice with trehalose, an mTOR-independent autophagy activator, for 2.5 months prevented dopaminergic neuron loss in the ventral midbrain, reduced phosphorylated tau and total tau in the striatum and limbic system, prevented brain astrogliosis and improved motor and cognitive behavior. Biochemical and electron microscopy data suggested that the protective effects of trehalose were mediated, at least in part, by autophagy activation²⁰².

Tau degradation can also be enhanced by specific activation of the immune system. Active immunization targeting phosphorylated tau reduced filamentous tau inclusions and neuronal dysfunction in transgenic mice overexpressing K257T/P301S human 4R0N tau under the rat tau promoter or P301L human 4R0N tau (JNPL3 model)^{203,204}. The mechanism by which intracellular proteins, including tau and α -synuclein, are cleared by immunization is not known but may involve lysosomal degradation²⁰⁵⁻²⁰⁷. Once antibodies enter into brain, they could be taken up by receptor-mediated endocytosis and activate autophagy²⁰⁷ or interact with tau in the extracellular matrix. Extracellular tau in cerebrospinal fluid (CSF) is

used in combination with other biomarkers to diagnose AD²⁰⁸; phosphorylated tau and total tau ratios in the CSF can also predict disease severity^{209,210}. Extracellular tau could come from the death of neurons or be released from live cells²¹¹. If there is an equilibrium between intracellular and extracellular tau, clearance of tau/antibody complexes from the extracellular space may ultimately lower intracellular tau levels^{207,212}.

Microtubule stabilizers

Microtubule disruption has been observed in several models of AD and FTL, including transgenic mice overexpressing wildtype human 0N3R tau under the mouse prion promoter (T44 model)¹⁰⁰ or P301S human 4R1N tau (PS19 model)¹⁸¹, and wildtype neuronal cultures exposed to A β oligomers^{58,114}. Some FTDP-17 tau mutations²¹³ and tau hyperphosphorylation^{214,215} reduce the binding of tau to microtubules. Although tau overexpression seems to be associated with destabilization of microtubules, it is unclear whether this phenomenon is always pathogenic and whether it results from a loss- or gain-of-function of tau. Indeed, tau is necessary for A β -induced microtubule disassembly *in vitro*⁵⁸, suggesting that tau is actually required for microtubule destabilization. A loss-of-function mechanism seems also unlikely because tau knockout mice have a rather benign phenotype, and tau reduction protects neurons from A β -induced impairments *ex vivo*^{58,65,84,88} and *in vivo*^{71,83,98}.

Despite these caveats regarding underlying mechanism, microtubule stabilizers have shown promise in preclinical and clinical trials for AD. For example, paclitaxel prevented A β -induced toxicity *in vitro*¹¹⁴ as well as axonal transport deficits and motor impairments in transgenic mice overexpressing wildtype human 0N3R tau (T44 model)¹⁰⁰. Etoposide, which has better blood–brain barrier permeability, improved microtubule density and cognition in P301S human 4R1N tau mice (PS19 model)²¹⁶. The peptide NAP stabilizes microtubules²¹⁷ and reduces tau hyperphosphorylation²¹⁸, suggesting that microtubule-stabilizing compounds can have more than one mechanism of action. While NAP showed some promise in a phase II clinical trial of amnesic mild cognitive impairment²¹⁹, no efficacy was observed in a phase III clinical trial against the tauopathy PSP²²⁰ suggesting that it may not function in pure tauopathies.

Conclusions regarding tau

While tau has long been implicated in neurodegenerative conditions, its functions in the adult brain and the precise mechanisms by which it contributes to neuronal dysfunction and degeneration in these disorders remain to be elucidated. A flurry of recent publications has challenged major dogmas in this field, including the notion that filamentous tau aggregates are the most pernicious forms of tau, that loss of tau function plays a major role in the pathogenesis of tauopathies, that tau enters dendritic spines only under pathological circumstances and that the adverse activities of tau aggregates are restricted to intracellular compartments. Provocative discoveries suggest that tau regulates neuronal excitability and that it is required for A β and other excitotoxins to cause neuronal deficits, aberrant network activity and cognitive decline. Indeed, tau has ‘graduated’ from a putative microtubule stabilizer to a multifunctional protein with many interacting signaling networks and to a master regulator of the intracellular trafficking of organelles and molecules involved in synaptic functions at the pre- and postsynaptic level. The hunt has also been intensified for the most pathogenic forms of tau, some of which have been traced into dendritic spines, and more has been learned about the complex posttranslational modification of tau, particularly acetylation, which appears to regulate the ubiquitination, turnover and aggregation of tau. These and other findings are providing critical guidance in the development of better treatments for tauopathies aimed at tau itself, tau regulators or factors mediating its putative functions. Identifying the functions and precise roles of tau in neurodegenerative disorders will likely require the analysis of conditional knockout models and the clinical evaluation of pertinent drugs with well-defined modes of action.

Part II: α -Synuclein, a pre-synaptic protein involved in disease

Much like tau, α -synuclein (SYN) is an intrinsically disordered protein which becomes hyperphosphorylated, mislocalizes and aggregates in neurodegenerative disease. Neuronal aggregates of SYN, called Lewy bodies, are the primary pathologic feature of Parkinson’s disease (PD), Parkinson’s disease with dementia (PDD) and dementia with Lewy bodies (DLB), a closely related set of diseases differentiated by the relative onset of motor and cognitive symptoms and Lewy body distribution. Point mutations and increased SYN gene dosage cause familial Lewy body diseases²²¹⁻²³⁰. Though this review

focuses on the pathophysiology of neuronal SYN, glial aggregates of SYN are associated with multiple-system atrophy (MSA)^{231,232}.

SYN is a small, 140 amino acid protein which primarily localizes to the neuronal pre-synapse under physiologic conditions. The structure of SYN can be divided into three regions: the N-terminal region, the hydrophobic NAC peptide and the C-terminal acidic region^{233,234}. In solution, SYN is an intrinsically disordered protein; however, the combined N-terminal and NAC regions form an amphipathic helix when bound to anionic membranes, or two helices on highly curved anionic membranes²³⁵⁻²³⁷. There is some evidence that SYN forms a physiologic α -helical tetramer *in vivo*²³⁸, distinct from the β -sheet oligomers found in disease conditions, however this result is still highly controversial²³⁹.

All 5 SYN mutations thought to cause PD are in the N-terminal region, but they appear to have varying effects on SYN structure^{221,222,226-228,230,240}. The A30P SYN mutation disrupts α -helix formation, thereby reducing membrane binding²⁴¹. The A53T SYN mutation allows for helix formation, but extends the β -sheet-forming region of the NAC which can facilitate aggregation²⁴¹. E46K, H50Q and G51D mutations all preserve α -helix formation, but E46K and H50Q both facilitate aggregation²⁴², while G51D may not affect aggregation²⁴⁰.

SYN function and aggregation can be also modified by post-translational modifications. Phosphorylation of the C-terminal region changes its binding affinity for synaptic, cytoskeletal and mitochondrial proteins²⁴³. SYN aggregation may be inhibited by O-GlcNAcylation in the NAC region^{244,245} and enhanced by C-terminal truncation²⁴⁶. While some C-terminal cleavage is present in normal brain, Lewy body pathology is associated with additional C-terminal cleavage products²⁴⁷ which may contribute to Lewy body aggregation. SYN in Lewy bodies also tends to be highly modified by phosphorylation and ubiquitination²⁴⁷⁻²⁴⁹, but the exact role of these modifications in pathology is unclear²⁵⁰.

Evidence for multiple functions of SYN

Much like tau, genetic ablation of SYN only produces subtle phenotypes. SYN knockout mice, generated from targeted gene knockout or spontaneous gene deletion, are viable and have normal fertility, brain anatomy and longevity^{251,252}. The spontaneous deletion model of SYN, Harlan C57Bl/6S mice, has

been widely used to study the effects of SYN knockout and to ablate endogenous SYN in transgenic models²⁵²⁻²⁵⁴. However, the exact range of this small deletion²⁵² and any other genes affected by it are unknown, so studies using this model should be interpreted cautiously.

Due to the subtle SYN knockout phenotype, researchers often study mice lacking other synuclein family members. β - and γ -synuclein share a high sequence similarity to SYN and have many of the same functions^{255,256}, so researchers often use double- or triple-synuclein knockout (DKO or TKO, respectively) mice to investigate the physiologic roles of synuclein proteins. TKO mice have a more pronounced phenotype than SYN knockout mice, with motor impairments and mortality around 1 year of age²⁵⁷.

SYN modulates synaptic vesicles

Although the precise physiologic functions of SYN are still highly debated, most evidence points to a role in the regulation of synaptic vesicle dynamics. SYN was initially identified through its association with synaptic vesicles²³³, which may be mediated through an affinity for highly curved membranes^{235,258}. However, much like other proteins which sense highly curved membranes, this affinity involves more than passive membrane binding. All three synuclein family members can induce membrane curvature at physiologically relevant concentrations, which is inhibited in the membrane-binding-defective A30P SYN mutant²⁵⁶. As endophilin A1, an endocytic membrane bending protein, is increased in TKO models and reduced by transgenic SYN expression in the TKO model, the authors suggest that SYN may have a role in endocytosis²⁵⁶. Exocytosis regulates the dispersion of both SYN and endophilin 1A from the synapse, suggesting that the two proteins share some regulatory mechanisms, and this regulation requires intact membrane binding^{259,260}. However, most evidence indicates that SYN acts as a negative regulator of exocytosis²⁶¹ without altering the rate of endocytosis or exocytosis²⁶². While the molecular mechanisms of this exocytic regulation are still debated, it relies on membrane binding²⁶² and may involve soluble NSF attachment protein receptor (SNARE) proteins.

Analysis of a novel model of neurodegeneration led to evidence that SYN regulates SNARE assembly. Knockout of cysteine string protein α (CSP α), a SNARE chaperone and regulator of exocytosis²⁶³, causes synaptic degeneration, motor impairment and premature mortality. SYN overexpression partially

ameliorates these phenotypes and an α/β -DKO mouse worsened them, suggesting SYN and CSP α have some functional redundancy²⁶⁴. On a molecular level, SYN overexpression rescued SNARE complex assembly in CSP α knockout mice without rescuing the loss of the SNARE protein SNAP-25²⁶⁴, leading to the discovery that SYN increases the formation of SNARE complexes²⁵⁷. This SNARE regulation requires C-terminal binding to synaptobrevin-2, a SNARE protein, and N-terminal membrane binding²⁵⁷. The physiologic significance of SNARE regulation by SYN remains unclear; one TKO model showed reduced SNARE complex assembly²⁵⁷, however, a second TKO model could not confirm this reduction²⁵⁵.

SYN binding to membranes and SNARE proteins may negatively regulate exocytosis by altering vesicle clustering. Cell-free studies indicate that SYN clusters synaptobrevin vesicle-SNARE (v-SNARE) vesicles together through membrane and synaptobrevin binding²⁶⁵. *In vivo* this activity could alter vesicle density and the availability of synaptic vesicles for release. In the CA1 of SYN transgenic mice, vesicle density was shifted away from the pre-synaptic active zone and pre-synaptic release was decreased²⁶². A second SYN transgenic mouse, with human SYN expression directed by a bacterial artificial chromosome on a mouse SYN knockout background (SYN BAC), showed increased vesicle clustering and decreased dopamine release at striatal synapses²⁶⁶. It is possible that vesicle clustering by SYN differentiates the resting or reserve pool of vesicles from the readily-releasable pool of synaptic vesicles (RRP). SYN transgenic mice have a smaller RRP without a change in synaptic vesicle number²⁶², implying a larger number of vesicles in the reserve pool, while SYN knockout mice have a smaller reserve pool and fewer synaptic vesicles²⁶⁷. Notably, SYN monomers don't alter vesicle fusion in cell-free conditions^{265,268}, confirming that monomeric SYN does not interfere with the dynamics of SNARE function.

Synuclein family proteins seem to play a specific role in the release of striatal dopamine. Though the magnitude of the effects on dopamine release vary depending on the strain background and knockout used, studies of SYN knockout and TKO mice have shown decreased levels of striatal dopamine and a blunted response to amphetamine, which enhances dopamine release^{251,255}. This regulation was specific to striatal synapses because the dopamine content of the ventral tegmental area was unaffected in the TKO model²⁵⁵. Both the biochemical and behavioral phenotypes could result from enhanced basal release of dopamine in the striatum, which would deplete the synaptic stores of dopamine²⁵¹. TKO mice showed enhanced release

of dopamine after a single stimulus²⁵⁵, while SYN knockout mice show enhanced synaptic release after a paired pulse stimulus²⁵¹. The mechanism behind the specific modulation of striatal dopaminergic terminals by synuclein proteins remains controversial. While several studies point to the negative regulation of the RRP by SYN^{251,253,262}, altered vesicle clustering could not be detected at striatal synapses in TKO mice²⁵⁵. However, the authors acknowledge that striatal synapses do not physically segregate the RRP and reserve pool of synaptic vesicles like hippocampal synapses²⁵⁵, so this subtle ultrastructural phenotype may be difficult to detect in a knockout model at striatal synapses. Altered vesicle clustering has been observed at striatal dopaminergic synapses in the SYN BAC model²⁶⁶.

Other functions of SYN

Using unbiased screening methods, SYN was identified as an inhibitor of phospholipase D2 (PLD2)²⁶⁹. PLD2 is a constitutively active enzyme which cleaves phosphatidylcholine into phosphatidic acid and choline. In cell-free conditions, all three synuclein proteins inhibit PLD2^{269,270}. Inhibition by SYN requires N-terminal α -helical structure, is prevented by C-terminal phosphorylation, and is enhanced by the A53T SYN mutation²⁷⁰. Toxicity from overexpression of PLD2 in the substantia nigra of rats is prevented by co-overexpression of SYN²⁷¹, however, endogenous PLD2 inhibition by SYN has not been investigated.

Post-mortem inhibition of PLD2 may confound the reported decrease in cortical acetylcholine levels in a SYN transgenic mouse²⁷². After decapitation, acetylcholine was measured indirectly by an assay which converts acetylcholine to choline prior to generating a fluorescent indicator (A12217, Invitrogen). Our lab achieved a similar decrease in fluorescence using the same assay in the same line of mice after cervical dislocation, however, this was due to a change in the level of choline (data not shown). Acetylcholine was not quantifiable in our assay. Based on the literature, acetylcholine levels fall rapidly after death by decapitation or cervical dislocation, while choline levels rise due to enzymatic production²⁷³. We hypothesize that overexpressed SYN may inhibit this *post-mortem* production of choline, possibly through PLD2 inhibition.

The pathologic interactions of SYN and mitochondria are well known, however, their physiologic interactions are relatively unexplored. Under normal conditions a portion of SYN binds to cardiolipin²⁷⁴, a

mitochondria-specific lipid, and localizes to mitochondria²⁷⁵. C57Bl/6S mice, with a spontaneous deletion of SYN, have reduced levels of cardiolipin and impaired activity of the electron transport chain specifically when measured through complex I/III linked activity²⁷⁶. Linked complex I/III activity impairment was confirmed in cultures of primary fetal midbrain neurons treated with SYN shRNA²⁷⁵. However, the molecular function of SYN on mitochondria and significance of these mitochondrial impairments *in vivo* remains unclear.

Mechanisms by which SYN contributes to disease

As the primary protein aggregate in PD, PDD, DLB and MSA, SYN dysfunction is very likely to contribute to sporadic human neurodegeneration. Furthermore, gene multiplication and point mutations in the N-terminal region of SYN cause familial Lewy body disease^{221-228,230,240}. As with tau, SYN pathogenesis may utilize several mechanisms, including loss- and gain-of-function. It is also possible that physiologic SYN functions enable disease pathogenesis after specific neuronal insults.

Loss of function

SYN is unlikely to cause neurodegenerative disease through a complete loss of function mechanism. Though SYN knockout mice have not been as thoroughly characterized as tau knockout lines, they have normal viability, fertility and brain anatomy^{251,252}. Alterations specifically in striatal dopaminergic terminals in SYN knockout mice do show an important role for SYN in their function, however, the functional redundancy of other synuclein family members reduces the magnitude of the SYN knockout phenotype²⁵⁵. Conversely, overexpression of even low levels of SYN are sufficient to alter neuronal neurotransmitter release in multiple neuronal populations²⁶² and higher levels of wildtype or mutant SYN can impair mouse behavior and cause premature mortality^{272,277}.

The A30P mutation causes a partial loss of SYN function. The normal pre-synaptic localization of SYN and its functions clustering v-SNARE vesicles and reducing neuronal exocytosis are all inhibited by the A30P SYN mutation^{259,262,265}. The inhibition of exocytosis by SYN was preserved when transfecting the A30P mutant into PC12 cells²⁷⁸, but not when acutely transfected into primary cultured neurons²⁶². However, the A30P mutation retains normal binding to synaptobrevin²⁵⁷, and enhances the nuclear

localization²⁷⁹ and oligomerization²⁴¹ of SYN, all of which may contribute to the *in vivo* toxicity of A30P SYN.

SYN functions enabling pathogenesis

SYN function is required for the toxicity of some mitochondrial toxins, which are used to acutely model dopaminergic cell death in PD. SYN knockout mice are resistant to toxicity from 1-methyl-4-phenyl-1,2,3,6-tetrahydropyridine (MPTP), 3-nitropropionic acid (3-NP) and malonate, but not rotenone²⁸⁰⁻²⁸². In the case of acute 3-NP and MPTP administration, the damage inflicted is SYN gene-dose dependent²⁸². Though the mechanism of this resistance remains obscure, proposed mechanisms include an increase of the neuroprotective β -synuclein²⁸³ or reduced dopamine storage in the striatum of SYN knockout mice^{280,282}, or the reduction of abnormal SYN species which inhibit ubiquitin-proteasomal degradation²⁸¹ and generate radical oxygen species²⁸². The neuroprotective effects of SYN ablation appear specific for dopaminergic nigrostriatal neurons, in agreement with a specific role for SYN in this neuronal population, because SYN knockout mice show no resistance to the noradrenergic/serotonergic toxin NH₂-MPTP²⁸³.

SYN is required for the toxicity of leucine-rich repeat kinase 2 (LRRK2) in primary neuronal culture. The G2019S LRRK2 mutation in iPS-derived neurons or overexpression of LRRK2 in primary rat cortical cell culture increases SYN levels and causes SYN-dependent cell death²⁸⁴. Part of this protective effect was mediated by lower LRRK2 levels in TKO neurons and neurons treated with SYN shRNA, however, reduced LRRK2 expression did not explain all of the protective effect conferred by SYN reduction²⁸⁴. The authors speculate that LRRK2 and SYN functions may converge on a single toxic pathway such as disruption of protein degradation²⁸⁴.

Gain of function

Abnormal nuclear localization of SYN can result in toxicity. While a portion of SYN localizes to the nucleus under normal circumstances²³³, oxidative stress and A30P and A53T mutations in cell culture, or paraquat treatment of mice can induce higher nuclear localization of SYN^{279,285-287}. Nuclear SYN was associated with reduced histone H3 acetylation²⁷⁹ and reduced transcription of monoamine synthetic

enzymes²⁸⁷ and peroxisome proliferator-activated receptor gamma coactivator 1 α (PGC1 α)-driven genes²⁸⁵. In turn, impairment of PGC1 α -mediated transcription was associated with altered mitochondrial structure, impaired mitochondrial complex I activity and cell death²⁸⁵. Inhibition of histone deacetylases or adding a SYN nuclear export signal prevented SYN toxicity in cell culture and in transgenic *Drosophila*²⁷⁹.

SYN aggregation is likely to be toxic in Lewy body disease. A53T, E46K and H50Q SYN all aggregate more rapidly than wildtype SYN^{241,242,288,289}. Interestingly, SYN aggregation may require binding to synaptobrevin to induce toxicity. A study examining the relationship between SYN function and toxicity found that mutations which increased aggregation and bound synaptobrevin also induced motor deficits and loss of dopaminergic neurons when virally expressed in the substantia nigra of mice²⁹⁰. The effect of the mutations on membrane binding, pre-synaptic localization and SNARE assembly did not account for *in vivo* toxicity²⁹⁰. C-terminal truncation mutants, which enhance aggregation but do not bind synaptobrevin, produced a less reliable correlation between aggregation and toxicity; only one of four aggregating C-terminal truncation constructs showed toxicity *in vivo*²⁹⁰. SNARE proteins are redistributed into SYN aggregates in A30P mice, transgenic mice expressing a partial SYN C-terminal truncation and PD patients²⁵⁴.

SYN oligomers have some unique properties which may make them more toxic than larger fibrils. SYN oligomers selectively permeabilize highly curved membranes to Ca²⁺ and other small ions²⁹¹, which may interfere with synaptic transmission. Large oligomeric SYN species inhibit fusion of v-SNARE vesicles containing synaptobrevin to target-SNARE vesicles, possibly by preventing vesicle docking²⁶⁸. However, the best studied route of oligomeric SYN toxicity relates to mitochondrial impairment.

Mitochondrial impairment is a common pathogenic mechanism for many of the pathways implicated in PD (for an in-depth review of SYN and mitochondria see Nakamura, *et.al.* 2012²⁹²). Oligomeric SYN species can selectively fragment mitochondria *in vitro* and *in vivo* without affecting the structure of other organelles²⁹³. Mitochondrial fragmentation is at least partly independent of Drp1, another protein implicated in the pathogenesis of PD, and relies on membrane binding; A30P mutant SYN could not induce mitochondrial fragmentation²⁹³ and may rely on other mechanisms of toxicity. In cell culture, SYN oligomer-induced fragmentation led to impaired mitochondrial respiration and cell death²⁹³. A similar

fragmentation of mitochondria was observed after A53T SYN transfection into primary neuronal culture, which led to induction of mitophagy, loss of mitochondria and a bioenergetic defect prior to cell death²⁹⁴. The mechanism of cell death after mitochondrial impairment may relate to the induction of reactive oxygen species²⁹⁵. Other studies have confirmed that SYN inhibited mitochondrial respiration, specifically complex I inhibition, in cell culture and transgenic mice, however, SYN oligomer levels did not correlate with mitochondrial defects^{275,296}. However, the observation of oligomeric species on a denaturing gel may not reflect the actual oligomeric species *in vivo*. Increased SYN levels and decreased complex I activity were shown in mitochondria isolated from the substantia nigra of PD patients²⁷⁵, but the SYN species involved were not determined.

Mutant or aggregated SYN can also inhibit protein degradation. In PC12 and primary midbrain neuronal cell culture, chaperone-mediated autophagy (CMA) can degrade SYN through lysosome-associated membrane protein type 2A (LAMP2A) binding and translocation of SYN into lysosomes²⁹⁷. In the same PC12 culture system, A53T and A30P SYN bind tightly to LAMP2A but inhibit CMA²⁹⁷. This impairment in degradation may promote SYN aggregation, which in turn impairs 26S proteasomal degradation²⁹⁸. The resulting accumulation of misfolded and damaged proteins could lead to cell dysfunction and death²⁹⁸.

Good evidence exists in humans and experimental models for the pathologic spread of SYN between neurons. The stereotyped progression of SYN pathology in many PD cases²⁹⁹ and the acquisition of Lewy body pathology by fetal neurons grafted into the substantia nigra of PD patients³⁰⁰ generated the hypothesis that SYN pathology could spread, prion-like, between neurons and seed aggregation in recipient neurons. Follow-up *in vivo* experiments supported this hypothesis. A prion-like spread of SYN pathology across multiple brain regions could be induced by injection of synthetic SYN fibrils into the striatum of a wildtype mouse³⁰¹. Like prion diseases, the spread of SYN pathology in the injected mouse relied on the presence of endogenous SYN³⁰¹. Mechanistic studies have implicated multiple parts of the endosomal-lysosomal degradation pathways in SYN release and uptake. SYN monomers and aggregates can be released from vesicles in SH-SY5Y cells in culture independently of the classical endoplasmic reticulum/Golgi secretion pathway³⁰². This release is increased by blocking lysosomal degradation or autophagy³⁰³⁻³⁰⁵, providing a

potential mechanism by which A30P and A53T SYN mutants may increase SYN release from neurons in disease conditions²⁹⁷. SYN monomers and aggregates have several potential fates once outside the cell. Free floating SYN monomers enter recipient cells by diffusion, while free floating SYN oligomers and fibrils are endocytosed and usually degraded in lysosomes³⁰⁶. Exosome-associated SYN oligomers are readily taken up by recipient neurons and are more toxic to H4 cells in culture than free floating oligomers³⁰⁵. Aggregates of G51D SYN are more toxic than wildtype SYN aggregated when applied to cells in culture²⁴⁰, though the mechanism is not known.

Treatments targeting SYN

Treatments targeting SYN follow similar strategies as treatments targeting tau, although there are fewer potential therapies in clinical trials. Most preclinical studies target SYN phosphorylation, aggregation or reduction of SYN levels, with a few studies focusing on the inhibition of SYN functions involved in disease or their downstream effects. Reducing the reactive oxygen species created downstream of SYN is an active area of preclinical investigation and one drug, phenylbutyrate, has progressed to Phase I clinical trials³⁰⁷.

SYN phosphorylation inhibitors

The primary modification of SYN in Lewy bodies is phosphorylation of S129^{247,249}. While the effects of this particular SYN phosphorylation are still controversial²⁵⁰, it may promote SYN aggregation²⁴⁹. Recently, PP2A was identified as the main enzyme responsible for dephosphorylation of SYN at S129³⁰⁸ which led to PP2A activation as a therapeutic target for PD. FDA-approved drugs metformin and rapamycin activate PP2A through inhibition of mTOR and were shown to reduce pS129 SYN in cell culture and in wildtype mice³⁰⁹.

Methylation of PP2A activates its enzymatic activity and reduces levels of SYN phosphorylation at S129³⁰⁸. A natural product library screened for inhibition of PP2A demethylation yielded eicosanoyl-5-hydroxytryptamide (EHT), derived from coffee extracts, which decreased demethylated-PP2A levels in primary neuronal culture and in mice³⁰⁸. In SYN transgenic mice, EHT treatment lowered levels of pS129 SYN, reduced inflammation, restored neuronal cfos in the dentate gyrus and improved motor performance

on the Rota rod test³⁰⁸. It should be noted, however, that the reported toxicity of S129 phosphorylated SYN varies between models²⁵⁰ and that polo-like kinase 2 expression, which reduces dopaminergic cell loss in a rat AAV SYN model, requires phosphorylation of S129 to target SYN for autophagic degradation²⁵⁰.

SYN aggregation inhibitors

Generally speaking, drug screening for chemical inhibitors of SYN aggregation has been hampered by the long incubation time for SYN aggregate formation *in vitro*. Many of the aggregation inhibitors tested against SYN aggregation have been selected due to prior efficacy against A β or prion protein aggregation and oligomer formation³¹⁰⁻³¹³. Reducing SYN aggregates using these broadly active aggregation inhibitors in an A53T SYN *drosophila* and an A30P SYN transgenic mouse improved performance in motor tasks^{310,312}. In SYN transgenic zebrafish embryos, inhibition of SYN aggregation increased SYN degradation by the proteasome and improved survival³¹³.

Recently, a technique called protein misfolding cyclic amplification, originally developed for prion aggregation, was modified to enhance the formation of aggregates from SYN without requiring high levels of recombinant protein³¹¹. This assay formed proteinase K-resistant beta sheet aggregates of varying lengths within 12 hours, as measured by thioflavin T fluorescence, whereas normal aggregation conditions at the same SYN concentration could not reach the same aggregation levels within 6 days³¹¹. This assay should greatly facilitate future screens for SYN-specific aggregation inhibitors.

SYN aggregation can also be inhibited by expression of β -synuclein³¹⁴. A double transgenic mouse model expressing SYN and β -synuclein showed fewer SYN aggregates, improved synaptic density and improved motor performance compared to singly transgenic SYN mice³¹⁴.

Reducing SYN levels

Improving clearance of SYN by autophagy and lysosomal degradation is another promising therapeutic strategy. Increasing autophagic degradation of SYN using a variety of mechanisms protects dopaminergic neurons in human neuronal culture and transgenic SYN models, though the species of SYN reduced depend on the methods used³¹⁵⁻³¹⁷. Reduction of a single SYN oligomer effectively reduced toxicity in cultured

human mesencephalic neurons when autophagy was induced with trifluoperazine³¹⁷, reinforcing the importance of SYN oligomers in neuronal toxicity.

Increasing the activity of the ubiquitin ligase Nedd4 reduces SYN levels and toxicity in cell culture and animal models^{318,319}. Overexpression of Nedd4 can reduce SYN levels and dopaminergic cell death in *drosophila* and rat AAV-SYN injection models of PD³¹⁸. Both Nedd4 overexpression and treatment with NBA2, a small molecule activator of the Nedd4 pathway, prevented nitrosative stress and ER dysfunction in A53T SYN iPS neurons³¹⁹.

SYN degradation can also be enhanced through increasing Hsp70 and CHIP activity. Chemically increasing Hsp70 expression using carbenoxolone, 115-7c or mannitol decreases SYN aggregation in cell culture and in mice^{320,321}. While initially mannitol was thought to act through inhibiting SYN aggregation, treatment of SYN transgenic mice with mannitol up-regulates Hsp70 and decreases levels of soluble SYN monomers³²¹. Overexpression of the Hsp70 interacting protein CHIP reduces SYN monomer and aggregate levels in H4 neuroglioma cell culture³²².

Active immunization also reduces abnormal SYN species. Immunization with recombinant SYN reduced SYN oligomers in brain and increased synaptic density³²³. However, further studies raised the concern that a T-cell response to active immunization, in this case nitrosylated SYN, may worsen dopaminergic cell loss during oxidative stress³²⁴. Immunization with a SYN AFFITOPE[®], a short peptide which mimics the SYN sequence, generates anti-SYN antibodies while avoiding a T cell immune response³²⁵. AFFITOPE[®] immunization of two lines of transgenic mice reduced SYN oligomers, and improved cognition in PDGF-SYN mice and motor impairments in Thy1-SYN mice³²⁵. Vaccination also reduced neuroinflammation and neurodegeneration while increasing anti-inflammatory cytokines in PDGF-SYN mice³²⁵.

Reducing SYN function in disease

Reactive oxygen species generated by mitochondrial malfunction are thought to play a central role in dopaminergic cell death in PD. Overexpression of DJ1, another protein implicated in familial PD, reduced A53T oligomerization and toxicity in cell culture and prevented the generation of reactive oxygen species

during oxidative stress³²⁶. Increasing DJ1 levels by treatment with phenylbutyrate, a histone deacetylase inhibitor, prevented neuronal loss in mice treated with MPTP and decreased SYN aggregation while improving motor function in a SYN transgenic mouse³²⁷. However, the study may be confounded by the use of an artificial Y39C mutation to enhance SYN aggregation through disulfide bond formation³²⁷ because increased glutathione levels from DJ1 induction may reduce the artificial SYN disulfide bonds³²⁶. Phenylbutyrate has progressed to phase I clinical trials to assess the effects of treatment on SYN levels in the blood of PD patients³⁰⁷.

Direct stabilization of a partially folded native state of SYN by small molecule binding can modulate SYN functions required for pathogenesis. An *in silico* screen for small molecules that bound transiently folded SYN monomers uncovered ELN484228, a small molecule which inhibited some functions and toxicity of SYN without affecting SYN aggregation³²⁸. In a phagocytosis assay, which mimics the effects of SYN on vesicle dynamics, ELN484228 prevented the localization of SYN to phagocytic sites and SYN-induced phagocytic impairment³²⁸. In primary neurons, ELN484228 reduced synaptic localization of SYN and reduced cell death and neurite retraction after transduction with A53T SYN³²⁸. Though this small molecule has yet to be tested in animal models, the use of small molecule structure modulators is a promising strategy for reducing SYN functions required for disease.

Conclusions regarding SYN

The relatively recent discovery of SYN as a major pathogenic protein in PD has been met with a huge effort by researchers to uncover the normal and pathogenic functions of SYN. While much of this research has focused on the pathological interaction between SYN and mitochondria, exciting new evidence has accumulated for the regulation of vesicle dynamics by SYN. Other intriguing experiments demonstrate the regulated release of cytosolic SYN into the extracellular space and how that process may become dysregulated in disease conditions, possibly contributing to the prion-like spread of SYN pathology. These and other findings may provide critical guidance in the development of better treatments aimed at reducing abnormal SYN function in synucleinopathies.

Part III: Pathologic interactions between SYN, tau and A β

SYN was first identified in human disease not as the primary component of Lewy bodies, but as the precursor protein to the non-A β component of plaques in AD²³⁴. While the role of SYN fragments in A β plaques is still unknown, Lewy body and AD pathology frequently co-occur^{14,329} and the clinical contribution of each pathologic protein to dementia is still controversial³³⁰. Lewy body pathology occurs in up to 60% of AD cases³²⁹ and may be more common in cases with frequent neuritic plaques³³¹. Aggregation of SYN is facilitated by A β ₁₋₄₂ in cell-free conditions, in cell culture and in mice doubly transgenic for SYN and human amyloid precursor protein (hAPP), which leads to high levels of A β and plaques³³². SYN and A β synergistically worsened behavioral impairments and loss of cholinergic neurons in double transgenic mice without altering A β deposition³³².

The biochemical and clinical interactions of SYN and tau are also well established. Common variants of SYN and tau provide the strongest genetic risk factors for sporadic PD^{333,334} and the two proteins have been shown to co-aggregate in Lewy bodies³³⁵⁻³³⁷. This co-aggregation may be mediated by a physical interaction between the two proteins, which enhances the aggregation of both proteins in cell-free conditions and *in vivo*^{277,338,339}. Notably, tau aggregates are induced only by specific strains of SYN aggregates³³⁹, which may account for the somewhat sparse co-localization and varied aggregation patterns of tau in Lewy bodies in human disease³⁴⁰. Despite the extensive interactions between these two proteins, the exact role of tau in Lewy body disease is unclear. In dementia cases, tau and Lewy body pathology may compete, rather than synergize, to dictate a clinical phenotype^{14,330}.

We carried out the following studies to clarify the functional interactions between A β , SYN and tau in mouse models of neurodegenerative disease (Figure 1.6). As the functional role of tau in mediating neurodegenerative disease was explored using a tau knockout mouse model, *we began by investigating the effects of reduction or ablation of endogenous tau in aged mice* (Chapter 2). For tau reduction to be used either to probe the role of tau in mediating neurodegenerative disease or as a potential therapeutic strategy, tau knockout mice should show no behavioral impairments and minimal biochemical alterations at all ages. While there was a consensus in the literature that tau reduction had no adverse effects at young ages, the effects of tau ablation in aged mice was controversial^{97,107}. Thus we compared aged mice with or without

endogenous tau reduction using behavior and biochemical measurements previously found to be altered in aged, impaired tau knockout mice¹⁰⁷.

As discussed previously, tau reduction in the hAPP J20 model prevents premature mortality and many behavioral and electrophysiologic deficits. Tau may mediate A β -induced impairments through a toxic gain of function or tau may facilitate signaling in a pathway critical for A β -induced pathology. *We investigated whether abnormal modification of tau contributes to A β -induced impairments in hAPP J20 mice* using mass spectrometry to identify and quantify post-translational modifications of tau in wildtype and hAPP mice. An alternate gain-of-function hypothesis, in which altered tau localization may contribute to impairments in hAPP J20 mice, is being explored as part of an ongoing collaboration.

Given the abnormal tau species found in PD and the extensive interactions between tau and SYN, *we tested the hypothesis that tau mediates impairments in mouse models of PD and other synucleinopathies* (Chapter 4). Tau lowering may constitute a valid therapeutic strategy for PD and DLB if tau were required for acute dopaminergic cell death or SYN-induced behavioral impairments. Conversely, tau phosphorylation and aggregation in synucleinopathies may constitute an epiphenomenon that contributes little to the pathogenesis of the disease. We explored the effects of tau reduction on motor behavior and immunohistochemistry in an acute model of dopaminergic cell death and in a transgenic model of synucleinopathy, which overexpresses human wildtype SYN in neurons.

Finally, *we determined whether SYN induced cortical neural network dysfunction in transgenic mice and compared it to neural network dysfunction in human DLB patients*. While synucleinopathies are associated with dementia and SYN aggregates, the contribution of SYN to cognitive impairment and neural network dysfunction is unknown. Cortical network dysfunction in synucleinopathies is often attributed to co-occurring AD pathology or to loss of cholinergic innervation in the cortex. We used electroencephalography and biochemical markers to examine neural network dysfunction in SYN transgenic mice and compared them to signs of neural network dysfunction in human DLB patients (Chapter 5). Uniquely, tau ablation in this study was used for its anti-epileptic properties, rather than as a mediator of neural network dysfunction. We hope through these studies to provide insight into the pathologic interactions of A β , SYN and tau in neural network dysfunction.

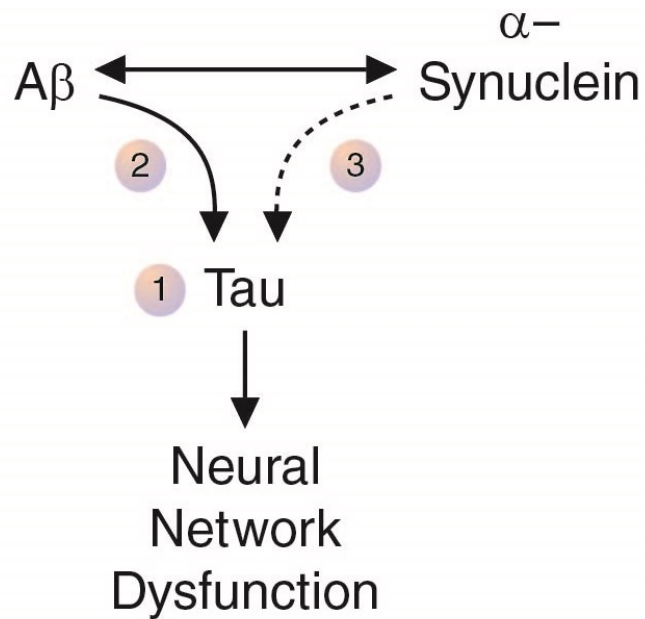


Figure 1.6 Determining the pathologic interactions between $A\beta$, SYN and tau. 1) Is reduction or ablation of endogenous tau a safe therapeutic strategy in aged mice? 2) Does $A\beta$ alter the post-translational modification state of tau in hAPP mice? 3) What types of neural network dysfunction are caused by SYN, and does tau mediate neural network dysfunction in SYN transgenic mice and acute models of PD?

Chapter 2

Age-Appropriate Cognition and Subtle Dopamine-Independent Motor Deficits in Aged Tau Knockout Mice

By

Meaghan Morris, Patricia Hamto, Anothony Adame, Nino Devidze, Eliezier Masliah and Lennart Mucke

Modified from *Neurobiol Aging* 2013; 34: 1523-1529

Used with permission

Introduction

Reduction of the microtubule-associated protein tau prevents cognitive impairments in transgenic models designed to assess the pathogenic effects of amyloid- β (A β) or apolipoprotein E4^{71,83,98,99}, proteins that – like tau itself – are thought to promote the development of Alzheimer’s disease (AD)³⁴¹. Alzheimer’s disease is the most common neurodegenerative disease. It causes prolonged suffering and disability in the elderly and takes an enormous toll on patient families and society in general³⁴². Its prevalence is expected to increase ≥ 3 -fold by 2050³⁴², threatening health care systems worldwide and underscoring the need to develop better strategies to prevent and halt this devastating illness^{341,343}.

Because tau reduction might be beneficial in AD and other “tauopathies”³⁴⁴, it is interesting to study the consequences of this intervention in experimental models, especially in regards to cognitive and motor functions. Up to 8 months of age, *Tau*^{-/-} mice had no impairments in the Morris water maze and other tests of learning, memory and exploratory behaviors^{71,83,98,107}. At 10-12 months, *Tau*^{-/-} mice also performed like wildtype *Tau*^{+/+} controls in the Morris water maze and radial arm water maze⁹⁷. However, a recent study identified Y-maze deficits in *Tau*^{-/-} mice at 12 months of age¹⁰⁷. We were unable to find information in the literature on the cognitive performance of older *Tau*^{-/-} mice.

Tau^{-/-} mice have also been reported to have motor deficits. One line of *Tau*^{-/-} mice showed deficits in rod walking and wire hang tests at 10-11 weeks of age¹⁰⁶. However, no additional behavioral analyses of this line appear to have been published since this original report. In a second, more widely used line of *Tau*^{-/-} mice⁷³, the effects of tau ablation on motor behavior in aged *Tau*^{-/-} mice are controversial. One group found no impairment on the Rota rod at 10-12 months⁹⁷, whereas another found deficits in the Rota rod, pole test and open field test at 12 months¹⁰⁷. Lei, et al. (2012) attributed the deficits they observed to a loss of dopaminergic neurons in the substantia nigra caused by iron accumulation in the brain¹⁰⁷.

To address these discrepancies and fill the knowledge gaps identified above, we assessed middle-aged and old *Tau*^{+/+}, *Tau*^{+/-} and *Tau*^{-/-} mice in a battery of behavioral tests and evaluated motor components of their central nervous system histopathologically and pharmacologically.

Results

Chronic lack of tau does not impair learning and memory in old age

Tau^{+/+}, *Tau*^{+/-}, and *Tau*^{-/-} littermates were obtained from breedings between *Tau*^{+/-} mice (C57Bl/6J). To determine whether chronic reduction (*Tau*^{+/-}) or ablation (*Tau*^{-/-}) of tau impairs learning and memory in middle-aged or old mice, we behaviorally tested two independent cohorts of mice at 11-17 or 21-22 months of age. The Morris water maze and a novel object recognition test were used to assess spatial versus non-spatial learning and memory, respectively. In the Morris water maze, tau ablation had no effect on learning and memory in 11–17-month-old mice (Figure 2.1A,B). Reduction and ablation of tau did not significantly affect learning and memory in 21–22-month-old mice either (Figure 2.1C,D). Tau ablation did not affect learning and memory in the novel object recognition test in 11–17-month-old mice (Figure 2.1E) and neither did tau reduction or ablation in 21–22-month-old mice (Figure 2.1F).

Ablation of tau and aging cause weight gain and subtle motor deficits

To determine whether chronic reduction or ablation of tau impairs motor functions in middle-aged or old mice, we assessed two cohorts of *Tau*^{+/+}, *Tau*^{+/-}, and *Tau*^{-/-} mice in several motor tests at 12-15 or 21-22 months of age. Mice of all genotypes gained weight as they aged, but *Tau*^{-/-} mice weighed more than *Tau*^{+/+} and *Tau*^{+/-} mice at 12-15 months and showed a trend in this direction at 21-22 months (Figure 2.2A). Tau genotype did not significantly alter rearing or overall activity in the open field, although both were reduced by aging (Figure 2.2B,C) and *Tau*^{-/-} mice showed a trend towards increased rearing at the older age (Figure 2.2B). Aging also reduced the latency to fall off the Rota rod, as did tau ablation (Figure 2.2D). Because fall latency in 12–15-month-old *Tau*^{-/-} mice strongly correlated with body weight at 12-15 months of age ($R^2=0.64$, $p=0.001$; Figure 2.3A), this deficit may be caused primarily by their increased weight.

At 12-15 months, *Tau*^{-/-} mice took longer to descend the pole than *Tau*^{+/+} and *Tau*^{+/-} mice, whereas at 21-22 months all groups showed comparable latencies (Figure 2.2E). In contrast to the Rota rod results, pole test performance in 12–15-month-old *Tau*^{-/-} mice did not correlate with body weight (Figure 2.3B). Tau ablation also increased the latency to cross a balance beam at 12-15 months of age (Figure 2.2F);

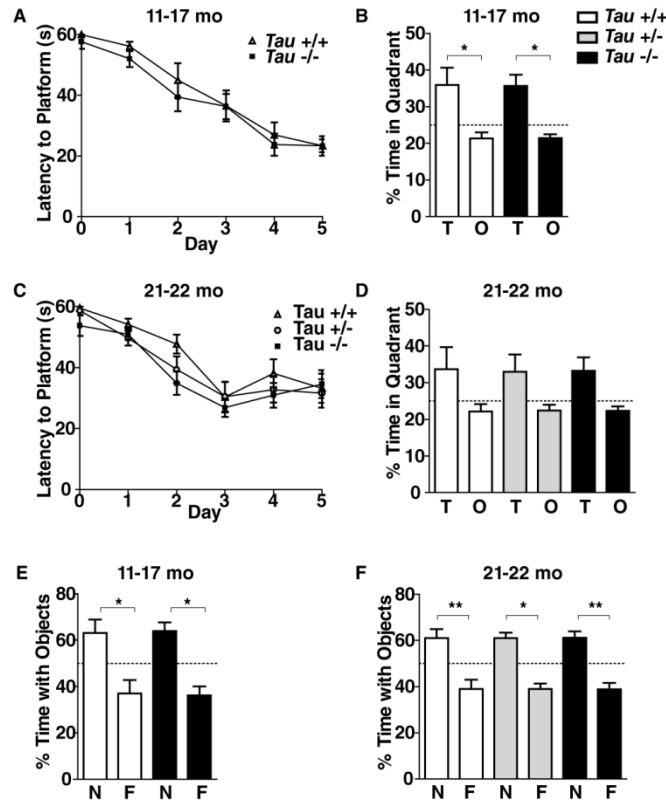


Figure 2.1. Lack of tau since early development does not impair learning and memory in middle-aged and old mice. (A-D) Independent cohorts of mice comprising the indicated genotypes were tested in the Morris water maze at 11-17 months (A, B; n=8 mice per genotype) or 21-22 months (C, D; n=11-13 mice per genotype) of age. mo, months (A, C) Learning curves during hidden-platform training. Repeated-measures ANOVA: time effect (A, $p < 0.0001$; C, $p < 0.0001$), but no genotype effect (A, $p = 0.37$; C, $p = 0.28$) or interaction (A, $p = 0.95$; C, $p = 0.70$). (B, D) Memory retention in the probe trial (platform removed) 24 h after the end of the last training trial. Repeated measures ANOVA: quadrant effect (B, $p = 0.002$; D, $p = 0.006$), but no genotype effect (B, $p = 0.98$; D, $p = 1.0$) or interaction (B, $p = 0.98$; D, $p = 1.0$). T, target quadrant; O, other quadrant. Dotted line indicates chance. (E, F) The same groups of mice were trained in a novel object recognition paradigm and tested 48h later. Repeated measures ANOVA: object effect (E, $p = 0.002$; F, $p < 0.0001$), but no genotype effect (E, $p = 0.47$; F, $p = 0.42$) or interaction (E, $p = 0.91$; F, $p = 1.0$). N, novel object; F, familiar object. * $p < 0.05$, ** $p < 0.01$ (Bonferroni post hoc test). Data are means \pm SEM.

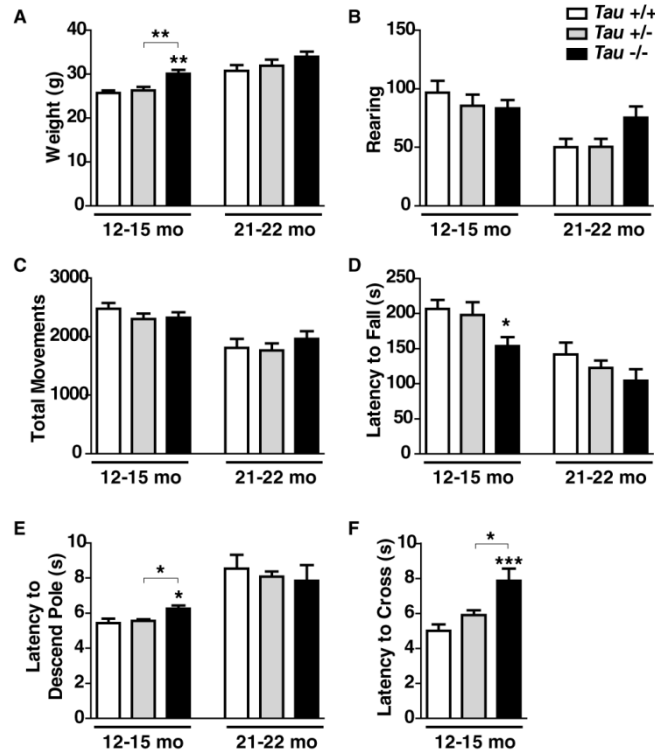


Figure 2.2. Complete, but not partial, tau reduction and aging are associated with weight gain and subtle motor deficits. Mice of the indicated genotypes were weighed and analyzed in different motor tests at 12-15 or 21-22 months of age ($n=11-14$ mice per age and genotype). (A) Body weight. Two-way ANOVA: genotype ($p=0.002$) and age ($p<0.0001$) effects but no interaction ($p=0.69$). (B, C) Rearing (B) and total movements (C) were measured in the open field test. Two-way ANOVA: age effect (B, $p<0.0001$; C, $p<0.0001$) but no genotype effect (B, $p=0.42$; C, $p=0.55$) or interaction (B, $p=0.09$; C, $p=0.44$). (D) Rota rod test. Two-way ANOVA: genotype ($p=0.01$) and age ($p<0.0001$) effects but no interaction ($p=0.67$). (E) Pole test. Two-way ANOVA: age effect ($p<0.0001$) but no genotype effect ($p=0.88$) or interaction ($p=0.31$). (F) Balance beam. * $p<0.05$, ** $p<0.01$, *** $p<0.001$ vs. age-matched wildtype mice or as indicated by brackets (Tukey test). Data are means \pm SEM.

correlation of latencies with body weight ($R^2=0.34$, $p=0.04$; Figure 2.3C) again suggested that this may not represent a genuine motor deficit. Independent of genotype, the oldest age group could not complete the balance beam test. These findings suggest that complete tau ablation causes subtle motor deficits, in part, by increasing body weight. In contrast, partial reduction of tau had no adverse effects on motor functions even at 21-22 months of age.

Motor deficits in *Tau*^{-/-} mice are probably not caused by dopaminergic dysfunction

Motor deficits in aging *Tau*^{-/-} mice have been attributed to impairments of dopaminergic neurons projecting to the striatum¹⁰⁷. We therefore assessed striatal dopamine and tyrosine hydroxylase (TH) levels of *Tau*^{+/+}, *Tau*^{+/-}, and *Tau*^{-/-} mice at 9-11, 14-20 or 25-26 months of age. We found a gene dose-dependent trend for tau reduction to lower striatal dopamine levels as mice aged (11-16% reduction, Figure 2.4A), but this trend did not reach statistical significance. Western blot analysis revealed a statistically significant decrease in TH levels only in *Tau*^{+/-} mice (16% reduction, Figure 2.4B,C) at 25-26 months. Notably, these were the same *Tau*^{+/-} mice that, compared with age-matched controls, failed to show any behavioral deficits at 21-22 months of age, suggesting that this subtle TH loss may not have a significant impact on motor function. Because others recently reported a much greater (40%) loss of striatal dopamine and TH in 12-month-old *Tau*^{-/-} mice from the same strain¹⁰⁷, we confirmed by post hoc power calculations (see Methods for details) that our analysis of striatal dopamine and TH levels was powered to detect such a change in all of the groups, if it were present. In contrast to Lei and colleagues, we did not find any iron accumulation in the hippocampus, striatum or substantia nigra of 14-month-old *Tau*^{-/-} mice (Figure 2.5).

To further test the hypothesis that motor deficits in *Tau*^{-/-} mice are caused by dopaminergic deficits, we treated an independent cohort of 12–15-month-old *Tau*^{+/+}, *Tau*^{+/-}, and *Tau*^{-/-} mice with a combination of L-DOPA and benserazide. To determine the efficacy of the treatment, we used the pole test, because it was the only test in which 12–15-month-old *Tau*^{-/-} mice showed weight-independent motor deficits (Figure 2.3B). In this second cohort, pole test latency also did not correlate with body weight in *Tau*^{-/-} mice, and acute i.p. injections of L-DOPA (20mg/kg) and benserazide (5mg/kg) did not improve latency to descend in the pole test in any of the groups (data not shown). We then treated the same mice with L-DOPA/

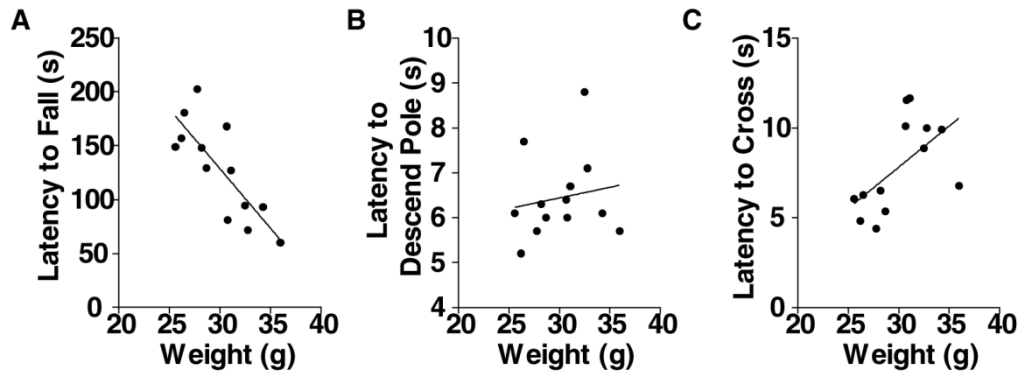


Figure 2.3. Correlation between weight and motor performance in 12–15-month-old *Tau*^{-/-} mice (n=11-14). (A) Rota rod ($R^2=0.64$, $p=0.001$ by linear regression). (B) Pole test ($R^2=0.03$, $p=0.29$). (C) Balance beam ($R^2=0.34$, $p=0.04$).

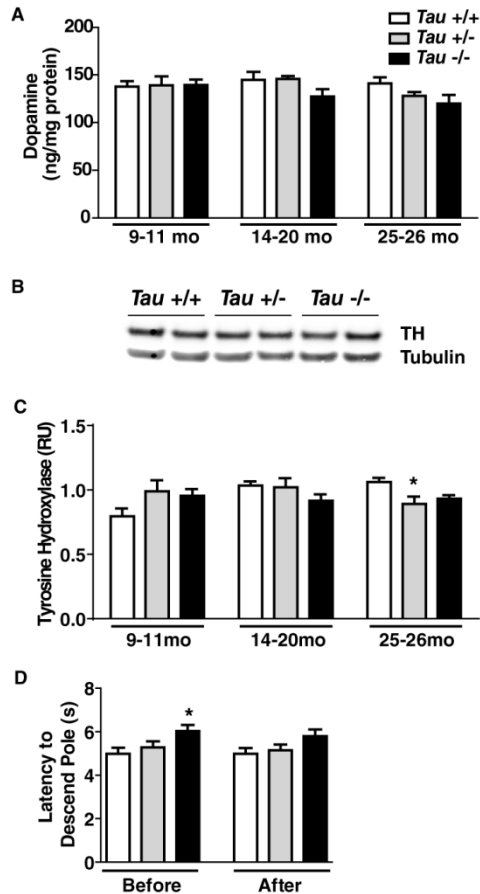


Figure 2.4. Mild dopaminergic deficits do not contribute to motor deficits in *Tau*^{-/-} mice. (A-C) Levels of dopamine (A) and tyrosine hydroxylase (TH) in the striatum (B, C) were measured in mice of the indicated genotypes at 9-11 months (n=5 per genotype), 14-20 months (n=6-7 per genotype) or 25-26 months (n=7-10 per genotype) of age. RU, relative units; TH, tyrosine hydroxylase. (A) Striatal dopamine levels determined by HPLC. Two-way ANOVA: no effects of genotype ($p=0.10$) or age ($p=0.14$) and no interaction ($p=0.40$). (B) Representative western blot showing tyrosine hydroxylase (TH) levels in the striatum of two mice per genotype (age 25-26 months). Alpha tubulin served as a loading control. (C) Quantitation of striatal tyrosine hydroxylase by western blot analysis (n=4-10 mice per genotype and age as specified above). Two-way ANOVA: interaction ($p=0.011$), but no effects of genotype ($p=0.72$) or age ($p=0.26$). Average signals in two 25-26 month wildtype mice on each blot were arbitrarily defined as 1.0 and used to normalize signals across western blots. (D) Pole test deficits in middle-aged *Tau* knockout mice are not significantly improved by chronic treatment with L-DOPA/benserazide. Mice (n=11-14 per genotype, age: 12-15 months) were assessed in the pole test before and on the 7th day of treatment with L-DOPA (200mg/L) and benserazide (50mg/L) in 0.2% ascorbic acid in their drinking water. Repeated measures two-way ANOVA: genotype effect ($p=0.014$) but no treatment effect ($p=0.97$) or interaction ($p=0.71$). * $p<0.05$ vs. age-matched wildtype mice (Bonferroni post hoc test of selected columns). Data are means \pm SEM.

benserazide dissolved in their drinking water for 7 days. On average, the mice received roughly 24 mg/kg/day of L-DOPA and 6 mg/kg/day of benserazide, which is close to the doses (20mg/kg/day L-DOPA and 5mg/kg/day benserazide) Lei et al. reported to significantly improve motor functions in 12-month-old *Tau*^{-/-} mice¹⁰⁷. On the 7th day of treatment, the mice were again tested in the pole test. Compared to *Tau*^{+/+} and *Tau*^{+/-} mice, *Tau*^{-/-} mice again took longer to descend the pole, but L-DOPA/benserazide treatment did not significantly improve their performance (Figure 2.4D). Thus, compared with age-matched *Tau*^{+/+} controls, *Tau*^{-/-} mice have only subtle dopaminergic deficits and it is unlikely that these deficits contribute significantly to the pole test deficits seen in 12–15-month-old *Tau*^{-/-} mice.

Discussion

Several new findings and conclusions emerged from this study. Middle-aged and old *Tau*^{-/-} mice had age-appropriate spatial and non-spatial learning and memory. Motor deficits were subtle in middle-aged *Tau*^{-/-} mice and undetectable in old *Tau*^{-/-} mice, most likely because deficits caused by aging became more prominent than those caused by tau ablation. Because middle-aged *Tau*^{-/-} mice had no significant reductions in striatal levels of dopamine or TH and L-DOPA/benserazide treatment did not improve their motor deficits, it is unlikely that these deficits were caused by dopaminergic impairments. Some of these deficits may be caused by weight gain and others by alternative mechanisms that have yet to be identified.

Reducing tau by half had no adverse effects on any of the outcome measures until 25-26 months of age. At this age, *Tau*^{+/-} mice showed a slight reduction in striatal TH levels but no behavioral deficits, compared with age-matched *Tau*^{+/+} mice, demonstrating that partial reduction of tau is well tolerated even in old mice. These results extend previous studies demonstrating that *Tau*^{+/-} mice showed no deficits in the Morris Water maze at 4-7 months⁹⁸. They also have potential therapeutic implications, as 50% reduction of tau was sufficient to improve neuronal network activity and cognitive functions in human amyloid precursor protein transgenic mice^{71,83,98} and to improve axonal transport in primary neuronal cultures exposed to A β oligomers⁶⁵.

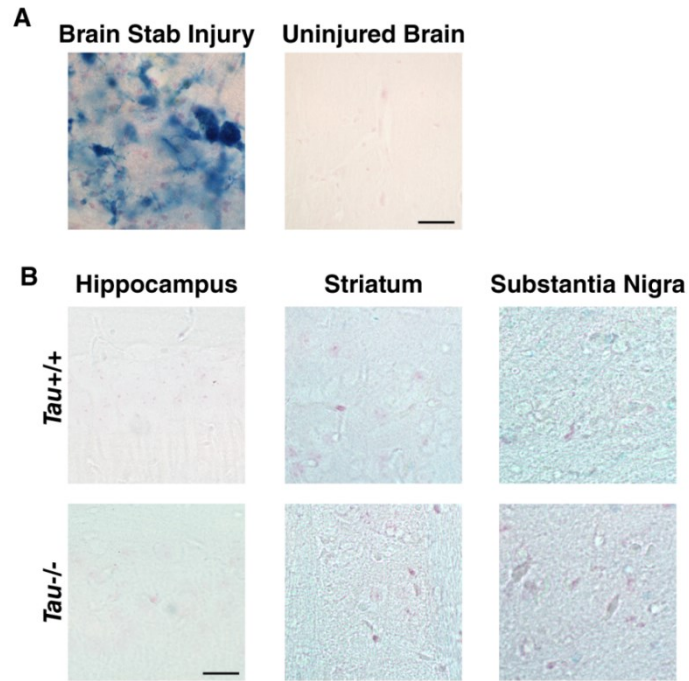


Figure 2.5. Lack of iron staining in the brains of 14-month-old *Tau*^{-/-} mice. (A) *Tau*^{+/+} mice that did (left) or did not (right) receive a cerebral needle stab injury were used as a positive control for cerebral iron staining. (B) No iron staining was observed in the brains of uninjured *Tau*^{+/+} and *Tau*^{-/-} mice (n=3 mice per genotype). Scale bars: 10μm, magnification: 430X.

The findings of the current study differ in several respects from those reported by Lei and colleagues¹⁰⁷. Specifically, we did not find behavioral deficits in the open field test, abnormal iron accumulation in the brain, or significant decreases in striatal levels of dopamine or TH in middle-aged and old *Tau*^{-/-} mice, compared with age-matched *Tau*^{+/+} controls. In addition, other types of subtle motor deficits we detected in 12–15-month-old *Tau*^{-/-} mice were not significantly improved by treatment with L-DOPA/benserazide. Because both studies assessed the same *Tau*^{-/-} model⁷³ at comparable ages (12 and 24 months versus 12-15 and 21-22 months), it is unlikely that these variables accounted for the differences in our results. Additional studies, including by independent groups, are needed to resolve the discrepancies, which might relate to a variety of other factors, including the diet and housing conditions of the mice and the methodological approaches used to study their phenotypes.

Because we did observe a trend towards lower striatal dopamine and TH levels in middle-aged and old *Tau*^{+/-} and *Tau*^{-/-} mice, it is possible that genetic reduction or ablation of tau slightly increases the susceptibility of dopaminergic neurons to various injuries, including those caused by aging, exposure to 6-hydroxydopamine³⁴⁵ and iron accumulation¹⁰⁷. However, we consider it unlikely that the motor impairments we observed in middle-aged *Tau*^{-/-} mice reflect extrapyramidal motor dysfunction because these mice showed only subtle trends towards dopaminergic deficits and their motor impairments did not improve with dopamine treatment. One potential cause of motor dysfunction is abnormal weight gain, which was evident in *Tau*^{-/-} mice at 12-15 months of age and correlated with their impairments on the Rota rod and balance beam. However, pole test deficits did not correlate with weight gain, suggesting the involvement of additional factors that remain to be defined.

In conclusion, the genetic ablation of tau causes minimal neurological dysfunction in middle-aged, but not in old *Tau*^{-/-} mice, as compared with age-matched wildtype controls, and there is little evidence that partial reduction of tau is detrimental. To further assess the safety of this potential therapeutic strategy, it would be desirable to reduce tau levels in rodent models at different ages after their nervous system has developed and matured in the presence of wildtype tau levels.

Chapter 3

How Tau Mediates A β -induced Dysfunction: Gain-of-Function versus Physiological Mediator

Endogenous mouse tau studies by

Meaghan Morris*, Giselle Knudsen*, Sumihiro Maeda, Johnathan Trinidad, Alexandra Ianoviciu, Alma Burlingame and Lennart Mucke

*These authors contributed equally to this work.

Endogenous rat tau studies by

Zihao Wang, Namrata D. Udeshi, Meaghan Morris, Jeffery Shabanowitz, Donald F. Hunt and Gerald W. Hart

Rat studies modified from *Molecular and Cellular Proteomics* 2010; 9 (1): 153-160

Used with permission

Introduction

Abnormal modification and accumulation of the microtubule-associated protein tau is associated with Alzheimer's disease (AD) and other neurodegenerative disorders collectively referred to as "tauopathies". A large body of experimental evidence suggests that cerebral accumulation of amyloid- β ($A\beta$) peptides contributes causally to AD³⁴⁶ and that pathologic tau species may mediate the effects of $A\beta$ on cognitive decline^{12,13,71,83,84,98}, though the nature of the $A\beta$ and tau species involved remain a topic of intense investigation.

Transgenic mice with neuronal overexpression of human amyloid precursor protein (hAPP) bearing familial AD-linked mutations have pathologically elevated levels of $A\beta$ in the brain and develop a range of other AD-like abnormalities^{347,348}. Although most lines of hAPP mice do not spontaneously develop abnormal modification or accumulation of endogenous mouse tau, genetic ablation of tau prevents or reduces behavioral impairments, synaptic deficits, neural network dysfunction and related molecular alterations in several lines of hAPP mice without affecting their levels of soluble $A\beta$, amyloid plaques, or neuritic dystrophy^{71,83,93,98,119}. In addition, tau reduction markedly increases resistance to seizure induction in various models of epilepsy^{71,98,111,349,350}. Taken together, these findings led us to propose two possible mechanisms by which tau enables $A\beta$ -induced impairments. In the first hypothesis, physiological forms of tau enable aberrant neural network activity caused by diverse pathogenic triggers⁷¹. The alternative hypothesis is that pathologically elevated levels of $A\beta$ change the posttranslational modification of tau causing an adverse gain of tau function, turning it into an active mediator of $A\beta$ -induced neuronal dysfunction¹¹⁴. As discussed elsewhere³⁴¹, these possibilities are not mutually exclusive. Characterizing the posttranslational modifications of tau may help identify strategies to block the pathological processes it enables or mediates.

Most studies of post-translational tau modifications have focused on the phosphorylation of abnormal tau or were carried out in cell-free conditions or cultured cell lines. While these studies have provided important information on abnormal tau, much less is known about the nature and extent of physiological tau modifications that occur *in vivo*. Furthermore, many tau modifications have not yet been studied as

widely as phosphorylation, including O-GlcNAc modification, ubiquitination, methylation and acetylation. Methylation of tau on lysine and arginine residues has been described very recently³⁵¹⁻³⁵³, but the functional effects of these two types of methylation remain mostly unknown. O-GlcNAc modification has been proposed to prevent tau phosphorylation by occupying many serine and threonine residues³⁵⁴⁻³⁵⁶, thereby preventing the dissociation of tau from microtubules and tau aggregation. However, prior to our studies no O-GlcNAc sites had been found on endogenous tau, compared to 34 phosphorylation sites^{352,357}. Ubiquitination of tau has been studied primarily on abnormal tau aggregates^{31,358}, while tau acetylation has been primarily studied in cell culture with some acetylation observed on abnormal tau aggregates^{23,24,195}. Interestingly, acetylation can oppose tau ubiquitination, which marks tau for degradation²³, but almost nothing appears to be known about the baseline ubiquitination or acetylation state of physiological tau.

Further complicating the interpretation of tau modifications, the quality of the site-assignment for tau modifications has often been suboptimal or uncertain. Assignment of tau phosphorylation sites in particular can be difficult due to the clustering of potential phosphorylation sites and the abundance of multiply phosphorylated peptides. Recent advances in mass spectrometry have enabled the calculation of confidence scores for modification site assignments, such as the Slip score or Ascore^{359,360}. However, the tau modification sites in online databases do not yet include this information, making it difficult to assess the quality of the information provided³⁶¹⁻³⁶⁵.

Here we used mass spectrometry to extensively interrogate physiological modifications of endogenous tau in brain tissues from untreated wildtype and hAPP mice. We focused on mouse tau because working with mice made it possible to standardize *peri-mortem* variables and optimize sample preservation, the sequence of mouse tau is similar to human tau (89% identical, 92% similar, blastp vs. human tau 441), and this approach allowed for the reliable quantitative comparison of tau modifications in wildtype controls and hAPP mice.

Results

Investigation of Endogenous Tau Modifications in Wildtype Mice

Our investigations into endogenous tau modification began by site mapping O-GlcNAc modification of endogenous rat tau. To identify O-GlcNAc modification on endogenous tau, we took advantage of a new technique recently developed by our lab for specific, high affinity enrichment of O-GlcNAc modified peptides (Figure 3.1A). Tau was enriched from rat brain by homogenization in 1% perchloric acid then the neutralized, concentrated supernatant was passed through a gel filtration column, which separates proteins based on size. The tau-containing fractions were combined and digested with trypsin, then tagged in successive steps with galactose-azide and a photo-cleavable biotin tag (Figure 3.1A). This tagging process allowed for high affinity avidin enrichment of O-GlcNAc modified peptides and facilitated the release of the tightly bound peptides by cleaving the biotin with exposure to ultraviolet light. From electron transfer dissociation mass spectrometry of the O-GlcNAc modified peptides we were able to assign a single O-GlcNAc modification site on tau, S400 (Figure 3.1B), as well as novel O-GlcNAc modifications of α -synuclein (SYN) and several other proteins.

Next, using endogenous tau samples isolated from wildtype mouse hippocampus and cortex (Table B.2), we were able to identify and carry out site assignments for six different types of post-translational modifications: arginine methylation, lysine acetylation, lysine methylation, lysine ubiquitination, serine O-GlcNAc modification, and serine / threonine / tyrosine phosphorylation (Figure 3.2, Tables 3.1,3.2). Lysine ubiquitination was inferred from the detection of GlyGly modified lysine, which results from trypsin cleavage of ubiquitin. Our experiments covered 96% of the tau sequence and assigned modifications at 63 sites, which are listed in Table 3.2 by position within mouse tau 430 and the homologous position in human tau 441. As is the convention in tau literature, all amino acid numbering in the text refers to the homologous site in human tau 441. To our knowledge, 18 of the 63 sites have not been previously reported and all of these novel modifications occurred on arginine or lysine residues which are conserved in human tau (Table 3.1, bold and red font Table 3.2; instruction for access to all peptide identification data in Appendix A: Peptide identification and label-free quantitation by mass spectrometry).

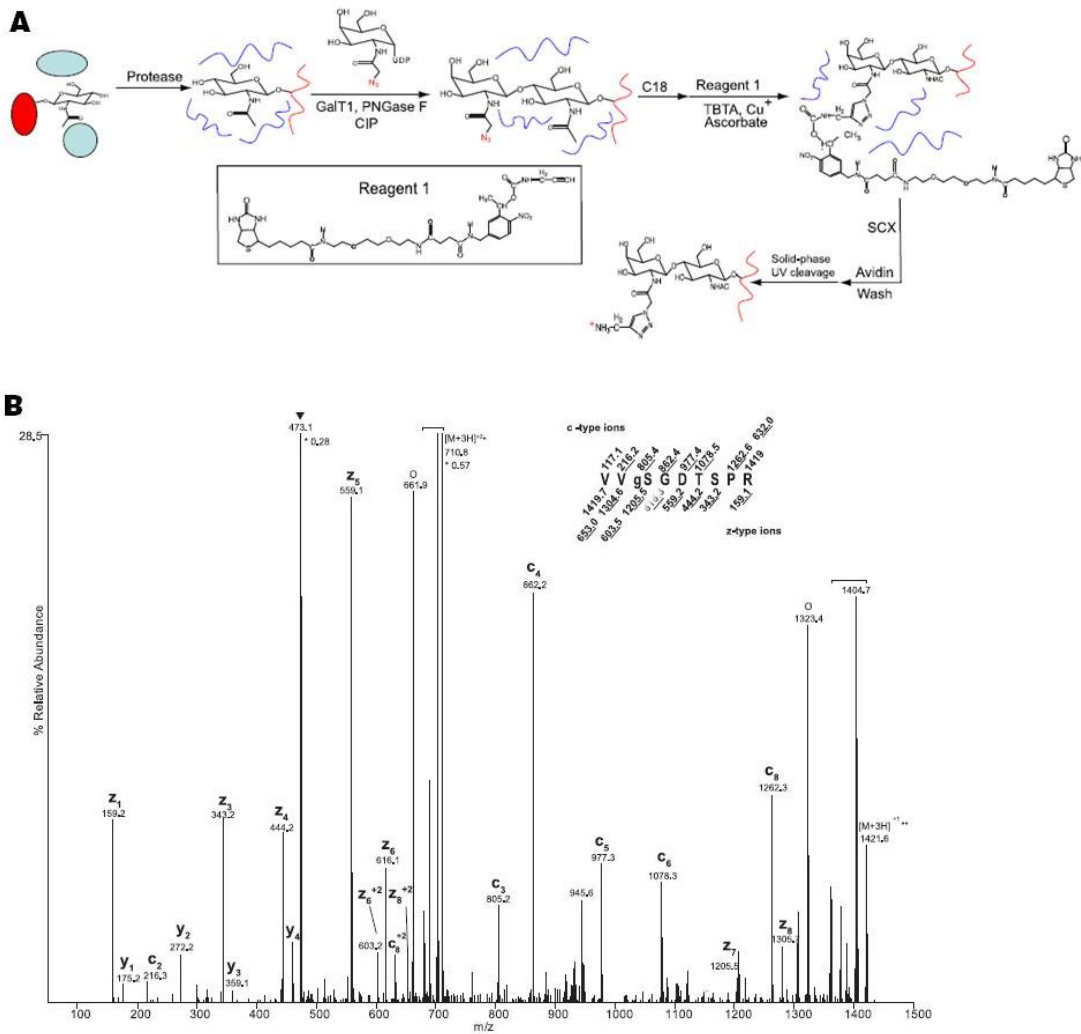


Figure 3.1. Identification of O-GlcNAc modification of S400 on tau by chemical/enzymatic enrichment. (A) Flow chart showing the overall strategy. *Inset*, structure of the photocleavable PC-PEG-biotin-alkyne reagent. (B) Electron-transfer dissociation tandem mass spectrometry spectrum recorded on $[M+3H]^{3+}$ ions (m/z 474.2) for the derivatized peptide VVgSDTPR from the tau protein. CIP, calf intestinal phosphatase; PNGase F, peptide:N-Glycosidase F; TBTA, tris[(1-benzyl-1*H*-1,2,3-triazole-4-yl)methyl]amine.

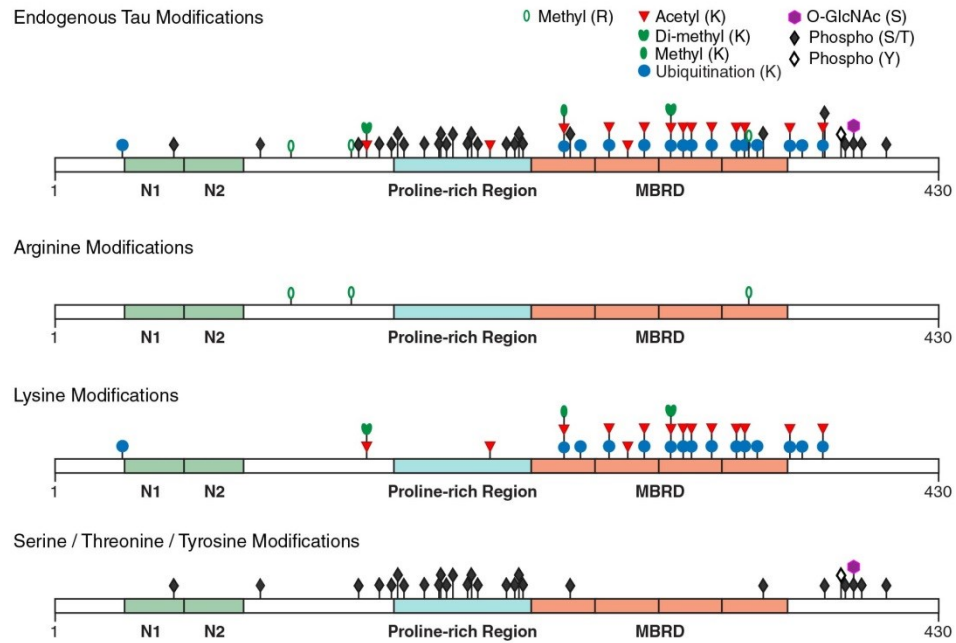


Figure 3.2. Post-translational modifications identified in endogenous mouse tau. Mouse tau was isolated from brains of wildtype mice and post-translational modifications were assigned by mass spectrometry. Modifications are shown on the longest tau isoform expressed in the mouse central nervous system (430 amino acids). All unambiguously assigned endogenous tau modifications are shown in the top panel, while the lower panels show the same modifications separated by the type of residue modified. The N-terminal exons expressed in mouse tau 430 are shown in blue, the proline-rich region in green and the four microtubule binding repeats are shown in orange. Only unambiguously assigned sites from wildtype mice reported (Table 3.2) are indicated, and all sites are positioned to scale. Note that some amino acid residues can be alternately modified and that these modifications are mutually exclusive, e.g., ubiquitination and acetylation. N1, N2, N-terminal exons subject to alternative splicing; MBRD, microtubule binding repeat domain.

Table 3.1. Summary of unambiguously assigned tau modifications in wildtype mice.

Modification	Sites Assigned	Previously Reported Sites^a	Residue Conserved in Human Tau 441	Sites in the MBRD	Sites with Alternate Modifications
Arginine Methylation	3	1 (0.33)	3 (1.0)	1 (0.33)	0 (0)
Lysine Acetylation	14	11 (0.79)	14 (1.0)	10 (0.71)	12 (0.86)
Lysine Methylation	mono – 1 di - 2	3 (1.0)	3 (1.0)	2 (0.67)	3 (1.0)
Lysine Ubiquitination	15	3 (0.20)	15 (1.0)	11 (0.73)	11 (0.73)
Serine O-GlcNAc	1	0	1	0	1
Serine / Threonine / Tyrosine Phosphorylation	27	27 (1.0)	25 (0.93)	2 (0.07)	1 (0.04)

Numbers in parentheses indicate the proportion of total for each modification. MBRD, microtubule binding repeat domain.

^aReported based on *in vitro* or *in vivo* experiments.

Contrary to the prevailing literature view, O-GlcNAc modification in mouse brain was detected only at a single site at very low stoichiometry. Detection of this O-GlcNAc modification required enrichment for O-GlcNAc modified peptides from the digests of a few large-scale tau preparations (Table B.2).

The majority of phosphorylation sites resided outside the microtubule binding repeat domain (MBRD) (Figure 3.2). To determine the likely site assignments for multiply phosphorylated peptides, we generated highly phosphorylated tau samples by subjecting wildtype mice to anesthesia/hypothermia³⁶⁶. Results obtained in this model suggested that the endogenous di-phosphorylation detected in the 210–224 region likely represents phosphorylation of T212 and T217. However, the model failed to resolve double- and triple-phosphorylated sites in the tryptic peptide representing residues 407–438. Because this peptide contained ten candidate serine/threonine sites for phosphorylation and showed partial methionine-oxidation, only one phosphorylation site (S409) could be unambiguously assigned.

Lysine modifications tended to be enriched in the microtubule binding repeat domain (MBRD), though the enrichment was not statistically significant. The vast majority of acetylation sites (86%) were alternately modified, usually by ubiquitination (Figure 3.2). Conversely, alternative modification of

ubiquitination sites always included acetylation. Acetylation and ubiquitination targeted the same lysine residue more often than would be predicted by chance ($p=0.00002$ by Pearson's Chi-squared test) and lysine methylation targeted residues that were targeted by both acetylation and ubiquitination ($p=0.0005$ by Likelihood Ratio test).

Table 3.2. Endogenous tau modifications in wildtype and hAPP mice.

Modification Site(s)	PTM	Number of PTM's	Modified Residue (Mouse 430 isoform)	Homologous Residue (Human 441 isoform)
DHGL <u>K</u> ESPP	GlyGly	1	33 ^a	44
DHGL <u>K</u> AEEA	GlyGly	1	33 ^b	44
PG <u>S</u> E <u>T</u> SDAK	Phospho	1	50 52 53 ^a	61 63 64 ³⁶⁷
SDAK <u>S</u> TPAE	Phospho	1	57 58 ^a	68 69 ³⁵⁷
DAK <u>S</u> TPAE	Phospho	1	58 ^a	69 ³⁵⁷
GIGD <u>T</u> PNQE	Phospho	1	100 ^c	111 ^{357,368}
VTQAR <u>V</u> ASK	Methyl	1	115 ^c	126
IATPR <u>R</u> GAAS	Methyl	1	144	155
RGAAS <u>S</u> PAQK	Phospho	1	148	_d 369
RGAAS <u>S</u> PAQKGTSNAT <u>R</u> IPA	Phospho	2	148,158 ^e	_d ,169 ^{357,369}
SPAQ <u>K</u> GTSN	Acetyl	1	152	163 ^{23,24}
SPAQ <u>K</u> GTSN	Dimethyl	1	152	163 ³⁵¹
IPAK <u>T</u> TP <u>S</u> PKTP	Phospho	2	164 165,167	175 _d 370
IPAK <u>T</u> TP <u>S</u> PK <u>T</u> PPGS	Phospho	3	164,167,170	175, _d 181 ^{368,370,371}
K <u>T</u> TP <u>S</u> PKTP	Phospho	1	167	_d 370
K <u>T</u> TP <u>S</u> PK <u>T</u> PPGS	Phospho	2	167,170	_d ,181 ^{368,370,371}
PSPK <u>T</u> PPGS	Phospho	1	170	181 ^{368,371}
PSPK <u>T</u> PPGS <u>G</u> EP <u>P</u> K <u>S</u> GER <u>S</u>	Phospho	2	170,180	181,191 ^{368,371,372}
RSGY <u>S</u> SPG <u>S</u> PG <u>T</u> P	Phospho	2	187,191	198,202 ³⁶⁹
RSGY <u>S</u> SPG <u>S</u> PG <u>T</u> PGSR <u>S</u> RT <u>P</u> S	Phospho	3	187 188 191 194 199	198 199 202 205 210 ^{368,369,373,374}
SGY <u>S</u> SPG <u>S</u> P	Phospho	1	188	199 ³⁷³
SGY <u>S</u> SPG <u>S</u> PG <u>T</u> P	Phospho	2	188,191	199,202 ^{369,373}
SSPG <u>S</u> PG <u>T</u> P	Phospho	1	191	202 ³⁶⁹
SSPG <u>S</u> PG <u>T</u> PGSR	Phospho	2	191,194	202,205 ^{368,369}
GSPG <u>T</u> PGSR	Phospho	1	194	205 ³⁶⁸
PGSR <u>S</u> RT <u>P</u> SL <u>T</u> PP <u>T</u> R	Phospho	2	199 201 203 206	210 212 214 217 ^{368,372,374,375}
SRSR <u>T</u> PSLP	Phospho	1	201	212 ^{372,375}
SRT <u>P</u> SL <u>T</u> P	Phospho	1	203	214 ³⁶⁸
PSL <u>T</u> PP <u>T</u> R	Phospho	1	206	217 ³⁶⁸
REP <u>K</u> VAVV	Acetyl	1	214	225
AVVR <u>T</u> PPKS	Phospho	1	220	231 ^{368,371,373,375}

AVVR <u>T</u> PPK <u>S</u> PS <u>A</u> SKSRL	Phospho	2	220 224 226 228	231 235 237 239 ^{357,367,375}
AVVR <u>T</u> PPK <u>S</u> PSAS	Phospho	2	220,224	231,235 ³⁷⁵
AVVR <u>T</u> PPKSPSA <u>S</u> KSRL	Phospho	2	220,228	231,239 ^{367,375}
PK <u>S</u> PS <u>A</u> SKS	Phospho	1	226	237 ³⁵⁷
NVRS <u>K</u> IGST	Acetyl	1	248	259 ^{23,24}
NVRS<u>K</u>IGST	GlyGly	1	248	259
NVRS <u>K</u> IGST	Methyl	1	248	259 ³⁵²
SKIG <u>S</u> TENL	Phospho	1	251	262 ^{371,376}
TENL<u>K</u>HQPG	GlyGly	1	256	267
IINK <u>K</u> LDLS	Acetyl	1	270	281 ^{23,24}
IINK<u>K</u>LDLS	GlyGly	1	270	281
<i>IINK<u>K</u>LDLS</i>	<i>Methyl</i>	<i>1</i>	<i>270^f</i>	<i>281</i>
NVQS <u>K</u> CGSK	Acetyl	1	279	290 ^{23,24}
<i>NVQS<u>K</u>CGSK</i>	<i>GlyGly</i>	<i>1</i>	<i>279^f</i>	<i>290</i>
KDNI <u>K</u> HVPG	Acetyl	1	287	298 ²³
KDNI<u>K</u>HVPG	GlyGly	1	287	298
QIVY <u>K</u> PVDL	Acetyl	1	300	311 ²⁴
QIVY <u>K</u> PVDL	Dimethyl	1	300	311 ³⁵²
QIVY <u>K</u> PVDL	GlyGly	1	300	311 ^{31,351,358}
VDLS <u>K</u> VTSK	Acetyl	1	306	317 ²³
VDLS <u>K</u> VTSK	GlyGly	1	306	317 ³⁵⁸
KVTS <u>K</u> CGSL	Acetyl	1	310	321 ²³
KVTS<u>K</u>CGSL	GlyGly	1	310	321
<i>SKCG<u>S</u>LGNI</i>	<i>Phospho</i>	<i>1</i>	<i>313^f</i>	<i>324^{377,378}</i>
NIHH <u>K</u> PGGG	Acetyl	1	320	331 ²³
NIHH<u>K</u>PGGG	GlyGly	1	320	331
<i>NIHH<u>K</u>PGGG</i>	<i>Methyl</i>	<i>1</i>	<i>320^f</i>	<i>331</i>
VKSE <u>K</u> LDFK	Acetyl	1	332	343
VKSE<u>K</u>LDFK	GlyGly	1	332	343
KLDF<u>K</u>DRVQ	Acetyl	1	336	347
KLDF<u>K</u>DRVQ	GlyGly	1	336	347
DFK <u>R</u> VQSK	Methyl	1	338	349 ³⁵³
RVQS <u>K</u> IGSL	GlyGly	1	342	353 ^{351,358}
SKIG <u>S</u> LDNI	Phospho	1	345	356 ³⁶⁸
GGGN <u>K</u> KIET	Acetyl	1	358	369 ^{23,24}
GGGN<u>K</u>KIET	GlyGly	1	358	369
KKIE <u>T</u> HKL <u>T</u> FREN	Phospho	1	362 366	373 377 ³⁷⁸
IE<u>T</u>H<u>K</u>L<u>T</u>FR	GlyGly	1	364	375
NAKA <u>K</u> TDHG	Acetyl	1	374	385 ²³
NAKA<u>K</u>TDHG	GlyGly	1	374	385
<i>AKAK<u>T</u>DHGAEIVYK<u>S</u>PVVS</i>	<i>Phospho</i>	<i>2</i>	<i>375,385^f</i>	<i>386,396^{375,378-380}</i>
AKAK <u>T</u> DHGAEIVYK <u>S</u> PVVSGD <u>T</u> <u>S</u> PRHL	Phospho	3	375,385,392 393	386,396,403 404 ^{375,378-380}
<i>AEIVYK<u>S</u>PVVS</i>	<i>Phospho</i>	<i>2</i>	<i>383,385^f</i>	<i>394,396³⁸¹</i>

AEIV <u>Y</u> KSPV <u>V</u> <u>S</u> GD <u>T</u> SPRHL	Phospho	3	383,389,392 393	394,400,403 404 ³⁸¹
<i>AEIV<u>Y</u>KSPV<u>V</u><u>S</u>GD<u>T</u>SPRHL</i>	<i>Phospho</i>	<i>3</i>	<i>383,385,392 393^f</i>	<i>394,396,403 404³⁸¹</i>
IVYK <u>S</u> PV <u>V</u> S	Phospho	1	385	396 ^{368,371}
IVYK <u>S</u> PV <u>V</u> <u>S</u> GD <u>T</u> S	Phospho	2	385,389	396,400 ^{368,371}
IVYK <u>S</u> PV <u>V</u> <u>S</u> GD <u>T</u> SPRHL	Phospho	2	385,392 393	396,403 404 ^{368,371}
IVYK <u>S</u> PV <u>V</u> <u>S</u> GD <u>T</u> SPRHL	Phospho	3	385,389,393	396,400,404 ^{368,371}
IVYK <u>S</u> PV <u>V</u> <u>S</u> GD <u>T</u> SPRHL	Phospho	3	385,389,392 393	396,400,403 404 ^{368,371}
SPV<u>V</u><u>S</u>GD<u>T</u>S	HexNAc	1	389	400
SPV <u>V</u> <u>S</u> GD <u>T</u> S	Phospho	1	389	400 ^{368,371}
SPV <u>V</u> <u>S</u> GD <u>T</u> SPRHL	Phospho	2	389,392 393	400,403 404 ^{368,371}
<i>SGD<u>T</u>SPRHL</i>	<i>Phospho</i>	<i>1</i>	<i>393^f</i>	<i>404</i>
PRHL <u>S</u> NV <u>S</u> STG <u>S</u> IDMV	Phospho	2	398 401 402 403 405	409 412 413 414 416 ^{357,382}
<i>PRHL<u>S</u>NV<u>S</u>STG<u>S</u>IDMV</i>	<i>Phospho</i>	<i>3</i>	<i>398 401 402 403 405^f</i>	<i>409 412 413 414 416^{357,382}</i>
SSTG <u>S</u> IDMV	Phospho	1	405 ^g	416 ³⁵⁷

PTM, post-translational modification. Novel modification sites found in wildtype mice are in bold and red font (HexNAc site was identified in rat), sites found only in hAPP mice are italicized and in blue font. Sites for which unambiguous assignment was not possible are indicated with a vertical bar between alternative assignments.

^a Mouse tau isoform A peptide

^b Mouse tau isoform B,C or D peptide

^c Mouse tau isoform A,B,C or D peptide

^d Not conserved in human tau

^e Site identified in PSD experiments

^f Modified species was only observed in hAPP samples

^g Peptide site was unambiguously assigned with AspN digestion

Similar Tau Modifications in Wildtype and hAPP Transgenic Mice

We next used our extensive dataset to investigate whether tau modifications are altered by neuronal overexpression of hAPP/A β *in vivo*. We identified 5 additional tau modifications in hAPP mice which had not been observed in wildtype mice (Table 3.2 italicized and in blue font, Table B.2). However, the abundance of these modifications approached the lower limit of detection and we could not determine whether they were truly specific to hAPP mice or whether they were present in wildtype mice just below the detection threshold.

Our combined list of tau modifications from wildtype and hAPP mice was used for quantitative comparison between hAPP mice and wildtype controls (Table 3.2). Because some spectra in these experiments could not be unambiguously assigned in all mice, modified peptides containing the same potential modification site were combined for quantitative comparison (Table 3.3). Although we compared

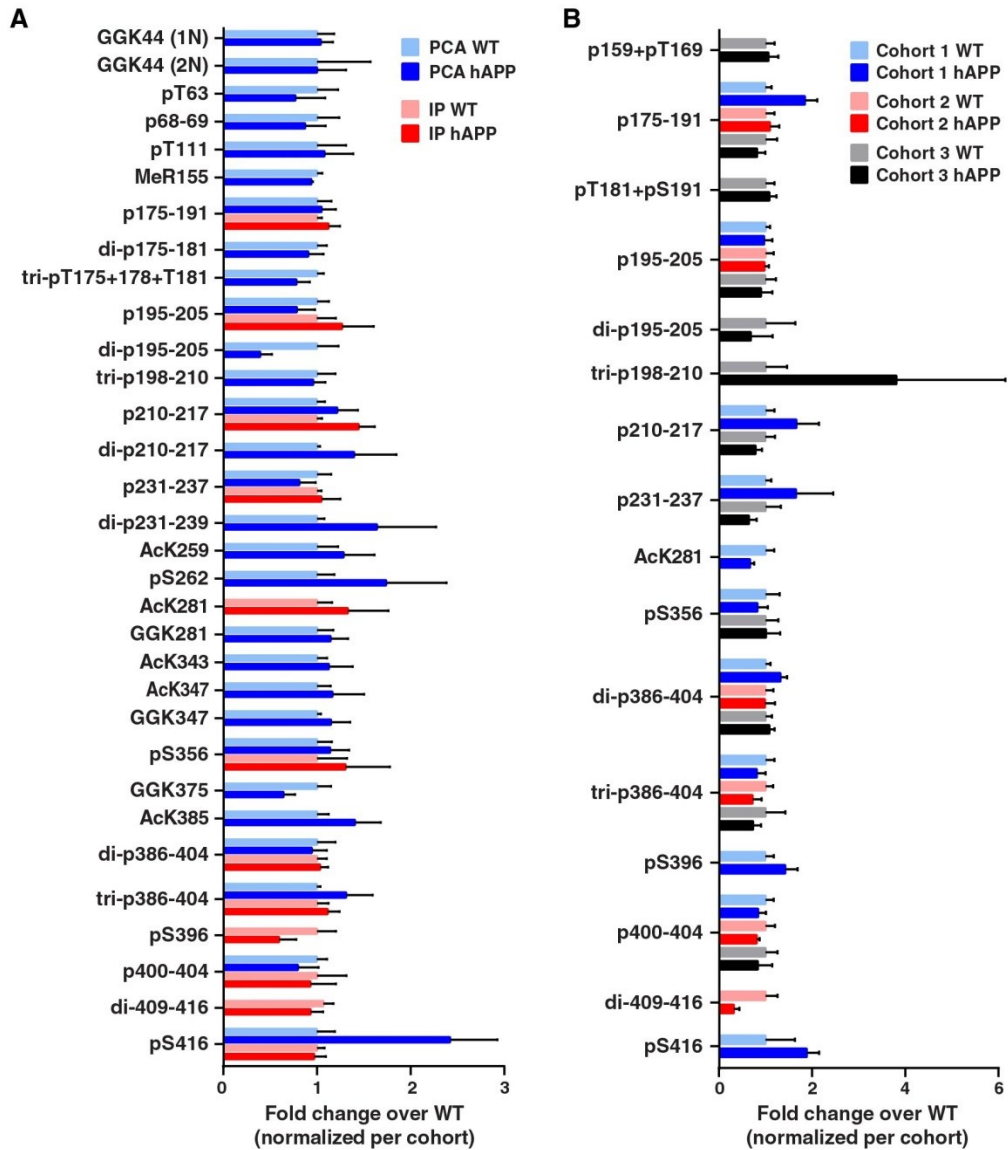


Figure 3.3. Comparison of post-translational modifications in hAPP and wildtype mice. Tau was isolated from hAPP and wildtype mice and the levels of all quantifiable post-translational modifications were assessed by mass spectrometry. (a) Tau was isolated from whole lysate either by selective solubility in perchloric acid in wildtype mice and symptomatic hAPP (PCA cohort, n=3 per group, age 6 months) or by immunoprecipitation in randomly selected wildtype and hAPP mice (IP cohort, n=10-12 mice per group, ages 7-10 months). (b) Tau was immunoprecipitated from the post-synaptic density of randomly-selected wildtype and hAPP mice using 3 separate cohorts (n=10-12 mice per group, ages 7-10 months). After correcting for multiple comparisons, no *p*-values were ≤ 0.05 . Modified amino acids are indicated if conserved in human tau 441 and unambiguously assigned, with multiple unambiguous modifications marked with ‘+’; if the site is ambiguous, a range containing the modified sites is indicated with a ‘di-’ or ‘tri-’ marking dual and tri-modified peptides, respectively. Ac, modified by acetylation; GG, modified by GlyGly; Me, modified by methylation; p, modified by phosphorylation; WT, wildtype; hAPP, human amyloid precursor protein transgenic; PCA, isolated by perchloric acid solubility; IP, immunoprecipitated.

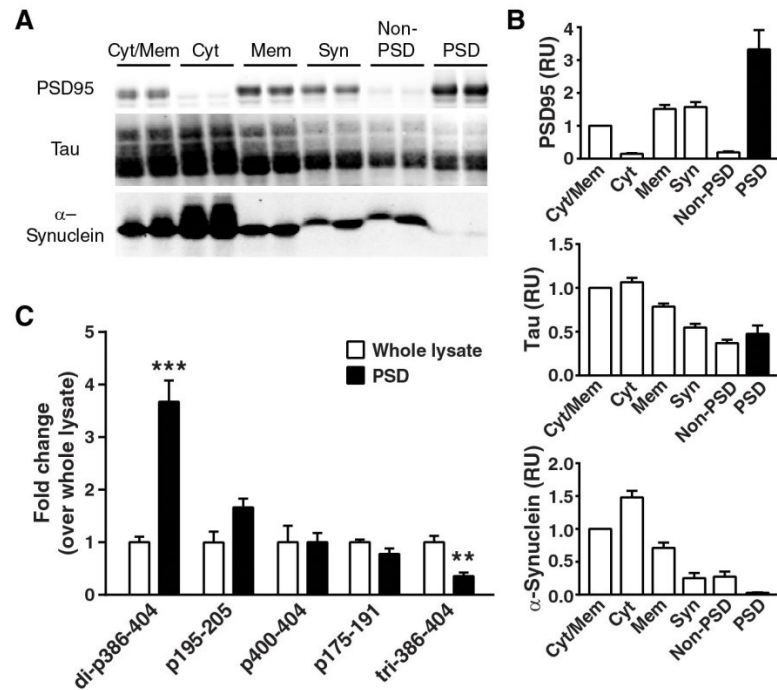


Figure 3.4. Differential modification of tau in the post-synaptic density. (a) Western blot showing PSD95, tau and α -synuclein levels at each step of post-synaptic density fractionation in a replicate cohort of mice and (b) quantification (n=8 mice, ages 5-6 months). Quantitative values were normalized to cytosolic/membrane fraction for each mouse. (c) Quantification of the 5 most commonly found tau modifications in the post-synaptic density fraction compared to hippocampal and cortical whole lysate (n=10-12 mice per group, ages 7-10 months). Due to site ambiguity, a range containing the modified sites is indicated and a 'di-' or 'tri-' denotes dual and tri-modified peptides, respectively. ** $p \leq 0.01$, *** $p \leq 0.001$ by Student's t-test with a Holm correction for multiple comparisons. Cyt/Mem, cytosolic- and membrane-containing fraction; Cyt, cytosolic fraction; Mem, membrane fraction; Syn, synaptosomal fraction; Non-PSD, fraction remaining after PSD extraction; PSD, post-synaptic density; RU, relative units. Quantitative values are means \pm SEM, though some error bars of fractionated samples are too small to be seen.

32 different peptide modifications across two independent experiments (Table 3.3A, B.3), we found no tau modifications that were significantly and consistently different between hAPP mice and wildtype controls.

Recent studies suggest that even small amounts of abnormal tau may be highly pathogenic when they are associated with the post-synaptic density (PSD)^{114,158}. Therefore, we also compared tau modifications in PSD fractions isolated from the hippocampus and cortex (Figure 3.4A,B) of hAPP mice and wildtype controls. Tau levels were similar in the PSD of hAPP mice and wildtype controls (replicate cohort age 5-6 months, n=8 mice per genotype, data not shown). Because of the low amount of tau isolated from PSD fractions, only the most abundant modifications could be compared. A total of 16 modified peptides were measured over the course of 3 independent experiments (Figure 3.3B, Table 3.3, B.2). Besides acetylated K281 detected in a single experiment, all peptide modifications identified in the PSD were phosphorylations. None of the tau modifications detected in PSD fractions were significantly and consistently different between hAPP mice and wildtype controls (Figure 3.3B). Phosphorylation at S416 tended to be found more often in the PSD of hAPP mice (35%) compared to wildtype controls (16%), so this site may merit further investigation despite the lack of a significant alteration between genotypes.

Many modified tau peptides could not be quantified because of the high variability in the detection of low abundance modifications among animals. Five modifications could be quantified in all unfractionated whole lysate and PSD experiments, and another four in both of the whole lysate experiments. The majority (7/9) of these modifications were mono-phosphorylations. The most consistent mono-phosphorylations were identified in peptides containing residues 175–191, 195–205 or 400–404, and the most consistent di- and tri-phosphorylations in peptides containing residues 386–404 (Figure 3.4C). The four additional modifications quantified in whole lysate, but not PSD, experiments were mono-phosphorylations in peptides containing residues 210–217 or 231–237, and at S356 and S416. Notably, di-phosphorylation in the 386-404 region was enriched in the PSD, while tri-phosphorylation of the 386-404 region was depleted in the PSD fraction in a side-by-side comparison with whole hippocampal and cortical lysate (Figure 3.4C).

Table 3.3. Tau modifications quantified in hAPP and wildtype mice.

Modification Site(s)	PTM	Number of Modified Residues	Modified Residue (Mouse 430 isoform)	Homologous Human Residue (441 isoform)	Quant.in Whole Lysate	Quant in PSD
DHGL <u>K</u> ESPP	GlyGly	1	33 ^a	44	+	-
DHGL <u>K</u> AEEA	GlyGly	1	33 ^b	44	+	-
PGSE <u>T</u> SDAK	Phospho	1	52 ^a	63	+	-
SDAK <u>S</u> TPTAE	Phospho	1	57 58 ^a	68 69	+	-
GIGD <u>T</u> PNQE	Phospho	1	100 ^c	111	+	-
IATP <u>R</u> GAAAS	Methyl	1	144	155	+	-
RGAA <u>S</u> PAQKGTSNAT <u>R</u> IPA	Phospho	2	148,158 ^d	- ^e ,169	-	+
IPAK <u>T</u> TPSPK <u>T</u> PPG <u>S</u> GEP <u>P</u> K <u>S</u> G <u>E</u>	Phospho	1	164 170 174 180	175 181 185 191	+	+
IPAK <u>T</u> TP <u>S</u> PK <u>T</u> PPGS	Phospho	2	164 167 170	175 ^e 181	+	-
IPAK <u>T</u> TPSPK <u>T</u> PPGS	Phospho	3	164,167,170	175, ^e 181	+	-
PSPK <u>T</u> PPG <u>S</u> GEP <u>P</u> K <u>S</u> G <u>E</u> R <u>S</u>	Phospho	2	170,180	181,191	-	+
SGER <u>S</u> GY <u>S</u> SPG <u>S</u> PG <u>T</u> PGSR	Phospho	1	184 187 191 194	195 198 202 205	+	+
SGER <u>S</u> GY <u>S</u> SPG <u>S</u> PG <u>T</u> PGSR	Phospho	2	184 187 188 191 194	195 198 199 202 205	+	+
RS <u>G</u> Y <u>S</u> SPG <u>S</u> PG <u>T</u> PGSR <u>S</u> R <u>T</u> PS	Phospho	3	187 188 191 194 199	198 199 202 205 210	+	+
PGSR <u>S</u> R <u>T</u> PS <u>L</u> PT <u>P</u> PTR	Phospho	1	199 201 203 206	210 212 214 217	+	+
PGSR <u>S</u> R <u>T</u> PS <u>L</u> PT <u>P</u> PTR	Phospho	2	199 201 203 206	210 212 214 217	+	-
AVVR <u>T</u> PPK <u>S</u> PS <u>A</u> SK <u>S</u>	Phospho	1	220 224 226	231 235 237	+	+
AVVR <u>T</u> PPK <u>S</u> PS <u>A</u> SK <u>S</u> R <u>L</u>	Phospho	2	220 224 226 228	231 235 237 239	+	-
NVRS <u>K</u> IGST	Acetyl	1	248	259	+	-
SKIG <u>S</u> TENL	Phospho	1	251	262	+	-
IINK <u>K</u> LDLS	Acetyl	1	270	281	+	+
IINK <u>K</u> LDLS	GlyGly	1	270	281	+	-
VKSE <u>K</u> LDFK	Acetyl	1	332	343	+	-
KLDF <u>K</u> DRVQ	Acetyl	1	336	347	+	-
KLDF <u>K</u> DRVQ	GlyGly	1	336	347	+	-
SKIG <u>S</u> LDNI	Phospho	1	345	356	+	+
IETH <u>K</u> LTFR	GlyGly	1	364	375	+	-
NAKA <u>K</u> TDHG	Acetyl	1	374	385	+	-
AKAK <u>T</u> DHGAEIVYK <u>S</u> PPV <u>S</u> GD	Phospho	2	375 385 389 392 393	386 396 400 403 404	+	+
AKAK <u>T</u> DHGAEIVYK <u>S</u> PPV <u>S</u> GD	Phospho	3	375 385 389 392 393	386 396 400 403 404	+	+
IVYK <u>S</u> PPV <u>S</u>	Phospho	1	385	396	+	+
SPV <u>S</u> GD <u>T</u> SPRHL	Phospho	1	389 392 393	400 403 404	+	+
PRHL <u>S</u> NV <u>S</u> STG <u>S</u> IDMV	Phospho	2	398 401 402 405	409 412 413 416	+	+
SSTG <u>S</u> IDMV	Phospho	1	405 ^f	416	+	+

PTM, post-translational modification; Quant, quantified. Sites for which unambiguous assignment was not possible are indicated with a vertical bar between alternative assignments.

^aPeptide from mouse isoform A

^bPeptide from mouse isoforms B, C or D

^cPeptide from mouse isoforms A, B, C or D

^dIdentified in PSD experiments

^eNot conserved in human tau

^fSite unambiguously assigned with AspN digestion

Discussion

Our study describes six distinct types of physiological tau modifications at 63 sites on endogenous mouse tau, approximately one quarter of which represent novel modifications. Because we wanted to carry out an unbiased assessment of endogenous tau modifications, we did not enrich for specific modification types during most of our site assignment experiments. However, some samples were enriched for O-GlcNAc because the unexpectedly low stoichiometry of this modification warranted more detailed investigation.

There is robust targeting of acetylation, ubiquitination and methylation to the same set of lysine residues on endogenous tau, suggesting cross-talk between these three modifications. Previous findings obtained in cultures of primary neurons and HEK293 cells suggested a potential competition between acetylation and ubiquitination of specific lysines in tau²³. Our tau modification data suggests that acetylation and ubiquitination also compete for lysine modification on tau *in vivo*. Nearly all acetylation sites on tau were alternately modified with ubiquitin, including three of the four KXGS motifs, which regulate neurite extension and the binding of tau to microtubules^{383,384}. In support of the hypothesis that acetylation may compete with KXGS phosphorylation¹⁹⁵ we did not detect any peptides modified by both phosphorylation and acetylation in our study. However, it's possible that any such doubly modified peptides in the MBRD would be too low in abundance on tau to detect even without competitive modification.

We found that methylation targets two critical lysine residues on endogenous tau also targeted by acetylation and ubiquitination. These highly regulated, triply-targeted lysine residues reside in the first KXGS motif and in the PHF6 sequence, two regions that regulate the microtubule binding function and aggregation of tau. Lysine modification of the first KXGS motif (K259-S262) may prevent the binding of tau to microtubules, similar to the effect of KXGS phosphorylation³⁸³. Lysine mutation in the PHF6

(³⁰⁶VQIVYK³¹¹) sequence, which is critical for tau aggregation³⁸⁵, inhibits both the binding of tau to microtubules and tau aggregation²⁴. It is possible that modification of K311 has similar effects. K281, which is adjacent to PHF6* (²⁷⁵VQIINK²⁸⁰) and targeted by acetylation and ubiquitination in wildtype mice, may also control tau aggregation⁴⁶. We found this residue to be methylated at low levels only in hAPP mice. Notably, different types of lysine modifications at triply-targeted residues probably have different effects on tau function. However, the alternate modification of lysines residues by at least three different processes suggests that these residues may play a strategic role in the regulation of tau.

The complex effects of acetylation on tau aggregation highlight the challenges involved in investigating tau modification by enzyme manipulation without assessing site-specific modifications. Acetylation of tau by CREB-binding protein (CBP) enhances tau aggregation²⁴, whereas acetylation of tau by p300 inhibits aggregation¹⁹⁵, possibly due to the acetylation of different lysine residues. Indeed, the contributions of different lysine modifications to tau function are likely to vary by modification type and location and deserve to be further explored in both health and disease.

Another modification that has been proposed to have a strategic role in tau regulation is O-GlcNAc modification. In these studies, we were able to identify only a single O-GlcNAc modification site at S400, which has been subsequently confirmed by antibody labeling³⁸⁶. Results obtained *in vitro* and *in vivo* after pharmacological blockade of OGase, the O-GlcNAc removing enzyme, suggested a potential inverse relationship between O-GlcNAc modification and phosphorylation at many sites on tau³⁵⁴⁻³⁵⁶. However, chronic treatment of mice with OGase inhibitors increased O-GlcNAc on S400 of tau without changing tau phosphorylation, the first indication that these modifications are not necessarily reciprocal³⁸⁷. Our data is inconsistent with the hypothesis that O-GlcNAc modification can block pathologic tau phosphorylation by occupying many potential phosphorylation sites. The relative abundance and number of sites occupied by phosphorylation on endogenous tau contrasts with the single residue modified by O-GlcNAc, which was only detectable after specific enrichment. Nonetheless, the conservation of O-GlcNAc on tau across species^{30,244,386} suggests that this modification does fulfill an important function. Recent *in vitro* and *in vivo* studies suggest that O-GlcNAc modification of tau may prevent tau aggregation or toxicity without altering tau phosphorylation³⁸⁷⁻³⁸⁹.

Arginine methylation is the most recently described modification of tau³⁵³. The MBRD arginine methylation site on tau (Table 3.2) was found in a broad survey of arginine methylation in mouse brain³⁵³. We found only arginine mono-methylation of tau, which could be catalyzed by type I or type II protein arginine methyltransferases³⁹⁰, and the functional impact of this mono-methylation is unknown. Because two of the arginine methylation sites clustered just N-terminal to the proline-rich region it is tempting to speculate that arginine methylation could affect the binding of tau to membrane proteins, which is mediated by the N-terminal region⁷⁶, or to SH3 domain-containing proteins, mediated by the proline-rich region^{39,102}. Conceivably, arginine methylation could also alter the nucleo-cytoplasmic shuttling of tau^{89,390}, the regulation of which is unclear.

Most of the tau phosphorylations were observed at sites adjacent to MBRD domains, consistent with previous reports³⁹¹. A recent study observed 31 phosphorylation sites in human brain tissue from cognitively normal individuals³⁵², similar to the 27 sites we observed. Among their 4 cognitively normal samples, only 6 of the 31 described phosphorylation sites were found in all samples, 4 known phosphorylation sites and 2 novel sites³⁵². The 4 known sites (T181, S202, T231 and S404) were consistent with 4 of our most commonly detected singly modified phosphopeptides quantified in whole lysate, suggesting that the phosphorylation state of endogenous tau is similar in wildtype mouse brain and normal human brain tissue.

Notably, we did not detect any difference in tau modifications between symptomatic hAPP-J20 mice and wildtype controls, consistent with our earlier findings⁹⁸. We have previously reported similar levels of hippocampal tau phosphorylation in young, symptomatic hAPP mice by western blot and local increases in tau phosphorylation near neuritic plaques in old mice⁹⁸. By contrast, other studies have found increased tau phosphorylation in hAPP mice by western blot^{392,393}, including in the hippocampus of young symptomatic hAPP-J20 mice³⁹⁴. Using quantitative mass spectrometry, we assessed many more tau modifications than we could previously assess by western blot analysis and we were able to quantify 31 peptide modifications. The few modifications found only in hAPP mice were enriched in MBRD modifications, particularly lysine methylation, which could suggest some dislocation of tau from microtubules in hAPP mice. However, these modifications did not appear in our quantitative experiments and we could not confirm whether they were

specific to hAPP mice. We found no quantitative change in tau modification in either unfractionated whole lysates or PSD preparations from hAPP-J20 mice relative to wildtype controls. These findings support our hypothesis that normally modified endogenous tau fulfills a physiological function that allows A β and other epileptogenic factors to elicit aberrant network activity^{83,98,111,341,350}. However, we cannot exclude the possibility that the less abundant modifications which we could not quantify may contribute to a gain-of-function mechanism. Nor can we exclude the possibility that tau modifications could be altered at other ages, other brain regions or in other cellular compartments, including the cytosolic compartment of dendritic spines, or that tau mislocalization could result in an adverse gain of tau function in hAPP mice.

Even if tau modifications are not altered in hAPP mice, these modifications may play an important role in A β -induced pathology *in vivo*. Because tau modifications regulate tau function and localization, including the entry of tau into dendritic spines¹⁵⁸, altering normal tau modifications may interfere with A β -induced pathology. We did not find a significant difference in S262 phosphorylation in hippocampal and cortical whole lysates from hAPP and wildtype mice. However, a recent study was able to reduce spine loss in CA3 pyramidal neurons of hAPP-J20 mice by transfection of tau with a serine to alanine mutation at position 262, which prevents S262 phosphorylation¹¹⁸. Regulation of tau functions by phosphorylation of S262, including neurite extension³⁸⁴ and microtubule binding³⁸³, may be critical for A β -induced pathology but not actively regulated by chronic A β *in vivo*.

The extensive modification of tau in normal brains suggests that tau regulation is important, although the exact functions of tau in the adult brain are unclear. It is interesting in this regard that many, if not all, of these modifications are sub-stoichiometric. Phosphorylation of tau was the most abundant modification identified in our study; however, normal tau isolated from human brain tissue appears to carry only an average of 2–4 phosphorylations per molecule³⁹⁵, which we found to be spread out over approximately 9 abundant sites and more than 18 less abundant sites. Lysine and arginine modifications on physiological tau were even less abundant and O-GlcNAc was not detectable without targeted enrichment. Because several tau modifications, particularly those located within the MBRD, prevent tau from binding to microtubules^{24,383} we speculate that many of the modifications we found belong to a small, highly regulated pool of tau that is not bound to microtubules and is free to interact with diverse molecules in different

neuronal compartments. Additional studies are clearly needed to further elucidate the regulation and function of the many posttranslational modifications of tau that occur in health and/or disease.

Chapter 4

Tau Reduction Does Not Prevent Motor Deficits in Two Mouse Models of Parkinson's Disease

By

Meaghan Morris, Akihiko Koyama, Eliezer Masliah and Lennart Mucke

Modified from *PLoS ONE* 2011; 6: e29257

Used under Common Creative Attribution License

Introduction

Neurodegenerative disorders are on the rise, most likely because greater longevity is increasing the age of populations around the world and age is a major risk factor for these conditions³⁹⁶⁻³⁹⁸. Alzheimer's disease (AD) and Parkinson's disease (PD) are the most prevalent of these disorders and no treatments are available to prevent them or halt or reverse their progression. If these diseases had pathogenic mechanisms in common, drugs might be developed to target these mechanisms for the benefit of both patient groups. It is interesting in this regard that AD and PD overlap clinically. A proportion of patients show manifestations of both diseases³⁹⁹⁻⁴⁰³, and first-degree relatives of patients with early-onset AD are at increased risk of developing PD⁴⁰⁴. The two diseases also overlap pathologically. A substantial proportion of AD patients have Lewy bodies in their brain, which are hallmarks of PD^{329,405,406}. Conversely, a proportion of PD patients have amyloid plaques in their brain, which are hallmarks of AD^{407,408}. Both AD and non-demented PD patients have hyperphosphorylated tau^{7,37,409,410}, which aggregates in AD and in some cases of PD without dementia^{3,5,6,10,335,336,411}. In addition, specific variants of the human tau (MAPT) gene appear to be genetic risk factors for PD^{333,412-414}.

Reduction of endogenous murine tau prevents cognitive deficits and various pathological alterations in several transgenic mouse models of AD^{71,83,98,99}. Furthermore, neuronal overexpression of human α -synuclein in transgenic mice causes phosphorylation and aggregation of endogenous tau^{277,410,415,416}. In light of these findings and a recent report that tau reduction prevented dendritic degeneration in a neuronal culture model of mutant LRRK2-linked PD⁴¹⁷, we wondered whether tau reduction is also beneficial in mouse models of PD.

Human PD is characterized, among other things, by motor abnormalities such as slowed movements, rigidity, unstable posture and abnormal gait⁴¹⁸. Pathologically, PD is characterized by loss of dopaminergic neurons in the substantia nigra, degeneration of their tyrosine hydroxylase (TH)-containing projections into the striatum and aggregation of α -synuclein into Lewy bodies⁴¹⁸.

Several of these abnormalities can be simulated in rodent models through administration of neurotoxins that target dopaminergic neurons or neuronal expression of transgenes that encode relevant pathogenic proteins. Unilateral injection of 6-hydroxydopamine (6-OHDA) into the striatum of wildtype

mice causes loss of TH-positive terminals in the striatum on the ipsilateral side and motor deficits⁴¹⁹. This model can be used to address the question whether tau reduction protects dopaminergic neurons in the substantia nigra against neurotoxins and whether tau reduction can prevent motor deficits caused by dopaminergic cell loss. Either of these effects could be beneficial in PD. In a different PD-related model, neuronal expression of human wildtype α -synuclein (SYN) causes motor deficits in transgenic mice⁴²⁰⁻⁴²². This model can be used to address the question whether tau is necessary for α -synuclein-induced pathogenesis. Here, we evaluated both of these models on $Tau^{+/+}$, $Tau^{+/-}$ and $Tau^{-/-}$ backgrounds to determine whether tau reduction diminishes the severity of their motor deficits and pathological alterations.

Results

Tau ablation does not prevent motor deficits caused by 6-OHDA and worsens some deficits

To evaluate the effects of tau reduction acutely and after recovery from 6-OHDA injection, $Tau^{+/+}$, $Tau^{+/-}$ and $Tau^{-/-}$ mice received unilateral injections of 6-OHDA into the striatum and were examined for motor abnormalities in the open field, Rota Rod and pole tests beginning 3 days (Figure 4.1) and 24 days (Figure 4.2) thereafter. Acutely, 6-OHDA injected mice of all three genotypes showed reduced movements and in the open field (Figure 4.1A,B) and reduced latency to fall off the accelerating Rota Rod (Figure 4.1C). 6-OHDA increased the latency to descend the pole in the pole test only in mice with reduced tau levels, but not in wildtype mice (Figure 4.1D). In vehicle injected mice, tau ablation reduced activity in the open field (Figure 4.1A) but did not significantly affect performance in the other tests (Figure 4.1B-D).

After the recovery period, all groups of mice showed a similar level of activity in the open field (Figure 4.2A). Tau ablation also had no effects on recovery of motor functions in the other tests at this stage, with 6-OHDA injected $Tau^{+/+}$ and $Tau^{-/-}$ mice showing no significant differences in rearing, Rota Rod fall latency or pole descent latency (Figure 4.2B-D).

To assess the effect of 6-OHDA on striatal projections from dopaminergic neurons in the substantia nigra, we immunostained brain sections from the behaviorally tested mice for TH (Figure 4.3A). Vehicle treated mice showed no loss of TH staining (Figure 4.3A, quantification not shown). 6-OHDA treatment caused a loss of striatal TH in all three genotypes, and there was a strong trend towards increased TH losses

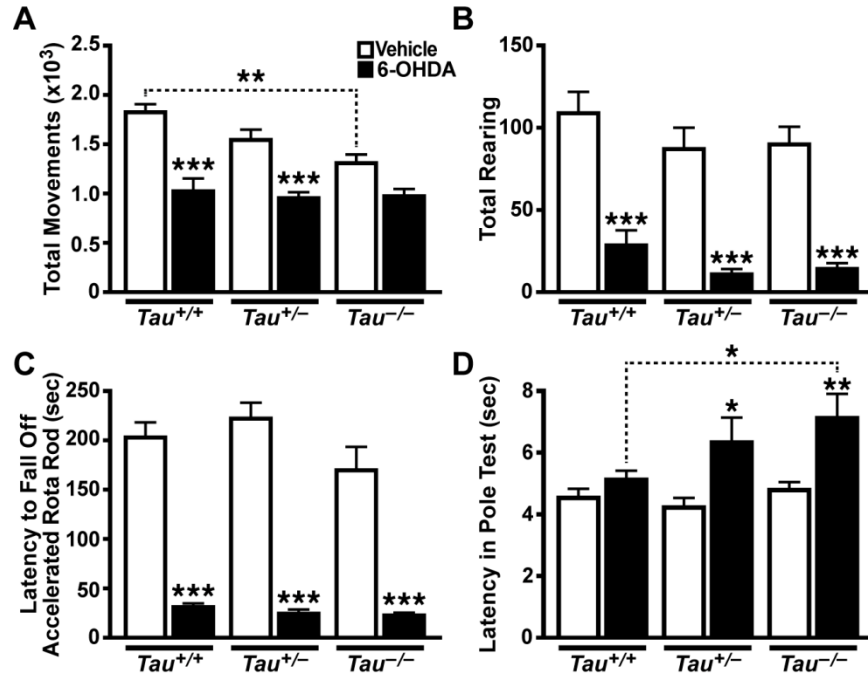


Figure 4.1. Tau reduction does not prevent motor deficits induced by acute striatal 6-OHDA injection. Mice (n=9-12 per treatment and genotype) received a unilateral striatal injection of 6-OHDA or vehicle at 2.6–5.8 months of age and were tested behaviorally beginning 3 days later. A) Total movements in the open field were reduced by 6-OHDA treatment and by tau reduction ($p < 0.0001$ for treatment effect, $p = 0.01$ for genotype effect, and $p = 0.054$ for interaction by two-way ANOVA). B) Rearing in the open field was reduced by 6-OHDA regardless of tau levels ($p < 0.0001$ for treatment effect, $p = 0.09$ for genotype effect, and $p = 0.15$ for interaction by two-way ANOVA after cube-root transformation). C) Latency to fall off an accelerating Rota Rod was reduced by 6-OHDA but not by tau reduction ($p < 0.0001$ for treatment effect, $p = 0.40$ for genotype effect, and $p = 0.22$ for interaction by two-way ANOVA after cube-root transformation). D) Latency to descend in the pole test was increased by 6-OHDA and by tau reduction ($p < 0.0001$ for treatment effect, $p = 0.05$ for genotype effect, and $p = 0.11$ for interaction by two-way ANOVA). * $p < 0.05$, ** $p < 0.01$, *** $p < 0.0001$ vs. vehicle-treated mice of same tau genotype or as indicated by bracket (Bonferroni test with selected comparisons of vehicle vs. 6-OHDA treatment within each genotype, and Tau^{+/+} vs. Tau^{-/-} for each treatment). Error bars represent SEM.

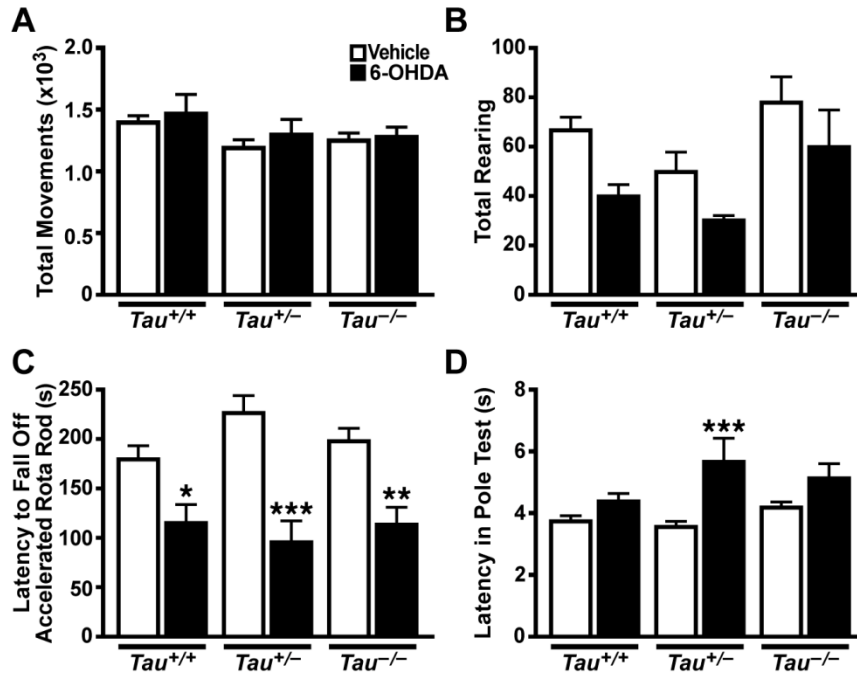


Figure 4.2. Tau reduction does not alter recovery of motor function after 6-OHDA injection. Mice (n=7-12 per genotype and treatment) received a unilateral striatal injection of 6-OHDA or vehicle at 2.6–5.8 months of age and were tested behaviorally beginning 24 days later. A) Total movements in the open field were similar in all groups. B) Rearing in the open field was reduced by 6-OHDA and this abnormality was improved by tau ablation ($p=0.003$ for treatment effect, $p=0.04$ for genotype effect, and $p=0.44$ for interaction by two-way ANOVA after log transformation). C) Fall latency on the accelerated Rota Rod was decreased by 6-OHDA treatment regardless of Tau genotype ($p<0.0001$ for treatment effect, $p=0.71$ for genotype effect, and $p=0.15$ for interaction). D) Latency to descend in the pole test was increased by 6-OHDA mostly in *Tau*^{+/-} mice ($p<0.0001$ for treatment effect, $p=0.04$ for genotype effect, and $p=0.09$ for interaction). * $p<0.05$, ** $p<0.01$, *** $p<0.0001$ vs. vehicle-treated mice of same Tau genotype or as indicated by bracket (Bonferroni test with selected comparisons as in Figure 4.1). Error bars represent SEM.

in 6-OHDA injected mice with reduced tau levels (Figure 4.3B). Thus, tau ablation does not prevent, and may partly enhance, acute motor and pathological deficits induced by 6-OHDA injection.

Tau reduction does not prevent motor deficits in human wildtype α -Synuclein transgenic mice

Mice with neuronal expression of SYN directed by the Thy1 promoter (SYN mice) were crossed onto the *Tau*^{+/+}, *Tau*^{+/-} or *Tau*^{-/-} background. Motor functions of the resulting offspring were assessed at 3.0-4.5 months of age. Independent of Tau genotype, SYN expression caused abnormalities in fall latency in the Rota Rod test (Figure 4.4A), stride length (Figure 4.4B), hind limb clasp reflex (Figure 4.4C), latency to cross a balance beam (Figure 4.4D) and foot slips on the balance beam (Figure 4.4E). Tau reduction did not significantly modulate these effects (Figure 4.4A-E). In mice without SYN, tau ablation increased latency to cross and foot slips on the balance beam (Figure 4.4D and E), but had no significant effect on the other measures.

To assess the effect of tau ablation on the pathology of SYN mice, we examined striatal TH staining in the behaviorally tested mice. Compared with wildtype mice, SYN mice showed no decreases in striatal TH staining on any of the Tau backgrounds (data not shown), consistent with previous findings in SYN/*Tau*^{+/+} mice at this age⁴²³.

Discussion

These findings demonstrate that tau reduction does not protect mice against motor deficits and pathological alterations caused by striatal injection of 6-OHDA or transgene-mediated neuronal expression of SYN. Thus, wildtype murine tau does not appear to contribute causally to PD-like motor deficits and pathological alterations in these models. In contrast, endogenous tau is required for amyloid- β (A β) peptides to impair neurons in primary cultures^{58,65,88} and in human amyloid precursor protein (hAPP) transgenic mice^{71,83,98}. It is also needed for apolipoprotein E4, the most important genetic risk factor for AD, to cause cognitive decline and neuronal loss in knockin mice⁹⁹. However, tau reduction did not alter the age of disease onset or mortality in a mouse model of amyotrophic lateral sclerosis⁸³, providing further support for the conclusion that tau specifically contributes to functional and pathological abnormalities in experimental models of some neurodegenerative disorders but not of others.

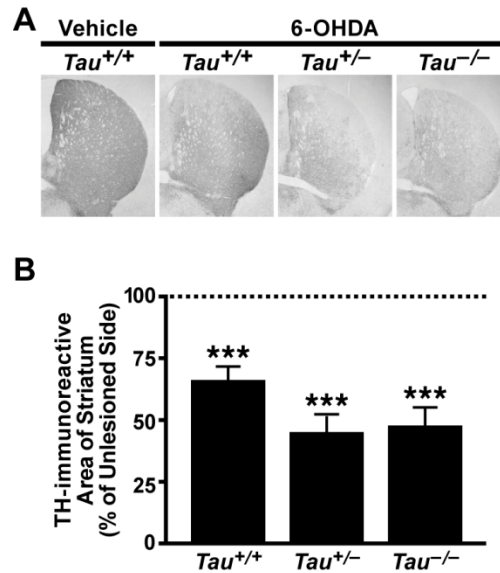


Figure 4.3. Tau reduction does not prevent loss of tyrosine hydroxylase after striatal injection of 6-OHDA. Mice ($n=7-12$ per treatment and genotype) received a unilateral striatal injection of 6-OHDA or vehicle at 2.6–5.8 months of age and were analyzed by tyrosine hydroxylase immunohistochemistry and light microscopy 50 days later. A) Representative photomicrographs from a vehicle-injected wildtype mouse and 6-OHDA injected mice of different Tau genotypes demonstrating loss of tyrosine hydroxylase immunoreactivity in the striatum. B) The effect of 6-OHDA was quantitated by expressing the area of tyrosine hydroxylase immunostaining on the lesioned side as a percentage of that on the unlesioned side of the brain. 6-OHDA caused loss of tyrosine hydroxylase immunoreactivity in the striatum and there was a trend toward greater losses in groups with reduced tau levels. *** $p < 0.0001$ vs. 100% (no loss of dopaminergic projections) by one-sample t-test with a Benjamini-Hochberg correction. One-way ANOVA between groups showed no significant changes. Error bars represent SEM.

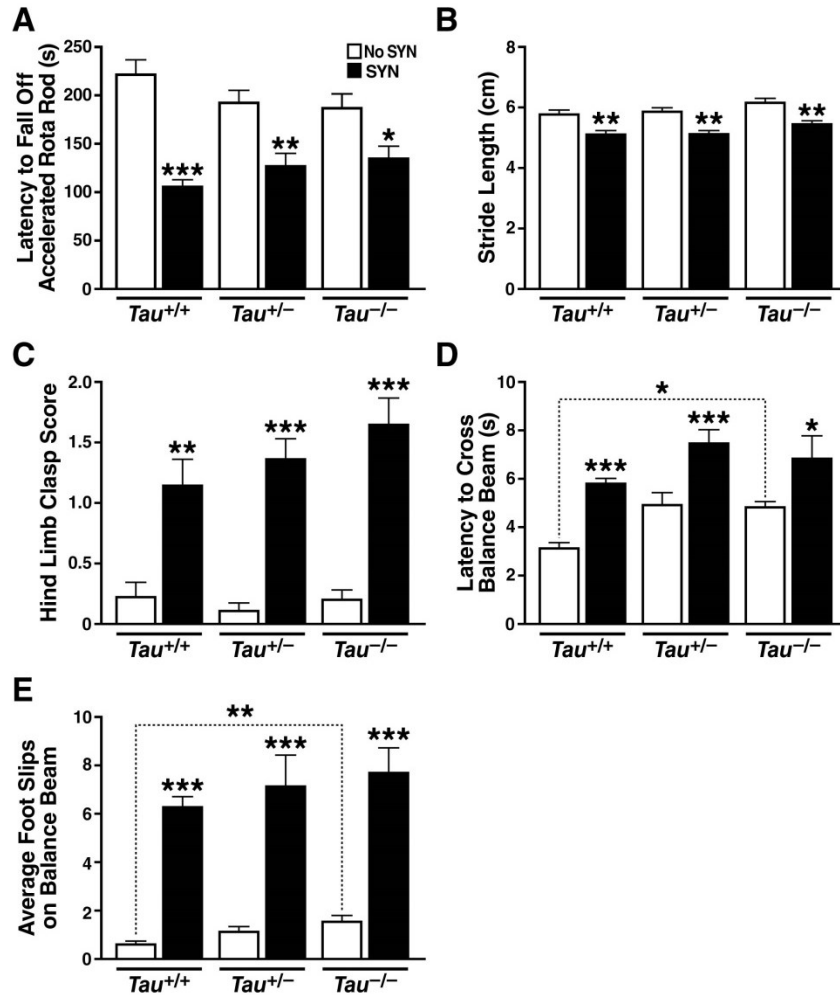


Figure 4.4. Tau reduction does not prevent motor deficits in SYN transgenic mice. SYN mice on different Tau backgrounds ($n=12-15$ per group) were analyzed behaviorally at 3.0–4.5 months of age. A) Transgenic expression of SYN impaired performance on an accelerating Rota Rod, reducing fall latencies. Tau reduction was associated with non-significant trends towards improved fall latencies in mice with SYN and towards impaired fall latencies in mice without SYN ($p<0.0001$ for SYN effect, $p=0.96$ for Tau effect, and $p=0.04$ for genotype interaction by two-way ANOVA). B) SYN mice had shortened stride lengths regardless of Tau genotype ($p<0.0001$ for SYN effect, $p=0.014$ for Tau effect, and $p=0.97$ for interaction by two-way ANOVA). C) SYN mice showed prominent increases in hind limb clasp reflex and tau reduction showed a non-significant trend to worsen this abnormality ($p<0.001$ for SYN effect, $p=0.45$ ($Tau^{+/-}$) and $p=0.91$ ($Tau^{-/-}$) for Tau effects, and $p=0.46$ ($Tau^{+/-}$) and $p=0.48$ ($Tau^{-/-}$) for SYN interaction by probit regression). D, E) Transgenic expression of SYN and tau reduction both increased (D) the latency to cross a balance beam ($p<0.0001$ for SYN effect, $p=0.07$ for Tau effect, and $p=0.94$ for interaction by two-way ANOVA) and (E) the number of foot slips while crossing a balance beam ($p<0.0001$ for SYN effect, $p=0.022$ for Tau effect, and $p=0.19$ for interaction by two-way ANOVA after square root transformation). Between 33–54% of mice in each SYN group had to be excluded from balance beam analysis because they dragged their hind limbs across the beam. * $p<0.05$, ** $p<0.01$, *** $p<0.0001$ vs. mice without SYN on the same Tau genotype or as indicated by bracket (Bonferroni test (A, B, D, E) or Welch's t-test with a Benjamini-Hochberg correction (C) for selected comparisons of + vs. – SYN for each Tau genotype and $Tau^{+/+}$ vs. $Tau^{-/-}$ for each SYN genotype). Error bars represent SEM.

It is important to consider the limitations of the mouse models used in this study and the extent to which one can extrapolate from these models to human PD. Because the 6-OHDA model is caused by an acute insult, it probably does not simulate the etiology of sporadic PD, a notoriously chronic condition. However, it is a robust model of dopaminergic cell loss and of motor deficits resulting from deficient dopaminergic input to the striatum, two cardinal features of PD. Our data suggest that wildtype tau does not enable the neural network dysfunction that underlies such motor deficits. This result was not predictable as tau enables neuronal hypersynchrony in models of AD⁸³ and neuronal hypersynchrony has also been implicated in the pathophysiology of PD^{424,425}. The differential effects of tau reduction in models of AD versus PD suggest that tau plays distinct roles in their pathogenic mechanisms. The SYN mice used in this study model α -synuclein-induced behavioral alterations and may be relevant to the early pathogenesis of PD and other synucleinopathies. However, they do not replicate PD-like neurodegeneration in the substantia nigra at this age⁴²⁶, possibly due to low α -synuclein expression levels in this structure. Our results indicate that tau does not enable or mediate early α -synuclein-induced motor deficits in this model.

Notably, we cannot exclude a pathogenic role of tau in humans with PD or other synucleinopathies or that tau reduction might be of benefit in specific forms of PD, for example, those caused by LRRK2 mutations⁴¹⁷. It is therefore interesting to comment on potential risks of tau reduction beyond lack of therapeutic benefit in forms of PD simulated by the models examined in the current study. Of all the functional outcome measures we evaluated in 6-OHDA injected mice and untreated SYN mice, tau reduction significantly worsened only one: descent latency of 6-OHDA injected mice in the pole test (Figure 4.1D), suggesting that the risk of enhancing PD-like alterations by tau reduction may be low. Tau reduction also had rather subtle effects on pathological measures in the PD models analyzed here. Although tau reduction appeared to exacerbate the 6-OHDA-induced loss of TH immunoreactivity in the striatum, this trend did not reach statistical significance.

Furthermore, tau reduction *per se* had relatively subtle effects in only two of our behavioral tests in vehicle injected controls and untreated mice lacking SYN. In vehicle injected mice, tau reduction was associated with decreased total movements in the open field acutely after the injection (Figure 4.1A), but not after a three week recovery period (Figure 4.2A). In untreated mice lacking SYN, tau reduction

impaired performance on the balance beam (Figure 4.3D, E). However, these impairments were much less severe than those caused by SYN expression ($p=0.009$ for balance beam latency and $p<0.0001$ for foot slips comparing $Tau^{-/-}$ with SYN/ $Tau^{+/+}$ mice by two-tailed t-test). Thus, tau reduction was well tolerated overall and caused only minimal motor deficits. Additional studies are needed to further explore the potential therapeutic value of this strategy in different neurological conditions.

Because tau reduction effectively prevented AD-like abnormalities in hAPP transgenic mice but not PD-like deficits in the models analyzed here, it is tempting to speculate that tau plays different roles also in the human conditions and that tau reduction might be beneficial in AD, but not in the most common forms of PD. Additional studies are needed to further test these hypotheses.

Chapter 5

Network Dysfunction in α -Synuclein Transgenic Mice and Human Lewy Body Dementia

By

Meaghan Morris, Pascal E. Sanchez, Laure Verret, Alexander J. Beagle, Weikun Guo, Dena Dubal,

Kamalini G. Ranasinghe, Akihiko Koyama, Keith A. Vossel, Lennart Mucke

Introduction

Dementia with Lewy bodies (DLB) belongs to a family of common neurodegenerative diseases called synucleinopathies, which are pathologically characterized by the mislocalization and aggregation of the α -synuclein (SYN). DLB, Parkinson's disease (PD), and Parkinson's disease with dementia (PDD) are closely related synucleinopathies, but are distinguished by differences in the relative onset of motor and cognitive impairments and in the distribution of SYN pathology³³⁰. While much is known about the motor impairments in PD, very little is known about the mechanisms of cognitive impairment and cortical network dysfunction in DLB and PDD. DLB and PDD patients have dementia with visual hallucinations, attentional fluctuations, and parkinsonism³³⁰. These symptoms are associated with a prominent slowing of cortical oscillations on electroencephalography (EEG), resulting in a shift in spectral power from higher (alpha, beta, gamma) to lower (delta, theta) frequency bands^{427,428}. However, it remains uncertain whether the neural network and cognitive dysfunction in these conditions are actually caused by SYN.

EEG slowing in neurodegenerative diseases is often attributed to the loss of cholinergic neurons projecting to the cortex. In some Alzheimer's disease (AD) patients, treatment with inhibitors of acetylcholinesterase, administered to compensate for cholinergic denervation, can improve frontal EEG activity and some cognitive functions^{429,430}. DLB patients have a greater loss of cholinergic neurons⁴³¹ and more EEG slowing than AD patients^{427,428}. Although DLB and PDD patients show loss of cholinergic projections in most cortical areas^{431,432}, cholinergic treatment normalizes brain activity only over the frontal cortex, as measured by resting-state fMRI⁴³³, suggesting that other mechanisms contribute to network dysfunction in other cortical regions.

Pharmacologically decreasing presynaptic release of neurotransmitters decreases the power of high-frequency brain oscillations on EEG⁴³⁴. Notably, neuronal overexpression of SYN impairs presynaptic release^{261,262} and causes behavioral deficits in SYN transgenic mice^{272,435}. These findings raise the possibility that SYN causally contributes to neural network dysfunction in DLB and PDD patients. To test this hypothesis, we performed EEG recordings and analyzed the expression of neuronal activity-dependent gene products in SYN transgenic mice, and carried out comparative analyses in humans with DLB.

Results

Table 5.1. Human EEG cohort

Diagnosis (n)	Control Cases (8)	DLB Cases (4)
Age (mean \pm SD)	68.4 \pm 3.0	73.3 \pm 8.3
Gender (M/F)	5/3	2/2
Education (Years) (mean \pm SD)	17.3 \pm 3.0	21.5 \pm 8.1
Handedness (R/L)	4/4	4/0

R, right-handed; L, left-handed

To detect changes in spectral power distribution in DLB patients across a wide frequency range, we recorded EEGs with a high sampling frequency in human subjects (Table 5.1) while they were awake but had their eyes closed. Average spectral power analysis revealed the average dominant peak frequency to be in the alpha range (8–12 Hz) in control subjects and in the theta range (4–8 Hz) in DLB subjects (Figure 5.1A), consistent with previous findings^{427,428}. Typical EEG analysis breaks spectral power into frequency bands, but this provides a relatively poor overall view of spectral power alterations. This is especially true in DLB where the relative power of many frequency bands is altered^{427,428}. Therefore, we analyzed the cumulative distribution function (CDF) of spectral power, which provides a continuous picture of the spectral power changes from 0 to 100 Hz. DLB patients showed a marked left-shift in the spectral power distribution towards slower frequencies as compared to controls (Figure 5.1B). Although DLB subjects had more variable total power than controls ($p=0.0007$, F test), total power was not different between the groups, indicating that their altered power distribution cannot be attributed to a change in total power.

To assess whether neuronal accumulation of SYN could causally contribute to these network abnormalities, we recorded EEGs from 4- to 8-month-old transgenic mice in which the Thy-1 promoter directs expression of human wildtype SYN in neurons^{435,436}. At this age, these mice are cognitively impaired and show abnormal neuronal SYN accumulation in the hippocampus and cortex^{272,435}. EEG and video recordings were obtained while mice were resting in a state of quiet wakefulness or early sleep. Similar to humans with DLB, SYN mice showed a slowing in the dominant resting rhythm and a marked left shift in the spectral power distribution (Figure 5.1C–E). This shift consisted of an increase in delta power and a decrease in the power of theta and higher frequency bands (Figure 5.1C,E). Total spectral power was comparable in NTG and SYN mice, indicating that the power shift in SYN mice reflects primarily a change in power distribution.

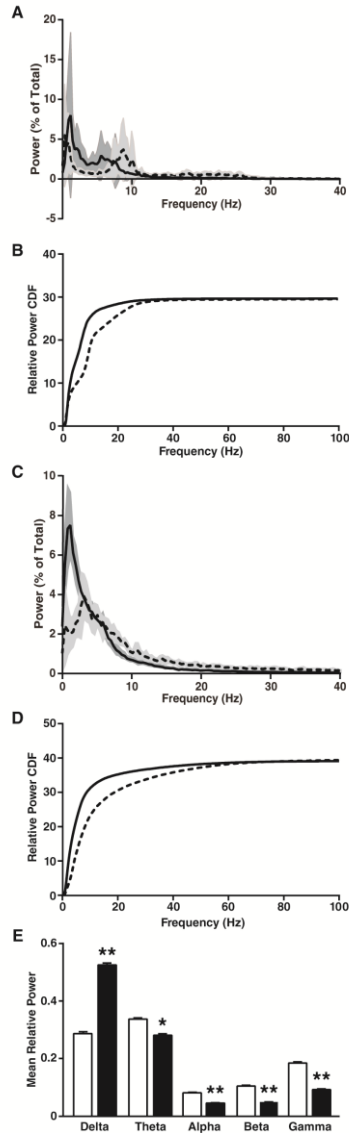


Figure 5.1. Dementia with Lewy bodies (DLB) in humans and neuronal expression of wildtype human α -synuclein (SYN) in transgenic mice cause a similar left shift in EEG spectral power. **(A,B)** Brain oscillations in patients with DLB ($n=4$, solid line) and control subjects ($n=8$, dashed line) were recorded by high sampling frequency EEG/MEG. **(A)** Relative power (in percent of total power) of brain oscillations of different frequencies recorded by EEG over the parietal cortex (0–40 Hz zoom shown for clarity). **(B)** The cumulative distribution function (CDF) of relative power was calculated from high sampling frequency EEG recordings and revealed a shift to lower frequencies in DLB patients ($p<0.0001$ by Kolmogrov-Smirnov test). **(C–E)** SYN mice ($n=14$, solid line and black bars) and NTG littermates ($n=9$, dashed line and white bars) were analyzed by EEG at 4–8 months of age. **(C)** Relative power (in percent of total power) of brain oscillations of different frequencies recorded over the parietal cortex (0–40 Hz zoom shown for clarity). **(D)** Cumulative distribution function of relative power revealed a shift to lower frequencies in SYN mice ($p<0.0001$ by Kolmogrov-Smirnov test). **(E)** Relative power (in percent of total power) of brain oscillations of different frequency bands. Delta 0.5–4 Hz, Theta 4–10 Hz, Alpha 10–13 Hz, Beta 13–20 Hz, Gamma 20.1–99.9 Hz. **A–D:** Black curves represent means and shadings 95% confidence intervals. **E:** * $p<0.05$, ** $p<0.01$ vs. NTG (repeated-measures mixed-effects model of relative power over time with Holm correction). Values are means \pm SEM; some error bars are too small to be visible.

Unexpectedly, EEGs recorded from SYN mice also revealed epileptiform spikes, multi-spike complexes and seizures (Figure 5.2A–E). During the first 24 h of recording, 25% (7/28) of SYN mice and 0% (0/14) of NTG controls had at least one seizure. The seizures we observed in SYN mice were of two types. The first, more common type (Figure 5.2D) had a typical electrographic seizure pattern and was usually accompanied by forelimb clonus, abnormal tonic posture and tail extension. These seizures were typically of moderate intensity and rarely caused only behavioral arrest or escalated into full running/jumping activity. The second type of seizure (Figure 5.2E), which we refer to as a myoclonic burst seizure, consisted of periodic, large amplitude spikes or multi-spike complexes and was accompanied by myoclonic jerks typically involving the neck, shoulder and forelimb. Myoclonic burst seizures did not usually evolve into other types of seizures. Both types of seizures symmetrically involved both hemispheres. During a 24-h recording session, most SYN mice with seizures demonstrated only one or the other of these seizure types.

We next looked for immunohistochemical changes in the hippocampus that are typically caused by epileptic activity⁴³⁷⁻⁴⁴⁰. Compared with NTG controls, SYN mice had reduced levels of calbindin in granule cells of the dentate gyrus and the stratum radiatum of CA1 (Figure 5.3F–H), increased or ectopic expression of neuropeptide Y (NPY) in the molecular layer of the dentate gyrus and the mossy fiber pathway (Figure 5.2F,I–J), and fewer cfos-positive granule cells (Figure 5.2F,K). All of these changes are seen in the presence of recurrent seizure activity^{437,438,441}. An independent line of transgenic mice expressing SYN under the PDGF promoter showed similar hippocampal alterations (Figure 5.3), making it unlikely that the abnormalities we detected in the Thy1-SYN line were caused by insertional mutagenesis or other positional effects resulting from the integration of the transgene into the genome.

To determine whether epileptic activity is sufficient to cause a left shift in spectral power, we examined transgenic mice with neuronal expression of mutant human amyloid precursor protein (hAPP) from line J20^{83,347,439,442}. These mice exhibit robust epileptic activity and have dysregulated gamma activity^{439,443}. A side-by-side comparison of EEG recordings in SYN and hAPP mice matched for age and background strain revealed clear differences in resting spectral power. SYN mice again showed a left shift in spectral power compared to NTG littermates, whereas hAPP mice and NTG littermates showed a similar

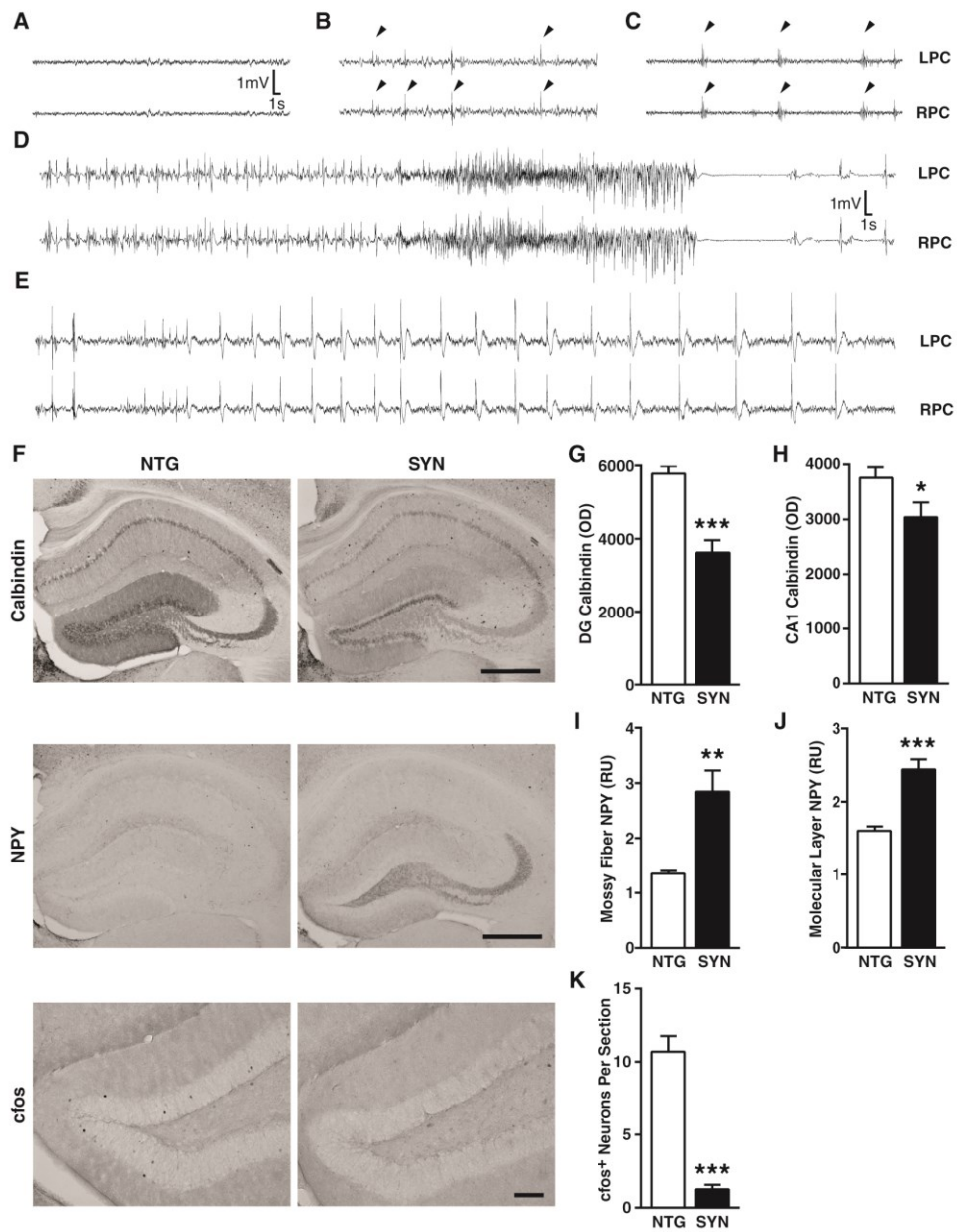


Figure 5.2. Epilepsy and related immunohistochemical alterations in SYN mice. (A–E) Representative EEG traces showing normal activity in a NTG mouse (A) and frequent epileptiform spikes (arrowheads in B), multi-spike complexes (arrowheads in C), a seizure (D) accompanied by tail extension and bilateral forelimb clonus (not shown), and a myoclonic burst seizure (E) in SYN mice. (F–K) Hippocampal changes in neuronal activity-dependent proteins in SYN mice (n=11–15 mice per genotype, age 5–7 months). Hippocampal sections from SYN and NTG mice were immunostained for calbindin, NPY or cfos and analyzed by densitometry (calbindin/NPY) and cell counting (cfos). (F) Representative images from NTG and SYN mice. Scale bars: 0.5 mm (Calbindin/NPY) and 0.1 mm (cfos). Calbindin was measured in the molecular layer of the dentate gyrus (G) and the stratum radiatum of CA1 (H), NPY in the mossy fibers (I) and the molecular layer (J), and cfos-positive cells in the granular layer (K). LPC, left parietal cortex; RPC, right parietal cortex; DG, dentate gyrus; OD, optical density; RU, relative units. * $p < 0.05$, ** $p < 0.01$, *** $p < 0.001$ (Student's *t*-test). Quantitative values represent means \pm SEM.

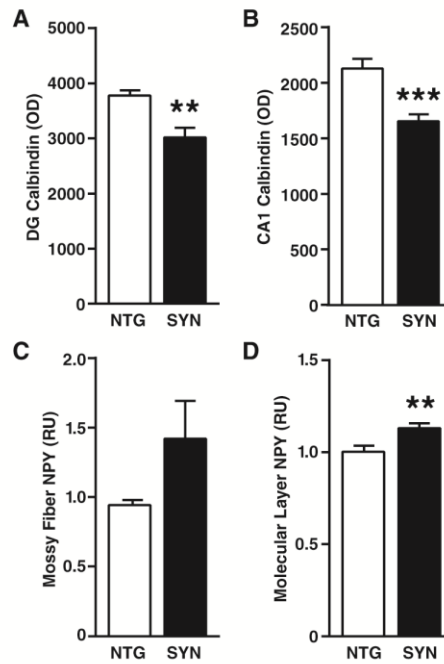


Figure 5.3. Neuronal expression of SYN directed by the PDGF promoter also causes hippocampal changes in activity-dependent proteins in an independent line of transgenic mice. (**A–D**) Hippocampal sections from PDGF-SYN mice and NTG controls were immunostained for calbindin or NPY and analyzed by densitometry (n=8 mice per genotype). Calbindin was measured in the molecular layer of the dentate gyrus (**A**) and the stratum radiatum of CA1 (**B**), and NPY in the mossy fibers (**C**) and the molecular layer (**D**) of the dentate gyrus. DG, dentate gyrus; OD, optical density; RU, relative units. ** $p < 0.01$, *** $p < 0.001$ (Student's t-test). The age of mice ranged from 3–17 months and was not significantly different between NTG and SYN mice (mean \pm SEM: 9.1 ± 1.39 for NTG and 10.4 ± 1.75 for SYN mice, $p = 0.57$ by Student's t-test). Bars represent means \pm SEM.

resting spectral power distribution (Figure 5.4A). Therefore, neuronal expression of transgene-derived proteins and epileptic activity are not sufficient to cause a left shift in spectral power during a resting EEG.

We next assessed more directly if epileptic activity contributed to spectral changes in SYN mice. Acute injection of phenobarbital (5 mg/kg, *i.p.*) decreased interictal epileptiform events by 55% but did not affect spectral power in SYN mice (Figure 5.4B–C). Similarly, ablation of the microtubule-associated protein tau, which has been shown to reduce epileptic activity in a variety of seizure models^{71,83,98,111,350}, tended to reduce interictal events by roughly 50% but, if anything, tended to slightly increase the left shift in spectral power in SYN mice (Figure 5.4D–E). Tau ablation also reduced some seizure-related biochemical alterations in the hippocampus of SYN mice (Figure 5.4F–H), although alterations in granule cell calbindin and mossy fiber NPY were not affected (data not shown). Thus, neither acute nor chronic reduction of epileptiform activity altered spectral power in SYN mice, suggesting that epileptiform activity may not be a critical cause or mediator of the left shift in spectral power.

Inhibiting cholinergic signaling in rats caused a left shift in spectral power similar to the shift we observed in untreated SYN mice^{444,445}. We therefore wondered whether increasing cholinergic neurotransmission by inhibiting acetylcholinesterase might reverse spectral changes in SYN mice. Donepezil, an acetylcholinesterase inhibitor, was injected daily (1 mg/kg, *i.p.*) for 14 days and EEG recordings were performed just before the treatment began (baseline), after the last injection, and after a washout period of 7 days. Donepezil did not reverse the spectral power shift in SYN mice, although there was a trend toward a right-shift in the power distribution in both NTG and SYN mice (Figure 5.4I).

Although oscillatory abnormalities in DLB patients have been well documented^{427,428}, few studies have examined neural network excitability in these patients. One small study raised the possibility of an increased incidence of seizures in DLB patients⁴⁴⁶ and a second group documented cortical myoclonus, a form of cortical hyperexcitability, in DLB patients⁴⁴⁷. To look for additional evidence of aberrant network excitability in these patients, we examined calbindin levels in their dentate gyrus. Patients with temporal lobe epilepsy or AD show reduced calbindin levels in dentate granule cells, and such calbindin reductions are thought to reflect aberrant hippocampal excitability^{348,448,449}. Using qRT-PCR, we determined calbindin

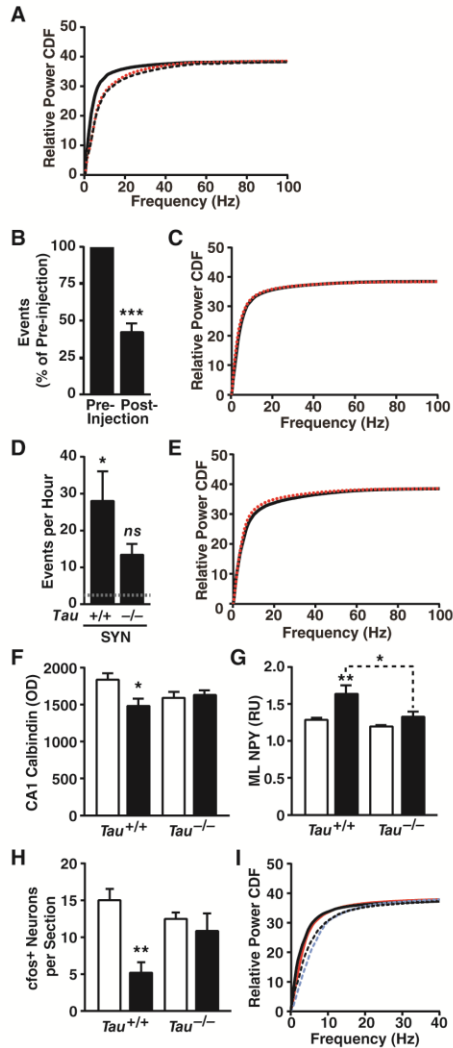


Figure 5.4. Modulation of epileptic activity does not shift spectral power. **(A)** Thy1-SYN mice (black solid line), hAPP-J20 mice (red dotted line) and their combined NTG littermate controls (black dashed line) were compared by EEG (n=3–7 mice per group, age 4–5 months). SYN mice showed a left shift, whereas hAPP mice did not (NTG vs. SYN $p < 0.0003$, hAPP vs. SYN $p < 0.0003$, NTG vs. hAPP $p = 0.06$, by Kolmogrov-Smirnov test with Holm correction). **(B,C)** Acute injection of phenobarbital (5 mg/kg, *i.p.*) reduced interictal spike activity **(B)** but did not alter the spectral power distribution **(C)**, $p = 0.70$ by Kolmogrov-Smirnov test) in SYN mice (pre-injection, black solid line; post-injection, red dotted line; n=6–10 mice, age 3–7 months). **(D, E)** Genetic ablation of tau caused a trend towards reduced epileptic activity **(D)**, $p = 0.17$ by Tukey test multiply adjusted p value) and a trend toward an increased left shift in spectral power distribution **(E)**, $p = 0.09$ by Kolmogrov-Smirnov test) in SYN mice ($Tau^{+/+}$, black solid line; $Tau^{-/-}$, red dotted line; n=6–7 mice per genotype, age 4–7 months). Dotted line in D represents the average level in NTG controls. **(F–H)** Hippocampal sections from $Tau^{+/+}$, $Tau^{-/-}$, SYN/ $Tau^{+/+}$ and SYN/ $Tau^{-/-}$ littermates (No SYN, white bars; SYN, black bars; n=10–13 mice per genotype, age 4–5 months) were immunostained for calbindin, NPY or cfos and analyzed by densitometry (calbindin/NPY) or cell counting (cfos). Calbindin was measured in the stratum radiatum of CA1 **(F)**, NPY in the molecular

layer **(G)**, and cfos-positive cells in the granular layer **(H)**. **(I)** Donepezil (1 mg/kg, *i.p.*) was injected once daily for 14 days in SYN mice and NTG controls (n=3–6 mice per genotype and treatment, age 4–6 months). Spectral power distribution in NTG and SYN mice is shown for the last day of donepezil treatment (NTG, blue dashed line; SYN, red solid line) and after 7 days of drug washout (NTG, black dashed line; SYN, black solid line). Kolmogorov-Smirnov test with Holm correction revealed a genotype effect during ($p = 0.002$) and after ($p < 0.005$) donepezil treatment, but no effects of treatment in SYN mice ($p = 0.84$) or NTG controls ($p = 0.90$). 0–40 Hz zoom shown for clarity. **A,C,E,I:** Quantitative values are means. **B,D,F–H:** * $p < 0.05$, ** $p < 0.01$ vs. NTG or as indicated by brackets (Tukey test), *** $p < 0.001$ vs. pre-injection baseline (one-sample t-test). Bars represent means \pm SEM. ML, molecular layer; OD, optical density; RU, relative units.

Table 5.2. Human *postmortem* tissues

Diagnosis (n)	Age (mean ± SD)	Sex (M/F)	RNA Integrity Number (mean ± SD)
No neurodegenerative disease (3)	84 ± 5.0	2/1	7.8 ± 0.2
DLB with marked AD pathology (6)	78 ± 4.5	5/1	6.1 ± 2.0
DLB with minimal AD pathology (5)	77 ± 5.4	4/1	5.3 ± 0.6
AD (7)	79 ± 2.9	2/5	6.5 ± 1.3

mRNA levels in the dentate gyrus obtained *postmortem* from humans with neocortical DLB pathology and low or high levels of AD pathology (Table 5.2). Dentate gyrus samples from AD cases and from people without neurodegenerative disease were used as positive and negative controls, respectively^{348,449}. DLB cases without AD pathology showed markedly reduced levels of calbindin mRNA in the dentate gyrus, similar in extent to reductions seen in AD (Figure 5.5). The most striking loss of calbindin mRNA was observed in DLB cases with a high level of AD pathology (Figure 5.5).

To further assess whether aberrant network excitability may contribute to SYN-related dementia, we reviewed the charts of patients who were seen at the UCSF Memory and Aging Center between 2007 and 2012 and who met research criteria for DLB³³⁰ (Table 5.3). We searched the charts for myoclonus and seizure disorders, both of which are thought to result from aberrant network excitability^{447,450,451}.

Table 5.3. Humans with DLB analyzed

Characteristic	DLB (158)	Age at Onset Model (<i>p</i> -value)
Sex (M/F)	94/64	0.002
Education (Years) (mean ± SD) ¹	15.5 ± 3.9	0.42
Handedness (R/L/A)	140/14/4	0.95
Patients with fluctuations (%)	100 (61.7%)	0.60
Patients with a seizure disorder (%)	5 (3.2%)	0.71
Patients with myoclonus (%) ²	34 (21.5%)	0.007
Age at onset of cognitive decline (mean ± SD) ³	69.7 ± 8.85	-

DLB, dementia with Lewy bodies; R, right-handed; L, left-handed; A, ambidextrous

¹One DLB patient was missing education information.

²One DLB patient had both myoclonus and a seizure disorder.

³Three DLB patients had an unclear age at onset.

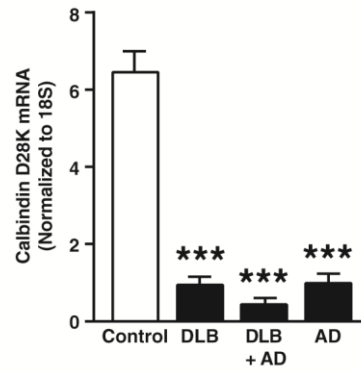


Figure 5.5. Reduction of calbindin mRNA levels in the dentate gyrus of humans with DLB and/or AD pathology. Calbindin mRNA levels in *postmortem* tissue samples were quantified by qRT-PCR and normalized to 18S RNA as a loading control. n=3 controls without neurodegenerative disease, n=5–7 cases per disease group. In cases with DLB plus high AD pathology (DLB+AD), there was an interaction between AD and Lewy body pathology ($p < 0.001$ by two-way ANOVA). *** $p < 0.001$ vs control (Tukey test). Values are means \pm SEM.

Myoclonus was noted in 21.5% (34/158) of patients with clinically diagnosed DLB, consistent with the estimated prevalence of myoclonus in pathologically-confirmed cases of diffuse Lewy body disease⁴⁵². Myoclonus and male gender were associated with a lower age of onset of cognitive impairment (65.9 ± 8.22 with myoclonus, 70.68 ± 8.77 without myoclonus; 67.9 ± 8.77 male, 72.4 ± 8.32 female) in a mixed effects linear model (Table 5.3). The incidence of myoclonus in DLB was markedly higher than that in an age-matched reference population (Table 5.4 and Caviness, *et.al.* 1999⁴⁵³).

Roughly 3% (5/158) of patients with DLB were noted to have a seizure disorder. An additional 7.6% (12/158) of DLB patients were suspected to have a seizure disorder but were not formally diagnosed. The first unprovoked seizure in epileptic DLB patients typically occurred near the time of dementia diagnosis (median -1 year relative to diagnosis, range -4 to +1), but was not related to the age of onset of cognitive impairment (73.0 ± 7.55 with epilepsy vs. 69.6 ± 8.89 without epilepsy). The incidence of new-onset, unprovoked seizures in our DLB population tended to be higher than that of an age-matched general population (Table 5.4 and ⁴⁵⁴). However, the magnitude of the effect was difficult to evaluate due to the small number of events during the incidence study period.

Table 5.4. Incidence of seizures and myoclonus in humans with DLB by age

Clinical Sign	Age ¹	n	Population	Incidence ²	Relative Rate (95% CI)
Seizures	70-79	1	71	234.7	1.5 (0.2-11.2) ³
	80+	2	36	925.9	5.4 (1.3-22.8) ³
Myoclonus	50-69	7	42	2777.8	1450.1 (424.5-4953.7) ⁴
	70+	11	102	1797.4	248.3 (96.2-640.4) ⁴

¹Age-ranges dictated by epidemiological studies in control populations

²per 100,000 person-years

³compared to Forsgren, *et.al.* 1996⁴⁵⁴

⁴compared to Caviness, *et.al.* 1999⁴⁵³

Autopsies were obtained in 12 DLB patients and revealed a high diagnostic accuracy for neocortical Lewy bodies: 11 out of 12 cases were confirmed pathologically; one case showed only AD pathology. Based on McKeith criteria³³⁰, there was a high likelihood that Lewy body pathology accounted for dementia in 6 cases and an intermediate likelihood for the remaining 5 cases, which had high levels of concomitant AD pathology. Four DLB patients with myoclonus that came to autopsy all had neocortical Lewy bodies; two of them also had numerous plaques and tangles, one had a high level of plaques without

tangles, and one had no appreciable AD pathology. However, the low number of autopsies precluded us from reliably assessing the relative contributions of DLB and AD pathology to clinical features.

Discussion

Our study demonstrates that neuronal overexpression of wildtype human SYN causes a left shift in spectral power in transgenic mice that closely resembles spectral alterations in humans with DLB. This finding supports the hypothesis that accumulation of SYN, which characterizes DLB pathologically, is at least partly responsible for network dysfunction in DLB patients. We further obtained evidence for aberrant network excitability in SYN mice and in humans with DLB.

The most direct evidence for aberrant network excitability in SYN mice consisted of interictal spikes and intermittent seizures that were associated with typical alterations on EEG and in motor behavior. These functional changes were accompanied by immunohistochemical alterations in the hippocampus that typically result from aberrant network excitability, including reduced calbindin levels. Reduced calbindin expression in the dentate gyrus was also detected in DLB patients. Notably, it is likely that calbindin depletion in the hippocampus is a more sensitive indicator of aberrant network excitability than routine scalp EEG, which can easily miss intermittent epileptiform events and is notoriously insensitive to epileptic activity in deeper brain regions such as the hippocampus^{455,456}.

A limitation of our mouse experiments is that all spectral analyses were performed on EEG recordings obtained over the parietal cortex of resting mice. We focused on this brain region because it shows a spectral shift in DLB (Figure 5.1 and Bonanni, *et.al.* 2008⁴²⁸), and on resting behavior in mice to mimic human EEG conditions. Recordings from other brain regions and task-related spectral analyses may provide additional insights into neuronal network dysfunction. For example, EEG recordings over the frontal cortex might be more suitable for assessing potential contributions of cholinergic deficits to spectral alterations in SYN mice, and analysis of individual EEG recordings in actively exploring mice could help reveal the kind of dysregulation of gamma oscillations we observed in hAPP-J20 mice⁴⁴³.

While overexpression of human SYN caused obvious seizure activity in transgenic mice, the more chronic accumulation of endogenous SYN in DLB patients may primarily cause more subtle signs of

aberrant network excitability such as myoclonus. Myoclonus in DLB and PD consists of a sudden brief jerk that is accompanied by a sharp transient in the contralateral sensorimotor cortex on EEG^{447,450}. This type of myoclonus, called cortical myoclonus, may be caused by aberrant cortical excitability^{447,450,451} and has been successfully treated with anti-epileptic drugs⁴⁵⁷⁻⁴⁵⁹. Interestingly, levels of SYN in the sensorimotor cortex were higher in PD patients with myoclonus than in those without⁴⁶⁰. Increased cortical SYN pathology may also explain why myoclonus is more frequent, and is thought to be more severe, in DLB patients than in PD patients^{447,452}.

In patients with early AD and a seizure disorder, a substantial proportion of the seizure activity was non-convulsive and could have easily been missed on routine exams⁴⁵⁶. This caveat may also apply to DLB. Indeed, symptoms similar to those associated with non-convulsive seizures, such as staring spells and disorganized speech, can occur during the episodes of fluctuating consciousness often seen in DLB patients. These episodes make it particularly difficult to distinguish between epileptic and non-epileptic symptoms. Among the DLB cases we reviewed, 2 out of 5 patients with a diagnosed seizure disorder had only non-convulsive seizures and another 10 patients were suspected to have this type of seizure. Although we compared the incidence of myoclonus and seizures to the best reference populations we could find in the literature⁴⁶¹, our relative rate calculations may be confounded by differences in racial and age distributions in the San Francisco Bay Area versus Rochester, Minnesota and Umeå, Sweden^{453,454}. A prospective clinical study is needed to more accurately determine the incidence of seizures and myoclonus in DLB patients.

We previously identified co-pathogenic interactions between A β and SYN in hAPP/SYN doubly transgenic mice³³² that may be relevant to the frequent co-occurrence of DLB and AD pathology^{14,329,462}. Because clinical assessment alone cannot reliably detect the co-occurrence of these pathologies¹⁴, an obvious limitation of our study is the lack of autopsy confirmation of most cases we analyzed by chart review or EEG. However, spectral slowing has been documented in autopsy-confirmed cases of DLB⁴⁶³ and was confirmed here with a different approach to spectral analysis. Furthermore, the reduction in calbindin mRNA was identified in cases with pathologically confirmed DLB, AD, or both and suggests that

SYN pathology is sufficient to cause aberrant network excitability. Again, a prospective study of DLB with imaging for AD pathology and/or autopsy confirmation is needed to further test this hypothesis.

In conclusion, our analysis of experimental models clearly demonstrates that SYN accumulation causes both a shift in the EEG spectrum towards slower brain oscillations as well as aberrant network excitability. We also obtained evidence suggesting that the mechanisms underlying these network effects may be at least partly distinct. While treatments targeting SYN should block both types of network dysfunction, drugs with different modes of action may have to be combined in order to block divergent branches of the SYN-induced pathogenic cascade further downstream. Recent evidence suggests that the hyperactivation of specific neural networks may contribute to cognitive deficits in early stages of AD and that specific anti-epileptic drugs may be able to reverse synaptic, network and cognitive dysfunction in this condition and related models^{442,456,464}. Although acute or chronic reduction in epileptiform activity in SYN mice did not affect their abnormal spectral distribution, it should be noted that the interventions used in this study achieved only a partial suppression of epileptiform activity in these mice. Additional studies are needed to further evaluate the interdependence between the different types of DLB-associated network dysfunctions and to determine the extents to which they contribute to the cognitive decline and behavioral alterations observed in this condition.

Chapter 6

Insights into the Functional Roles of Tau and α -Synuclein in Neurodegenerative Disease

By

Meaghan Morris

Tau and α -synuclein (SYN) are both critical proteins for the development of several common neurodegenerative diseases. Our studies provide further insights into the different functional roles of tau and SYN in these diseases. Genetic tau ablation, which is relatively benign by itself, reduces epileptiform activity and interrupts A β -induced pathogenic mechanisms, raising the possibility that A β converts tau into an active mediator of its pathogenic effects. Our studies suggest that abnormal tau modification by A β -induced signaling pathways may not be required for tau to enable A β -induced adverse effects because tau was similarly modified at many sites in hAPP and wildtype mice. However, as we discuss below, the study of tau modifications was suggestive, rather than conclusive. Tau does not mediate oscillatory neural network abnormalities and motor impairment in SYN mice, though tau ablation tends to reduce epileptic activity in these mice consistent with its anti-epileptic effects.

We were able to conclusively demonstrate that tau reduction is safe in aged tau knockout mice under normal conditions. Tau ablation had no effect on learning or memory, and caused mild weight gain and motor impairments that were indistinguishable from wildtype mice by 21 months of age. These mild impairments were not L-DOPA responsive, nor were they associated with loss of striatal dopamine, loss of tyrosine hydroxylase, or iron accumulation. In agreement with the first studies of aged tau knockout mice⁹⁷, tau ablation is benign in the absence of iron accumulation. Tau reduction, which more closely models a therapeutic situation, caused no behavioral alterations whatsoever.

We were unable to fully address whether altered tau modifications may contribute to impairments in the human amyloid precursor protein (hAPP) J20 model of AD. We mapped more than 63 endogenous tau modifications in hAPP and wildtype mice, but we could only compare 31 of these modifications in whole cortical and hippocampal lysate. These 31 modifications failed to show significant, consistent changes between genotypes. In the post-synaptic density, we compared 16 tau modifications between the two genotypes, which also failed to show significant changes. There were 5 modifications mapped only in hAPP mice, 4 of which were in the MRBD. Nearly half of all lysine methylation sites mapped (2/5) were found in the MRBD only in hAPP mice, suggesting that lysine methylation may be increased in hAPP mice. However, these modifications were low abundance, appeared rarely in our hAPP samples and were not observed in the quantitative experiments, making it difficult to determine whether the modifications

were truly specific to hAPP mice. Our data supports the hypothesis that tau mediates impairments in hAPP mice through its normal function, however, we cannot exclude that low abundance tau modifications are altered, or that tau modifications are altered at another age, in another cellular compartment, or that changes in tau localization can mediate impairments in hAPP mice. We were able to map many novel tau modifications on endogenous tau which should facilitate future studies of tau regulation.

Tau did not mediate motor impairments or dopaminergic cell death in two mouse models of PD-like pathology. Tau ablation tended to worsen motor impairments and acute dopaminergic cell death induced by 6-hydroxydopamine treatment, implying that tau may be required for the preservation of dopaminergic cell health in specific stressor conditions. Tau ablation had no effect on the motor impairments in a SYN transgenic model, implying that SYN does not require tau for some types of neural network dysfunction. The extent to which these findings generalize to other toxic models of dopaminergic cell death or other synucleinopathy models remains to be determined. However, our findings imply that tau-targeted therapies would not benefit motor impairments in synucleinopathy patients.

In addition to motor impairments, SYN induces a left-shift in the spectral power of cortical oscillations and seizures in transgenic mice. DLB patients showed a similar left-shift in spectral power and calbindin reduction in the dentate gyrus, indicative of aberrant network excitability. This reduction occurred in the absence of significant AD pathology, though co-occurrence of DLB and AD pathology synergistically lowered calbindin in the dentate gyrus. Myoclonus, a clinical sign of aberrant network excitability, was present in nearly one quarter of DLB patients, however future studies with a higher proportion of autopsies or with imaging for AD pathology will be required to determine the degree of aberrant network excitability attributable to SYN pathology. Aberrant network excitability in SYN mice could be reduced by acute administration of phenobarbital or tau ablation; neither intervention significantly altered the spectral power shift. Aberrant network excitability in hAPP mice was insufficient to cause a left shift in spectral power, which suggests, in combination with the previous results, that spectral power alterations are not caused by aberrant network excitability. While our suppression of epileptiform activity is similar to the 50% suppression of epileptiform activity required to rescue cognitive impairment in hAPP mice⁴⁴², it is possible

that a reduction greater than 50% in SYN mice is required to alter spectral power. Future studies are needed to determine how SYN causes these two, potentially distinct, types of neural network dysfunction.

After our publication in 2013, two other investigators published studies regarding the effects of tau reduction in aging mice. One study of tau knockout mice at 22-25 months of age confirmed the absence of cognitive or motor deficits, iron accumulation or loss of tyrosine hydroxylase (TH), while the mice retained the seizure resistance characteristic of younger tau knockout mice³⁴⁹. The second study found mild motor impairment and TH loss at 8-9 months of age, with cognitive impairments by 21 months of age⁴⁶⁵. Interestingly, TH-positive neurons did not die in motor-impaired tau knockout mice because TH staining in the substantia nigra could be restored by dietary supplementation of docosahexaenoic acid and α -lipoate starting at 14-15 months of age⁴⁶⁵. Some of the contradictory findings in tau knockout mice may be due to the differential susceptibility of tau knockout neurons to different types of stress. As we suggested earlier, dopaminergic neurons in tau knockout mice may be particularly susceptible to specific challenge conditions, which may include iron accumulation¹⁰⁷, neuroinflammation or a high fat diet deficient in neuroprotective fish oils⁴⁶⁵. One caveat to the cognitive and dopaminergic impairments in tau knockout mice is that they have only been described when unrelated mice on the same genetic background were compared^{107,465}, while littermate-controlled studies of aged tau knockout mice show normal cognition and no neuronal loss¹⁰⁷ (Chapter 2). Future studies should determine whether neuroinflammation or cerebral iron accumulation can induce robust deficits in tau knockout mice compared to wildtype littermates. Notably, no behavioral deficits have been shown in tau hemizygous mice at any ages (Chapter 2) and tau reduction continues to confer resistance to PTZ-induced seizures at old ages³⁴⁹. The normal behavior of aged tau hemizygous mice suggests that tau reduction in aged humans may be safe, while the resistance to induced aberrant network excitability suggests that tau reduction may continue to be effective against an important mechanism of AD pathogenesis at older ages.

Tau appears to be a specific mediator of AD and aberrant network excitability. Tau is phosphorylated in response to many different challenging conditions *in vitro* and *in vivo*, and is increased in many neurodegenerative conditions, including AD, PD, prion diseases and in glia in multiple sclerosis^{466,467} (Chapters 1&4). However, tau ablation only improves behavioral impairments, biomarker alterations and

premature mortality in models of AD and epilepsy^{71,83,98,99,350}. Mouse models of amyotrophic lateral sclerosis⁸³, prion infection⁴⁶⁶, multiple sclerosis⁴⁶⁷ and PD (Chapter 4) do not seem to benefit from tau reduction. Tau ablation tended to worsen acute motor impairment and dopaminergic cell loss in the 6-hydroxydopamine model of PD (Chapter 4), and significantly worsened behavioral scores and spinal axon damage in the acute phase of an experimental autoimmune encephalomyelitis model of multiple sclerosis⁴⁶⁷. This confirms our hypothesis that tau reduction is not a general neuroprotective intervention, but interferes with specific pathways involved in aberrant network excitability. These findings also imply that tau may not be the primary mediator of cellular toxicity in PD, multiple sclerosis or prion diseases, even when hyperphosphorylated tau is present. It is possible that hyperphosphorylated tau requires a specific cellular environment or localization to confer toxicity, or that the hyperphosphorylated tau in PD, multiple sclerosis and prion diseases is not toxic. The modification and aggregation states which are required for tau to cause toxicity are not known.

The numerous and varied endogenous tau post-translational modifications imply a multiplicity of highly regulated tau functions. We described a large number of modifications on endogenous tau, including the largely unexamined arginine methylation. This recently discovered³⁵³ type of tau modification has no known competing arginine modifications and clusters in the N-terminal projection domain of tau, which presents an exciting opportunity to discover novel mechanisms of tau regulation. Future studies using immunohistochemistry and mass spectrometry should determine whether arginine methylation alters the subcellular localization of tau or the affinity of tau for Fyn, tubulin, actin and other binding partners.

Endogenous tau modification in the MRBD may create a small pool of tau not bound to microtubules. Tau phosphorylation and acetylation in the MBRD can prevent the binding of tau to microtubules^{24,383} and were found on a fraction of endogenous tau in our study. MRBD modification may serve to direct a portion of tau to other locations or functions in the cell. For example, phosphorylation of S262 in the MBRD prevents tau from binding to microtubules³⁸³ but is necessary for proper neurite extension³⁸⁴, suggesting that S262 phosphorylation directs tau away from microtubules into a signaling pathway for neurite extension. We speculate that tau pathology in disease may emerge from such non-microtubule-bound tau, which is probably also more accessible for enzymatic modification.

Future studies are needed to dissect the role of tau and tau modifications in aberrant network excitability. Tau facilitates genetically- and chemically-induced epileptic activity^{71,111,350} (Chapter 5). As tau modifications may play a role in the impairments of hAPP transgenic mice, tau modifications may also play a role in the facilitation of epileptic activity, regardless of whether chronic epileptic activity alters tau modifications. Dynamic changes in tau phosphorylation are observed after acute induction of seizures by kainic acid injection; tau phosphorylation is reduced within 6 hours after injection, then elevated 10-48 hours after injection⁴⁶⁸. Whether acute epileptic activity changes other tau modifications is not known. The tau modification state in chronic epileptic models is also unclear, however, the similar modification levels of hAPP and wildtype tau would indicate the chronic epilepsy may not alter tau modifications. Determining which tau modifications are required for aberrant excitatory activity may provide alternate therapeutic strategies for the treatment of epilepsy and AD.

Tau ablation did tend to reduce epileptic activity and the associated hippocampal remodeling in SYN mice without affecting motor deficits or spectral alterations. The mechanisms by which SYN produces these diverse types of network dysfunction remain unclear. While SYN-induced seizures may seem inconsistent with the notion that SYN decreases pre-synaptic release, it is possible that specific populations of interneurons may be preferentially affected by SYN or that a chronic, widespread decrease in pre-synaptic release causes compensatory remodeling resulting in aberrant network excitability. Future studies using depth electrode recordings in awake, behaving SYN mice are necessary to determine the brain regions involved in generating SYN-induced epileptic activity.

The mechanism of SYN-induced spectral dysfunction (Chapter 5) is obscure. There are few mechanistic studies examining cortical brain oscillations in rodents. Lesions of the nucleus basalis of Meynert and cannabinoid treatment both simulate aspects of the oscillatory changes in SYN mice but both change the total power of the EEG signal, which is not altered in SYN mice. Lesion of the nucleus basalis, which drastically reduces cortical cholinergic innervation, increases delta and theta power and lowers beta power in rats, but it also appears to raise the total EEG power⁴⁴⁵. Widespread reduction of pre-synaptic release by cannabinoid injection lowers the power of high frequency oscillations, but it also lowers the total EEG power⁴³⁴. It is therefore probable that multiple mechanisms or brain regions are involved in the

spectral alterations in SYN mice. We speculate that SYN could decrease cortical presynaptic release, thereby reducing the power of high frequency oscillations, and release the suppression of delta power during wakefulness by decreasing pre-synaptic release in another brain region, possibly the thalamus. A less likely scenario is that SYN mice lose coordination of neuronal firing at high frequencies without altering basal release, which could preserve total oscillatory power but decrease high frequency oscillations. Or SYN could cause spectral alterations through a completely different mechanism altogether. In addition to determining the mechanism of spectral alterations, the relative contributions of spectral dysfunction and epileptiform activity on cognitive and motor abnormalities should also be examined.

In conclusion, we propose the following model for SYN, tau and A β interactions in neurodegenerative disease (Figure 6.1). SYN and A β can both cause neural network dysfunction and, when acting on the same network, can synergize to increase aberrant network excitability in humans. A β acts through tau to induce neural network dysfunction without necessarily altering the basal modifications of tau, while SYN-induced spectral and motor dysfunction is independent of tau. Further studies are required to determine whether interfering with network excitability improves cognition in the setting of SYN pathology.

Tau lowering is a promising therapeutic strategy for aberrant network excitability in human epilepsy and AD. Our studies and others^{111,349} indicate that partial reduction of tau is likely to be safe in adults and the elderly population. Our studies also suggest that tau lowering may be more effective than targeting abnormal tau phosphorylation or aggregation because deficits in hAPP mice are mediated by monomeric tau with no detectable changes in phosphorylation. Tau lowering would specifically target aberrant network excitability, but would not be effective against most SYN-induced neural network dysfunction. Given the high prevalence of SYN pathology in AD³²⁹ and AD pathology in Lewy body dementia¹⁴, many dementia patients would benefit from a combination of therapies targeting tau and SYN.

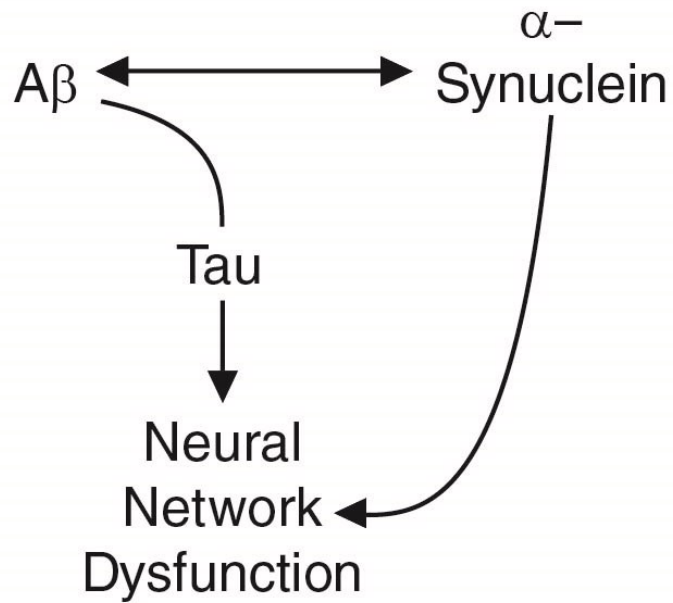


Figure 6.1. Model of pathologic interactions between $A\beta$, α -synuclein and tau in neurodegenerative disease. We propose the following model of neurodegeneration: $A\beta$ causes neural network dysfunction through tau without altering tau modifications, and α -synuclein (SYN) causes motor and spectral dysfunction independently of tau. Interactions between $A\beta$ and SYN can synergistically worsen neural network dysfunction.

Appendix A: Methods

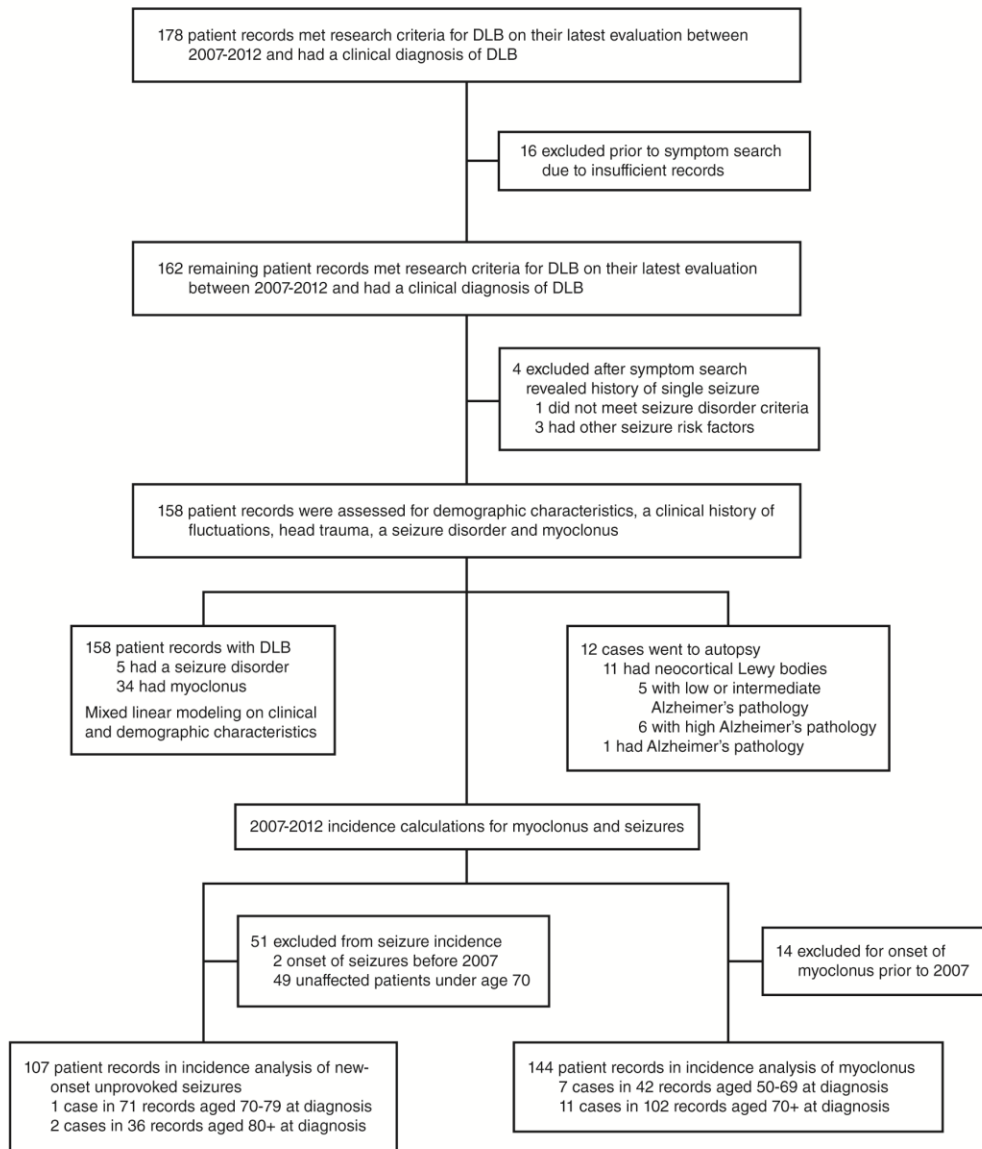


Figure A.1. Workflow of the chart review analysis.

Chart review and analysis of clinical data

We searched the electronic database of the UCSF Memory and Aging Center for patients who were seen between 2007–2012, who met McKeith criteria³³⁰ for DLB on their latest evaluation during that period, and who had a clinical diagnosis of DLB (n=178) (Figure A.1). Of these, 16 DLB patients were removed because the records were incomplete. We searched the remaining patient records for seizures, epilepsy, myoclonus, head trauma, and fluctuations using the word stems “seiz-“, “spells”, “epil-“, “eeg”, “myo-“, “head”, and “fluc-”. A seizure disorder, aka epilepsy, was defined as two or more unprovoked seizures or one unprovoked seizure with EEG evidence of epileptiform activity⁴⁶⁹. We excluded patients who had a seizure but who did not meet the criteria for a seizure disorder (n=1) or who had other seizure risk factors, including urinary tract infection with a fever (n=1), normal pressure hydrocephalus with a shunt and fever (n=1), and stroke (n=1). Among the remaining 158 DLB patients, 5 (3.2%) patients met the criteria for a seizure disorder and 34 (21.5%) patients were noted to have myoclonus. In 12 (7.6%) patients without the diagnosis of a seizure disorder EEGs had been obtained for suspected seizures. None of the patients with a seizure disorder, but one patient with myoclonus, had a history of mild head trauma with loss of consciousness for several minutes. A mixed effects linear model was fit to age of onset of cognitive impairment with sex, education, handedness, fluctuations, seizure disorder and myoclonus as independent variables. The presence versus absence of a clinical history of fluctuations, a seizure disorder, or myoclonus was quantified using 1 or 0, respectively. Reported *p*-values were derived from the mixed effects linear model including all variables. Significance was retained in a mixed effects linear model of age of onset of cognitive impairment using only sex (*p*=0.002) and myoclonus (*p*=0.009) as independent variables.

Incidence rates for myoclonus and a first unprovoked seizure (FUS) were calculated separately using 6 person-years per DLB patient in the study (Figure A.1). Fourteen patients with myoclonus and 2 patients with FUS prior to 2007 were excluded from the respective incidence calculations. Two patients who were unaffected during the incidence study period (2007–2012) developed myoclonus in 2013. There were 18 new cases of myoclonus and 3 new cases of FUS in our population between 2007 and 2012. As onset of myoclonus was not usually noted in the clinical history, the time of onset of myoclonus was estimated using the first mention of myoclonus in clinic notes after the initial evaluation. Both myoclonus (median:

+2 years relative to diagnosis, range –5 to +9) and seizure (median: –1 year relative to diagnosis, range –4 to +1) incidence tended to occur near the diagnosis of dementia. Therefore, the age of dementia diagnosis was used to stratify the DLB population without myoclonus or seizures. Relative rates and confidence intervals were calculated according to published formulas⁴⁷⁰.

Twelve DLB cases came to autopsy. The likelihood that clinical dementia was caused by Lewy body pathology seen on autopsy was estimated using McKeith criteria³³⁰. The presence of neocortical DLB was either directly stated by the pathologist (n=9) or inferred from the distribution of Lewy body pathology (n=2). The presence of AD pathology was based on autopsy summary statements and NIA-Reagan criteria⁴⁷¹. Because NIA-Reagan criteria require complete concordance between Braak and CERAD staging, two cases were not classifiable by these criteria: both cases had frequent plaques but a Braak stage below 5. In these cases, Braak stage was used as a surrogate to estimate the relative likelihood that dementia resulted from Lewy body pathology by McKeith criteria. All studies in human subjects were approved by the Committee on Human Research of the University of California, San Francisco. All human research subjects provided written informed consent before participating in protocols from which data were derived and were not required to re-consent for this analysis.

EEG recordings in human subjects

EEG recordings were obtained using an international 10–20 electrode placement. Participants were placed in the recumbent position with eyes closed and resting-state EEG activity was recorded for 50 min. One minute from the initial 20 min of recording, during which all subjects were awake, was used for analysis.

Human tissues

Human *postmortem* brain samples were obtained from the brain bank of the University of California at San Diego (UCSD) and the New York Brain Bank (NYBB) at Columbia University. The dentate gyrus was isolated over dry ice from larger tissue blocks. Calbindin mRNA levels, normalized to 18S RNA levels in the dentate gyrus, were similar in the disease groups from both brain banks (data not shown).

RNA isolation and RT-qPCR analysis

Frozen tissue (approximately half of the dissected dentate gyrus) was homogenized for 20 s in 500 μ L of TRIzol reagent at 20,000–21,000 rpm (Polytron homogenizer) and incubated on ice for 5 min. Samples were then mixed with 100 μ L chloroform, incubated briefly on ice, and centrifuged in heavy phase lock gel tubes at 12,000 $\times g$ and 4°C for 5 min. The supernatant was mixed with 250 μ L isopropanol, incubated for 10 min at room temperature, and centrifuged at 12,000 $\times g$ and 4°C for 10 min. The pellet was re-suspended in 75% ethanol and briefly spun at 7,500 $\times g$ at 4°C. The resulting pellet was then dissolved in 100 μ L of water and incubated at 56°C for 10 min, followed by addition of 350 μ L RLT buffer from the RNeasy Mini Kit (Qiagen) and 250 μ L ethanol. The RNA was further purified using the RNeasy Mini Kit following the “On-column DNase digestion” protocol using 30 μ L water for final elution. RNA concentration was measured by Nanodrop (ND-1000, Thermo Scientific). RNA integrity was determined on a 2100 Bioanalyzer (Agilent) according to the manufacturer’s instructions. All RNA samples were diluted to the same concentration and reverse transcribed with oligo-dTs and random hexamers according to the manufacturer’s instructions (TaqMan® Reverse Transcription Reagents, Applied Biosystems). Negative controls were generated by combining several samples and running RT-qPCR without reverse transcriptase. qPCR was carried out with SYBR green (SYBR green PCR Master Mix, Applied Biosystems) on a 7900HT Fast Real-Time PCR System (Applied Biosystems). To ensure that RNA quality was sufficient for RT-qPCR measurements, only samples with an RNA integrity number greater than 4.0 were analyzed. RNA integrity was not significantly different between groups by one-way ANOVA (data not shown). The experimenter was blinded to the pathological diagnosis of human cases.

Mice and mouse tissues

Detailed lists of the mouse cohorts used in this manuscript are found in Appendix B. For most experiments in this study, we used mice expressing human wildtype α -synuclein (Thy1-SYN line 61⁴³⁶), human amyloid precursor protein with Swedish and Indiana mutations (PDGF β -hAPP line J20³⁴⁷), or mice lacking endogenous tau⁷³ on a pure C57Bl/6J background, as specified in the text. Heterozygous transgenic mice expressing SYN directed by the Thy1 promoter on a mixed C57Bl/6 and DBA/2 background⁴³⁶ were crossed with *Tau*^{-/-} C57Bl/6 mice and their F1 offspring were intercrossed to generate mice with or

without SYN on the $Tau^{+/+}$, $Tau^{+/-}$, or $Tau^{-/-}$ backgrounds. EEG studies on Thy1-SYN mice revealed similar levels of epileptiform activity and spectral alterations on both backgrounds (data not shown). For all experiments involving Thy1-SYN mice, only male mice were used because the SYN transgene in line 61 is located on the X-chromosome²⁷². Food (Picolab Rodent Diet 20) and water were given *ad libitum* and mice were kept on a standard 12-h light/dark cycle. At the end of experiments, mice were deeply anesthetized with Avertin (2.5% w/v in 2.5% tert-amyl alcohol/phosphate-buffered saline) and killed by transcardial perfusion with saline. Usually, one hemibrain was fixed in 4% paraformaldehyde (from 32% solution, Electron Microscopy Services, PA) in phosphate buffer (pH 7.4) and one hemibrain was frozen on dry ice. For 6-OHDA experiments, both hemibrains were fixed. Sections from PDGF β -SYN mice (line D⁴³⁶) were a gift from Dr. Eliezer Masliah (Departments of Neuroscience and Pathology, University of California at San Diego). All experiments were approved by the Institutional Animal Care and Use Committee of the University of California, San Francisco.

Chemicals

Phosphatase inhibitor cocktails 1 or 3, and 2 (100X, Sigma) and protease inhibitor tablets (cOmplete, EDTA-free and cOmplete-mini, EDTA-free; Roche) were used interchangeably with Halt protease and phosphatase inhibitor cocktails (Thermo Scientific); all were used at 1X according to the manufacturers' instructions. Thiamet G (4390, Tocris) was used in a range of concentrations, as specified. Trichostatin A ([R-(E,E)]-7-[4-(Dimethylamino)phenyl]-N-hydroxy-4,6-dimethyl-7-oxo-2,4-heptadienamidine, Sigma) and niacinamide (pyridine-3-carboxylic acid amide, Sigma) were used at a concentration of 3 μ M and 10 mM, respectively. Other chemical reagents used were: ketamine HCl (Bionichepharma), medetomidine (dexdomitor, Henry Schein), perchloric acid (Fisher), methanol (Fisher), 4-(2-hydroxyethyl)piperazine-1-ethanesulfonic acid (HEPES, Sigma), sodium chloride (5M solution, Cellgrow), sodium dodecyl sulfate (SDS from 10% solution, Teknova), TritonX-100 (Sigma), sodium deoxycholate (Sigma), avertin prepared from 99% purity tribromoethanol (A18706, Alfa Aesar), tert-amyl alcohol (Aldrich), 6-hydroxydopamine (Sigma), L-DOPA (Sigma), benserazide HCl (Sigma), phenobarbital sodium (5-ethyl-5-phenyl-2,4,6-trioxohexahydropyrimidine sodium salt, P5178, Sigma), paraformaldehyde diluted from 32% solution (Electron Microscopy Sciences), TRIzol reagent (Life Technologies), chloroform (Sigma), glycerol

(Fisher), ethylene glycol (Fisher), phosphate-buffered saline diluted from 10X stock solution (Mediatech, Inc., VA), and donepezil hydrochloride (4385, Tocris). The PC-PEG-biotin alkyne was synthesized by Dr. Wang using the published protocols²⁴⁴ and all other reagents for chemical/enzymatic tagging of O-GlcNAc modifications were purchased from Sigma. All reagents for peptide digestions were purchased from Sigma, except proteomic grade trypsin (Promega) and AspN (Roche).

Hypothermia Induction

Mice were injected intraperitoneally with ketamine HCl (75 mg/kg) and medetomidine (1 mg/kg), or with saline as a negative control, and returned to their home cage for 1 hour before analysis. Mice were killed by cervical dislocation and their brain tissues were immediately frozen on dry ice.

6-OHDA injection

Mice were anesthetized, placed in a stereotaxic device and injected with either 2 μ l containing 4 μ g of 6-OHDA (Sigma, MO) in a solution of 2% L-ascorbic acid (Sigma, MO) in saline or the ascorbic acid-saline solution alone (vehicle). A single injection was performed in the striatum at the following coordinates relative to bregma: anterior-posterior = +0.4, medial-lateral = +2.0, dorsal-ventral = -3.3. Injections were made at a rate of 0.5 μ l/min with a 10- μ l syringe (Hamilton Company USA, NV). Behavioral testing for acute effects of 6-OHDA began on the third day after injection and was completed within seven days. Behavioral testing to assess recovery began 24 days after the injection and was also completed within seven days.

EEG recordings in mice

Lightweight EEG plugs were constructed in-house by soldering four Teflon-coated silver wires (0.125mm diameter) to a multichannel electrical connector. These plugs were surgically implanted into avertin-anesthetized mice, placing the silver wire leads into the subdural space. Reference leads were placed approximately 1 mm posterior and \pm 1 mm mediolateral to bregma, and recording leads approximately 1 mm anterior and \pm 2 mm mediolateral to lambda. Mice were allowed at least one week to recover from surgery before EEG recordings. EEG activity was recorded for 24 h in freely moving mice using Harmonie

5.0b software (Stellate), with one of the rostral leads serving as the reference electrode. For experiments shown in Figure 5.4B-C, phenobarbital sodium (0.5 mg/mL in sterile saline) was injected *i.p.* after four or more hours of baseline recording. For experiments shown in Figure 5.4I, donepezil hydrochloride (0.1 mg/mL in sterile saline) was injected *i.p.* every morning for 14 days; recording began immediately after the last injection.

Spectral analysis

For spectral analysis in humans, 60 s artifact-free EEG segments from the PZ electrode were selected manually. In two subjects (1 control and 1 DLB patient), who had no artifact-free periods, a recording segment with minimal artifacts was selected.

For spectral analysis in mice, 20–140 s EEG segments were selected during daytime resting behavior; the exact segment length depended on the time mice displayed resting behavior. Resting behavior was defined as lack of movement in the absence of EEG patterns suggestive of sleep entry such as sinusoidal changes in EEG amplitudes in the 5–15 Hz range. This approach does not exclude the possibility that some time points analyzed occurred during early sleep. Spectral analysis in phenobarbital- or donepezil-treated mice was conducted during the period of spike reduction or 3–4 hours⁴⁷² after the drug injection, respectively. EEG recordings were evaluated by a reader blinded to the *Tau* genotype. However, blinding to SYN genotype was not possible because of the epileptiform activity associated with this genotype.

Selected segments were converted into European Data Format files and imported into LabChart 7 Pro (AD Instruments) for spectral analysis. A 60-Hz notch filter was applied to all cases in which an electrical artifact was observed. Spectral power was obtained by subjecting the recordings to a fast Fourier transform (FFT) using a Hann cosine-bell window with no overlap between windows. Using the EEG sampling rate, we calculated the FFT size necessary for a resolution of 0.5 Hz and selected the nearest higher FFT size available in LabChart. Human EEGs were recorded at a 600-Hz sampling rate and FFT was performed with a 2048 point FFT size to obtain a resolution of 0.29 Hz. Mouse EEGs were recorded at a 200-Hz sampling rate and FFT was performed with a 512 point FFT size to obtain a resolution of 0.39 Hz. Spectrogram text files were analyzed in Excel by removing time points containing movement or epileptiform activity and averaging the remaining 20–60 s of data. Average power for each frequency block was then normalized to

the total averaged power to obtain relative spectral power. Relative power cumulative distribution functions (CDF) were obtained using the integral function in Prism (GraphPad).

For frequency band analysis in chapter 5, selected segments were exported as a text file and spectral power was obtained using a custom-written Matlab script and an FFT size of 1000 points to obtain data at 5-s intervals⁴⁴³. Spectral frequency bands were defined as follows: delta 0.5–4 Hz, theta 4–10 Hz, alpha 10–13 Hz, beta 13–20 Hz, and gamma 20.1–99.9 Hz. The EEG signal during resting behavior in was analyzed over time in each frequency band using a repeated measures mixed model analysis with a Holm *p*-value correction for multiple comparisons.

Analysis of epileptiform activity

Epileptiform activity was detected with the Gotman spike detector set to threshold 8 (Harmonie, Stellate). Events marked as epileptiform that coincided with large or sudden movements, such as rapid turns, grooming, digging and eating, were removed as possible artifacts. Myoclonic jerks, defined as epileptiform activity accompanied by sudden abnormal movements in an otherwise motionless mouse, were not excluded. Baseline epileptiform activity was quantified during 12–16 h of EEG recordings (50% during light cycle, 50% during dark cycle), excluding the first hour of recording and the first half hour after the change in light condition. Drug effects were assessed by comparing the extent of epileptiform activity during the 2 h preceding and 2.5 h following the injection, excluding from analysis the first half hour after the injection.

Behavioral testing

Unless specified otherwise, mice were acclimated to the testing room for at least one hour before testing. All testing apparatuses were cleaned with 70% ethanol between mice, unless otherwise indicated, and with 10% bleach after each testing day. Open field, pole and balance beam tests were carried out as described³⁴⁵. Experimenters were blinded to the genotype of mice.

Morris water maze

Spatial learning and memory was assessed as described⁴⁷³ in a Morris water maze consisting of a pool (120 cm in diameter) of water made opaque with white, non-toxic tempura paint. Water temperature was held at $20\pm 1^\circ\text{C}$. Extra maze cues were posted on the walls of the testing room. Data were acquired with Ethovision XT (Noldus Information Technology, the Netherlands).

Pre-training: Before hidden platform training, mice were exposed to the water maze by having them swim down a rectangular channel for 4 trials. The hidden escape platform was placed in the middle of the channel. If a mouse was unable to find and mount the platform for 60 s, it was guided to it and allowed to sit on it for up to 10 s.

Hidden platform training: Following pre-training, mice were trained for 5 days to locate a hidden platform (10x10 cm) submerged 1.5 cm below the water surface. The platform location was fixed, while the mouse drop locations were changed between trials. Mice were trained in four sessions per day with 3 hours of rest between sessions. Each session consisted of two trials with inter-trial intervals of approximately 15 min. Trials were terminated after 60 s. If a mouse did not find the platform within this time period, it was gently guided to the platform and allowed to sit on it for 15 s. Latency to locate the platform, as well as distance to the platform and swim speeds were recorded for the subsequent data analysis.

Probe trials: Twenty four hours after the last hidden platform training, the platform was removed and mice were allowed to swim in the pool for 60 s. The drop location was opposite to where the platform used to be during hidden platform training. The percentage of time mice spent in the target quadrant and the number of times they crossed the original platform location were recorded.

Novel object recognition (NOR)

On two consecutive days, mice were placed into a Plexiglas chamber (20x20 cm) containing two identical objects and allowed to explore for 10 min. Forty-eight hours after training, mice were tested in the same chamber for 10 min after one of the objects was replaced with a novel object. Time spent exploring each

object was recorded. The novel object position alternated between mice to eliminate any possible right-left bias. Objects were cleaned with 70% ethanol between each mouse.

Open field

Spontaneous movements in the open field were assessed using a Flex-Field/Open Field Photobeam Activity System (San Diego Instruments, CA). Each mouse was placed in the center of a clear plastic chamber (41x41x30 cm) with two 16x16 photobeam arrays and allowed to explore for 15 min. Movements were recorded through the number of beam breaks and rearing was determined by beam breaks on the higher of the two arrays.

Rota rod

Five mice were placed on the Rota Rod (Med Associates Inc, VT) for simultaneous testing and the computer recorded photobeam interruption when mice fell off the rotating rod. Photobeams were interrupted by the tester if the mouse held onto the rod without walking for three full rotations. Each mouse was given three trials with a maximum time on the Rota Rod of 300 seconds and with a 10-min rest between trials. The mice were first trained on the Rota Rod at a constant speed of 16 rpm. For the next two days they were trained on the Rota Rod in the morning and afternoon at an accelerating speed of 4 rpm to 40 rpm over 300 s. The average latency to fall off the Rota Rod was analyzed on the afternoon of day 2 for SYN $Tau^{-/-}$ cohorts and on the afternoon of day 3 for older $Tau^{-/-}$ mouse cohorts.

Pole test

The pole consisted of a thin wooden dowel and a cross-shaped wooden base placed in a clean cage. Rubber bands were wrapped around the dowel at intervals of approximately 1.5 inches to increase traction. Mice were placed at the top of the pole facing downwards and latency to descend the pole was measured. Trials were excluded if the mouse jumped or slid down the pole rather than climbed down. On the first day, mice were trained in two trials with approximately 10 min of rest between trials. On the second day, they were given five trials and the shortest latency to descend the pole was analyzed. The pole was cleaned with 70% ethanol between testing groups of mice from separate home cages.

Pole test with 3,4-dihydroxyphenylalanine (L-DOPA)/benserazide treatments

Acute treatment with L-DOPA/benserazide was designed as a cross-over trial. On day 1, mice were trained twice on the pole without injection. On day 2, mice were given an intraperitoneal (*i.p.*) injection of saline or of L-DOPA (20 mg/kg) and benserazide HCl (5 mg/kg) (Sigma) in saline. The mice were then transferred to the testing room and, 30 min later, given five pole test trials. On day 3, treatments were reversed, so that mice injected with saline on day 2 now received L-DOPA/benserazide and vice versa. Mice were then transferred to the testing room and tested as on day 2.

The same cohort of mice was used to assess the effect of chronic L-DOPA/benserazide treatment. Three days after finishing the acute treatments, mice were given five trials on the pole test to assess their performance before chronic drug treatment. They were then given water bottles containing L-DOPA (200 mg/L) and benserazide (50 mg/L) in 0.2% ascorbic acid (Sigma) as described¹⁰⁷. The bottles were changed daily and fluid/drug intake per cage of group-housed mice was monitored daily. The average weight of each mouse was calculated from measurements obtained at the beginning and end of the treatment. For each cage, the average daily drug intake was divided by the total weight of mice in the cage to estimate their approximate daily dose in mg of drug per kg of body weight. On the seventh day of chronic treatment, mice were given five trials in the pole test. Half of the mice were sacrificed the day after the last pole test. The remaining mice were placed on normal drinking water to allow for drug washout and sacrificed six days later.

Gait analysis

Gait analysis was done using the DigiGait software and treadmill (Mouse Specifics, Inc., MA). Mice were placed on the treadmill and the belt speed was set at a constant pace of 15 cm/s. Mice were allowed to walk for several seconds until a regular gaiting pattern was observed; 4-5 s of gait video were then recorded. Mice were excluded if a regular gait pattern could not be recorded. Variable thresholds were set on the DigiGait software to allow the computer to identify and analyze the mouse paws from the recorded video clips. After the software analyzed each video, the data was manually curated to ensure that the analysis

corresponded to actual paw placement. Any data that consistently misidentified paw placement on the belt was excluded from analysis.

Hind limb clasp

The hind limb clasp test was performed as described⁴⁷⁴. Each mouse was lifted by the tail and slowly lowered toward a surface for 10 s. The hind limbs were observed and each mouse was given a score for each trial. A score of 0 indicated that the hind limbs were extended for >50% of the trial period, a score of 1 indicated that one hind limb was retracted for >50% of the trial period, a score of 2 indicated that both hind limbs were partially retracted for >50% of the trial period, and a score of 3 indicated that both hind limbs were fully retracted and touching the abdomen for >50% of the trial period. Each mouse was tested three times and the scores were analyzed as described in the statistics section.

Balance beam

The balance beam consisted of two platforms connected by a removable plastic beam leading to an opaque box on top of one platform. On the first day, mice were trained on a thick, round beam by placing them first a few inches from the box and leading them into the box, and then by placing them halfway across the beam and leading them into the box, if leading was required. The mice were then trained three times across the whole length of the beam with approximately 10 min rest periods between trials. On the second day, mice were again trained three times on the thick beam. On the third day, the thick beam was replaced with a thin, square beam and the mice were tested three times. The average latency to cross the thin beam and the average number of times a foot slipped while crossing the beam during the testing sessions were analyzed. A trial was excluded from analysis if the mouse dragged its hind limbs across the beam for >50% of the distance. At 21-22 months of age, mice of all genotypes were unable to walk across the thin balance beam.

Preparation of tau- and O-GlcNAc-enriched peptides from rat brain tissue

Rat brain (3.4 g) was homogenized in 12.5 ml of ice-cold 1% perchloric acid (Polytron homogenizer, Glen Mills, Clifton, NJ). The resulting suspension was incubated on ice for 20 min and centrifuged at 20,000 x g

for 20 min. The supernatant was passed through a 1- μ m filter and concentrated with a 10-kDa molecular mass cutoff membrane with simultaneous buffer exchange to 10 mM HEPES, pH 7.5. The proteins (1.9 mg) were fractionated on a Superose 12 PC 3.2/30 gel filtration column (GE Healthcare) by using a buffer containing 20 mM HEPES and 50 mM NaCl, pH 7.5 and tau-containing fractions were combined. The total protein amount was estimated by UV absorbance at 280 nm. An aliquot of this material (about 1.3 μ g) was digested with trypsin (50:1 substrate/enzyme) in 100 mM ammonium bicarbonate, pH 8 overnight at 37 °C. Trypsin was removed with a 10-kDa molecular mass cutoff membrane (Millipore, Billerica, MA). Solvent was removed under vacuum, and the residue was then resuspended in 120 μ l of 10 mM HEPES, pH 7.9 containing 5 mM MnCl₂, UDP-N-azidoacetylgalactosamine (UDP-GalNAz), and 10 units of GalT1 (Invitrogen). The reaction mixture was incubated overnight at 4 °C, treated with 10 units calf intestine phosphatase (New England Biolabs, Ipswich, MA), incubated for an additional 2 h at room temperature, and then passed through a C18 spin column (Nest Group, Southborough, MA). UDP-GalNAz and the modified peptides were eluted in 0.1% TFA, 1% acetonitrile and 0.1% TFA, 80% acetonitrile, respectively. The solvent was removed under vacuum, and the sample was reconstituted in 20 μ l solution containing 0.05 μ mol of PC-PEG-biotin-alkyne, 10 mM sodium ascorbate, 1 mM tris[(1-benzyl-1H-1,2,3-triazol-4-yl)methyl]amine (in 4:1 t-butanol:DMSO), and 2 mM CuSO₄. The reaction mixture was incubated overnight at room temperature with gentle agitation. To remove excess PC-PEG-biotin-alkyne, the sample was diluted into strong cation exchange (SCX) loading buffer (5 mM KH₂PO₄, 25% acetonitrile, pH 3.0) and then passed through an SCX spin column (Nest Group). The column was washed with several column volumes of loading buffer, and the retained peptides were eluted with high salt buffer (5 mM KH₂PO₄, 400 mM KCl, 25% acetonitrile, pH 3.0). The eluent was adjusted to pH 7 with ammonium hydroxide and then allowed to interact with high capacity avidin beads (Pierce) for 2 h at room temperature. Avidin beads were washed 10 times with PBS solution and twice with 20% methanol/water and resuspended in 70% methanol/water. The suspension was transferred to a thin walled PCR tube, irradiated with 365 nm UV light (2 milliwatts/cm²) (Spectroline ENF-240C, Westbury, NY) for 25 min at a distance of 10 cm with rotation, and the supernatant was then dried under vacuum and stored at -20 °C. The overall process is demonstrated in Figure 3.1. The peptides were analyzed by electron-transfer dissociation as published²⁴⁴.

Perchloric acid enrichment of mouse tissue

Mouse hippocampus and cortex were isolated over ice and homogenized in 1% perchloric acid⁴⁷⁵. The suspension was incubated for 20 min on ice and then spun at 20,000xg at 4°C for 30 min. The supernatant was neutralized with NaOH and 1 M Tris (pH 7.4), phosphatase inhibitors and 25 µM Thiamet G were added, and the solution was concentrated over a 10-kDa MW filter (Vivaspin 20, Vivaproducts; Ultrafree, Millipore). For large-scale lectin weak affinity chromatography (LWAC) preparations, 10–14 hemibrains were combined from 8–10 mice. For the first quantitative experiment (Figure 3.3) wildtype mice were selected randomly, while the three most hyperactive hAPP mice were selected from a total of seven hAPP mice based on their behavior in the open field test.

Whole lysate preparation for immunoprecipitation

Mouse cortex and hippocampus were isolated on ice, then homogenized in Thermo IP Lysis buffer containing 25 µM Thiamet G and protease and phosphatase inhibitors. Trichostatin A and niacinamide were also added to the buffer for Chapter 3 quantitative experiments. The lysates were sonicated (Episonic multi-functional bioprocessor 1000, Epigentek Group Inc.) at an amplitude of 40% on ice twice for 5 min and spun for 10 min at 10,000xg at 4°C. The supernatant was collected and the protein concentration was measured by Bradford (Bio-Rad) assay according to the manufacturer's instructions.

Post-synaptic density preparation

Combined hippocampus and cortex from one whole mouse brain was homogenized with a Dounce homogenizer in 1 mL of buffer A (40 mM Tris-acetate (pH 7.5), 10 mM niacinamide, 3 µM trichostatin A, 1 µM Thiamet G, 0.3 M sucrose, and phosphatase and protease inhibitors). The suspension was transferred to a centrifuge tube, washed with an additional 1 mL of buffer A, and spun at 850xg (IEC CENTRA GP&R, rotor 216) at 4°C for 20 min. The supernatant was collected and stored on ice while the pellet was re-suspended in 2 mL buffer A and spun again. The resulting supernatant was combined with the first and 50 µL was retained as the cytosolic/membrane fraction. 8 mL of 40 mM Tris-acetate buffer were layered on top of the combined supernatants and then spun at 17,000xg (SW41 Ti rotor) at 4°C for 25 min. This supernatant was saved as the cytosolic fraction. The pellet was re-suspended in 1.2mL of buffer A, with 50

μL set aside for the membrane fraction, and loaded onto a sucrose density gradient consisting of 2.2 mL each of buffer A containing 1.2 M, 1.0 M or 0.8 M sucrose. 4 mL of 40 mM Tris-acetate buffer were added to the top and the samples were spun at 85,000xg (SW41 Ti rotor) at 4°C for 2 hours. The white layer at the 1.0 M/1.2 M sucrose interface were collected, re-suspended in 10–11 mL buffer A and spun at 85,000xg (SW41 Ti rotor) at 4°C for 30 min. The pellet was kept at -80°C overnight. The thawed pellet was then re-suspended using a 26-gauge needle in buffer B (10 mM Bicine-Tris (pH 7.5), 10 mM niacinamide, 3 μM trichostatin A, 1 μM Thiamet G, 5% N-octylglucoside, and phosphatase and protease inhibitors, and 50 μL was set aside for the synaptosomal fraction. The remaining suspension was loaded onto a sucrose gradient consisting of 3 mL each of buffer B/1% N-octylglucoside containing 2.2 M, 1.4 M or 1.0 M sucrose. Trichostatin A and niacinamide were used for PSD preparation only in the second and third quantitative PSD experiments in Chapter 3. Samples were spun at 85,000xg (SW41 Ti rotor) at 4°C for 2 hours and the top layer was collected for the non-PSD fraction. The translucent white layer at the 1.4 M/2.2 M sucrose interface was collected, resuspended in 12 mL of 10 mM Bicine-Tris (pH 7.5) and spun again at 85,000xg (SW41 Ti rotor) at 4°C for 2 hours. The pellet was stored at -80°C until immunoprecipitation. The pellet was resuspended in 35 μL of PSD buffer (20 mM HEPES, 5 mM sodium chloride, 1% TritonX-100, 1% SDS, 1% sodium deoxycholate, 25 μM Thiamet G, 3 μM trichostatin A, 10mM niacinamide, and phosphatase inhibitors), then either used for western blotting or tau immunoprecipitation. Samples for immunoprecipitation were diluted with 565 μL of IP lysis buffer (Pierce Crosslink IP kit) containing 25 μM Thiamet G, 3 μM trichostatin A, 10 mM niacinamide, and protease and phosphatase inhibitors. In the final quantitative PSD experiment (Chapter 3), tau was enriched prior to immunoprecipitation by heating the 600 μL solution at 95°C for 10 min, incubating on ice for 5–10 min, and spinning the sample at 20,817xg at 4°C for 30 min, and collecting the supernatant.

Tau immunoprecipitation

Tau was immunoprecipitated from brain whole lysate or PSD using BSA- and azide-free tau5 antibody (Abcam, ab80579) and a cross-link immunoprecipitation kit (Thermo-Pierce) following the manufacturer's instructions. Columns were used up to twice without noticeable loss of immunoprecipitation efficiency and 30 μL of elution buffer was used for the second elution step of the cross-link immunoprecipitation protocol.

For experiments using in-gel trypsin digestion of proteins prior to mass spectrometry, the immunoprecipitated proteins were run on a 4–12% bis-tris gel and stained with SafeStain (Life Technologies). A broad band around 50 kDa was then cut out for mass spectrometry analysis. For experiments using in-solution trypsin digestion prior to mass spectrometry, immunoprecipitated samples were neutralized with 1 M Tris (pH 9.6) containing 25 μ M Thiamet G and phosphatase inhibitors; 3 μ M trichostatin A and 10 mM niacinamide were also added for quantitative experiments. During the initial assignment of tau modifications, we used 1 mg whole lysate from cortex and hippocampus and 30 μ g of tau5. For quantitative immunoprecipitation experiments, we used 215 μ g of whole lysate from cortex and hippocampus or the entire PSD fraction from one mouse (approximately 215 μ g), and 10–20 μ g of tau5 antibody.

Peptide identification and label-free quantitation by mass spectrometry

Peptides in tau-enriched samples were identified by peptide sequencing with mass spectrometry. In-gel digestion was performed according to the UCSF Mass Spectrometry Facility protocol (<https://msf.ucsf.edu/ingel.html>). For in-solution digestion of tau enriched samples, the samples were incubated with urea (5 M final) and 10 mM tris(2-carboxyethyl)phosphine (TCEP) for 10 min at 56°C. Following reduction, the samples were alkylated with 20 mM iodoacetamide (30 min, dark, room temperature), then quenched with 10 mM additional TCEP, and the final volume was brought up to 250 μ L with 100 mM ammonium bicarbonate buffer. Trypsin and AspN digestions were performed overnight at 37°C using an enzyme to total protein ratio of 1:50. Samples were then acidified with 10% formic acid to pH 2–3, desalted using C18 Omix tips, and the extracted peptides were dried in a speedvac before analysis.

To target O-GlcNAcylated peptides, lectin weak affinity chromatography (LWAC) enrichment^{476,477} was performed on 1.2–1.8 mg of tau-enriched protein samples generated from large scale perchloric acid enrichment.

Peptide sequencing was performed using either LTQ-Orbitrap Velos or LTQ-Orbitrap XL (Thermo) mass spectrometers, each equipped with a 10,000 psi system nanoACUITY (Waters) UPLC instrument for reversed phase chromatography with a C18 column (BEH130, 1.7 μ m bead size, 100 μ m x 100 mm). The

liquid chromatography (LC) was operated at 600 nL/min flow rate, and peptides were separated using a linear gradient over 60 or 90 min from 2% to 30% acetonitrile in 0.1% formic acid.

Tau enriched samples were analyzed by several tandem mass spectrometry (MS/MS) techniques. For collision-induced dissociation (CID) and electron-transfer dissociation (ETD) experiments, survey scans were recorded over a 350–1500 m/z range and MS/MS was performed with CID or ETD activation on the three most intense precursor ions, with a minimum of 10,000 counts and 35% normalized collision energy. ETD isolation width was 3.0 amu with 200 μ s activation time; CID isolation width was 2.0 amu with 30 μ s activation time. For the higher-energy collisional dissociation (HCD) experiments, survey scans were recorded over a 350–1400 m/z range and MS/MS was performed with HCD activation on the ten most intense precursor ions, with minimum signal of 4000 counts, isolation width 2.5 amu, 0.1 μ s activation time, and 30% normalized collision energy over a mass range of 350–1500 m/z. Internal recalibration to a polydimethylcyclsiloxane (PCM) ion with m/z = 445.120025 was used for both MS and MS/MS scans⁴⁷⁸.

Mass spectrometry centroid peak lists were generated using in-house software called PAVA, and data were searched using Protein Prospector software v. 5.10.1⁴⁷⁹. For protein identification, database searches were performed against the *Mus musculus* subset of the UniProtKB database (*downloaded March 21, 2012*) totaling 77,771 entries. This database was concatenated with a fully randomized set of 77,771 entries for estimation of false discovery rate⁴⁸⁰. Data were also searched against a targeted library of tau isoform sequences (P10637, P10637-2, P10637-3, P10637-4, P10637-5 and P10637-6). Peptide sequences were matched as tryptic peptides with 0, 1 or 2 missed cleavages, and carbamidomethylated cysteines as a fixed modification. Variable modifications included: oxidation of methionine, N-terminal pyroglutamate from glutamine, start methionine processing, protein N-terminal acetylation, phosphorylation on serine, threonine, or tyrosine, O-GlcNAcylated serine and threonine, acetylated lysine, methylation on lysine or arginine, and diglycyl modified lysine. Mass accuracy tolerance was set to 20 ppm for parent and 30 ppm for fragment masses.

For reporting of protein identifications from this database search, score thresholds were selected that resulted in a protein false discovery rate of approximately 1%. The Protein Prospector parameters were: minimum protein score of 22, minimum peptide score of 15, and maximum expectation values of 0.02 for

protein and 0.05 for peptide matches. Post-translational modification assignments on tau were scored by “SLIP” scoring within Protein Prospector³⁵⁹, with unambiguous site assignments receiving a score ≥ 6 , and site assignments were manually confirmed. Ambiguous site assignments are denoted in tables using a vertical bar between the potential modification sites.

For label-free quantitation by selective reaction monitoring with HCD ionization, a list of parent masses was developed with a ± 10 ppm exclusion mass width window. The parent mass list included experimentally observed as well as predicted masses for tryptic peptides containing up to three phosphorylations on serine/threonine/tyrosine, O-GlcNAcylation on serine/threonine, diglycyl modified lysine, acetylation on lysine or arginine, and mono- or di-methylation on lysine or arginine, with up to two missed cleavages, as well as unmodified peptides that uniquely identify the known mouse isoforms of tau (SwissProt P10637, P10637-1, P10637-2, P10637-3, P10637-4, P10637-5, P10637-6). Dynamic exclusion was applied over a 10 second duration after a single repeat count, with an exclusion list size of 25 masses. All peptides utilized for site assignments were manually checked with alternate site-assignment hypotheses and the mass accuracy was sufficient to distinguish acetylation from potential tri-methylation modification. Data were searched as described above for information-dependent acquisition mode experiments. Quantitative analysis was performed with a previously reported label-free quantitation method that integrates the base peak intensity for each identified species⁴⁸¹.

Spectra and results for all identified tau peptides may be viewed with the freely available software MS Viewer, which can be accessed through the Protein Prospector suite of software at the following url: <http://prospector2.ucsf.edu/prospector/cgi-bin/msform.cgi?form=msviewer>. Search keys for the PTM site assignment data are listed for each set of experiments: Velos HCD: jtuvjpmrv, OrbitrapXL CID: kfjt07okcs, and OrbitrapXL ETD: m5jt1eadj7. Search keys for the peptides identified in the label free quantitation experiments are: Cohort 1: v5rszczgkcv, Cohort 1: 59gqdxjiwa, Cohort 3: ge5lvgitnp, Cohort 4: v6uklmtkyj.

Quantitative comparison of tau modifications

The value of modified tau peptides in each experiment was normalized to the median peak area of unmodified tau peptides from that sample, excluding unmodified tau peptides with a value of zero for more than 2 samples. Any peptide with a peak width of zero was assigned a value of zero for the quantitative analysis. Peptides with the same mass to charge ratio (m/z) represent different possible peptide species within the same quantified peak and were averaged to obtain the value for that tau modification. To obtain a value for one tau modification represented by multiple peptides, the value of peptides with the same m/z were averaged and added to the value of peptides with a different m/z . For each cohort, quantified values were normalized to the average value of that modification in wildtype mice and the normalized values of each modification were compared between wildtype and hAPP mice, excluding the zero values. To determine whether a modification appeared more frequently in one genotype, we also compared the number of zero values across genotypes for each tau modification.

Striatal tissue dissection

Frozen hemibrains were covered in 2% agarose and chopped into 450 μm slices (McIlwain Tissue Chopper, Mickle Laboratory Engineering Co. Ltd., UK). Slices were microdissected in sterile PBS on ice. The striatum was isolated from 4-5 slices per mouse. Striatal tissues were immediately frozen on dry ice and stored at -80°C . For each mouse, half of the striatal tissue was sent to the Vanderbilt Neurochemistry Core Laboratory for determination of bioamine levels by HPLC. The other half was homogenized in 100 μL buffer (PBS, 1mM DTT, 0.5mM EDTA, 0.5% Triton-X100, 0.1M PMSF, phosphatase inhibitor cocktails 2 and 3 (Sigma) and protease inhibitor tablets (Roche complete mini)) with a hand-held homogenizer. Samples were then sonicated (Episonic multi-functional bioprocessor 1000, Epigentek Group Inc., NY) at an amplitude of 40% in an ice bath twice for 5 min, incubated for 20-30 min on ice, and spun at 10,000 $\times g$ at 4°C for 10 min. The supernatant was collected.

Western blotting

Protein concentration was measured by BCA assay (Thermo Scientific). Samples were run on a 4-12% bis-tris gel (Bio-rad) and most samples were then transferred by iBlot onto a nitrocellulose membrane

(Invitrogen), which was blocked for 1 hour in 5% milk/PBS. For western blotting of fractionation samples (Chapter 3), the 4-12% bis-tris gel was incubated in 10% methanol/2xNuPAGE transfer buffer (NP0006-1, Life Technologies) for 10 minutes, then transferred by iBlot onto a nitrocellulose membrane (Invitrogen) and blocked for 1 hour in Odyssey blocking buffer (927-40000, LI-COR Biosciences). Blots were incubated overnight with primary antibodies (rabbit anti-tyrosine hydroxylase (1:1000 AB152, Millipore) plus anti-alpha tubulin (1:500,000 B512, Sigma), mouse anti-PSD95 (1:2000 MABN68, Millipore), or mouse anti- α -synuclein (1:2000 610787, BD Transduction laboratories) plus rabbit anti-tau (1/2000 EP2456Y, Millipore)), followed by incubation with secondary antibodies (680LT donkey anti-mouse (1:10,000-20,000, LI-COR Biosciences) and 800CW anti-rabbit (1:10,000-20,000, LI-COR Biosciences)) and quantitation of signals by an Odyssey system (LI-COR Biosciences). Membranes that were exposed to several primary antibodies in succession were not stripped between exposures.

Immunohistochemistry

Fixed hemibrains were stored at 4° C in phosphate-buffered saline (PBS) for 24 h and then in 30% sucrose/PBS until they were sectioned by microtome (Leica Microsystems Inc., IL) into 30 μ m sections, which were then stored at -20°C in a solution containing 30% glycerol (Fisher, PA), 30% ethylene glycol (Fisher, PA) and 40% phosphate-buffered saline (from 10X stock solution, Mediatech, Inc., VA) until immunostaining. Primary antibodies were rabbit anti-TH (1:2000 ab152, Abcam, MA), rabbit anti-calbindin (1:50,000, Swant), rabbit anti-NPY (1:8,000, Immunostar) and rabbit anti-cfos (1:10,000, Ab-5, Calbiochem). Primary antibody binding was detected with biotinylated donkey anti-rabbit (1:500, Jackson Immunoresearch), followed by avidin-biotin complex (Vector, CA). To determine the extent of the loss of striatal dopaminergic projections after 6-OHDA injection, the percent area occupied by TH immunoreactivity was determined with the BIOQUANT (BIOQUANT Image Analysis Corporation, TN) percent area function, in which the entire striatum was outlined by a variable region of interest and the percent area showing a staining signal above a set threshold was measured. Percent area on the injected side of the striatum was normalized to the percent area on the contralateral uninjected side. In SYN transgenic mice, striatal TH immunoreactivity was quantitated by densitometry. Calbindin, NPY and cfos quantification was done as described⁴⁴⁰, except that optical density measurements of calbindin

immunoreactivity in the dentate gyrus was not normalized to that in CA1, because calbindin was reduced in the latter region also. The experimenter was blinded to mouse treatment and genotype.

Perl iron staining

Brain sections were stained as previously described⁴⁸². Briefly, sections were stained in a solution of 1% potassium ferrocyanide and 1% hydrochloric acid. They were then rinsed with distilled water and counterstained at 60°C for 15 s in a solution of 0.1% nuclear fast red, 5% aluminum sulfate and trace amounts of thymol (storage preservative). The sections were rinsed well in water and then mounted and analyzed. Focal brain injury, elicited in anesthetized wildtype mice as described⁴⁸³, was used as a positive control.

Statistical analysis

Investigators were blinded with respect to the genotype and treatment of mice during behavioral testing, biochemistry and immunohistochemistry. Most data was analyzed by GraphPad Prism (GraphPad Software Inc., CA). Generally analyses were done using one- or two-way ANOVA, as appropriate, with the specified *post hoc* test. Tukey testing was used to compare between all groups, Bonferroni was used when only selected groups were compared. Findings were considered significant at $p \leq 0.05$ and outliers in mouse analyses were defined *a priori* as greater than 2SD from the mean. A *p*-value correction was used for multiple comparisons, as specified in the figure legends.

Power calculations for TH western blotting were done using the Statistical Solutions, LLC Power & Sample Size Calculator as a two-tailed t-test comparing $Tau^{+/+}$ and $Tau^{-/-}$ groups within each age group. Alpha was defined as 0.0167 for each test to correct for multiple comparisons. The lower sample number and the higher standard deviation between the two groups were used in power calculations for striatal dopamine and tyrosine hydroxylase levels. All comparisons made had power higher than 0.80 to detect a 40% decrease from levels in $Tau^{+/+}$ mice.

The TH quantification of 6-OHDA-treated mice was analyzed by one-way t-tests compared to 100% with a Benjamini-Hochberg *p*-value correction and by one-way ANOVA with a Bonferroni *post hoc* test to

compare treated groups to each other. To assess genotype effects and genotype interaction in the hind limb clasp test, the raw score data was analyzed by probit regression with random effects taken into account (Stata, StataCorp LP, TX). Comparisons between individual genotype groups were made by Welch's t-test of the average hind limb clasp scores for each mouse with a Benjamini-Hochberg p-value correction for multiple comparisons.

Contingency analysis was done in Prism (GraphPad) to determine significant enrichment of tau modifications in the microtubule binding repeat domain using a Holm correction for multiple comparisons. A chi-square test was used when all expected counts were more than 5 (acetylation, ubiquitination); otherwise, we used Fisher's exact test (methylation, phosphorylation). Pearson's chi-squared test and the likelihood ratio test to determine lysine targeting above chance was done in R (R-project).

For each tau modification found in more than 3 mice per genotype per cohort with a value greater than zero, values in hAPP and wildtype mice were compared by Student's t-test in Excel. P-values were adjusted using a Benjamini-Hochberg correction in R (R-project).

In behavioral data where the variance between groups was severely unequal (Bartlett's test $p < 0.0001$), the data was transformed by either a square-root, cube-root or log transformation to normalize variance between the groups. Whichever transformation best normalized variance was then analyzed by two-way ANOVA and a Bonferroni post-hoc test. All transformed data displayed equal variance across groups except rearing after four-weeks of recovery from a 6-OHDA injection (Bartlett's test $p = 0.03$).

Cumulative distribution functions were generated using the integral function in Prism. Repeated measures mixed effects model analysis in Stata was used to analyze the frequency band graph with multiple time points (Figure 5.1E). A mixed effects linear model in Stata was fit to the age of onset of cognitive impairment of DLB patients, as detailed in the chart review section above. Incidence rate ratios and 95% confidence intervals were calculated as described⁴⁷⁰.

Appendix B: Mouse Cohorts Studied

Table B.1: Mouse cohorts used in aged tau knockout studies

Fig. Panel	Analysis	Mice per Group (M/F)	Age at Analysis (mo)	Cohort
2.1A,B,E	Water maze, Novel object recognition	Tau ^{+/+} , 8 (3/5)	11-17	A
		Tau ^{-/-} , 8 (3/5)		
2.1C,D,F; 2.2A-E	Water maze, Novel object recognition, Weight, Open field, Rota rod, Pole test	Tau ^{+/+} , 12-13a (6/7)	21-22	B
		Tau ^{+/-} , 12-13a (6/7)		
		Tau ^{-/-} , 11-13a (6/7)		
2.2A,D,E,F; 2.3A-C	Weight, Rota rod, Pole test, Balance beam	Tau ^{+/+} , 13 (0/13)	12-15	C
		Tau ^{+/-} , 14 (0/14)		
		Tau ^{-/-} , 13 (0/13)		
2.2B,C	Open field	Tau ^{+/+} , 11 (0/11)	12-15	C
		Tau ^{+/-} , 13 (0/13)		
		Tau ^{-/-} , 12 (0/12)		
2.4A,C	Striatal dopamine and tyrosine hydroxylase	Tau ^{+/+} , 4-5b (5/0)	9-11	D
		Tau ^{+/-} , 5 (5/0)		
		Tau ^{-/-} , 5 (5/0)		
2.4A,C	Striatal dopamine and tyrosine hydroxylase	Tau ^{+/+} , 7 (2/5)	14-20	A
		Tau ^{-/-} , 6 (2/4)		
2.4A,C	Striatal dopamine and tyrosine hydroxylase	Tau ^{+/-} , 7 (0/7)	15-17	C
2.4A-C	Striatal dopamine and tyrosine hydroxylase	Tau ^{+/+} , 10 (5/5)	25-26	B
		Tau ^{+/-} , 8 (4/4)		
		Tau ^{-/-} , 7 (4/3)		
2.4D	Pole test with drug	Tau ^{+/+} , 14 (5/9)	12-15	E
		Tau ^{+/-} , 14 (9/5)		
		Tau ^{-/-} , 11 (3/8)		
2.5B	Perl staining analysis	Tau ^{+/+} , 3 (1/2)	14	F
		Tau ^{-/-} , 3 (1/2)		

mo, months; M, male; F, female

^aSome mice died over the course of testing

^bOne mouse was excluded from western blot analysis for technical reasons.

Table B.2: Summary of mice and experiments used to identify post-translational modifications of tau (reporting data available for viewing through MASSive)

Filename	Date	Mice ^a	Age ^b	Sex	hAPP	Treatment	Tau Isolation	Digest	Peptide Enrichment	MS
T9081407	2009-0814-07	1	6	F	-	-	IP	Solution	-	CID ETD
T9081408	2009-0814-08	1	6	F	-	-	IP	Gel	-	CID ETD
T9081410	2009-0814-10	1	6	F	-	-	IP	Gel	-	CID ETD
T9102604	2009-1026-04	2-9	5-13	3M, 5F	-	-	PCA	Solution	LWAC fraction 1	CID ETD
T9102605	2009-1026-05	2-9	5-13	3M, 5F	-	-	PCA	Solution	LWAC fraction 2	CID ETD
T9102606	2009-1026-06	2-9	5-13	3M, 5F	-	-	PCA	Solution	LWAC fraction 3	CID ETD
T9102607	2009-1026-07	2-9	5-13	3M, 5F	-	-	PCA	Solution	LWAC fraction 4	CID ETD
T9102608	2009-1026-08	2-9	5-13	3M, 5F	-	-	PCA	Solution	LWAC fraction 5	CID ETD
T9102609	2009-1026-09	2-9	5-13	3M, 5F	-	-	PCA	Solution	LWAC fraction 6	CID ETD
T9102610	2009-1026-10	2-9	5-13	3M, 5F	-	-	PCA	Solution	LWAC fraction 7	CID ETD
T9102611	2009-1026-11	2-9	5-13	3M, 5F	-	-	PCA	Solution	LWAC fraction 8	CID ETD
T9102612	2009-1026-12	2-9	5-13	3M, 5F	-	-	PCA	Solution	LWAC fraction 9	CID ETD
T9102613	2009-1026-13	2-9	5-13	3M, 5F	-	-	PCA	Solution	LWAC fraction 10	CID ETD
T9102614	2009-1026-14	2-9	5-13	3M, 5F	-	-	PCA	Solution	LWAC fraction 11	CID ETD
T9102615	2009-1026-15	2-9	5-13	3M, 5F	-	-	PCA	Solution	LWAC fraction 12	CID ETD
T9102616	2009-1026-16	2-9	5-13	3M, 5F	-	-	PCA	Solution	LWAC fraction 13	CID ETD
T9102617	2009-1026-17	2-9	5-13	3M, 5F	-	-	PCA	Solution	LWAC fraction 14	CID ETD
T9102618	2009-1026-18	2-9	5-13	3M, 5F	-	-	PCA	Solution	LWAC fraction 15	CID ETD
T9110607	2009-1106-07	10	4.5	M	-	-	PCA	Gel	-	CID ETD
T9113004	2009-1130-04	11	4.5	F	-	saline	PCA	Gel	-	CID ETD
T9113005	2009-1130-05	12	4.5	F	-	anesthesia	PCA	Gel	-	CID ETD
T9113006	2009-1130-06	13	4.5	F	-	anesthesia	PCA	Gel	-	CID ETD
T9113007	2009-1130-07	14	4	M	-	saline	PCA	Gel	-	CID ETD
T9113008	2009-1130-08	15	4	M	-	anesthesia	PCA	Gel	-	CID ETD
T9113009	2009-1130-09	16	4	M	-	saline	PCA	Gel	-	CID ETD
T2010012 3-01	2010-0123-01	17-26	3-12	5M, 5F	+	-	PCA	Solution	LWAC, RP fraction 1	CID ETD
T2010012 3-02	2010-0123-02	17-26	3-12	5M, 5F	+	-	PCA	Solution	LWAC, RP fraction 2	CID ETD
T2010012 3-03	2010-0123-03	17-26	3-12	5M, 5F	+	-	PCA	Solution	LWAC, RP fraction 3	CID ETD
T2010012 3-04	2010-0123-04	17-26	3-12	5M, 5F	+	-	PCA	Solution	LWAC, RP fraction 4	CID ETD
T2010012 3-05	2010-0123-05	17-26	3-12	5M, 5F	+	-	PCA	Solution	LWAC, RP fraction 5	CID ETD
T2010012 3-06	2010-0123-06	17-26	3-12	5M, 5F	+	-	PCA	Solution	LWAC, RP fraction 6	CID ETD

T2010012 3-07	2010- 0123-07	17-26	3-12	5M, 5F	+	-	PCA	Solution	LWAC, RP fraction 7	CID ETD
T2010012 3-08	2010- 0123-08	17-26	3-12	5M, 5F	+	-	PCA	Solution	LWAC, RP fraction 8	CID ETD
T2010012 3-09	2010- 0123-09	17-26	3-12	5M, 5F	+	-	PCA	Solution	LWAC, RP fraction 9	CID ETD
T2010012 3-10	2010- 0123-10	17-26	3-12	5M, 5F	+	-	PCA	Solution	LWAC, RP fraction 10	CID ETD
T2010012 3-11	2010- 0123-11	17-26	3-12	5M, 5F	+	-	PCA	Solution	LWAC, RP fraction 11	CID ETD
T2010012 3-12	2010- 0123-12	17-26	3-12	5M, 5F	+	-	PCA	Solution	LWAC, RP fraction 12	CID ETD
T2010012 3-13	2010- 0123-13	17-26	3-12	5M, 5F	+	-	PCA	Solution	LWAC, RP fraction 13	CID ETD
T2010012 3-14	2010- 0123-14	17-26	3-12	5M, 5F	+	-	PCA	Solution	LWAC, RP fraction 14	CID ETD
T2010012 3-15	2010- 0123-15	17-26	3-12	5M, 5F	+	-	PCA	Solution	LWAC, RP fraction 15	CID ETD
T2010012 3-16	2010- 0123-16	17-26	3-12	5M, 5F	+	-	PCA	Solution	LWAC, RP fraction 16	CID ETD
T2010012 3-17	2010- 0123-17	17-26	3-12	5M, 5F	+	-	PCA	Solution	LWAC, RP fraction 17	CID ETD
T2010012 3-18	2010- 0123-18	17-26	3-12	5M, 5F	+	-	PCA	Solution	LWAC, RP fraction 18	CID ETD
T2010012 3-19	2010- 0123-19	17-26	3-12	5M, 5F	+	-	PCA	Solution	LWAC, RP fraction 19	CID ETD
T2010012 3-20	2010- 0123-20	17-26	3-12	5M, 5F	+	-	PCA	Solution	LWAC, RP fraction 20	CID ETD
T2010012 3-21	2010- 0123-21	17-26	3-12	5M, 5F	+	-	PCA	Solution	LWAC, RP fraction 21	CID ETD
T2010012 3-22	2010- 0123-22	17-26	3-12	5M, 5F	+	-	PCA	Solution	LWAC, RP fraction 22	CID ETD
T2010012 3-23	2010- 0123-23	17-26	3-12	5M, 5F	+	-	PCA	Solution	LWAC, RP fraction 23	CID ETD
T2010012 3-24	2010- 0123-24	17-26	3-12	5M, 5F	+	-	PCA	Solution	LWAC, RP fraction 24	CID ETD
T2010012 3-25	2010- 0123-25	17-26	3-12	5M, 5F	+	-	PCA	Solution	LWAC, RP fraction 25	CID ETD
T2010012 3-26	2010- 0123-26	17-26	3-12	5M, 5F	+	-	PCA	Solution	LWAC, RP fraction 26	CID ETD
T2010012 3-27	2010- 0123-27	17-26	3-12	5M, 5F	+	-	PCA	Solution	LWAC, RP fraction 27	CID ETD
T2010012 3-28	2010- 0123-28	27-36	3.5	4M, 6F	-	-	PCA	Solution	LWAC, RP fraction 8	CID ETD
T2010012 3-29	2010- 0123-29	27-36	3.5	4M, 6F	-	-	PCA	Solution	LWAC, RP fraction 9	CID ETD
T2010012 3-30	2010- 0123-30	27-36	3.5	4M, 6F	-	-	PCA	Solution	LWAC, RP fraction 10	CID ETD
T2010012 3-31	2010- 0123-31	27-36	3.5	4M, 6F	-	-	PCA	Solution	LWAC, RP fraction 11	CID ETD
T2010012 3-32	2010- 0123-32	27-36	3.5	4M, 6F	-	-	PCA	Solution	LWAC, RP fraction 18	CID ETD
T2010012 3-33	2010- 0123-33	27-36	3.5	4M, 6F	-	-	PCA	Solution	LWAC, RP fraction 19	CID ETD
T2010012 3-34	2010- 0123-34	27-36	3.5	4M, 6F	-	-	PCA	Solution	LWAC, RP fraction 20	CID ETD
T2010012 3-35	2010- 0123-35	27-36	3.5	4M, 6F	-	-	PCA	Solution	LWAC, RP fraction 21	CID ETD
T2010012 3-36	2010- 0123-36	27-36	3.5	4M, 6F	-	-	PCA	Solution	LWAC, RP fraction 22	CID ETD
T2010012 3-37	2010- 0123-37	27-36	3.5	4M, 6F	-	-	PCA	Solution	LWAC, RP fraction 23	CID ETD
T2010012 3-38	2010- 0123-38	27-36	3.5	4M, 6F	-	-	PCA	Solution	LWAC, RP fraction 24	CID ETD
T2010012 3-39	2010- 0123-39	27-36	3.5	4M, 6F	-	-	PCA	Solution	LWAC, RP fraction 25	CID ETD
T2010012 3-40	2010- 0123-40	27-36	3.5	4M, 6F	-	-	PCA	Solution	LWAC, RP fraction 26	CID ETD
T2010020 5-04	2010- 0205-04	27-36	3.5	4M, 6F	-	-	PCA	Solution	LWAC, RP fraction 1	CID ETD

T2010020 5-05	2010- 0205-05	27-36	3.5	4M, 6F	-	-	PCA	Solution	LWAC, RP fraction 2	CID ETD
T2010020 5-06	2010- 0205-06	27-36	3.5	4M, 6F	-	-	PCA	Solution	LWAC, RP fraction 3	CID ETD
T2010020 5-07	2010- 0205-07	27-36	3.5	4M, 6F	-	-	PCA	Solution	LWAC, RP fraction 4	CID ETD
T2010020 5-08	2010- 0205-08	27-36	3.5	4M, 6F	-	-	PCA	Solution	LWAC, RP fraction 5	CID ETD
T2010020 5-09	2010- 0205-09	27-36	3.5	4M, 6F	-	-	PCA	Solution	LWAC, RP fraction 6	CID ETD
T2010020 5-10	2010- 0205-10	27-36	3.5	4M, 6F	-	-	PCA	Solution	LWAC, RP fraction 7	CID ETD
T2010020 5-11	2010- 0205-11	27-36	3.5	4M, 6F	-	-	PCA	Solution	LWAC, RP fraction 12	CID ETD
T2010020 5-12	2010- 0205-12	27-36	3.5	4M, 6F	-	-	PCA	Solution	LWAC, RP fraction 13	CID ETD
T2010020 5-13	2010- 0205-13	27-36	3.5	4M, 6F	-	-	PCA	Solution	LWAC, RP fraction 14	CID ETD
T2010020 5-14	2010- 0205-14	27-36	3.5	4M, 6F	-	-	PCA	Solution	LWAC, RP fraction 15	CID ETD
T2010020 5-15	2010- 0205-15	27-36	3.5	4M, 6F	-	-	PCA	Solution	LWAC, RP fraction 16	CID ETD
T2010020 5-16	2010- 0205-16	27-36	3.5	4M, 6F	-	-	PCA	Solution	LWAC, RP fraction 17	CID ETD
V2010081 3-09	2010- 0813-09	10	4.5	M	-	-	PCA	Gel	-	HCD
V2010081 3-10	2010- 0813-10	11	4.5	F	-	saline	PCA	Gel	-	HCD
V2010081 3-11	2010- 0813-11	12	4.5	F	-	anesthesia	PCA	Gel	-	HCD
V2010081 3-12	2010- 0813-12	13	4.5	F	-	anesthesia	PCA	Gel	-	HCD
V2010081 3-13	2010- 0813-13	14	4	M	-	saline	PCA	Gel	-	HCD
V2010081 3-14	2010- 0813-14	10	4.5	M	-	-	PCA	Gel	-	HCD
V2010081 3-15	2010- 0813-15	17-26	3-12	5M, 5F	+	-	PCA	Solution	-	HCD
V2010092 1-05	2010- 0921-05	37°	6	M	-	-	PCA	Gel	-	HCD
V2010092 1-06	2010- 0921-06	38°	6	M	-	-	PCA	Gel	-	HCD
V2010092 1-07	2010- 0921-07	39°	6	M	+	-	PCA	Gel	-	HCD
V2010092 1-08	2010- 0921-08	40°	6	M	+	-	PCA	Gel	-	HCD
V2010092 1-09	2010- 0921-09	41°	6	M	+	-	PCA	Gel	-	HCD
V2010092 1-10	2010- 0921-10	42°	6	M	-	-	PCA	Gel	-	HCD
V2010092 1-11	2010- 0921-11	42°	6	M	-	-	PCA	Gel	-	HCD
V2010092 1-12	2010- 0921-12	42°	6	M	-	-	PCA	Gel	-	HCD
V2010092 1-13	2010- 0921-13	42°	6	M	-	-	PCA	Gel	-	HCD
V2010092 1-14	2010- 0921-14	42°	6	M	-	-	PCA	Gel	-	HCD
V2010092 8-02	2010- 0928-02	37°	6	M	-	-	PCA	Gel	-	HCD
V2010092 8-03	2010- 0928-03	38°	6	M	-	-	PCA	Gel	-	HCD
V2010092 8-04	2010- 0928-04	42°	6	M	-	-	PCA	Gel	-	HCD
V2010092 8-05	2010- 0928-05	39°	6	M	+	-	PCA	Gel	-	HCD
V2010092 8-06	2010- 0928-06	40°	6	M	+	-	PCA	Gel	-	HCD
T2010092 8-07	2010- 0928-07	37°	6	M	-	-	PCA	Gel	-	CID ETD

V2010092 8-07	2010- 0928-07	41 ^c	6	M	+	-	PCA	Gel	-	HCD
T2010092 8-08	2010- 0928-08	38 ^c	6	M	-	-	PCA	Gel	-	CID ETD
T2010092 8-09	2010- 0928-09	42 ^c	6	M	-	-	PCA	Gel	-	CID ETD
T2010092 8-10	2010- 0928-10	39 ^c	6	M	+	-	PCA	Gel	-	CID ETD
T2010092 8-11	2010- 0928-11	40 ^c	6	M	+	-	PCA	Gel	-	CID ETD
T2010092 8-12	2010- 0928-12	41 ^c	6	M	+	-	PCA	Gel	-	HCD
V2010121 3-03	2010- 1213-03	37 ^c	6	M	-	-	PCA	Gel	-	HCD
V2010121 3-04	2010- 1213-04	37 ^c	6	M	-	-	PCA	Gel	-	HCD
V2010121 3-05	2010- 1213-05	42 ^c	6	M	-	-	PCA	Gel	-	HCD
V2010121 3-06	2010- 1213-06	42 ^c	6	M	-	-	PCA	Gel	-	HCD
V2011061 6-02	2011- 0616-02	43	9.5	F	-	-	PSD IP	Solution	-	HCD
V2011080 5-04	2011- 0805-04	43	9.5	F	-	-	PSD IP	Solution	-	HCD
V2011081 1-01	2011- 0811-01	43	9.5	F	-	-	PSD IP	Solution	-	HCD
V2011092 8-04	2011- 0928-04	44	4.5	M	-	-	PCA	Solution	-	HCD
V2011092 8-06	2011- 0928-06	45	4.5	M	-	-	PCA	Gel	-	HCD
V2011100 3-03	2011- 1003-03	46	7	F	-	-	PSD IP	Solution	-	HCD
V2011100 3-04	2011- 1003-04	44	4.5	M	-	-	PCA	Solution	-	HCD
V2011100 3-05	2011- 1003-05	44	4.5	M	-	-	PCA	Solution	-	HCD
V2011100 3-06	2011- 1003-06	47	7	M	+	-	PSD IP	Solution	-	HCD

MS, mass spectrometry method; hAPP, human amyloid precursor protein transgenic; F, female; M, male; IP, immunoprecipitation; PCA, 1% perchloric acid enrichment; PSD, post-synaptic density fractionation; Gel, in gel digestion; Solution, in solution digestion; ETD, electron transfer dissociation; CID, collision-induced dissociation; HCD, higher energy collisional dissociation

^aEach mouse was assigned a unique number for the inclusion list

^bAge in months

^cCohort A, Table B.3

Table B.3: Mouse cohorts used for quantitative mass spectrometry experiments

Cohort	Mice (Fractionation)	Sex	Age (Months)	Tau Enrichment
A	3 WT (none) 3 hAPP (none)	3M per group	6	Perchloric Acid
B	12 WT (none) 12 hAPP (none) 10 WT (PSD) 12 hAPP (PSD)	5-6M, 5- 7F per group	7-10	Immunoprecipitation
C	12 WT (PSD) 12 hAPP (PSD)	2M, 10F per group	7-9	Immunoprecipitation
D	10 WT (PSD) 10 hAPP (PSD)	10F per group	7-8	Immunoprecipitation

WT, wildtype; hAPP, human amyloid precursor protein transgenic; M, male; F, female; PSD, post-synaptic density

Table B.4: Mouse cohorts used in PD model studies

Fig. Panel	Analysis	Mice per Group (M/F)	Age at Analysis (mo)	Cohort
4.1-4.3	Open field, Rota Rod, pole test, tyrosine hydroxylase immunohistochemistry	Vehicle Tau ^{+/+} , 12 (9/3)	3-6	A
		Vehicle Tau ^{+/-} , 11-12 ^a (9/3)		
		Vehicle Tau ^{-/-} , 12 (9/3)		
		6-OHDA Tau ^{+/+} , 9-12 ^a (9/3)		
		6-OHDA Tau ^{+/-} , 7-12 ^a (9/3)		
		6-OHDA Tau ^{-/-} , 8-12 ^a (9/3)		
4.4	Rota Rod, stride length, hindlimb clasp, balance beam	Tau ^{+/+} , 15 (15/0)	3-4.5	B
		Tau ^{+/-} , 15 (15/0)		
		Tau ^{-/-} , 15 (15/0)		
		SYN Tau ^{+/+} , 15 (15/0)		
		SYN Tau ^{+/-} , 12-15 ^a (15/0)		
		SYN Tau ^{-/-} , 13-15 ^a (15/0)		

mo, months; M, male; F, female

^aSome mice died over the course of testing

Table B.5: Mouse cohorts used in SYN transgenic studies of neural network dysfunction

Fig. Panel	Analysis	Mice per Group (M/F)	Age at Analysis (mo)	Cohort
5.1C-E	EEG	NTG, 6 (6/0) Thy1-SYN, 11 (11/0)	4–8	A
5.1C-E, 5.4B, 5.4D-E	EEG	NTG, 3 (3/0) Thy1-SYN Tau ^{+/+} , 3 (3/0) Thy1-SYN Tau ^{-/-} , 3 (3/0)	5–7	B
5.2F-K	IHC	NTG, 12 (12/0) Thy1-SYN, 11 (11/0)	5–7	C
5.2K	IHC	NTG, 3 (3/0) Thy1-SYN, 2 (3/0)	5–7	D
5.3	IHC	NTG, 8 (4/4) PDGF-SYN, 8 (3/5)	3–17	E
5.4A-C	EEG	NTG, 7 (6/1) Thy1-SYN, 3 (3/0) hAPP, 5 (4/1)	4–5	F
5.4B-C	EEG	Thy1-SYN, 3-4 (4/0) ^{ab}	3	G
5.4D-E	EEG	Tau ^{+/+} , 3 (3/0) Thy1-SYN Tau ^{+/+} , 3-4 ^c (4/0) Thy1-SYN Tau ^{-/-} , 3 (3/0)	4–6	H
5.4F-H	IHC	Tau ^{+/+} , 10 (10/0) Tau ^{-/-} , 10 (10/0) Thy1-SYN Tau ^{+/+} , 11 (11/0) Thy1-SYN Tau ^{-/-} , 13 (13/0)	4–5	I
5.4I	EEG	NTG, 3 (3/0) SYN, 6 (6/0)	4–6	J

mo, months; IHC, immunohistochemistry

^aOne mouse was excluded from the spectral analysis because no suitable resting state could be found.

^bSYN mice were compared to themselves before and after treatment.

^cOne mouse with >250 events per hour was excluded as an outlier.

Bibliography

- 1 Weingarten, M. D., Lockwood, A. H., Hwo, S. Y. & Kirschner, M. W. A protein factor essential for microtubule assembly. *Proc. Natl. Acad. Sci. USA* **72**, 1858–1862, (1975).
- 2 Witman, G. B., Cleveland, D. W., Weingarten, M. D. & Kirschner, M. W. Tubulin requires tau for growth onto microtubule initiating sites. *Proc. Natl. Acad. Sci. USA* **73**, 4070–4074, (1976).
- 3 Kondo, J. *et al.* The carboxyl third of tau is tightly bound to paired helical filaments. *Neuron* **1**, 827–834, (1988).
- 4 Nukina, N. & Ihara, Y. One of the antigenic determinants of paired helical filaments is related to tau protein. *J. Biochem.* **99**, 1541–1544, (1986).
- 5 Grundke-Iqbal, I. *et al.* Microtubule-associated protein tau. A component of Alzheimer paired helical filaments. *J. Biol. Chem.* **261**, 6084–6089, (1986).
- 6 Wood, J. G., Mirra, S. S., Pollock, N. J. & Binder, L. I. Neurofibrillary tangles of Alzheimer disease share antigenic determinants with the axonal microtubule-associated protein tau (τ). *Proc. Natl. Acad. Sci. USA* **83**, 4040–4043, (1986).
- 7 Lee, V. M., Balin, B. J., Otvos, L., Jr. & Trojanowski, J. Q. A68: a major subunit of paired helical filaments and derivatized forms of normal Tau. *Science* **251**, 675–678, (1991).
- 8 Lee, V. M., Goedert, M. & Trojanowski, J. Q. Neurodegenerative tauopathies. *Annu. Rev. Neurosci.* **24**, 1121–1159, (2001).
- 9 Omalu, B. *et al.* Emerging histomorphologic phenotypes of chronic traumatic encephalopathy [CTE] in American athletes. *Neurosurgery*, In press.
- 10 Rajput, A. *et al.* Parkinsonism, Lrrk2 G2019S, and tau neuropathology. *Neurology* **67**, 1506–1508, (2006).
- 11 Santpere, G. & Ferrer, I. LRRK2 and neurodegeneration. *Acta Neuropathol.* **117**, 227–246, (2009).
- 12 Giannakopoulos, P. *et al.* Tangle and neuron numbers, but not amyloid load, predict cognitive status in Alzheimer's disease. *Neurology* **60**, 1495–1500, (2003).
- 13 Ihara, Y. PHF and PHF-like fibrils--cause or consequence? *Neurobiol. Aging* **22**, 123–126, (2001).
- 14 Merdes, A. R. *et al.* Influence of Alzheimer pathology on clinical diagnostic accuracy in dementia with Lewy bodies. *Neurology* **60**, 1586–1590, (2003).
- 15 Gu, Y., Oyama, F. & Ihara, Y. Tau is widely expressed in rat tissues. *J. Neurochem.* **67**, 1235–1244, (1996).
- 16 Trojanowski, J. Q., Schuck, T., Schmidt, M. L. & Lee, V. M. Distribution of tau proteins in the normal human central and peripheral nervous system. *J. Histochem. Cytochem.* **37**, 209–215, (1989).
- 17 Tashiro, K., Hasegawa, M., Ihara, Y. & Iwatsubo, T. Somatodendritic localization of phosphorylated tau in neonatal and adult rat cerebral cortex. *Neuroreport* **8**, 2797–2801, (1997).
- 18 Klein, C. *et al.* Process outgrowth of oligodendrocytes is promoted by interaction of fyn kinase with the cytoskeletal protein tau. *J. Neurosci.* **22**, 698–707, (2002).
- 19 Mandelkow, E. M. *et al.* Structure, microtubule interactions, and phosphorylation of tau protein. *Ann. NY Acad. Sci.* **777**, 96–106, (1996).
- 20 Goedert, M., Spillantini, M. G., Jakes, R., Rutherford, D. & Crowther, R. A. Multiple isoforms of human microtubule-associated protein tau: Sequences and localization in neurofibrillary tangles of Alzheimer's disease. *Neuron* **3**, 519–526, (1989).
- 21 Wei, M. L. & Andreadis, A. Splicing of a regulated exon reveals additional complexity in the axonal microtubule-associated protein tau. *J. Neurochem.* **70**, 1346–1356, (1998).
- 22 Lee, G. *et al.* Phosphorylation of tau by fyn: implications for Alzheimer's disease. *J. Neurosci.* **24**, 2304–2312, (2004).
- 23 Min, S. W. *et al.* Acetylation of tau inhibits its degradation and contributes to tauopathy. *Neuron* **67**, 953–966, (2010).
- 24 Cohen, T. J. *et al.* The acetylation of tau inhibits its function and promotes pathological tau aggregation. *Nat. Commun.* **2**, 252, (2011).
- 25 Wilhelmus, M. M. *et al.* Transglutaminases and transglutaminase-catalyzed cross-links colocalize with the pathological lesions in Alzheimer's disease brain. *Brain Pathol.* **19**, 612–622, (2009).
- 26 Ledesma, M. D., Bonay, P., Colaco, C. & Avila, J. Analysis of microtubule-associated protein tau glycation in paired helical filaments. *J. Biol. Chem.* **269**, 21614–21619, (1994).

- 27 Miyasaka, T. *et al.* Visualization of newly deposited tau in neurofibrillary tangles and neuropil
threads. *J. Neuropathol. Exp. Neurol.* **64**, 665–674, (2005).
- 28 Reyes, J. F. *et al.* A possible link between astrocyte activation and tau nitration in Alzheimer's
disease. *Neurobiol. Dis.* **31**, 198–208, (2008).
- 29 Dorval, V. & Fraser, P. E. Small ubiquitin-like modifier (SUMO) modification of natively
unfolded proteins tau and alpha-synuclein. *J. Biol. Chem.* **281**, 9919–9924, (2006).
- 30 Arnold, C. S. *et al.* The microtubule-associated protein tau is extensively modified with O-linked
N-acetylglucosamine. *J. Biol. Chem.* **271**, 28741–28744, (1996).
- 31 Cripps, D. *et al.* Alzheimer disease-specific conformation of hyperphosphorylated paired helical
filament-Tau is polyubiquitinated through Lys-48, Lys-11, and Lys-6 ubiquitin conjugation. *J.*
Biol. Chem. **281**, 10825–10838, (2006).
- 32 Kar, S., Fan, J., Smith, M. J., Goedert, M. & Amos, L. A. Repeat motifs of tau bind to the insides
of microtubules in the absence of taxol. *EMBO J.* **22**, 70–77, (2003).
- 33 Santarella, R. A. *et al.* Surface-decoration of microtubules by human tau. *J. Mol. Biol.* **339**, 539–
553, (2004).
- 34 Al-Bassam J, Ozer R S, Safer D, Halpain S & Milligan R A. MAP2 and tau bind longitudinally
along the outer ridges of microtubule protofilaments. *J. Cell Biol.* **157**, 1187–1196, (2002).
- 35 Maas, T., Eidenmuller, J. & Brandt, R. Interaction of tau with the neural membrane cortex is
regulated by phosphorylation at sites that are modified in paired helical filaments. *J. Biol. Chem.*
275, 15733–15740, (2000).
- 36 Frappier, T. F., Georgieff, I. S., Brown, K. & Shelanski, M. L. tau Regulation of microtubule-
microtubule spacing and bundling. *J. Neurochem.* **63**, 2288–2294, (1994).
- 37 Biernat, J. *et al.* The switch of tau protein to an Alzheimer-like state includes the phosphorylation
of two serine-proline motifs upstream of the microtubule binding region. *EMBO J.* **11**, 1593–1597,
(1992).
- 38 Augustinack, J. C., Schneider, A., Mandelkow, E. M. & Hyman, B. T. Specific tau
phosphorylation sites correlate with severity of neuronal cytopathology in Alzheimer's disease.
Acta Neuropathol. (Berl) **103**, 26–35, (2002).
- 39 Reynolds, C. H. *et al.* Phosphorylation regulates tau interactions with Src homology 3 domains of
phosphatidylinositol 3-kinase, phospholipase Cgamma1, Grb2, and Src family kinases. *J. Biol.*
Chem. **283**, 18177–18186, (2008).
- 40 Lee, G., Newman, S. T., Gard, D. L., Band, H. & Panchamoorthy, G. Tau interacts with src-family
non-receptor tyrosine kinases. *J. Cell Sci.* **111 (Pt 21)**, 3167–3177, (1998).
- 41 Gustke, N., Trinczek, B., Biernat, J., Mandelkow, E. M. & Mandelkow, E. Domains of tau protein
and interactions with microtubules. *Biochemistry* **33**, 9511–9522, (1994).
- 42 Jho, Y. S., Zhulina, E. B., Kim, M. W. & Pincus, P. A. Monte carlo simulations of tau proteins:
Effect of phosphorylation. *Biophys. J.* **99**, 2387–2397, (2010).
- 43 Li, X. *et al.* Novel diffusion barrier for axonal retention of Tau in neurons and its failure in
neurodegeneration. *The EMBO journal* **30**, 4825–4837, (2011).
- 44 Fischer, D. *et al.* Conformational changes specific for pseudophosphorylation at serine 262
selectively impair binding of tau to microtubules. *Biochemistry* **48**, 10047–10055, (2009).
- 45 von Bergen, M., Barghorn, S., Biernat, J., Mandelkow, E. M. & Mandelkow, E. Tau aggregation is
driven by a transition from random coil to beta sheet structure. *Biochim Biophys Acta* **1739**, 158–
166, (2005).
- 46 von Bergen, M. *et al.* Mutations of tau protein in frontotemporal dementia promote aggregation of
paired helical filaments by enhancing local beta-structure. *J. Biol. Chem.* **276**, 48165–48174,
(2001).
- 47 Higuchi, M. *et al.* Axonal degeneration induced by targeted expression of mutant human tau in
oligodendrocytes of transgenic mice that model glial tauopathies. *J. Neurosci.* **25**, 9434–9443,
(2005).
- 48 Kempf, M., Clement, A., Faissner, A., Lee, G. & Brandt, R. Tau binds to the distal axon early in
development of polarity in a microtubule- and microfilament-dependent manner. *J. Neurosci.* **16**,
5583–5592, (1996).
- 49 Fanara, P. *et al.* Changes in microtubule turnover accompany synaptic plasticity and memory
formation in response to contextual fear conditioning in mice. *Neuroscience* **168**, 167–178,
(2010).

- 50 Fleming, L. M., Weisgraber, K. H., Strittmatter, W. J., Troncoso, J. C. & Johnson, G. V. Differential binding of apolipoprotein E isoforms to tau and other cytoskeletal proteins. *Exp. Neurol.* **138**, 252–260, (1996).
- 51 Ahmed, T. V. d. J., A.; Blum, D.; Galas, Marie-Christine; D'Hooge, R.; Buee, L.; Balschun, D. Cognition and hippocampal plasticity in mice with a homozygous tau deletion. *Neurobiology of aging.*
- 52 Fulga, T. A. *et al.* Abnormal bundling and accumulation of F-actin mediates tau-induced neuronal degeneration in vivo. *Nature cell biology* **9**, 139–148, (2007).
- 53 Surridge, C. D. & Burns, R. G. The difference in the binding of phosphatidylinositol distinguishes MAP2 from MAP2C and Tau. *Biochemistry* **33**, 8051–8057, (1994).
- 54 Flanagan, L. A. *et al.* The structure of divalent cation-induced aggregates of PIP2 and their alteration by gelsolin and tau. *Biophys. J.* **73**, 1440–1447, (1997).
- 55 Hwang, S. C., Jhon, D. Y., Bae, Y. S., Kim, J. H. & Rhee, S. G. Activation of phospholipase C-gamma by the concerted action of tau proteins and arachidonic acid. *J. Biol. Chem.* **271**, 18342–18349, (1996).
- 56 Jenkins, S. M. & Johnson, G. V. Tau complexes with phospholipase C-gamma in situ. *Neuroreport* **9**, 67–71, (1998).
- 57 Qiang, L., Yu, W., Andreadis, A., Luo, M. & Baas, P. W. Tau protects microtubules in the axon from severing by katanin. *J. Neurosci.* **26**, 3120–3129, (2006).
- 58 King, M. E. *et al.* Tau-dependent microtubule disassembly initiated by prefibrillar β -amyloid. *The Journal of cell biology* **175**, 541–546, (2006).
- 59 DiTella, M. C., Feiguin, F., Carri, N., Kosik, K. S. & Caceres, A. MAP-1B/TAU functional redundancy during laminin-enhanced axonal growth. *Journal of cell science* **109 (Pt 2)**, 467–477, (1996).
- 60 Takei, Y., Teng, J., Harada, A. & Hirokawa, N. Defects in axonal elongation and neuronal migration in mice with disrupted *tau* and *map1b* genes. *J. Cell Biol.* **150**, 989–1000, (2000).
- 61 Dixit, R., Ross, J. L., Goldman, Y. E. & Holzbaur, E. L. Differential regulation of dynein and kinesin motor proteins by tau. *Science* **319**, 1086–1089, (2008).
- 62 Ebnet, A. *et al.* Overexpression of tau protein inhibits kinesin-dependent trafficking of vesicles, mitochondria, and endoplasmic reticulum: Implications for Alzheimer's disease. *J. Cell Biol.* **143**, 777–794, (1998).
- 63 Mandell, J. W. & Banker, G. A. A spatial gradient of tau protein phosphorylation in nascent axons. *J. Neurosci.* **16**, 5727–5740, (1996).
- 64 Kanaan, N. M. *et al.* Pathogenic forms of tau inhibit kinesin-dependent axonal transport through a mechanism involving activation of axonal phosphotransferases. *The Journal of neuroscience : the official journal of the Society for Neuroscience* **31**, 9858–9868, (2011).
- 65 Vossel, K. A. *et al.* Tau reduction prevents A β -induced impairments in axonal transport. *Science* **330**, 198, (2010).
- 66 Yuan, A., Kumar, A., Peterhoff, C., Duff, K. & Nixon, R.-A. Axonal transport rates *in vivo* are unaffected by tau deletion or overexpression in mice. *J. Neurosci.* **28**, 1682–1687, (2008).
- 67 He, H. J. *et al.* The proline-rich domain of tau plays a role in interactions with actin. *BMC Cell Biol.* **10**, 81, (2009).
- 68 Kotani, S., Nishida, E., Kumagai, H. & Sakai, H. Calmodulin inhibits interaction of actin with MAP2 and Tau, two major microtubule-associated proteins. *J. Biol. Chem.* **260**, 10779–10783, (1985).
- 69 Farias, G. A., Munoz, J. P., Garrido, J. & Maccioni, R. B. Tubulin, actin, and tau protein interactions and the study of their macromolecular assemblies. *J. Cell Biochem.* **85**, 315–324, (2002).
- 70 Yu, J. Z. & Rasenick, M. M. Tau associates with actin in differentiating PC12 cells. *FASEB J.* **20**, 1452–1461, (2006).
- 71 Ittner, L. M. *et al.* Dendritic function of tau mediates amyloid-beta toxicity in Alzheimer's disease mouse models. *Cell* **142**, 387–397, (2010).
- 72 Sharma, V. M., Litersky, J. M., Bhaskar, K. & Lee, G. Tau impacts on growth-factor-stimulated actin remodeling. *J. Cell. Sci.* **120**, 748–757, (2007).
- 73 Dawson, H. N. *et al.* Inhibition of neuronal maturation in primary hippocampal neurons from tau deficient mice. *J. Cell Sci.* **114**, 1179–1187, (2001).

- 74 Harada, A. *et al.* Altered microtubule organization in small-calibre axons of mice lacking *tau* protein. *Nature* **369**, 488–491, (1994).
- 75 Caceres, A., Potrebic, S. & Kosik, K. S. The effect of tau antisense oligonucleotides on neurite formation of cultured cerebellar macroneurons. *The Journal of neuroscience : the official journal of the Society for Neuroscience* **11**, 1515-1523, (1991).
- 76 Brandt, R., Leger, J. & Lee, G. Interaction of tau with the neural plasma membrane mediated by tau's amino-terminal projection domain. *J. Cell Biol.* **131**, 1327–1340, (1995).
- 77 Leugers, C. J. & Lee, G. Tau potentiates nerve growth factor-induced mitogen-activated protein kinase signaling and neurite initiation without a requirement for microtubule binding. *J. Biol. Chem.* **285**, 19125–19134, (2010).
- 78 Rouzier, R. *et al.* Microtubule-associated protein tau: A marker of paclitaxel sensitivity in breast cancer. *Proc. Natl. Acad. Sci. USA* **102**, 8315–8320, (2005).
- 79 Souter, S. & Lee, G. Microtubule-associated protein tau in human prostate cancer cells: Isoforms, phosphorylation, and interactions. *J. Cell Biochem.* **108**, 555–564, (2009).
- 80 Sapir, T., Frotscher, M., Levy, T., Mandelkow, E. M. & Reiner, O. Tau's role in the developing brain: implications for intellectual disability. *Human molecular genetics* **21**, 1681-1692, (2012).
- 81 Frandemich, M. L. *et al.* Activity-dependent tau protein translocation to excitatory synapse is disrupted by exposure to amyloid-beta oligomers. *The Journal of neuroscience : the official journal of the Society for Neuroscience* **34**, 6084-6097, (2014).
- 82 Chen, Q. *et al.* Tau protein is involved in morphological plasticity in hippocampal neurons in response to BDNF. *Neurochemistry international* **60**, 233-242, (2012).
- 83 Roberson, E. D. *et al.* Amyloid- β /Fyn-induced synaptic, network, and cognitive impairments depend on Tau levels in multiple mouse models of Alzheimer's disease. *J. Neurosci.* **31**, 700–711, (2011).
- 84 Shipton, O. A. *et al.* Tau protein is required for amyloid β -induced impairment of hippocampal long-term potentiation. *J. Neurosci.* **31**, 1688–1692, (2011).
- 85 Kimura, T. *et al.* Microtubule-associated protein tau is essential for long-term depression in the hippocampus. *Philosophical transactions of the Royal Society of London. Series B, Biological sciences* **369**, 20130144, (2014).
- 86 Sanchez-Mejia, R. & Mucke, L. Phospholipase A2 and arachidonic acid in Alzheimer's disease. *Biochim. Biophys. Acta* **1801**, 784–790, (2010).
- 87 Perez, M. *et al.* Tau--an inhibitor of deacetylase HDAC6 function. *J. Neurochem.* **109**, 1756–1766, (2009).
- 88 Rapoport, M., Dawson, H. N., Binder, L. I., Vitek, M. P. & Ferreira, A. Tau is essential to β -amyloid-induced neurotoxicity. *Proc. Natl. Acad. Sci. USA* **99**, 6364–6369, (2002).
- 89 Sultan A *et al.* Nuclear tau: A key player in neuronal DNA protection. *J. Biol. Chem.*, (2010).
- 90 Miao, Y., Chen, J., Zhang, Q. & Sun, A. Deletion of tau attenuates heat shock-induced injury in cultured cortical neurons. *J. Neurosci. Res.* **88**, 102–110, (2010).
- 91 Miyasaka, T. *et al.* Progressive neurodegeneration in *C. elegans* model of tauopathy. *Neurobiol. Dis.* **20**, 372–383, (2005).
- 92 Frost, B., Hemberg, M., Lewis, J. & Feany, M. B. Tau promotes neurodegeneration through global chromatin relaxation. *Nature neuroscience* **17**, 357-366, (2014).
- 93 Suberbielle, E. *et al.* Physiologic brain activity causes DNA double-strand breaks in neurons, with exacerbation by amyloid-beta. *Nature neuroscience* **16**, 613-621, (2013).
- 94 Bullmann, T., de Silva, R., Holzer, M., Mori, H. & Arendt, T. Expression of embryonic tau protein isoforms persist during adult neurogenesis in the hippocampus. *Hippocampus* **17**, 98–102, (2007).
- 95 Hong, X. P. *et al.* Essential role of tau phosphorylation in adult hippocampal neurogenesis. *Hippocampus*, (2009).
- 96 Zhao, C., Deng, W. & Gage, F. H. Mechanisms and functional implications of adult neurogenesis. *Cell* **132**, 645–660, (2008).
- 97 Dawson, H. N. *et al.* Loss of tau elicits axonal degeneration in a mouse model of Alzheimer's disease. *Neuroscience* **169**, 516–531, (2010).
- 98 Roberson, E. D. *et al.* Reducing endogenous tau ameliorates amyloid β -induced deficits in an Alzheimer's disease mouse model. *Science (New York, N.Y)* **316**, 750–754, (2007).

- 99 Andrews-Zwilling, Y. *et al.* Apolipoprotein E4 causes age- and Tau-dependent impairment of GABAergic interneurons, leading to learning and memory deficits in mice. *J. Neurosci.* **30**, 13707–13717, (2010).
- 100 Zhang, B. *et al.* Microtubule-binding drugs offset tau sequestration by stabilizing microtubules and reversing fast axonal transport deficits in a tauopathy model. *Proc. Natl. Acad. Sci. USA* **102**, 227–231, (2005).
- 101 Strittmatter, W. J. *et al.* Isoform-specific interactions of apolipoprotein E with microtubule-associated protein tau: implications for Alzheimer disease. *Proc. Natl. Acad. Sci. USA* **91**, 11183–11186, (1994).
- 102 Bhaskar, K., Yen, S. H. & Lee, G. Disease-related modifications in tau affect the interaction between Fyn and Tau. *J. Biol. Chem.* **280**, 35119–351125, (2005).
- 103 Arendt, T. *et al.* Reversible paired helical filament-like phosphorylation of tau is an adaptive process associated with neuronal plasticity in hibernating animals. *J. Neurosci.* **23**, 6972–6981, (2003).
- 104 Yu, Y. *et al.* Developmental regulation of tau phosphorylation, tau kinases, and tau phosphatases. *J. Neurochem.* **108**, 1480–1494, (2009).
- 105 Alonso, A. C., Grundke-Iqbal, I. & Iqbal, K. Alzheimer's disease hyperphosphorylated tau sequesters normal tau into tangles of filaments and disassembles microtubules. *Nat. Med.* **2**, 783–787, (1996).
- 106 Ikegami, S., Harada, A. & Hirokawa, N. Muscle weakness, hyperactivity, and impairment in fear conditioning in tau-deficient mice. *Neurosci. Lett.* **279**, 129–132, (2000).
- 107 Lei, P. *et al.* Tau deficiency induces parkinsonism with dementia by impairing APP-mediated iron export. *Nat. Med.* **18**, 291–295, (2012).
- 108 Tucker, K. L., Meyer, M. & Barde, Y. A. Neurotrophins are required for nerve growth during development. *Nat. Neurosci.* **4**, 29–37, (2001).
- 109 Muramatsu, K. *et al.* Neuron-specific recombination by Cre recombinase inserted into the murine tau locus. *Biochem. Biophys. Res. Commun.* **370**, 419–423, (2008).
- 110 Rudy, J. W., Huff, N. C. & Matus-Amat, P. Understanding contextual fear conditioning: Insights from a two-process model. *Neurosci. Biobehav. Rev.* **28**, 675–685, (2004).
- 111 Devos, S. L. *et al.* Antisense reduction of tau in adult mice protects against seizures. *J. Neurosci.* **33**, 12887–12897, (2013).
- 112 Cantero, J. L. *et al.* Role of tau protein on neocortical and hippocampal oscillatory patterns. *Hippocampus*, In press.
- 113 De Felice, F. G. *et al.* Alzheimer's disease-type neuronal tau hyperphosphorylation induced by Abeta oligomers. *Neurobiol. Aging* **29**, 1334–1347, (2008).
- 114 Zempel, H., Thies, E., Mandelkow, E. & Mandelkow, E. M. A{beta} Oligomers Cause Localized Ca²⁺ Elevation, Missorting of Endogenous Tau into Dendrites, Tau Phosphorylation, and Destruction of Microtubules and Spines. *J. Neurosci.* **30**, 11938–11950, (2010).
- 115 Zempel, H. *et al.* Amyloid-beta oligomers induce synaptic damage via Tau-dependent microtubule severing by TTL6 and spastin. *The EMBO journal* **32**, 2920-2937, (2013).
- 116 Leroy, K. *et al.* Lack of tau proteins rescues neuronal cell death and decreases amyloidogenic processing of APP in APP/PS1 mice. *The American journal of pathology* **181**, 1928-1940, (2012).
- 117 Brecht, W. J. *et al.* Neuron-specific apolipoprotein E4 proteolysis is associated with increased tau phosphorylation in brains of transgenic mice. *J. Neurosci.* **24**, 2527–2534, (2004).
- 118 Mairet-Coello, G. *et al.* The CAMKK2-AMPK kinase pathway mediates the synaptotoxic effects of Abeta oligomers through Tau phosphorylation. *Neuron* **78**, 94-108, (2013).
- 119 Seward, M. E. *et al.* Amyloid-beta signals through tau to drive ectopic neuronal cell cycle re-entry in Alzheimer's disease. *Journal of cell science* **126**, 1278-1286, (2013).
- 120 Chin, J. *et al.* Fyn kinase modulates synaptotoxicity, but not aberrant sprouting, in human amyloid precursor protein transgenic mice. *J. Neurosci.* **24**, 4692–4697, (2004).
- 121 Chin, J. *et al.* Fyn kinase induces synaptic and cognitive impairments in a transgenic mouse model of Alzheimer's disease. *J. Neurosci.* **25**, 9694–9703, (2005).
- 122 Bhaskar, K., Hobbs, G. A., Yen, S. H. & Lee, G. Tyrosine phosphorylation of tau accompanies disease progression in transgenic mouse models of tauopathy. *Neuropathol. Appl. Neurobiol.* **36**, 462–477, (2010).

- 123 Matsuo, E. S. *et al.* Biopsy-derived adult human brain tau is phosphorylated at many of the same
sites as Alzheimer's disease paired helical filament tau. *Neuron*. **13**, 989–1002, (1994).
- 124 Gentleman, S. M., Nash, M. J., Sweeting, C. J., Graham, D. I. & Roberts, G. W. β -Amyloid
precursor protein (β APP) as a marker for axonal injury after head injury. *Neurosci.Lett.* **160**, 139–
144, (1993).
- 125 Planel, E. *et al.* Insulin dysfunction induces in vivo tau hyperphosphorylation through distinct
mechanisms. *J. Neurosci.* **27**, 13635–13648, (2007).
- 126 Burkhart, K. K., Beard, D. C., Lehman, R. A. & Billingsley, M. L. Alterations in tau
phosphorylation in rat and human neocortical brain slices following hypoxia and glucose
deprivation. *Exp. Neurol.* **154**, 464–472, (1998).
- 127 Steinhilb, M. L., Dias-Santagata, D., Fulga, T. A., Felch, D. L. & Feany, M. B. Tau
phosphorylation sites work in concert to promote neurotoxicity in vivo. *Molecular biology of the
cell* **18**, 5060–5068, (2007).
- 128 Jeganathan, S. *et al.* Proline-directed pseudo-phosphorylation at AT8 and PHF1 epitopes induces a
compaction of the paperclip folding of Tau and generates a pathological (MC-1) conformation. *J.
Biol. Chem.* **283**, 32066–32076, (2008).
- 129 Kraemer, B. C. *et al.* Neurodegeneration and defective neurotransmission in a *Caenorhabditis
elegans* model of tauopathy. *Proc. Natl. Acad. Sci. USA* **100**, 9980–9985, (2003).
- 130 SantaCruz, K. *et al.* Tau suppression in a neurodegenerative mouse model improves memory
function. *Science* **309**, 476–481, (2005).
- 131 O'Leary, J. C., 3rd *et al.* Phenothiazine-mediated rescue of cognition in tau transgenic mice
requires neuroprotection and reduced soluble tau burden. *Mol. Neurodegener.* **5**, 45, (2010).
- 132 Mocanu, M. M. *et al.* The potential for beta-structure in the repeat domain of tau protein
determines aggregation, synaptic decay, neuronal loss, and coassembly with endogenous Tau in
inducible mouse models of tauopathy. *J. Neurosci.* **28**, 737–748, (2008).
- 133 Sydow, A. *et al.* Tau-induced defects in synaptic plasticity, learning, and memory are reversible in
transgenic mice after switching off the toxic Tau mutant. *J. Neurosci.* **31**, 2511–2525, (2011).
- 134 de Calignon, A., Spires-Jones, T. L., Pitstick, R., Carlson, G. A. & Hyman, B. T. Tangle-bearing
neurons survive despite disruption of membrane integrity in a mouse model of tauopathy. *J.
Neuropathol. Exp. Neurol.* **68**, 757–761, (2009).
- 135 de Calignon, A. *et al.* Caspase activation precedes and leads to tangles. *Nature* **464**, 1201–1204,
(2010).
- 136 Rocher, A. B. *et al.* Structural and functional changes in tau mutant mice neurons are not linked to
the presence of NFTs. *Exp. Neurol.* **223**, 385–393, (2010).
- 137 Feuillette, S., Miguel, L., Frebourg, T., Champion, D. & Lecourtis, M. Drosophila models of
human tauopathies indicate that Tau protein toxicity in vivo is mediated by soluble cytosolic
phosphorylated forms of the protein. *J. Neurochem.* **113**, 895–903, (2010).
- 138 Berger, Z. *et al.* Accumulation of pathological tau species and memory loss in a conditional model
of tauopathy. *J. Neurosci.* **27**, 3650–3662, (2007).
- 139 Maeda, S. *et al.* Granular tau oligomers as intermediates of tau filaments. *Biochemistry* **46**, 3856–
3861, (2007).
- 140 Sahara, N., Maeda, S. & Takashima, A. Tau oligomerization: a role for tau aggregation
intermediates linked to neurodegeneration. *Curr. Alzheimer Res.* **5**, 591–598, (2008).
- 141 Garg, S., Timm, T., Mandelkow, E. M., Mandelkow, E. & Wang, Y. Cleavage of Tau by calpain
in Alzheimer's disease: The quest for the toxic 17 kD fragment. *Neurobiol. Aging* **32**, 1–14,
(2011).
- 142 Park, S. Y. & Ferreira, A. The generation of a 17 kDa neurotoxic fragment: An alternative
mechanism by which tau mediates β -amyloid-induced neurodegeneration. *J. Neurosci.* **25**, 5365–
5375, (2005).
- 143 Gamblin, T. C. *et al.* Caspase cleavage of tau: linking amyloid and neurofibrillary tangles in
Alzheimer's disease. *Proc. Natl. Acad. Sci. USA* **100**, 10032–10037, (2003).
- 144 Wang, Y. *et al.* Tau fragmentation, aggregation and clearance: The dual role of lysosomal
processing. *Hum. Mol. Genet.* **18**, 4153–4170, (2009).
- 145 Gomez-Ramos, A., Diaz-Hernandez, M., Cuadros, R., Hernandez, F. & Avila, J. Extracellular tau
is toxic to neuronal cells. *FEBS Lett.* **580**, 4842–4850, (2006).

- 146 Frost, B., Jacks, R. L. & Diamond, M. I. Propagation of tau misfolding from the outside to the
inside of a cell. *J. Biol. Chem.* **284**, 12845–12852, (2009).
- 147 Gomez-Ramos, A., Diaz-Hernandez, M., Rubio, A., Miras-Portugal, M. T. & Avila, J.
Extracellular tau promotes intracellular calcium increase through M1 and M3 muscarinic receptors
in neuronal cells. *Mol. Cell Neurosci.* **37**, 673–681, (2008).
- 148 Clavaguera, F. *et al.* Transmission and spreading of tauopathy in transgenic mouse brain. *Nat. Cell
Biol.* **11**, 909–913, (2009).
- 149 Braak, H. & Braak, E. Frequency of stages of Alzheimer-related lesions in different age
categories. *Neurobiol. Aging* **18**, 351–357, (1997).
- 150 Harris, J. A. *et al.* Transsynaptic progression of amyloid- β -induced neuronal dysfunction within
the entorhinal-hippocampal network. *Neuron* **68**, 428–441, (2010).
- 151 Pooler, A. M., Phillips, E. C., Lau, D. H., Noble, W. & Hanger, D. P. Physiological release of
endogenous tau is stimulated by neuronal activity. *EMBO reports* **14**, 389–394, (2013).
- 152 Yamada, K. *et al.* Neuronal activity regulates extracellular tau in vivo. *The Journal of
experimental medicine* **211**, 387–393, (2014).
- 153 Coppola, G. *et al.* Evidence for a role of the rare p.A152T variant in MAPT in increasing the risk
for FTD-spectrum and Alzheimer's diseases. *Human molecular genetics* **21**, 3500–3512, (2012).
- 154 Kara, E. *et al.* The MAPT p.A152T variant is a risk factor associated with tauopathies with
atypical clinical and neuropathological features. *Neurobiology of aging* **33**, 2231 e2237–2231
e2214, (2012).
- 155 Mann, D. M., McDonagh, A. M., Pickering-Brown, S. M., Kowa, H. & Iwatsubo, T. Amyloid beta
protein deposition in patients with frontotemporal lobar degeneration: Relationship to age and
apolipoprotein E genotype. *Neurosci. Lett* **304**, 161–164, (2001).
- 156 Terwel, D. *et al.* Changed conformation of mutant Tau-P301L underlies the moribund tauopathy,
absent in progressive, nonlethal axonopathy of Tau-4R/2N transgenic mice. *J. Biol. Chem.* **280**,
3963–3973, (2005).
- 157 Kimura, T. *et al.* Aggregation of detergent-insoluble tau is involved in neuronal loss but not in
synaptic loss. *J. Biol. Chem.* **285**, 38692–38699, (2010).
- 158 Hoover, B. R. *et al.* Tau mislocalization to dendritic spines mediates synaptic dysfunction
independently of neurodegeneration. *Neuron* **68**, 1067–1081, (2010).
- 159 Burnouf, S. *et al.* NMDA receptor dysfunction contributes to impaired brain-derived neurotrophic
factor-induced facilitation of hippocampal synaptic transmission in a Tau transgenic model. *Aging
cell* **12**, 11–23, (2013).
- 160 Tackenberg, C. & Brandt, R. Divergent pathways mediate spine alterations and cell death induced
by amyloid-beta, wild-type tau, and R406W tau. *J. Neurosci.* **29**, 14439–14450, (2009).
- 161 Maruyama, M. *et al.* Imaging of tau pathology in a tauopathy mouse model and in Alzheimer
patients compared to normal controls. *Neuron* **79**, 1094–1108, (2013).
- 162 Mi, K. & Johnson, G. V. The role of tau phosphorylation in the pathogenesis of Alzheimer's
disease. *Curr. Alzheimer Res.* **3**, 449–463, (2006).
- 163 Noble, W. *et al.* Inhibition of glycogen synthase kinase-3 by lithium correlates with reduced
tauopathy and degeneration *in vivo*. *Proc. Natl. Acad. Sci. USA* **102**, 6990–6995, (2005).
- 164 Grandjean, E. M. & Aubry, J. M. Lithium: Updated human knowledge using an evidence-based
approach: Part III: Clinical safety. *CNS Drugs* **23**, 397–418, (2009).
- 165 Peineau, S. *et al.* LTP inhibits LTD in the hippocampus via regulation of GSK3beta. *Neuron* **53**,
703–717, (2007).
- 166 Kimura, T. *et al.* GSK-3beta is required for memory reconsolidation in adult brain. *PLoS One* **3**,
e3540, (2008).
- 167 Zheng Y L *et al.* A Cdk5 inhibitory peptide reduces tau hyperphosphorylation and apoptosis in
neurons. *EMBO J.* **24**, 209–220, (2005).
- 168 Alvarez, A., Toro, R., Cáceres, A. & Maccioni, R. B. Inhibition of tau phosphorylating protein
kinase cdk5 prevents beta-amyloid-induced neuronal death. *FEBS Lett.* **459**, 421–426, (1999).
- 169 Kim, D. *et al.* Dereglulation of HDAC1 by p25/Cdk5 in neurotoxicity. *Neuron* **60**, 803–817,
(2008).
- 170 Kampers, T., Friedhoff, P., Biernat, J., Mandelkow, E. M. & Mandelkow, E. RNA stimulates
aggregation of microtubule-associated protein tau into Alzheimer-like paired helical filaments.
FEBS Lett. **399**, 344–349, (1996).

171 Goedert, M. *et al.* Assembly of microtubule-associated protein tau into Alzheimer-like filaments
induced by sulphated glycosaminoglycans. *Nature* **383**, 550–553, (1996).

172 Crowe, A., Ballatore, C., Hyde, E., Trojanowski, J. Q. & Lee, V. M. High throughput screening
for small molecule inhibitors of heparin-induced tau fibril formation. *Biochem. Biophys. Res.
Commun.* **358**, 1–6, (2007).

173 Perez, M., Valpuesta, J. M., Medina, M., Montejo de Garcini, E. & Avila, J. Polymerization of tau
into filaments in the presence of heparin: The minimal sequence required for tau-tau interaction. *J.
Neurochem.* **67**, 1183–1190, (1996).

174 Chirita, C. N., Necula, M. & Kuret, J. Anionic micelles and vesicles induce tau fibrillization in
vitro. *J. Biol. Chem.* **278**, 25644–25650, (2003).

175 Masuda, M. *et al.* Small molecule inhibitors of alpha-synuclein filament assembly. *Biochemistry*
45, 6085–6094, (2006).

176 Pickhardt, M. *et al.* Anthraquinones inhibit tau aggregation and dissolve Alzheimer's paired helical
filaments in vitro and in cells. *J. Biol. Chem.* **280**, 3628–3635, (2005).

177 Gura, T. Hope in Alzheimer's fight emerges from unexpected places. *Nat. Med.* **14**, 894, (2008).

178 Wischik, C. M., Edwards, P. C., Lai, R. Y. K., Roth, M. & Harrington, C. R. Selective inhibition
of Alzheimer disease-like tau aggregation by phenothiazines. *Proc. Natl. Acad. Sci. USA* **93**,
11213–11218, (1996).

179 Schirmer, R. H., Adler, H., Pickhardt, M. & Mandelkow, E. "Lest we forget you - methylene blue
...". *Neurobiol. Aging*, In press.

180 Wischik, C. *TSingaporeite*, <<http://www.taurx.com/fact.htm>>

181 Yoshiyama, Y. *et al.* Synapse loss and microglial activation precede tangles in a P301S tauopathy
mouse model. *Neuron* **53**, 337–351, (2007).

182 Chambraud, B. *et al.* A role for FKBP52 in Tau protein function. *Proc. Natl. Acad. Sci. USA* **107**,
2658–2663, (2010).

183 Blair, L. J. *et al.* Accelerated neurodegeneration through chaperone-mediated oligomerization of
tau. *J Clin Invest* **123**, 4158–4169, (2013).

184 Taniguchi, S. *et al.* Inhibition of heparin-induced tau filament formation by phenothiazines,
polyphenols, and porphyrins. *J. Biol. Chem.* **280**, 7614–7623, (2005).

185 Cheng, I. *et al.* Accelerating amyloid- β fibrillization reduces oligomer levels and functional
deficits in Alzheimer disease mouse models. *J. Biol. Chem.* **282**, 23818–23828, (2007).

186 Shankar, G. M. *et al.* Amyloid-beta protein dimers isolated directly from Alzheimer's brains
impair synaptic plasticity and memory. *Nat. Med.* **14**, 837–842, (2008).

187 Ashe, K. H. & Zahs, K. R. Probing the biology of Alzheimer's disease in mice. *Neuron* **66**, 631–
645, (2010).

188 Sakono, M. & Zako, T. Amyloid oligomers: Formation and toxicity of Abeta oligomers. *FEBS J.*
277, 1348–1358, (2010).

189 Shimura, H., Schwartz, D., Gygi, S. P. & Kosik, K. S. CHIP-Hsc70 complex ubiquitinates
phosphorylated tau and enhances cell survival. *J. Biol. Chem.* **279**, 4869–4876, (2004).

190 Petrucelli, L. *et al.* CHIP and Hsp70 regulate tau ubiquitination, degradation and aggregation.
Hum. Mol. Genet. **13**, 703–714, (2004).

191 Hatakeyama, S. *et al.* U-box protein carboxyl terminus of Hsc70-interacting protein (CHIP)
mediates poly-ubiquitylation preferentially on four-repeat Tau and is involved in
neurodegeneration of tauopathy. *J. Neurochem.* **91**, 299–307, (2004).

192 Sahara, N. *et al.* In vivo evidence of CHIP up-regulation attenuating tau aggregation. *J.
Neurochem.* **94**, 1254–1263, (2005).

193 Dickey, C. A. *et al.* The high-affinity HSP90-CHIP complex recognizes and selectively degrades
phosphorylated tau client proteins. *The Journal of clinical investigation* **117**, 648–658, (2007).

194 Sahara, N. *et al.* Molecular chaperone-mediated tau protein metabolism counteracts the formation
of granular tau oligomers in human brain. *J. Neurosci. Res.* **85**, 3098–3108, (2007).

195 Cook, C. *et al.* Acetylation of the KXGS motifs in tau is a critical determinant in modulation of
tau aggregation and clearance. *Human molecular genetics* **23**, 104–116, (2014).

196 Sahara, N. *et al.* Assembly of two distinct dimers and higher-order oligomers from full-length tau.
Eur. J. Neurosci. **25**, 3020–3029, (2007).

- 197 Bi, X., Zhou, J. & Lynch, G. Lysosomal protease inhibitors induce meganeurites and tangle-like
structures in entorhinohippocampal regions vulnerable to Alzheimer's disease. *Exp. Neurol.* **158**,
312–327, (1999).
- 198 Auer, I. A. *et al.* Paired helical filament tau (PHFtau) in Niemann-Pick type C disease is similar to
PHFtau in Alzheimer's disease. *Acta Neuropathol.* **90**, 547–551, (1995).
- 199 Pacheco, C. D. & Lieberman, A. P. The pathogenesis of Niemann-Pick type C disease: A role for
autophagy? *Expert Rev. Mol. Med.* **10**, e26, (2008).
- 200 Bu, B. *et al.* Niemann-Pick disease type C yields possible clue for why cerebellar neurons do not
form neurofibrillary tangles. *Neurobiol. Dis.* **11**, 285–297, (2002).
- 201 Pacheco, C. D., Elrick, M. J. & Lieberman, A. P. Tau deletion exacerbates the phenotype of
Niemann-Pick type C mice and implicates autophagy in pathogenesis. *Hum. Mol. Genet.* **18**, 956–
965, (2009).
- 202 Rodriguez-Navarro, J. A. *et al.* Trehalose ameliorates dopaminergic and tau pathology in parkin
deleted/tau overexpressing mice through autophagy activation. *Neurobiol. Dis.* **39**, 423–438,
(2010).
- 203 Boimel M *et al.* Efficacy and safety of immunization with phosphorylated tau against
neurofibrillary tangles in mice. *Exp. Neurol.* **224**, 472–485, (2010).
- 204 Asuni A A, Boutajangout A, Quartermain D & Sigurdsson E M. Immunotherapy targeting
pathological tau conformers in a tangle mouse model reduces brain pathology with associated
functional improvements. *J. Neurosci.* **27**, 9115–9129, (2007).
- 205 Masliah, E. *et al.* Effects of a-synuclein immunization in a mouse model of Parkinson's disease.
Neuron **46**, 857–868, (2005).
- 206 Sigurdsson, E. M. Immunotherapy targeting pathological tau protein in Alzheimer's disease and
related tauopathies. *J. Alzheimers Dis.* **15**, 157–168, (2008).
- 207 Sigurdsson, E. M. Tau-focused immunotherapy for Alzheimer's disease and related tauopathies.
Curr. Alzheimer Res. **6**, 446–450, (2009).
- 208 Trojanowski, J. Q. *et al.* Update on the biomarker core of the Alzheimer's Disease Neuroimaging
Initiative subjects. *Alzheimers Dement.* **6**, 230–238, (2010).
- 209 Vanmechelen, E. *et al.* Quantification of tau phosphorylated at threonine 181 in human
cerebrospinal fluid: A sandwich ELISA with a synthetic phosphopeptide for standardization.
Neurosci. Lett. **285**, 49–52, (2000).
- 210 Wallin, A. K. *et al.* CSF biomarkers predict a more malignant outcome in Alzheimer disease.
Neurology **74**, 1531–1537, (2010).
- 211 Kim, W., Lee, S. & Hall, G. F. Secretion of human tau fragments resembling CSF-tau in
Alzheimer's disease is modulated by the presence of the exon 2 insert. *FEBS Lett.* **584**, 3085–
3088, (2010).
- 212 Brody, D. L. & Holtzman, D. M. Active and passive immunotherapy for neurodegenerative
disorders. *Annu. Rev. Neurosci.*, (2008).
- 213 Hong, M. *et al.* Mutation-specific functional impairments in distinct tau isoforms of hereditary
FTDP-17. *Science* **282**, 1914–1917, (1998).
- 214 Merrick, S. E., Trojanowski, J. Q. & Lee, V. M. Selective destruction of stable microtubules and
axons by inhibitors of protein serine/threonine phosphatases in cultured human neurons. *J.*
Neurosci. **17**, 5726–5737, (1997).
- 215 Alonso A C, Zaidi T, Grundke-Iqbal I & Iqbal K. Role of abnormally phosphorylated tau in the
breakdown of microtubules in Alzheimer disease. *Proc. Natl. Acad. Sci. U.S.A.* **91**, 5562–5566,
(1994).
- 216 Brunden, K. R. *et al.* Epothilone D improves microtubule density, axonal integrity, and cognition
in a transgenic mouse model of tauopathy. *J. Neurosci.* **30**, 13861–13866, (2010).
- 217 Divinski, I., Holtser-Cochav, M., Vulih-Schultzman, I., Steingart, R. A. & Gozes, I. Peptide
neuroprotection through specific interaction with brain tubulin. *J. Neurochem.* **98**, 973–984,
(2006).
- 218 Vulih-Schultzman, I. *et al.* Activity-dependent neuroprotective protein snippet NAP reduces tau
hyperphosphorylation and enhances learning in a novel transgenic mouse model. *J. Pharmacol.*
Exp. Ther. **323**, 438–449, (2007).
- 219 Gozes, I. *et al.* Addressing Alzheimer's disease tangles: From NAP to AL-108. *Curr Alzheimer*
Res **6**, 455–460, (2009).

- 220 Rogers, M. B. Tau-Targeting Drug Davunetide Washes Out in Phase 3 Trials
<http://www.alzforum.org/news/research-news/tau-targeting-drug-davunetide-washes-out-phase-3-trialsite>, 2012).
- 221 Polymeropoulos, M. H. *et al.* Mutation in the alpha-synuclein gene identified in families with Parkinson's disease. *Science* **276**, 2045-2047, (1997).
- 222 Kruger, R. *et al.* Ala30Pro mutation in the gene encoding alpha-synuclein in Parkinson's disease. *Nature genetics* **18**, 106-108, (1998).
- 223 Singleton, A. B. *et al.* alpha-Synuclein locus triplication causes Parkinson's disease. *Science* **302**, 841, (2003).
- 224 Ibanez, P. *et al.* Causal relation between alpha-synuclein gene duplication and familial Parkinson's disease. *Lancet* **364**, 1169-1171, (2004).
- 225 Chartier-Harlin, M. C. *et al.* Alpha-synuclein locus duplication as a cause of familial Parkinson's disease. *Lancet* **364**, 1167-1169, (2004).
- 226 Zarranz, J. J. *et al.* The new mutation, E46K, of alpha-synuclein causes Parkinson and Lewy body dementia. *Annals of neurology* **55**, 164-173, (2004).
- 227 Appel-Cresswell, S. *et al.* Alpha-synuclein p.H50Q, a novel pathogenic mutation for Parkinson's disease. *Movement disorders : official journal of the Movement Disorder Society* **28**, 811-813, (2013).
- 228 Proukakis, C. *et al.* A novel alpha-synuclein missense mutation in Parkinson disease. *Neurology* **80**, 1062-1064, (2013).
- 229 Fares, M. B. *et al.* The novel Parkinson's disease linked mutation G51D attenuates in vitro aggregation and membrane binding of alpha-synuclein, and enhances its secretion and nuclear localization in cells. *Human molecular genetics*, (2014).
- 230 Kiely, A. P. *et al.* alpha-Synucleinopathy associated with G51D SNCA mutation: a link between Parkinson's disease and multiple system atrophy? *Acta neuropathologica* **125**, 753-769, (2013).
- 231 Spillantini, M. G. *et al.* Filamentous alpha-synuclein inclusions link multiple system atrophy with Parkinson's disease and dementia with Lewy bodies. *Neuroscience letters* **251**, 205-208, (1998).
- 232 Tu, P. H. *et al.* Glial cytoplasmic inclusions in white matter oligodendrocytes of multiple system atrophy brains contain insoluble alpha-synuclein. *Annals of neurology* **44**, 415-422, (1998).
- 233 Maroteaux, L., Campanelli, J. T. & Scheller, R. H. Synuclein: a neuron-specific protein localized to the nucleus and presynaptic nerve terminal. *The Journal of neuroscience : the official journal of the Society for Neuroscience* **8**, 2804-2815, (1988).
- 234 Ueda, K. *et al.* Molecular cloning of cDNA encoding an unrecognized component of amyloid in Alzheimer disease. *Proceedings of the National Academy of Sciences of the United States of America* **90**, 11282-11286, (1993).
- 235 Davidson, W. S., Jonas, A., Clayton, D. F. & George, J. M. Stabilization of alpha-synuclein secondary structure upon binding to synthetic membranes. *The Journal of biological chemistry* **273**, 9443-9449, (1998).
- 236 Ulmer, T. S., Bax, A., Cole, N. B. & Nussbaum, R. L. Structure and dynamics of micelle-bound human alpha-synuclein. *The Journal of biological chemistry* **280**, 9595-9603, (2005).
- 237 Eliezer, D., Kutluay, E., Bussell, R., Jr. & Browne, G. Conformational properties of alpha-synuclein in its free and lipid-associated states. *Journal of molecular biology* **307**, 1061-1073, (2001).
- 238 Bartels, T., Choi, J. G. & Selkoe, D. J. alpha-Synuclein occurs physiologically as a helically folded tetramer that resists aggregation. *Nature* **477**, 107-110, (2011).
- 239 Lashuel, H. A., Overk, C. R., Oueslati, A. & Masliah, E. The many faces of alpha-synuclein: from structure and toxicity to therapeutic target. *Nature reviews. Neuroscience* **14**, 38-48, (2013).
- 240 Lesage, S. *et al.* G51D alpha-synuclein mutation causes a novel parkinsonian-pyramidal syndrome. *Annals of neurology* **73**, 459-471, (2013).
- 241 Bussell, R., Jr. & Eliezer, D. Residual structure and dynamics in Parkinson's disease-associated mutants of alpha-synuclein. *The Journal of biological chemistry* **276**, 45996-46003, (2001).
- 242 Ghosh, D. *et al.* The Parkinson's disease-associated H50Q mutation accelerates alpha-Synuclein aggregation in vitro. *Biochemistry* **52**, 6925-6927, (2013).
- 243 McFarland, M. A., Ellis, C. E., Markey, S. P. & Nussbaum, R. L. Proteomics analysis identifies phosphorylation-dependent alpha-synuclein protein interactions. *Molecular & cellular proteomics : MCP* **7**, 2123-2137, (2008).

244 Wang, Z. *et al.* Enrichment and site mapping of O-linked N-acetylglucosamine by a combination
of chemical/enzymatic tagging, photochemical cleavage, and electron transfer dissociation mass
spectrometry. *Molecular & cellular proteomics : MCP* **9**, 153-160, (2010).

245 Marotta, N. P., Cherwien, C. A., Abeywardana, T. & Pratt, M. R. O-GlcNAc modification
prevents peptide-dependent acceleration of alpha-synuclein aggregation. *Chembiochem : a
European journal of chemical biology* **13**, 2665-2670, (2012).

246 Murray, I. V. *et al.* Role of alpha-synuclein carboxy-terminus on fibril formation in vitro.
Biochemistry **42**, 8530-8540, (2003).

247 Anderson, J. P. *et al.* Phosphorylation of Ser-129 is the dominant pathological modification of
alpha-synuclein in familial and sporadic Lewy body disease. *The Journal of biological chemistry*
281, 29739-29752, (2006).

248 Kuzuhara, S., Mori, H., Izumiyama, N., Yoshimura, M. & Ihara, Y. Lewy bodies are
ubiquitinated. A light and electron microscopic immunocytochemical study. *Acta
neuropathologica* **75**, 345-353, (1988).

249 Fujiwara, H. *et al.* alpha-Synuclein is phosphorylated in synucleinopathy lesions. *Nat Cell Biol* **4**,
160-164, (2002).

250 Oueslati, A., Fournier, M. & Lashuel, H. A. Role of post-translational modifications in modulating
the structure, function and toxicity of alpha-synuclein: implications for Parkinson's disease
pathogenesis and therapies. *Progress in brain research* **183**, 115-145, (2010).

251 Abeliovich, A. *et al.* Mice lacking alpha-synuclein display functional deficits in the nigrostriatal
dopamine system. *Neuron* **25**, 239-252, (2000).

252 Specht, C. G. & Schoepfer, R. Deletion of the alpha-synuclein locus in a subpopulation of
C57BL/6J inbred mice. *BMC neuroscience* **2**, 11, (2001).

253 Yavich, L., Tanila, H., Vepsalainen, S. & Jakala, P. Role of alpha-synuclein in presynaptic
dopamine recruitment. *The Journal of neuroscience : the official journal of the Society for
Neuroscience* **24**, 11165-11170, (2004).

254 Garcia-Reitböck, P. *et al.* SNARE protein redistribution and synaptic failure in a transgenic mouse
model of Parkinson's disease. *Brain : a journal of neurology* **133**, 2032-2044, (2010).

255 Anwar, S. *et al.* Functional alterations to the nigrostriatal system in mice lacking all three
members of the synuclein family. *The Journal of neuroscience : the official journal of the Society
for Neuroscience* **31**, 7264-7274, (2011).

256 Westphal, C. H. & Chandra, S. S. Monomeric synucleins generate membrane curvature. *The
Journal of biological chemistry* **288**, 1829-1840, (2013).

257 Burre, J. *et al.* Alpha-synuclein promotes SNARE-complex assembly in vivo and in vitro. *Science*
329, 1663-1667, (2010).

258 Pranke, I. M. *et al.* alpha-Synuclein and ALPS motifs are membrane curvature sensors whose
contrasting chemistry mediates selective vesicle binding. *J Cell Biol* **194**, 89-103, (2011).

259 Fortin, D. L. *et al.* Neural activity controls the synaptic accumulation of alpha-synuclein. *The
Journal of neuroscience : the official journal of the Society for Neuroscience* **25**, 10913-10921,
(2005).

260 Bai, J., Hu, Z., Dittman, J. S., Pym, E. C. & Kaplan, J. M. Endophilin functions as a membrane-
bending molecule and is delivered to endocytic zones by exocytosis. *Cell* **143**, 430-441, (2010).

261 Bendor, J. T., Logan, T. P. & Edwards, R. H. The function of alpha-synuclein. *Neuron* **79**, 1044-
1066, (2013).

262 Nemani, V. M. *et al.* Increased expression of alpha-synuclein reduces neurotransmitter release by
inhibiting synaptic vesicle reclustering after endocytosis. *Neuron* **65**, 66-79, (2010).

263 Dawson-Scully, K., Bronk, P., Atwood, H. L. & Zinsmaier, K. E. Cysteine-string protein increases
the calcium sensitivity of neurotransmitter exocytosis in *Drosophila*. *The Journal of neuroscience
: the official journal of the Society for Neuroscience* **20**, 6039-6047, (2000).

264 Chandra, S., Gallardo, G., Fernandez-Chacon, R., Schluter, O. M. & Sudhof, T. C. Alpha-
synuclein cooperates with CSPalpha in preventing neurodegeneration. *Cell* **123**, 383-396, (2005).

265 Diao, J. *et al.* Native alpha-synuclein induces clustering of synaptic-vesicle mimics via binding to
phospholipids and synaptobrevin-2/VAMP2. *eLife* **2**, e00592, (2013).

266 Janežič, S. *et al.* Deficits in dopaminergic transmission precede neuron loss and dysfunction in a
new Parkinson model. *Proceedings of the National Academy of Sciences of the United States of
America* **110**, E4016-4025, (2013).

- 267 Cabin, D. E. *et al.* Synaptic vesicle depletion correlates with attenuated synaptic responses to
prolonged repetitive stimulation in mice lacking alpha-synuclein. *The Journal of neuroscience :
the official journal of the Society for Neuroscience* **22**, 8797-8807, (2002).
- 268 Choi, B. K. *et al.* Large alpha-synuclein oligomers inhibit neuronal SNARE-mediated vesicle
docking. *Proceedings of the National Academy of Sciences of the United States of America* **110**,
4087-4092, (2013).
- 269 Jenco, J. M., Rawlingson, A., Daniels, B. & Morris, A. J. Regulation of phospholipase D2:
selective inhibition of mammalian phospholipase D isoenzymes by alpha- and beta-synucleins.
Biochemistry **37**, 4901-4909, (1998).
- 270 Payton, J. E., Perrin, R. J., Woods, W. S. & George, J. M. Structural determinants of PLD2
inhibition by alpha-synuclein. *Journal of molecular biology* **337**, 1001-1009, (2004).
- 271 Gorbatyuk, O. S. *et al.* alpha-Synuclein expression in rat substantia nigra suppresses
phospholipase D2 toxicity and nigral neurodegeneration. *Molecular therapy : the journal of the
American Society of Gene Therapy* **18**, 1758-1768, (2010).
- 272 Magen, I. *et al.* Cognitive deficits in a mouse model of pre-manifest Parkinson's disease. *Eur. J.
Neurosci.* **35**, 870-882, (2012).
- 273 Stavinoha, W. B. & Weintraub, S. T. Choline content of rat brain. *Science* **183**, 964-965, (1974).
- 274 Nakamura, K. *et al.* Optical reporters for the conformation of alpha-synuclein reveal a specific
interaction with mitochondria. *The Journal of neuroscience : the official journal of the Society for
Neuroscience* **28**, 12305-12317, (2008).
- 275 Devi, L., Raghavendran, V., Prabhu, B. M., Avadhani, N. G. & Anandatheerthavarada, H. K.
Mitochondrial import and accumulation of alpha-synuclein impair complex I in human
dopaminergic neuronal cultures and Parkinson disease brain. *The Journal of biological chemistry*
283, 9089-9100, (2008).
- 276 Ellis, C. E. *et al.* Mitochondrial lipid abnormality and electron transport chain impairment in mice
lacking alpha-synuclein. *Molecular and cellular biology* **25**, 10190-10201, (2005).
- 277 Giasson, B. I. *et al.* Initiation and synergistic fibrillization of tau and alpha-synuclein. *Science* **300**,
636-640, (2003).
- 278 Larsen, K. E. *et al.* Alpha-synuclein overexpression in PC12 and chromaffin cells impairs
catecholamine release by interfering with a late step in exocytosis. *The Journal of neuroscience :
the official journal of the Society for Neuroscience* **26**, 11915-11922, (2006).
- 279 Kontopoulos, E., Parvin, J. D. & Feany, M. B. Alpha-synuclein acts in the nucleus to inhibit
histone acetylation and promote neurotoxicity. *Human molecular genetics* **15**, 3012-3023, (2006).
- 280 Dauer, W. *et al.* Resistance of alpha -synuclein null mice to the parkinsonian neurotoxin MPTP.
Proceedings of the National Academy of Sciences of the United States of America **99**, 14524-
14529, (2002).
- 281 Fornai, F. *et al.* Parkinson-like syndrome induced by continuous MPTP infusion: convergent roles
of the ubiquitin-proteasome system and alpha-synuclein. *Proceedings of the National Academy of
Sciences of the United States of America* **102**, 3413-3418, (2005).
- 282 Klivenyi, P. *et al.* Mice lacking alpha-synuclein are resistant to mitochondrial toxins.
Neurobiology of disease **21**, 541-548, (2006).
- 283 Thomas, B. *et al.* Resistance to MPTP-neurotoxicity in alpha-synuclein knockout mice is
complemented by human alpha-synuclein and associated with increased beta-synuclein and Akt
activation. *PLoS One* **6**, e16706, (2011).
- 284 Skibinski, G., Nakamura, K., Cookson, M. R. & Finkbeiner, S. Mutant LRRK2 toxicity in neurons
depends on LRRK2 levels and synuclein but not kinase activity or inclusion bodies. *The Journal
of neuroscience : the official journal of the Society for Neuroscience* **34**, 418-433, (2014).
- 285 Siddiqui, A. *et al.* Selective binding of nuclear alpha-synuclein to the PGC1alpha promoter under
conditions of oxidative stress may contribute to losses in mitochondrial function: implications for
Parkinson's disease. *Free radical biology & medicine* **53**, 993-1003, (2012).
- 286 Goers, J. *et al.* Nuclear localization of alpha-synuclein and its interaction with histones.
Biochemistry **42**, 8465-8471, (2003).
- 287 Kim, S., Park, J. M., Moon, J. & Choi, H. J. Alpha-synuclein interferes with cAMP/PKA-
dependent upregulation of dopamine beta-hydroxylase and is associated with abnormal adaptive
responses to immobilization stress. *Experimental neurology* **252**, 63-74, (2014).

288 Narhi, L. *et al.* Both familial Parkinson's disease mutations accelerate alpha-synuclein
aggregation. *The Journal of biological chemistry* **274**, 9843-9846, (1999).

289 Fredenburg, R. A. *et al.* The impact of the E46K mutation on the properties of alpha-synuclein in
its monomeric and oligomeric states. *Biochemistry* **46**, 7107-7118, (2007).

290 Burre, J., Sharma, M. & Sudhof, T. C. Systematic mutagenesis of alpha-synuclein reveals distinct
sequence requirements for physiological and pathological activities. *The Journal of neuroscience :
the official journal of the Society for Neuroscience* **32**, 15227-15242, (2012).

291 Volles, M. J. *et al.* Vesicle permeabilization by protofibrillar alpha-synuclein: implications for the
pathogenesis and treatment of Parkinson's disease. *Biochemistry* **40**, 7812-7819, (2001).

292 Nakamura, K. alpha-Synuclein and mitochondria: partners in crime? *Neurotherapeutics* **10**, 391-
399, (2013).

293 Nakamura, K. *et al.* Direct membrane association drives mitochondrial fission by the Parkinson
disease-associated protein alpha-synuclein. *The Journal of biological chemistry* **286**, 20710-
20726, (2011).

294 Choubey, V. *et al.* Mutant A53T alpha-synuclein induces neuronal death by increasing
mitochondrial autophagy. *The Journal of biological chemistry* **286**, 10814-10824, (2011).

295 Junn, E. & Mouradian, M. M. Human alpha-synuclein over-expression increases intracellular
reactive oxygen species levels and susceptibility to dopamine. *Neuroscience letters* **320**, 146-150,
(2002).

296 Loeb, V., Yakunin, E., Saada, A. & Sharon, R. The transgenic overexpression of alpha-synuclein
and not its related pathology associates with complex I inhibition. *The Journal of biological
chemistry* **285**, 7334-7343, (2010).

297 Cuervo, A. M., Stefanis, L., Fredenburg, R., Lansbury, P. T. & Sulzer, D. Impaired degradation of
mutant alpha-synuclein by chaperone-mediated autophagy. *Science* **305**, 1292-1295, (2004).

298 Snyder, H. *et al.* Aggregated and monomeric alpha-synuclein bind to the S6' proteasomal protein
and inhibit proteasomal function. *The Journal of biological chemistry* **278**, 11753-11759, (2003).

299 Braak, H. *et al.* Staging of brain pathology related to sporadic Parkinson's disease. *Neurobiology
of aging* **24**, 197-211, (2003).

300 Li, J. Y. *et al.* Lewy bodies in grafted neurons in subjects with Parkinson's disease suggest host-to-
graft disease propagation. *Nature medicine* **14**, 501-503, (2008).

301 Luk, K. C. *et al.* Pathological alpha-synuclein transmission initiates Parkinson-like
neurodegeneration in nontransgenic mice. *Science* **338**, 949-953, (2012).

302 Lee, H. J., Patel, S. & Lee, S. J. Intravesicular localization and exocytosis of alpha-synuclein and
its aggregates. *The Journal of neuroscience : the official journal of the Society for Neuroscience*
25, 6016-6024, (2005).

303 Emmanouilidou, E. *et al.* Cell-produced alpha-synuclein is secreted in a calcium-dependent
manner by exosomes and impacts neuronal survival. *The Journal of neuroscience : the official
journal of the Society for Neuroscience* **30**, 6838-6851, (2010).

304 Hasegawa, T. *et al.* The AAA-ATPase VPS4 regulates extracellular secretion and lysosomal
targeting of alpha-synuclein. *PLoS One* **6**, e29460, (2011).

305 Danzer, K. M. *et al.* Exosomal cell-to-cell transmission of alpha synuclein oligomers. *Molecular
neurodegeneration* **7**, 42, (2012).

306 Lee, H. J. *et al.* Assembly-dependent endocytosis and clearance of extracellular alpha-synuclein.
The international journal of biochemistry & cell biology **40**, 1835-1849, (2008).

307 University of Colorado, Denver. Phenylbutyrate As a Treatment for Abnormal Accumulation of
Brain Protein in Parkinson's Disease.
<http://www.clinicaltrials.gov/ct2/show/NCT02046434?term=phenylbutyrate+parkinsons&rank=1>
[title](#), 2014).

308 Lee, K. W. *et al.* Enhanced phosphatase activity attenuates alpha-synucleinopathy in a mouse
model. *The Journal of neuroscience : the official journal of the Society for Neuroscience* **31**, 6963-
6971, (2011).

309 Perez-Revuelta, B. I. *et al.* Metformin lowers Ser-129 phosphorylated alpha-synuclein levels via
mTOR-dependent protein phosphatase 2A activation. *Cell death & disease* **5**, e1209, (2014).

310 Shaltiel-Karyo, R. *et al.* Differential inhibition of alpha-synuclein oligomeric and fibrillar
assembly in parkinson's disease model by cinnamon extract. *Biochim Biophys Acta* **1820**, 1628-
1635, (2012).

- 311 Herva, M. E. *et al.* Anti-amyloid compounds inhibit alpha-synuclein aggregation induced by protein misfolding cyclic amplification (PMCA). *The Journal of biological chemistry* **289**, 11897-11905, (2014).
- 312 Wagner, J. *et al.* Anle138b: a novel oligomer modulator for disease-modifying therapy of neurodegenerative diseases such as prion and Parkinson's disease. *Acta neuropathologica* **125**, 795-813, (2013).
- 313 Prabhudesai, S. *et al.* A novel "molecular tweezer" inhibitor of alpha-synuclein neurotoxicity in vitro and in vivo. *Neurotherapeutics* **9**, 464-476, (2012).
- 314 Hashimoto, M., Rockenstein, E., Mante, M., Mallory, M. & Masliah, E. beta-Synuclein inhibits alpha-synuclein aggregation: a possible role as an anti-parkinsonian factor. *Neuron* **32**, 213-223, (2001).
- 315 Hebron, M. L., Lonskaya, I. & Moussa, C. E. Nilotinib reverses loss of dopamine neurons and improves motor behavior via autophagic degradation of alpha-synuclein in Parkinson's disease models. *Human molecular genetics* **22**, 3315-3328, (2013).
- 316 Oueslati, A., Schneider, B. L., Aebischer, P. & Lashuel, H. A. Polo-like kinase 2 regulates selective autophagic alpha-synuclein clearance and suppresses its toxicity in vivo. *Proceedings of the National Academy of Sciences of the United States of America* **110**, E3945-3954, (2013).
- 317 Hollerhage, M. *et al.* Trifluoperazine rescues human dopaminergic cells from wild-type alpha-synuclein-induced toxicity. *Neurobiology of aging* **35**, 1700-1711, (2014).
- 318 Davies, S. E. *et al.* Enhanced ubiquitin-dependent degradation by Nedd4 protects against alpha-synuclein accumulation and toxicity in animal models of Parkinson's disease. *Neurobiology of disease* **64**, 79-87, (2014).
- 319 Chung, C. Y. *et al.* Identification and rescue of alpha-synuclein toxicity in Parkinson patient-derived neurons. *Science* **342**, 983-987, (2013).
- 320 Kilpatrick, K. *et al.* Chemical induction of Hsp70 reduces alpha-synuclein aggregation in neuroglioma cells. *ACS chemical biology* **8**, 1460-1468, (2013).
- 321 Shaltiel-Karyo, R. *et al.* A blood-brain barrier (BBB) disrupter is also a potent alpha-synuclein (alpha-syn) aggregation inhibitor: a novel dual mechanism of mannitol for the treatment of Parkinson disease (PD). *The Journal of biological chemistry* **288**, 17579-17588, (2013).
- 322 Shin, Y., Klucken, J., Patterson, C., Hyman, B. T. & McLean, P. J. The co-chaperone carboxyl terminus of Hsp70-interacting protein (CHIP) mediates alpha-synuclein degradation decisions between proteasomal and lysosomal pathways. *The Journal of biological chemistry* **280**, 23727-23734, (2005).
- 323 Masliah, E. *et al.* Effects of alpha-synuclein immunization in a mouse model of Parkinson's disease. *Neuron* **46**, 857-868, (2005).
- 324 Benner, E. J. *et al.* Nitrated alpha-synuclein immunity accelerates degeneration of nigral dopaminergic neurons. *PLoS One* **3**, e1376, (2008).
- 325 Mandler, M. *et al.* Next-generation active immunization approach for synucleinopathies: implications for Parkinson's disease clinical trials. *Acta neuropathologica* **127**, 861-879, (2014).
- 326 Zhou, W. & Freed, C. R. DJ-1 up-regulates glutathione synthesis during oxidative stress and inhibits A53T alpha-synuclein toxicity. *The Journal of biological chemistry* **280**, 43150-43158, (2005).
- 327 Zhou, W. *et al.* Phenylbutyrate up-regulates the DJ-1 protein and protects neurons in cell culture and in animal models of Parkinson disease. *The Journal of biological chemistry* **286**, 14941-14951, (2011).
- 328 Toth, G. *et al.* Targeting the intrinsically disordered structural ensemble of alpha-synuclein by small molecules as a potential therapeutic strategy for Parkinson's disease. *PLoS One* **9**, e87133, (2014).
- 329 Hamilton, R. L. Lewy bodies in Alzheimer's disease: A neuropathological review of 145 cases using a-synuclein immunohistochemistry. *Brain Pathol.* **10**, 378-384, (2000).
- 330 McKeith, I. G. *et al.* Diagnosis and management of dementia with Lewy bodies: Third report of the DLB Consortium. *Neurology* **65**, 1863-1872, (2005).
- 331 Mikolaenko, I. *et al.* Alpha-synuclein lesions in normal aging, Parkinson disease, and Alzheimer disease: evidence from the Baltimore Longitudinal Study of Aging (BLSA). *Journal of neuropathology and experimental neurology* **64**, 156-162, (2005).

- 332 Masliah, E. *et al.* β -Amyloid peptides enhance α -synuclein accumulation and neuronal deficits in a transgenic mouse model linking Alzheimer's disease and Parkinson's disease. *Proc. Natl. Acad. Sci. USA* **98**, 12245–12250, (2001).
- 333 Golbe, L. I. *et al.* The tau A0 allele in Parkinson's disease. *Mov. Disord.* **16**, 442–447, (2001).
- 334 Simon-Sanchez, J. *et al.* Genome-wide association study reveals genetic risk underlying Parkinson's disease. *Nature genetics* **41**, 1308-1312, (2009).
- 335 Duda, J. E. *et al.* Concurrence of alpha-synuclein and tau brain pathology in the Contursi kindred. *Acta Neuropathol.* **104**, 7–11, (2002).
- 336 Kotzbauer, P. T. *et al.* Fibrillization of alpha-synuclein and tau in familial Parkinson's disease caused by the A53T alpha-synuclein mutation. *Exp. Neurol.* **187**, 279–288, (2004).
- 337 Ishizawa, T., Mattila, P., Davies, P., Wang, D. & Dickson, D. W. Colocalization of tau and alpha-synuclein epitopes in Lewy bodies. *Journal of neuropathology and experimental neurology* **62**, 389-397, (2003).
- 338 Jensen, P. H. *et al.* alpha-synuclein binds to Tau and stimulates the protein kinase A-catalyzed tau phosphorylation of serine residues 262 and 356. *The Journal of biological chemistry* **274**, 25481-25489, (1999).
- 339 Guo, J. L. *et al.* Distinct alpha-synuclein strains differentially promote tau inclusions in neurons. *Cell* **154**, 103-117, (2013).
- 340 Arima, K. *et al.* Cellular co-localization of phosphorylated tau- and NACP/alpha-synuclein-epitopes in lewy bodies in sporadic Parkinson's disease and in dementia with Lewy bodies. *Brain research* **843**, 53-61, (1999).
- 341 Huang, Y. & Mucke, L. Alzheimer mechanisms and therapeutic strategies. *Cell* **148**, 1204–1222, (2012).
- 342 2012 Alzheimer's disease facts and figures. *Alzheimers Dement.* **8**, 131–168, (2012).
- 343 Golde, T. E., Schneider, L. S. & Koo, E. H. Anti- β therapeutics in Alzheimer's disease: The need for a paradigm shift. *Neuron* **69**, 203–213, (2011).
- 344 Morris, M., Maeda, S., Vossel, K. & Mucke, L. The many faces of tau. *Neuron* **70**, 410–426, (2011).
- 345 Morris, M., Koyama, A., Masliah, E. & Mucke, L. Tau reduction does not prevent motor deficits in two mouse models of Parkinson's disease. *PLoS One* **6**, e29257, (2011).
- 346 Palop, J. J. & Mucke, L. Synaptic depression and aberrant excitatory network activity in Alzheimer's disease: two faces of the same coin? *Neuromolecular medicine* **12**, 48-55, (2010).
- 347 Mucke, L. *et al.* High-level neuronal expression of $A\beta_{1-42}$ in wild-type human amyloid protein precursor transgenic mice: Synaptotoxicity without plaque formation. *J. Neurosci.* **20**, 4050–4058, (2000).
- 348 Palop, J. J. *et al.* Neuronal depletion of calcium-dependent proteins in the dentate gyrus is tightly linked to Alzheimer's disease-related cognitive deficits. *Proc. Natl. Acad. Sci. USA* **100**, 9572–9577, (2003).
- 349 Li, Z., Hall, A. M., Kelinske, M. & Roberson, E. D. Seizure resistance without parkinsonism in aged mice after tau reduction. *Neurobiology of aging*, (2014).
- 350 Holth, J. K. *et al.* Tau loss attenuates neuronal network hyperexcitability in mouse and Drosophila genetic models of epilepsy. *J. Neurosci.* **33**, 1651–1659, (2013).
- 351 Thomas, S. N. *et al.* Dual modification of Alzheimer's disease PHF-tau protein by lysine methylation and ubiquitylation: a mass spectrometry approach. *Acta neuropathologica* **123**, 105-117, (2012).
- 352 Funk, K. E. *et al.* Lysine methylation is an endogenous post-translational modification of tau protein in human brain and a modulator of aggregation propensity. *The Biochemical journal*, (2014).
- 353 Guo, H. *et al.* Profiling substrates of protein arginine N-methyltransferase 3 with S-adenosyl-L-methionine analogues. *ACS chemical biology* **9**, 476-484, (2014).
- 354 Liu, F., Iqbal, K., Grundke-Iqbal, I., Hart, G. W. & Gong, C. X. O-GlcNAcylation regulates phosphorylation of tau: a mechanism involved in Alzheimer's disease. *Proceedings of the National Academy of Sciences of the United States of America* **101**, 10804-10809, (2004).
- 355 Liu, F. *et al.* Reduced O-GlcNAcylation links lower brain glucose metabolism and tau pathology in Alzheimer's disease. *Brain : a journal of neurology* **132**, 1820-1832, (2009).

- 356 Yuzwa, S. A. *et al.* A potent mechanism-inspired O-GlcNAcase inhibitor that blocks phosphorylation of tau in vivo. *Nature chemical biology* **4**, 483-490, (2008).
- 357 Hanger, D. P. *et al.* Novel phosphorylation sites in tau from Alzheimer brain support a role for casein kinase 1 in disease pathogenesis. *The Journal of biological chemistry* **282**, 23645-23654, (2007).
- 358 Morishima-Kawashima, M. *et al.* Ubiquitin is conjugated with amino-terminally processed tau in paired helical filaments. *Neuron* **10**, 1151-1160, (1993).
- 359 Baker, P. R., Trinidad, J. C. & Chalkley, R. J. Modification site localization scoring integrated into a search engine. *Molecular & cellular proteomics : MCP* **10**, M111 008078, (2011).
- 360 Beausoleil, S. A., Villen, J., Gerber, S. A., Rush, J. & Gygi, S. P. A probability-based approach for high-throughput protein phosphorylation analysis and site localization. *Nature biotechnology* **24**, 1285-1292, (2006).
- 361 Bradshaw, R. A., Medzihradzky, K. F. & Chalkley, R. J. Protein PTMs: post-translational modifications or pesky trouble makers? *Journal of mass spectrometry : JMS* **45**, 1095-1097, (2010).
- 362 Dinkel, H. *et al.* Phospho.ELM: a database of phosphorylation sites--update 2011. *Nucleic acids research* **39**, D261-267, (2011).
- 363 Chalkley, R. J. & Clauser, K. R. Modification site localization scoring: strategies and performance. *Molecular & cellular proteomics : MCP* **11**, 3-14, (2012).
- 364 Hornbeck, P. V. *et al.* PhosphoSitePlus: a comprehensive resource for investigating the structure and function of experimentally determined post-translational modifications in man and mouse. *Nucleic acids research* **40**, D261-270, (2012).
- 365 UniProt, C. Activities at the Universal Protein Resource (UniProt). *Nucleic acids research* **42**, D191-198, (2014).
- 366 Planel, E. *et al.* Anesthesia leads to tau hyperphosphorylation through inhibition of phosphatase activity by hypothermia. *The Journal of neuroscience : the official journal of the Society for Neuroscience* **27**, 3090-3097, (2007).
- 367 Huttlin, E. L. *et al.* A tissue-specific atlas of mouse protein phosphorylation and expression. *Cell* **143**, 1174-1189, (2010).
- 368 Trinidad, J. C. *et al.* Global identification and characterization of both O-GlcNAcylation and phosphorylation at the murine synapse. *Molecular & cellular proteomics : MCP* **11**, 215-229, (2012).
- 369 Tweedie-Cullen, R. Y., Reck, J. M. & Mansuy, I. M. Comprehensive mapping of post-translational modifications on synaptic, nuclear, and histone proteins in the adult mouse brain. *Journal of proteome research* **8**, 4966-4982, (2009).
- 370 Collins, M. O., Yu, L., Campuzano, I., Grant, S. G. & Choudhary, J. S. Phosphoproteomic analysis of the mouse brain cytosol reveals a predominance of protein phosphorylation in regions of intrinsic sequence disorder. *Molecular & cellular proteomics : MCP* **7**, 1331-1348, (2008).
- 371 Hanger, D. P., Betts, J. C., Loviny, T. L., Blackstock, W. P. & Anderton, B. H. New phosphorylation sites identified in hyperphosphorylated tau (paired helical filament-tau) from Alzheimer's disease brain using nano-electrospray mass spectrometry. *Journal of neurochemistry* **71**, 2465-2476, (1998).
- 372 Goswami, T. *et al.* Comparative phosphoproteomic analysis of neonatal and adult murine brain. *Proteomics* **12**, 2185-2189, (2012).
- 373 Wang, J. Z., Wu, Q., Smith, A., Grundke-Iqbal, I. & Iqbal, K. Tau is phosphorylated by GSK-3 at several sites found in Alzheimer disease and its biological activity markedly inhibited only after it is prephosphorylated by A-kinase. *FEBS letters* **436**, 28-34, (1998).
- 374 Leroy, A. *et al.* Spectroscopic studies of GSK3 β phosphorylation of the neuronal tau protein and its interaction with the N-terminal domain of apolipoprotein E. *The Journal of biological chemistry* **285**, 33435-33444, (2010).
- 375 Rudrabhatla, P., Jaffe, H. & Pant, H. C. Direct evidence of phosphorylated neuronal intermediate filament proteins in neurofibrillary tangles (NFTs): phosphoproteomics of Alzheimer's NFTs. *FASEB journal : official publication of the Federation of American Societies for Experimental Biology* **25**, 3896-3905, (2011).
- 376 Drewes, G. *et al.* Microtubule-associated protein/microtubule affinity-regulating kinase (p110mark). A novel protein kinase that regulates tau-microtubule interactions and dynamic

- instability by phosphorylation at the Alzheimer-specific site serine 262. *The Journal of biological chemistry* **270**, 7679-7688, (1995).
- 377 Hill, J. J., Callaghan, D. A., Ding, W., Kelly, J. F. & Chakravarthy, B. R. Identification of okadaic acid-induced phosphorylation events by a mass spectrometry approach. *Biochemical and biophysical research communications* **342**, 791-799, (2006).
- 378 Thornton, C., Bright, N. J., Sastre, M., Muckett, P. J. & Carling, D. AMP-activated protein kinase (AMPK) is a tau kinase, activated in response to amyloid beta-peptide exposure. *The Biochemical journal* **434**, 503-512, (2011).
- 379 Smet-Nocca, C. *et al.* Identification of O-GlcNAc sites within peptides of the Tau protein and their impact on phosphorylation. *Molecular bioSystems* **7**, 1420-1429, (2011).
- 380 Mondragon-Rodriguez, S., Perry, G., Luna-Munoz, J., Acevedo-Aquino, M. C. & Williams, S. Phosphorylation of tau protein at sites Ser(396-404) is one of the earliest events in Alzheimer's disease and Down syndrome. *Neuropathology and applied neurobiology* **40**, 121-135, (2014).
- 381 Tremblay, M. A., Acker, C. M. & Davies, P. Tau phosphorylated at tyrosine 394 is found in Alzheimer's disease tangles and can be a product of the Abl-related kinase, Arg. *Journal of Alzheimer's disease : JAD* **19**, 721-733, (2010).
- 382 Duka, V. *et al.* Identification of the sites of tau hyperphosphorylation and activation of tau kinases in synucleinopathies and Alzheimer's diseases. *PLoS One* **8**, e75025, (2013).
- 383 Biernat, J., Gustke, N., Drewes, G., Mandelkow, E. M. & Mandelkow, E. Phosphorylation of Ser262 strongly reduces binding of tau to microtubules: distinction between PHF-like immunoreactivity and microtubule binding. *Neuron* **11**, 153-163, (1993).
- 384 Biernat, J. & Mandelkow, E. M. The development of cell processes induced by tau protein requires phosphorylation of serine 262 and 356 in the repeat domain and is inhibited by phosphorylation in the proline-rich domains. *Mol Biol Cell* **10**, 727-740, (1999).
- 385 von Bergen, M. *et al.* Assembly of tau protein into Alzheimer paired helical filaments depends on a local sequence motif ((306)VQIVYK(311)) forming beta structure. *Proceedings of the National Academy of Sciences of the United States of America* **97**, 5129-5134, (2000).
- 386 Yuzwa, S. A. *et al.* Mapping O-GlcNAc modification sites on tau and generation of a site-specific O-GlcNAc tau antibody. *Amino acids* **40**, 857-868, (2011).
- 387 Yuzwa, S. A. *et al.* Increasing O-GlcNAc slows neurodegeneration and stabilizes tau against aggregation. *Nature chemical biology* **8**, 393-399, (2012).
- 388 Yuzwa, S. A., Cheung, A. H., Okon, M., McIntosh, L. P. & Vocadlo, D. J. O-GlcNAc modification of tau directly inhibits its aggregation without perturbing the conformational properties of tau monomers. *Journal of molecular biology* **426**, 1736-1752, (2014).
- 389 Borghgraef, P. *et al.* Increasing brain protein O-GlcNAc-ylation mitigates breathing defects and mortality of Tau.P301L mice. *PLoS One* **8**, e84442, (2013).
- 390 Bedford, M. T. & Clarke, S. G. Protein arginine methylation in mammals: who, what, and why. *Molecular cell* **33**, 1-13, (2009).
- 391 Mandelkow, E. M. *et al.* Tau domains, phosphorylation, and interactions with microtubules. *Neurobiology of aging* **16**, 355-362; discussion 362-353, (1995).
- 392 Sturchler-Pierrat, C. *et al.* Two amyloid precursor protein transgenic mouse models with Alzheimer disease-like pathology. *Proceedings of the National Academy of Sciences of the United States of America* **94**, 13287-13292, (1997).
- 393 Rockenstein, E. *et al.* Neuroprotective effects of regulators of the glycogen synthase kinase-3beta signaling pathway in a transgenic model of Alzheimer's disease are associated with reduced amyloid precursor protein phosphorylation. *The Journal of neuroscience : the official journal of the Society for Neuroscience* **27**, 1981-1991, (2007).
- 394 Simon, A. M. *et al.* Overexpression of wild-type human APP in mice causes cognitive deficits and pathological features unrelated to Abeta levels. *Neurobiology of disease* **33**, 369-378, (2009).
- 395 Kopke, E. *et al.* Microtubule-associated protein tau. Abnormal phosphorylation of a non-paired helical filament pool in Alzheimer disease. *The Journal of biological chemistry* **268**, 24374-24384, (1993).
- 396 Ferri, C. P. *et al.* Global prevalence of dementia: A Delphi consensus study. *Lancet* **366**, 2112-2117, (2005).
- 397 Dorsey, E. R. *et al.* Projected number of people with Parkinson disease in the most populous nations, 2005 through 2030. *Neurology* **68**, 384-386, (2007).

398 Thies, W. & Bleiler, L. 2011 Alzheimer's disease facts and figures. *Alzheimers Dement.* **7**, 208–
 244, (2011).

399 Pearce, J. The extrapyramidal disorder of Alzheimer's disease. *Eur. Neurol.* **12**, 94–103, (1974).

400 Lieberman, A. *et al.* Dementia in Parkinson disease. *Ann. Neurol.* **6**, 355–359, (1979).

401 Leverenz, J. & Sumi, S. M. Parkinson's disease in patients with Alzheimer's disease. *Arch. Neurol.*
43, 662–664, (1986).

402 Ditter, S. M. & Mirra, S. S. Neuropathologic and clinical features of Parkinson's disease in
 Alzheimer's disease patients. *Neurology* **37**, 754–760, (1987).

403 Mayeux, R. *et al.* An estimate of the prevalence of dementia in idiopathic Parkinson's disease.
Arch. Neurol. **45**, 260–262, (1988).

404 Hofman, A. *et al.* History of dementia and Parkinson's disease in 1st-degree relatives of patients
 with Alzheimer's disease. *Neurology* **39**, 1589–1592, (1989).

405 Lippa, C. F. *et al.* Lewy bodies contain altered α -synuclein in brains of many familiar Alzheimer's
 disease patients with mutations in presenilin and amyloid precursor protein genes. *Am. J. Pathol.*
153, 1365–1370, (1998).

406 Mikolaenko, I. *et al.* α -synuclein lesions in normal aging, Parkinson disease, and Alzheimer
 disease: Evidence from the Baltimore Longitudinal Study of Aging (BLSA). *J. Neuropathol. Exp.*
Neurol. **64**, 156–162, (2005).

407 Hakim, A. M. & Mathieson, G. Dementia in Parkinson disease: A neuropathologic study.
Neurology **29**, 1209–1214, (1979).

408 Boller, F., Mizutani, T., Roessmann, U. & Gambetti, P. Parkinson disease, dementia, and
 Alzheimer disease: Clinicopathological correlations. *Ann. Neurol.* **7**, 329–335, (1980).

409 Wills, J. *et al.* Elevated tauopathy and alpha-synuclein pathology in postmortem Parkinson's
 disease brains with and without dementia. *Exp. Neurol.* **225**, 210–218, (2010).

410 Wills, J. *et al.* Tauopathic changes in the striatum of A53T alpha-synuclein mutant mouse model
 of Parkinson's disease. *PLoS One* **6**, e17953, (2011).

411 Kosik, K. S., Joachim, C. L. & Selkoe, D. J. Microtubule-associated protein tau (τ) is a major
 antigenic component of paired helical filaments in Alzheimer disease. *Proc. Natl. Acad. Sci. USA*
83, 4044–4048, (1986).

412 Pastor, P. *et al.* Significant association between the tau gene A0/A0 genotype and Parkinson's
 disease. *Ann. Neurol.* **47**, 242–245, (2000).

413 Martin, E. R. *et al.* Association of single-nucleotide polymorphisms of the tau gene with late-onset
 Parkinson disease. *JAMA* **286**, 2245–2250, (2001).

414 Elbaz, A. *et al.* Independent and joint effects of the MAPT and SNCA genes in Parkinson disease.
Ann. Neurol. **69**, 778–792, (2011).

415 Frasier, M. *et al.* Tau phosphorylation increases in symptomatic mice overexpressing A30P alpha-
 synuclein. *Exp. Neurol.* **192**, 274–287, (2005).

416 Haggerty, T. *et al.* Hyperphosphorylated Tau in an alpha-synuclein-overexpressing transgenic
 model of Parkinson's disease. *Eur. J. Neurosci.* **33**, 1598–1610, (2011).

417 Lin, C. H., Tsai, P. I., Wu, R. M. & Chien, C. T. LRRK2 G2019S mutation induces dendrite
 degeneration through mislocalization and phosphorylation of tau by recruiting autoactivated
 GSK3 α . *J. Neurosci.* **30**, 13138–13149, (2010).

418 Shulman, J. M., De Jager, P. L. & Feany, M. B. Parkinson's disease: Genetics and pathogenesis.
Annu. Rev. Pathol. **6**, 193–222, (2011).

419 Matsuura, K., Kabuto, H., Makino, H. & Ogawa, N. Pole test is a useful method for evaluating the
 mouse movement disorder caused by striatal dopamine depletion. *J. Neurosci. Methods* **73**, 45–48,
 (1997).

420 Masliah, E. *et al.* Dopaminergic loss and inclusion body formation in α -synuclein mice:
 Implications for neurodegenerative disorders. *Science* **287**, 1265–1269, (2000).

421 Fleming, S. M. *et al.* Early and progressive sensorimotor anomalies in mice overexpressing wild-
 type human α -synuclein. *J. Neurosci.* **24**, 9434–9440, (2004).

422 Fleming, S. M. *et al.* Behavioral effects of dopaminergic agonists in transgenic mice
 overexpressing human wildtype α -synuclein. *Neuroscience* **142**, 1245–1253, (2006).

423 Fernagut, P. O. *et al.* Behavioral and histopathological consequences of paraquat intoxication in
 mice: Effects of alpha-synuclein over-expression. *Synapse* **61**, 991–1001, (2007).

- 424 Hammond, C., Bergman, H. & Brown, P. Pathological synchronization in Parkinson's disease:
networks, models and treatments. *Trends Neurosci.* **30**, 357–364, (2007).
- 425 Gittis, A. H. *et al.* Rapid target-specific remodeling of fast-spiking inhibitory circuits after loss of
dopamine. *Neuron* **71**, 858–868, (2011).
- 426 Lam, H. A. *et al.* Elevated tonic extracellular dopamine concentration and altered dopamine
modulation of synaptic activity precede dopamine loss in the striatum of mice overexpressing
human alpha-synuclein. *J. Neurosci. Res.* **89**, 1091–1102, (2011).
- 427 Andersson, M., Hansson, O., Minthon, L., Rosen, I. & Londos, E. Electroencephalogram
variability in dementia with lewy bodies, Alzheimer's disease and controls. *Dementia and
geriatric cognitive disorders* **26**, 284–290, (2008).
- 428 Bonanni, L. *et al.* EEG comparisons in early Alzheimer's disease, dementia with Lewy bodies and
Parkinson's disease with dementia patients with a 2-year follow-up. *Brain : a journal of neurology*
131, 690–705, (2008).
- 429 Almkvist, O. *et al.* Responder characteristics to a single oral dose of cholinesterase inhibitor: A
double-blind placebo-controlled study with tacrine in Alzheimer patients. *Dementia and geriatric
cognitive disorders* **12**, 22–32, (2001).
- 430 Adler, G., Brassens, S., Chwalek, K., Dieter, B. & Teufel, M. Prediction of treatment response to
rivastigmine in Alzheimer's dementia. *Journal of neurology, neurosurgery, and psychiatry* **75**,
292–294, (2004).
- 431 Lippa, C. F., Smith, T. W. & Perry, E. Dementia with Lewy bodies: Choline acetyltransferase
parallels nucleus basalis pathology. *Journal of neural transmission* **106**, 525–535, (1999).
- 432 Perry, E. K. *et al.* Cholinergic transmitter and neurotrophic activities in Lewy body dementia:
Similarity to Parkinson's and distinction from Alzheimer disease. *Alzheimer disease and
associated disorders* **7**, 69–79, (1993).
- 433 Possin, K. L. *et al.* Rivastigmine is associated with restoration of left frontal brain activity in
Parkinson's disease. *Mov. Disord.* **28**, 1384–1390, (2013).
- 434 Sales-Carbonell, C. *et al.* Striatal GABAergic and cortical glutamatergic neurons mediate
contrasting effects of cannabinoids on cortical network synchrony. *Proc. Natl. Acad. Sci. USA*
110, 719–724, (2013).
- 435 Chesselet, M. F. *et al.* A progressive mouse model of Parkinson's disease: the Thy1-aSyn ("Line
61") mice. *Neurotherapeutics* **9**, 297–314, (2012).
- 436 Rockenstein, E. *et al.* Differential neuropathological alterations in transgenic mice expressing α -
synuclein from the PDGF-B and Thy-1 promoters. *J. Neurosci. Res.* **68**, 568–578, (2002).
- 437 Miller, J. J. & Baimbridge, K. G. Biochemical and immunohistochemical correlates of kindling-
induced epilepsy: Role of calcium binding protein. *Brain Res.* **278**, 322–326, (1983).
- 438 Marksteiner, J., Ortler, M., Bellmann, R. & Sperk, G. Neuropeptide Y biosynthesis is markedly
induced in mossy fibers during temporal lobe epilepsy of the rat. *Neurosci. Lett.* **112**, 143–148,
(1990).
- 439 Palop, J. J. *et al.* Aberrant excitatory neuronal activity and compensatory remodeling of inhibitory
hippocampal circuits in mouse models of Alzheimer's disease. *Neuron* **55**, 697–711, (2007).
- 440 Palop, J. J., Mucke, L. & Roberson, E. D. Quantifying biomarkers of cognitive dysfunction and
neuronal network hyperexcitability in mouse models of Alzheimer's disease: Depletion of
calcium-dependent proteins and inhibitory hippocampal remodeling. *Methods Mol. Biol.* **670**,
245–262, (2011).
- 441 Winston, S. M., Hayward, M. D., Nestler, E. J. & Duman, R. S. Chronic electroconvulsive
seizures down-regulate expression of the immediate-early genes c-fos and c-jun in rat cerebral
cortex. *J. Neurochem.* **54**, 1920–1925, (1990).
- 442 Sanchez, P. E. *et al.* Levetiracetam suppresses neuronal network dysfunction and reverses synaptic
and cognitive deficits in an Alzheimer's disease model. *Proc. Natl. Acad. Sci. USA* **109**, E2895–
E2903, (2012).
- 443 Verret, L. *et al.* Inhibitory interneuron deficit links altered network activity and cognitive
dysfunction in Alzheimer model. *Cell* **149**, 708–721, (2012).
- 444 Buzsaki, G. *et al.* Nucleus basalis and thalamic control of neocortical activity in the freely moving
rat. *J. Neurosci.* **8**, 4007–4026, (1988).

- 445 Riekkinen, P., Jr., Riekkinen, M., Sirvio, J., Miettinen, R. & Riekkinen, P. Loss of cholinergic neurons in the nucleus basalis induces neocortical electroencephalographic and passive avoidance deficits. *Neuroscience* **47**, 823–831, (1992).
- 446 Weiner, M. F. *et al.* Can alzheimer's disease and dementias with Lewy bodies be distinguished clinically? *J. Geriatr. Psychiatry Neurol.* **16**, 245–250, (2003).
- 447 Caviness, J. N., Adler, C. H., Caselli, R. J. & Hernandez, J. L. Electrophysiology of the myoclonus in dementia with Lewy bodies. *Neurology* **60**, 523–524, (2003).
- 448 Magloczky, Z., Halasz, P., Vajda, J., Czirjak, S. & Freund, T. F. Loss of Calbindin-D_{28K} immunoreactivity from dentate granule cells in human temporal lobe epilepsy. *Neuroscience* **76**, 377–385, (1997).
- 449 Bandopadhyay, R., Liu, J. Y., Sisodiya, S. M. & Thom, M. A comparative study of the dentate gyrus in hippocampal sclerosis in epilepsy and dementia. *Neuropathol. Appl. Neurobiol.* **40**, 177–190, (2014).
- 450 Caviness, J. N., Adler, C. H., Beach, T. G., Wetjen, K. L. & Caselli, R. J. Small-amplitude cortical myoclonus in Parkinson's disease: Physiology and clinical observations. *Mov. Disord.* **17**, 657–662, (2002).
- 451 Kojovic, M., Cordivari, C. & Bhatia, K. Myoclonic disorders: A practical approach for diagnosis and treatment. *Therapeutic advances in neurological disorders* **4**, 47–62, (2011).
- 452 Louis, E. D., Klatka, L. A., Liu, Y. & Fahn, S. Comparison of extrapyramidal features in 31 pathologically confirmed cases of diffuse Lewy body disease and 34 pathologically confirmed cases of Parkinson's disease. *Neurology* **48**, 376–380, (1997).
- 453 Caviness, J. N. *et al.* The incidence and prevalence of myoclonus in Olmsted County, Minnesota. *Mayo Clinic proceedings* **74**, 565–569, (1999).
- 454 Forsgren, L., Bucht, G., Eriksson, S. & Bergmark, L. Incidence and clinical characterization of unprovoked seizures in adults: A prospective population-based study. *Epilepsia* **37**, 224–229, (1996).
- 455 Pillai, J. & Sperling, M. R. Interictal EEG and the diagnosis of epilepsy. *Epilepsia* **47 Suppl 1**, 14–22, (2006).
- 456 Vossel, K. A. *et al.* Seizures and epileptiform activity in the early stages of Alzheimer disease. *JAMA Neurol.* **70**, 1158–1166, (2013).
- 457 Brown, P. *et al.* Effectiveness of piracetam in cortical myoclonus. *Mov. Disord.* **8**, 63–68, (1993).
- 458 Ikeda, A., Shibasaki, H., Tashiro, K., Mizuno, Y. & Kimura, J. Clinical trial of piracetam in patients with myoclonus: Nationwide multiinstitution study in Japan. The Myoclonus/Piracetam Study Group. *Mov. Disord.* **11**, 691–700, (1996).
- 459 Frucht, S. J., Louis, E. D., Chuang, C. & Fahn, S. A pilot tolerability and efficacy study of levetiracetam in patients with chronic myoclonus. *Neurology* **57**, 1112–1114, (2001).
- 460 Caviness, J. N. *et al.* Parkinson's disease, cortical dysfunction, and alpha-synuclein. *Mov. Disord.* **26**, 1436–1442, (2011).
- 461 Kotsopoulos, I. A., van Merode, T., Kessels, F. G., de Krom, M. C. & Knottnerus, J. A. Systematic review and meta-analysis of incidence studies of epilepsy and unprovoked seizures. *Epilepsia* **43**, 1402–1409, (2002).
- 462 Del Ser, T., Hachinski, V., Merskey, H. & Munoz, D. G. Clinical and pathologic features of two groups of patients with dementia with Lewy bodies: effect of coexisting Alzheimer-type lesion load. *Alzheimer disease and associated disorders* **15**, 31–44, (2001).
- 463 Briel, R. C. G. *et al.* EEG findings in dementia with Lewy bodies and Alzheimer's disease. *Journal of neurology, neurosurgery, and psychiatry* **66**, 401–403, (1999).
- 464 Bakker, A. *et al.* Reduction of hippocampal hyperactivity improves cognition in amnesic mild cognitive impairment. *Neuron* **74**, 467–474, (2012).
- 465 Ma, Q. L. *et al.* Loss of MAP Function Leads to Hippocampal Synapse Loss and Deficits in the Morris Water Maze with Aging. *The Journal of neuroscience : the official journal of the Society for Neuroscience* **34**, 7124–7136, (2014).
- 466 Lawson, V. A. *et al.* Gene knockout of tau expression does not contribute to the pathogenesis of prion disease. *Journal of neuropathology and experimental neurology* **70**, 1036–1045, (2011).
- 467 Weinger, J. G. *et al.* Mice devoid of Tau have increased susceptibility to neuronal damage in myelin oligodendrocyte glycoprotein-induced experimental autoimmune encephalomyelitis. *Journal of neuropathology and experimental neurology* **71**, 422–433, (2012).

- 468 Liang, Z., Liu, F., Iqbal, K., Grundke-Iqbal, I. & Gong, C. X. Dysregulation of tau phosphorylation in mouse brain during excitotoxic damage. *Journal of Alzheimer's disease : JAD* **17**, 531-539, (2009).
- 469 Fisher, R. S. *et al.* Epileptic seizures and epilepsy: Definitions proposed by the International League Against Epilepsy (ILAE) and the International Bureau for Epilepsy (IBE). *Epilepsia* **46**, 470-472, (2005).
- 470 Rothman, K. & Greenland, S. *Modern Epidemiology*. 3rd edn, (Lippincott Williams & Wilkins, 2008).
- 471 Consensus recommendations for the postmortem diagnosis of Alzheimer's disease. The National Institute on Aging, and Reagan Institute Working Group on Diagnostic Criteria for the Neuropathological Assessment of Alzheimer's Disease. *Neurobiol. Aging* **18**, S1-S2, (1997).
- 472 Kinney, G. G., Patino, P., Mermet-Bouvier, Y., Starrett, J. E., Jr. & Gribkoff, V. K. Cognition-enhancing drugs increase stimulated hippocampal theta rhythm amplitude in the urethane-anesthetized rat. *J. Pharmacol. Exp. Ther.* **291**, 99-106, (1999).
- 473 Morris, R. G., Garrud, P., Rawlins, J. N. & O'Keefe, J. Place navigation impaired in rats with hippocampal lesions. *Nature* **297**, 681-683, (1982).
- 474 Guyenet, S. J. *et al.* A simple composite phenotype scoring system for evaluating mouse models of cerebellar ataxia. *J. Vis. Exp.*, (2010).
- 475 Ivanovova, N., Handzusova, M., Hanes, J., Kontsekova, E. & Novak, M. High-yield purification of fetal tau preserving its structure and phosphorylation pattern. *Journal of immunological methods* **339**, 17-22, (2008).
- 476 Vosseller, K. *et al.* O-linked N-acetylglucosamine proteomics of postsynaptic density preparations using lectin weak affinity chromatography and mass spectrometry. *Molecular & cellular proteomics : MCP* **5**, 923-934, (2006).
- 477 Chalkley, R. J., Thalhammer, A., Schoepfer, R. & Burlingame, A. L. Identification of protein O-GlcNAcylation sites using electron transfer dissociation mass spectrometry on native peptides. *Proceedings of the National Academy of Sciences of the United States of America* **106**, 8894-8899, (2009).
- 478 Olsen, J. V. *et al.* Parts per million mass accuracy on an Orbitrap mass spectrometer via lock mass injection into a C-trap. *Molecular & cellular proteomics : MCP* **4**, 2010-2021, (2005).
- 479 Chalkley, R. J., Baker, P. R., Medzihradzky, K. F., Lynn, A. J. & Burlingame, A. L. In-depth analysis of tandem mass spectrometry data from disparate instrument types. *Molecular & cellular proteomics : MCP* **7**, 2386-2398, (2008).
- 480 Elias, J. E. & Gygi, S. P. Target-decoy search strategy for increased confidence in large-scale protein identifications by mass spectrometry. *Nature methods* **4**, 207-214, (2007).
- 481 Guan, S., Price, J. C., Prusiner, S. B., Ghaemmaghami, S. & Burlingame, A. L. A data processing pipeline for mammalian proteome dynamics studies using stable isotope metabolic labeling. *Molecular & cellular proteomics : MCP* **10**, M111 010728, (2011).
- 482 Perl, D. P. & Good, P. F. Comparative techniques for determining cellular iron distribution in brain tissues. *Ann. Neurol.* **32 Suppl**, S76-S81, (1992).
- 483 Mucke, L., Oldstone, M. B. A., Morris, J. C. & Nerenberg, M. I. Rapid activation of astrocyte-specific expression of GFAP-lacZ transgene by focal injury. *New Biol.* **3**, 465-474, (1991).

The Johns Hopkins University School of Medicine

Meaghan Morris

6/23/2014

Educational History

Ph.D. expected 2014 Program in Biology, Chemistry and Molecular Biology
Johns Hopkins School of Medicine
Mentors: Dr. Gerald Hart, PhD and Dr. Lennart Mucke, MD
B.S. 2006 Chemistry, Boston College

Other Professional Experience

Summer Internship 2006 Roche, Palo Alto, CA
Undergraduate Research 2003-2006 Lab of Dr. T. Ross Kelly, Boston College

Fellowships

2004 Summer Undergraduate Research Fellowship, Pfizer

Honors and Awards

2006	Phi Beta Kappa Membership	Boston College
2006	Albert McGuinn, SJ Award	Boston College
2006	McCarthy Award	Boston College
2006	Graduated summa cum laude	Boston College
2005	Dean's Scholar as a Chemistry Major	Boston College
2002 – 2006	College of Arts and Sciences Honors Program	Boston College
2002 – 2005	Dean's List First Honors	Boston College
2004	Sophomore Scholar as a Chemistry Major	Boston College
2004	Leadership Award	Boston College Varsity Women's Fencing Team

Peer Reviewed Publications

Morris M, Hamto P, Adame A, Devidze N, Masliah E, Mucke L (2013) Age-appropriate cognition and subtle dopamine-independent motor deficits in aged Tau knockout mice. *Neurobiol Aging*. 34:1523-1529. PMID: PMC3596503

Morris M, Koyama A, Masliah E, Mucke L (2011) Tau reduction does not prevent motor deficits in two mouse models of Parkinson's disease. *PLoS ONE*. 6:e29257. PMID: PMC3242771

Morris M, Maeda S, Vossel K, Mucke L (2011) The many faces of tau. *Neuron*. 70:410-426. PMID: PMC3319390

Wang Z, Udeshi ND, **O'Malley M**, Shabanowitz J, Hunt DF, Hart GW (2010) Enrichment and site mapping of O-linked N-acetylglucosamine by a combination of chemical/enzymatic tagging, photochemical cleavage, and electron transfer dissociation mass spectrometry. *Mol Cell Proteomics*. 9:153-160. PMID: PMC2808261

Iyer PS, **O'Malley MM**, Lucas MC. (2007) Microwave-enhanced rhodium-catalyzed conjugate-addition of aryl boronic acids to unprotected maleimides. *Tet Lett*. 48:4413-4418.

O'Malley MM, Damkaci F, Kelly TR (2006) Synthesis of Pterocellin A. *Org Lett.* 8:2651-2652.

Posters

Morris M, Sanchez P, Verret L, Dubal DB, Koyama A, Masliah E, Mucke L (2012) Human wildtype α -synuclein causes neuronal network dysfunction in transgenic mice. Society for Neuroscience 42nd Annual Meeting, New Orleans, LA, October 13, 2012.